NAVAL POSTGRADUATE SCHOOL

Monterey, California

THESIS

AN INVESTIGATION OF BANK-TO-TURN MISSILES

by

Nicolaos G. Protonotarios

June 1986

Thesis Advisor: D. J. Collins

Approved for public release; distribution unlimited.

Unclassified

RITY CLASSIFICATION OF THIS PAGE

REPORT DOCUMENTATION PAGE

REPORT SECURITY CLASSIFICATION	1b RESTRICTIVE MARKINGS
SECURITY CLASSIFICATION AUTHORITY	3 DISTRIBUTION / AVAILABILITY OF REPORT Approved for public release; distribution unlimited.
DECLASSIFICATION / DOWNGRADING SCHEDULE	
ERFORMING ORGANIZATION REPORT NUMBER(S)	5 MONITORING ORGANIZATION REPORT NUMBER(S)
NAME OF PERFORMING ORGANIZATION: Naval Postgraduate School 6b OFFICE SYMBOL (If applicable): Code 67Co	7a NAME OF MONITORING ORGANIZATION: Naval Postgraduate School
ADDRESS (City, State, and ZIP Code): Monterey, California 93943-5000	7b. ADDRESS (City, State, and ZIP Code): Monterey, California 93943-5000
NAME OF FUNDING / SPONSORING ORGANIZATION 8b. OFFICE SYMBOL (If applicable)	9 PROCUREMENT INSTRUMENT IDENTIFICATION NUMBER
ADDRESS (City, State, and ZIP Code)	10 SOURCE OF FUNDING NUMBERS PROGRAM ELEMENT NO / PROJECT NO / TASK NO / WORK UNIT ACCESSION NO

TITLE (Include Security Classification)

AN INVESTIGATION OF B.T.T. MISSILES

PERSONAL AUTHOR(S) PROTONOTARIOS, Nicolaos G.

TYPE OF REPORT	13b TIME COVERED	14 DATE OF REPORT (Year, Month, Day)	15 PAGE COUNT
Master's Thesis	FROM _____ TO _____	1986 June 20	221

SUPPLEMENTARY NOTATION

COSATI CODES			18 SUBJECT TERMS (Continue on reverse if necessary and identify by block number)
FIELD	GROUP	SUB-GROUP	Bank-to-Turn, autopilot, pitch, roll, yaw, longitudinal, lateral coupled, split up, reconfiguration, robustness.

ABSTRACT (Continue on reverse if necessary and identify by block number)

The purpose of this thesis was to examine the control deficiencies in a Bank-to-Turne TT) cruise missile, due to specific impairments at its control surfaces, during the termediate phase of its mission.

A linearized mathematical model is developed, which simulates the dynamic response of e missile, circular airframe, for the study of flight control configuration.

In the development, a classical design and analysis was performed using both, longitudinal d lateral channels for the circular airframe.

For each channel, the control surfaces were split into independent components, and the rresponding continuous open loop uncoupled autopilots were analyzed in terms of their ansient response.

DISTRIBUTION / AVAILABILITY OF ABSTRACT UNCLASSIFIED/UNLIMITED ☐ SAME AS RPT ☐ DTIC USERS	21 ABSTRACT SECURITY CLASSIFICATION
NAME OF RESPONSIBLE INDIVIDUAL: D. J. Collins	22b TELEPHONE (Include Area Code): (408) 646 2826 22c OFFICE SYMBOL: 67Co

ORM 1473, 84 MAR — 83 APR edition may be used until exhausted; All other editions are obsolete

SECURITY CLASSIFICATION OF THIS PAGE

Unclassified

Then specific kinds of impairments were examined and analyzed.

Finally, the combined continuous pitch and roll channel autopilots are investigated and the robustness of the complete system is analyzed in Chapter V.

Approved for public release, distribution unlimited

An Investigation of Bank-to-Turn Missiles

by

Nicolaos, G. Protonotarios
Lieutenant Commander, Hellenic Navy
B.S., Hellenic Naval Academy, 1973

Submitted in partial fulfillment of the
requirements for the degree of

MASTER OF SCIENCE IN ENGINEERING SCIENCE

from the

NAVAL POSTGRADUATE SCHOOL
June 1986

ABSTRACT

The purpose of this thesis was to examine the control deficiencies in a Bank-to-Turne (BTT) cruise missile, due to specific impairments at its control surfaces, during the intermediate phase of its mission.

A linearized mathematical model is developed, which simulates the dynamic response of the missile, circular airframe, for the study of flight control configuration.

In the development, a classical design and analysis was performed using both, longitudinal and lateral channels for the circular airframe.

For each channel, the control surfaces were split into independent components, and the corresponding continuous open loop uncoupled autopilots were analyzed in terms of their transient response.

Then specific kinds of impairments were examined and analyzed.

Finally, the combined continuous pitch and roll channel autopilots are investigated and the robustness of the complete system is analyzed in Chapter V.

TABLE OF CONTENTS

LIST OF TABLES

LIST OF FIGURES

ACKNOWLEDGEMENT

I would like to express my sincere appreciation to Professor D. J. Collins, whose assistance and encouragement contributed immeasurably to this thesis.

I would also like to dedicate this thesis to my wife Nicole, and my mother Irini. Without their constant love, support, and understanding this work would not have been possible.

I. INTRODUCTION

A guided missile is one which is usually fired in a direction approximately towards the target and subsequently receives steering commands from the guidance system to improve its accuracy.

In recent years, the application of Bank-to-Turn (BTT) guidance to tactical missiles has generated conciderable interest, motivated by certain advantages that a Bank-to-Turn control configuration can offer.

First, against high performance threats, there is a need for defensive missiles to develope increasingly higher lift accelerations, which requires banking maneuver to properly direct the control vector.

Second, the need for greatly increased stand off ranges has led the design of tactical missiles towards airbreathing propulsion systems such as the ramjet. These designs generally have configuration geometries that are not cruciform, due to exposed inlets beneath the vehicle. As a result, there are often stringent limits on the sideslip angle that can be developed during engine operation, and this too, dictates some types of Bank-to-Turn control scheme.

This thesis investigates the controllability of a Bank-to-Turn missile, when one or more control surfaces are damaged, at fixed flight conditions (i.e. constant altitude, Mach number and missile weight and inertias).

The approach is to design a control reconfiguration module to be placed between the flight control laws and the control surfaces. In the face of missile damage the reconfiguration module would reallocate control

commands to the unimpaired control surfaces so that flight critical pitch, yaw, and rolling moments would be preserved to the maximum extent possible. Using the reconfiguration module control laws, the existing flight control laws would not be altered.

In the first part of the thesis the control surfaces conventions, definitions and the manoeuvre by banking are reviewed.

The second and third part reviews the design of the longitudinal and lateral channels and involves the uncoupled pitch, roll and yaw channels for the circular and elliptical airframes of a B.T.T. missile. The resultant continuous open loop designs are analyzed and found to be in accordance with the desired specified requirements. Applying the convention control theory, the corresponding modified longitudinal and lateral autopilots are obtained, analyzed and compared with the original system. The effect of damage to one or more control surfaces, on the controllability of each system, is obtained, analyzed and compared with the unimpaired models respectively.

Finally, the combined linear open loop pitch and roll channel autopilots, for the circular airframe configuration, are investigated. The effect of damage to one or more actuators, on the control of the combined unimpaired system is obtained and analyzed. The most severe type of impairment considered in this thesis, i.e., the hard over type, is extensively investigated in Chapter V. Corrective actions are then developed and presented.

The robustness of the complete system is analyzed in chapter five. Conclusions and recommendations for future study are then given.

The investigation and analysis in all the above cases was performed using the existing at Naval Postgraduate School (NPS), Optimal Systems Control Program (OPTSYS) for the continuous system, Robustness Design Program (POPLAR) for the robustness of the system, and EASYPLOT program for the plotting of different kind of impairments and comparisons.

II. GUIDED MISSILE CONTROL SURFACES CONVENTIONS AND MANOEUVRE BY BANKING

In this chapter, before going into mathematical details concerning the motion of a guided missile in space as a result of guidance commands, some definitions and discussion concerning the control surfaces are given.

A. GENERAL

The task of a Missile Control system is to manoeuvere the missile quickly and efficiently as a result of the following two control singnals:

(a) Detection whether the missile is flying too high or too low, or too much to the left or right.

(b) Measure the deviations or errors and develope commands to the control system to reduce these errors to zero.

B. CONTROL SURFACES DEFINITIONS

Suppose that the control surfaces 1 and 3, as is shown in the Figure 2.1, are mechanichally linked together such that a servo must impart the same rotation to both. Then these surfaces are essentially elevators. Positive elevator deflection produces a negative force in the z-direction and an anti-clockwise moment about the y-axis.

If now surfaces 1 and 3 each have their own servo it is possible for them to act as ailerons. Positive aileron deflection produces an anti-clockwise moment about the x-axis.

If looking in the direction y one surface is rotated δ^0 clockwise and the other surface δ^0 anti-clockwise then a pure couple is imparted to the missile about the fore and aft axis and this will tend to make the missile roll. Such control surfaces are now called ailerons, and by doing the same thing to control surfaces 2 and 4, the turning effect of the ailerons can be doubled.

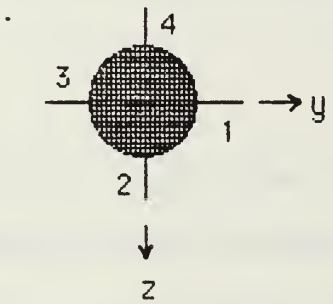

Figure 2.1 Control surfaces looking from rear of the Missile.

If the aerodynamics are linear i.e., the normal forces are proportional to incidence then the principle of superposition applies. Commmands for elevator rudder and aileron movements can be added electrically resulting in unequal movements to opposite control surfaces. Positive rudder deflection produces a positive force in the y-direction and negative moment about the z-axis. In this way we have the means to control roll motion as well as the up-down i.e., pitch motion and left-right i.e., yaw motion.

C. CONTROL SURFACE CONVETION

As is shown in the Figure 2.1 deflections δ_1, δ_2, δ_3, δ_4 are defined as positive if the leading edge of the control surface is rotated clockwise as one looks outwards along the individual hinge axis. The total aileron deflection is defined as:

$$\text{Aileron deflection } \delta = 1/4\,(\delta_1+\delta_2+\delta_3+\delta_4) \qquad \text{(II.C-1)}$$

$$\text{or} \quad 1/2\,(\delta_1+\delta_3) \quad \text{or} \quad 1/2\,(\delta_2+\delta_4) \qquad \text{(II.C-2)}$$

if only two surfaces act differentially.

D. BANK-TO-TURN CONTROL SURFACES CONFIGURATION

The same kind of analysis can be applied for the Bank-to-Turn missile configuration, shown in Figure 2.2. Note that the arrow on the control surface indicates the direction of positive leading edge deflection.

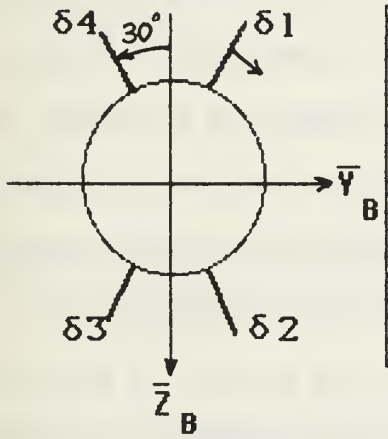

Tail Command	Tail Incidence			
	δ_1	δ_2	δ_3	δ_4
$+\delta_{Pc}$	-	+	-	+
$+\delta_{Yc}$	+	+	+	+
$+\delta_{Rc}$	+	-	-	+

Figure 2.2 B.T.T Aerodynamic Sign Convention.

The maneuver plane is the $\bar{x}_B$-$\bar{z}_B$ plane. The downwards movement is defined as positive. This is the configuration investigated in this thesis.

The B.T.T. missile configuration is tail-controlled using four identical control surfaces. The control surfaces are located flush with the body base with a ±30 degrees dihedral. With tail control configurations the pitching moment or control effectiveness is quite high in view of the fact that the tail moment arm is generally fairly large. Also there is no adverse downwash from deflection of the forward surfaces, in comparison with the canard control configuration. A more complete model of the B.T.T. circular confinguration is also shown in Figures 3.1 and 3.4 , taken from Arrow, A. [Ref. 1].

E. MANEUVER BY BANKING.

The Conventional method of altering course to the right or left in a missile or aircraft is to use the ailerons to bank i.e, roll by an angle φ, as is shown in Figure 2.3. If the lift force is increased slightly by the use of the elevators so that the vertical component of lift equals the weight then there is a horizontal component of lift equal to the total lift times sin θ. It is this component of lift which causes the flight path to change. An exact analysis of the maneuver is not simple as the airflow over the outer control surface is faster than that over the inner control surface due to the rate of turn. In practice a small amount of rudder is applied in an attempt to make the general airflow directly along the fore and aft axis of the cordinated B.T.T. missile and in the plane of the control surfaces. In this condition there is no "sideslip" and hence no net sideforce. This is the preferred method of manoeuvring since lifting forces are most efficiently generated perpendicular to the control surfaces; the lift-to-drag ratio is a maximum

in this condition. Even so there is some additional induced drag when manoeuvring. An additional manoeuvring force is obtained by increasing the incidence and this means that the normal force is inclined backwards to the velocity vector by the angle of incidence. There is a useful component equal to the normal force times the cosine of the angle of incidence and a component proportional to the sine of the incidence opposing the velocity vector. This "induced drag" will always occur whenever a lifting force is produced irrespective of the method of manoeuvre.

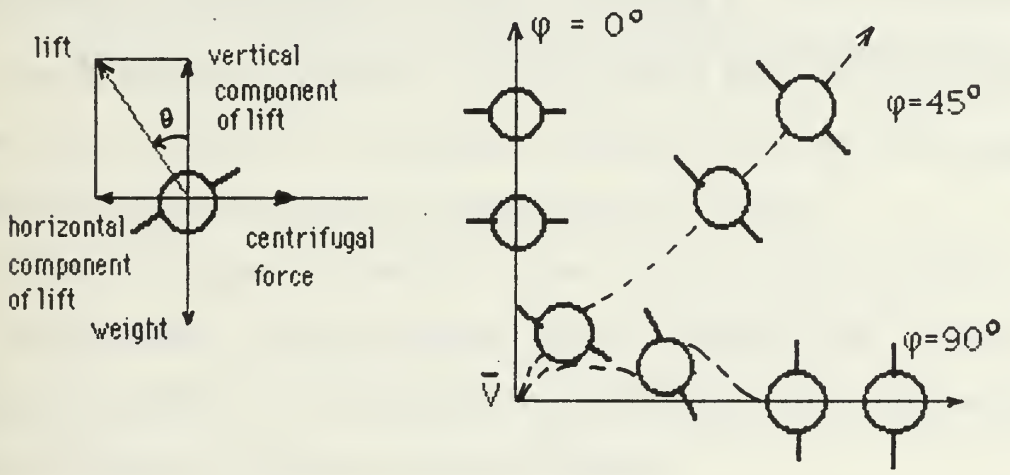

Figure 2.3 Forces Acting on a Banking Missile and Coordinated Missile Motion for coordinated B.T.T. Control Policies.

Because it is desired that the B.T.T. missile avoid negative angles of attack, the missile is forced to roll about its velocity vector when the desired manouvre direction is in the negative angle-of-attack direction. Although some negative angles of attack may be possible with certain missiles.

Coordinated motion or zero sideslip angle is achieved by directing the body fixed pitch axis of the missile at the missile velocity vector so that there is no component of missile velocity vector along the body fixed yaw axis of the missile. The Figure 2.3 (b) shows the attitude of the missile body with respect to its velocity vector $\overline{V}$. When an upward command is applied, i.e., $\varphi = 0$, the missile body moves upward with its pitch axis directed at the velocity vector until it reaches manoeuver level or angle of attack. No roll motion is required to maintain coordination of this manoeuver. The circular airframe configuration of this thesis is a planar configuration which is symmetric about its wing planes and therefore have two perfect directions which are normal to the planes of its wing.

III. LONGITUDINAL MODEL METHODOLOGY

A. INTRODUCTION

In this Chapter the design of the continuous uncoupled pitch channel (longitudinal) autopilot is reviewed, as was analyzed by Arrow, A. and Karaiskos, I. [Ref. 1 and 2]. A modified longitudinal autopilot is then designed with the four control surfaces split into independent components, for the circular configuration model shown in Figure 3.1.

Then a comparison between the two systems (original and modified) shows that are identical. The transient response plots and their analysis demonstrate the performance of the modified pitch channel.

Having established the validity of the modified system one then uses the multiple-input multiple-output control theory and state-space representation [Ref. 3], to investigate the performance of the modified pitch channel autopilot for various classes of damages.

For this thesis, two classes of impairments are considered namely, locked or hard over and inoperative with the control surfaces centered. The plots of a modified pitch autopilot without impairment are used as a basis for comparison, the impairment induced effects on normal acceleration, rate and tail incidence are assessed.

A general block diagram, of a B.T.T. autopilot is shown in Figure 3.2 taken from [Ref. 1]. Inertial acceleration commands are applied in polar coordinates (i.e., magnitude of the command (η_C) applied to the pitch autopilot and the direction (ψ_C) is applied to the roll autopilot. Achieved

manoeuver plane or inertial acceleration in rectangular coordinates (i.e., η_Z and η_Y) is determined by resolving achieved body-fixed accelerations (i.e., η_Z and η_Y) through missile roll angle (φ).

Before going into the details concerning the various kinds of damages it is prefered to make here clear some terms used in this work.

ORIGINAL SYSTEM is called the unmodified pitch channel autopilot presented in [Ref. 1].

UNIMPAIRED SYSTEM is called the modified, i.e., with the split control surfaces system, and without any kind of damage.

IMPAIRMENT, HARD OVER OR INOPERATIVE are terms expressing a specific kind of damage to one or more control surfaces.

B. UNCOUPLED LINEAR PITCH CHANNEL (ORIGINAL)

1. Aerodynamic Model

The linear pitch channel dynamic model which is used for the circular airframe, is shown in Figure 3.3, with the following requirements :

a. In actuator command branch, the high attenuation frequency must be ≥ 15 db at 100 rad/sec and zero angle-of-attack. This requirement limits the autopilot speeds of time response.

b. Relative stability with gain margins ≥ 6 db, phase margins ≥ 30 degrees with a goal at 12 db and 50 degrees.

c. An acceleration time responce with 63% time constant of 0.5 seconds for a step command of acceleration at the flight condition of interest, overshoot ≤ 10%, and zero steady-state error to reduce variations of guidance navigation gain.

The linear pitch channel dynamic model which is used, is shown in Figure 3.3. This Figure is taken from [Ref. 1]. The model is linearized for stability studies and the following three assumptions were made :

a. Manoeuver plane is the plane $\overline{x_B} - \overline{z_B}$, as is shown in Figure 3.4 in which the arrow indicates the direction of positive leading edge deflection.

b. The missile is trimmed in pitch, at fixed values of angle of attack (a), pitch angular rate (q), and pitch tail incidence (δ_P), that is $M_y = 0$.

c. The roll rate (P) of the missile is constant.

Using the foregoing assumptions, and the approximation that the variation in forward velocity (u), is equal to zero a simplified set of longitudinal equations of motion are constructed applicable to the short period of motion. These equations describe the two degree of freedom, short period longitudinal mode.

Linearized aerodynamic derivatives for M = 3.95 and Altitude = 60 KFT are provided in Table 3.1, as is given in [Ref.1].

2. Pitch Control Law

The longitudinal control law model for the circular airframe was developed from the block diagrams and information provided in [Ref. 1], and is shown in Figure 3.5. Lead-lag filters were used in the system to shape the output response, provide adequate gain and phase margins, and finally to prevent guidance noise saturation problems. The guidance requirement of zero steady-state error is satisfied by using an integrator in the acceleration error branch of the circulare control law. The rate error conpensation determines the high frequency attenuation and was used to minimize the effect of aerodynamic variations on acceleration time

response. The acceleration error compensation determines the acceleration time response.

The blocks in the pitch control law of Figure 3.5 for the circular model represent the basic transfer functions in which a normal acceleration command (n_{Zc}) equal to 1 gee, is applied to the pitch control law which uses measurements of:

a. Missile body pitch angular rate (q) and

b. Pitch normal acceleration (n_Z)

to determine the required actuator comand (δ_{P_C}). The actuator is modeled as a first order lag at 188.4 rad/sec and is shown in Figure 3.2.

3. Basic Transfer functions of the Aerodynamic Model

The equations which are represented by the block diagram of the aerodynamic model, of the uncoupled pitch channel are presented below and taken from [Ref.2] .

a. The pitch aerodynamic transfer function for the pitch angular rate (q) about the $\overline{Y}_B$ axis:

$$\frac{q}{\delta_P} = \frac{-1.3361s - 0.15}{22.545 \times 10^{-3} s^2 + 3.3634 \times 10^{-3} s + 1} \text{ (1/sec)} \qquad \text{(III.B.3-1)}$$

b. The pitch aerodynamic transfer function for the achieved maneuver normal acceleration (n_Z) in the $\overline{Z}_B$ direction:

$$\frac{n_z}{\delta_P} = \frac{106.074 \times 10^{-3} s^2 - 18.82}{22.545 \times 10^{-3} s^2 + 3.3634 \times 10^{-3} s + 1} \text{ (g's/rad)} \qquad \text{(III.B.3-2)}$$

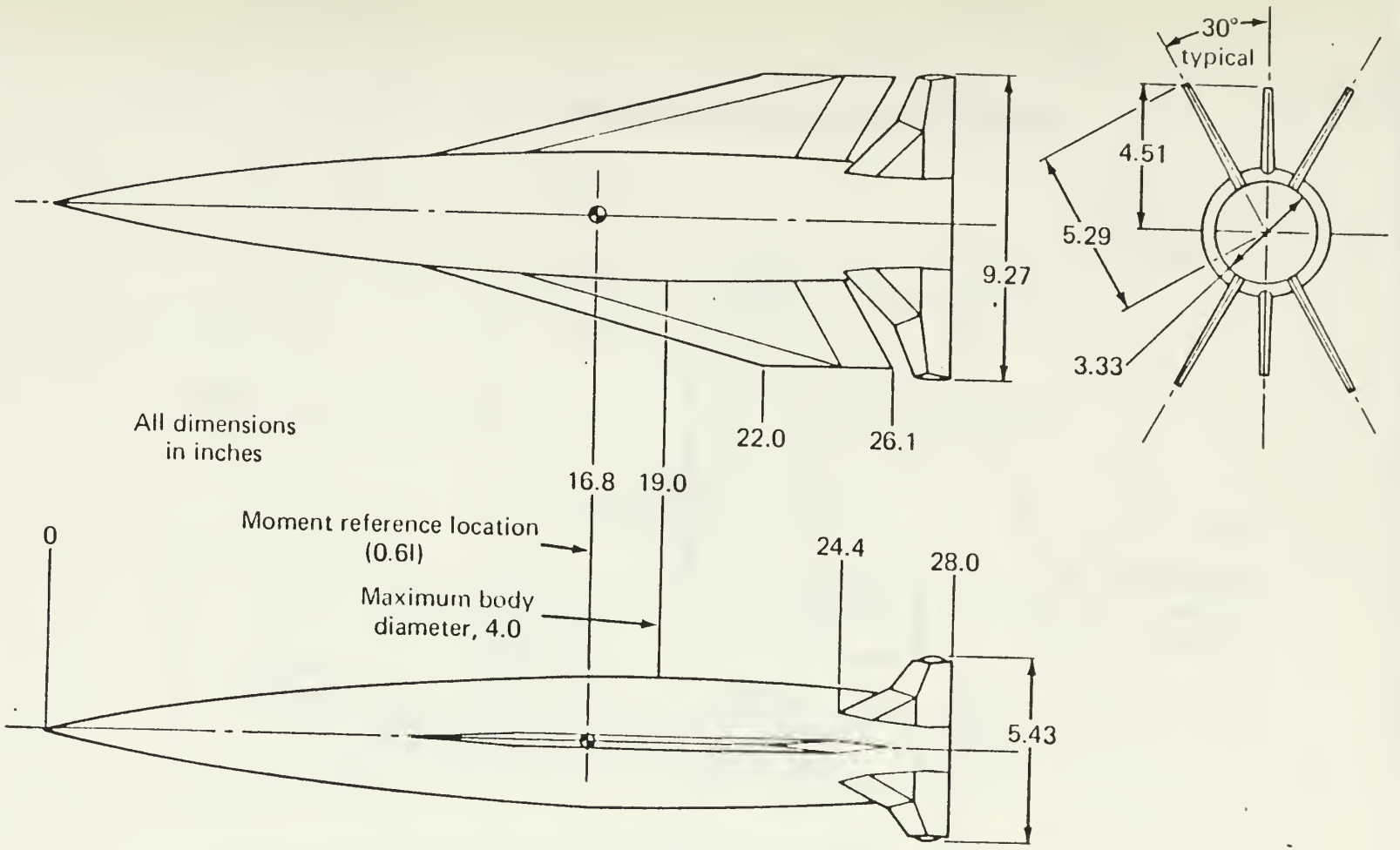

Figure 3.1 B.T.T. Model of Circular Configuration; Scale 1/6.

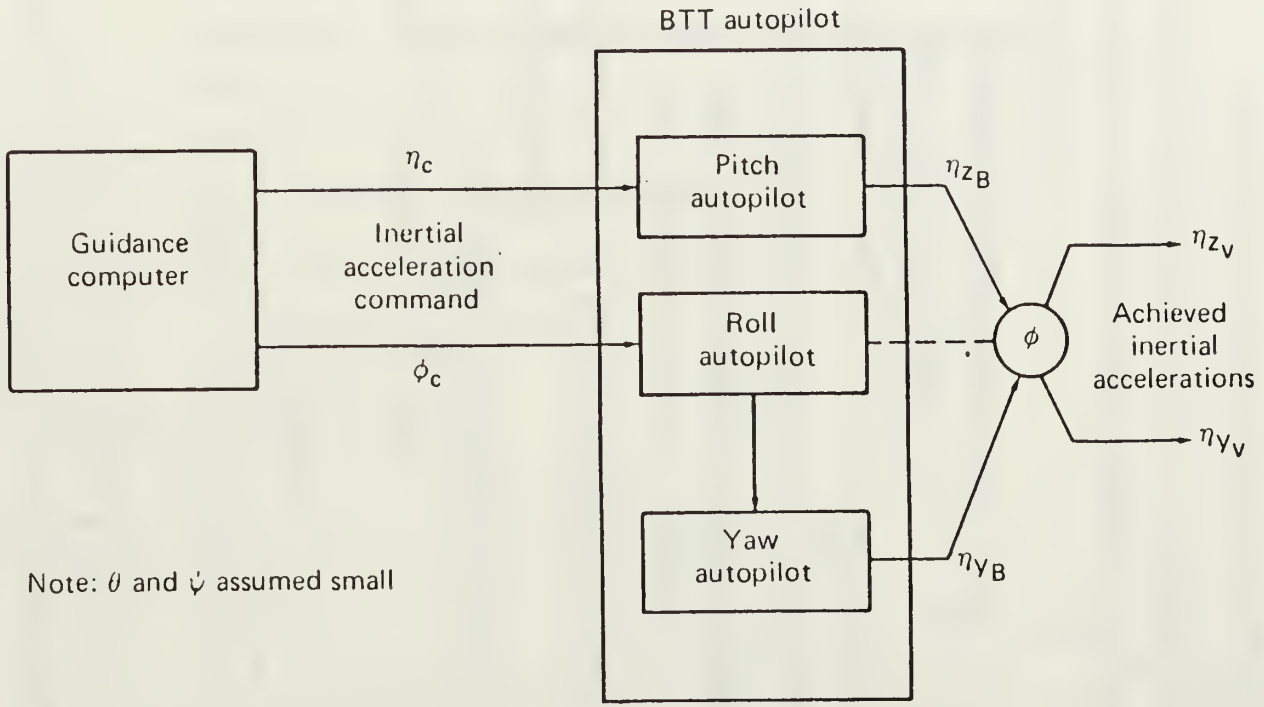

Figure 3.2 Block Diagram of the Bank-to Turn Autopilot.

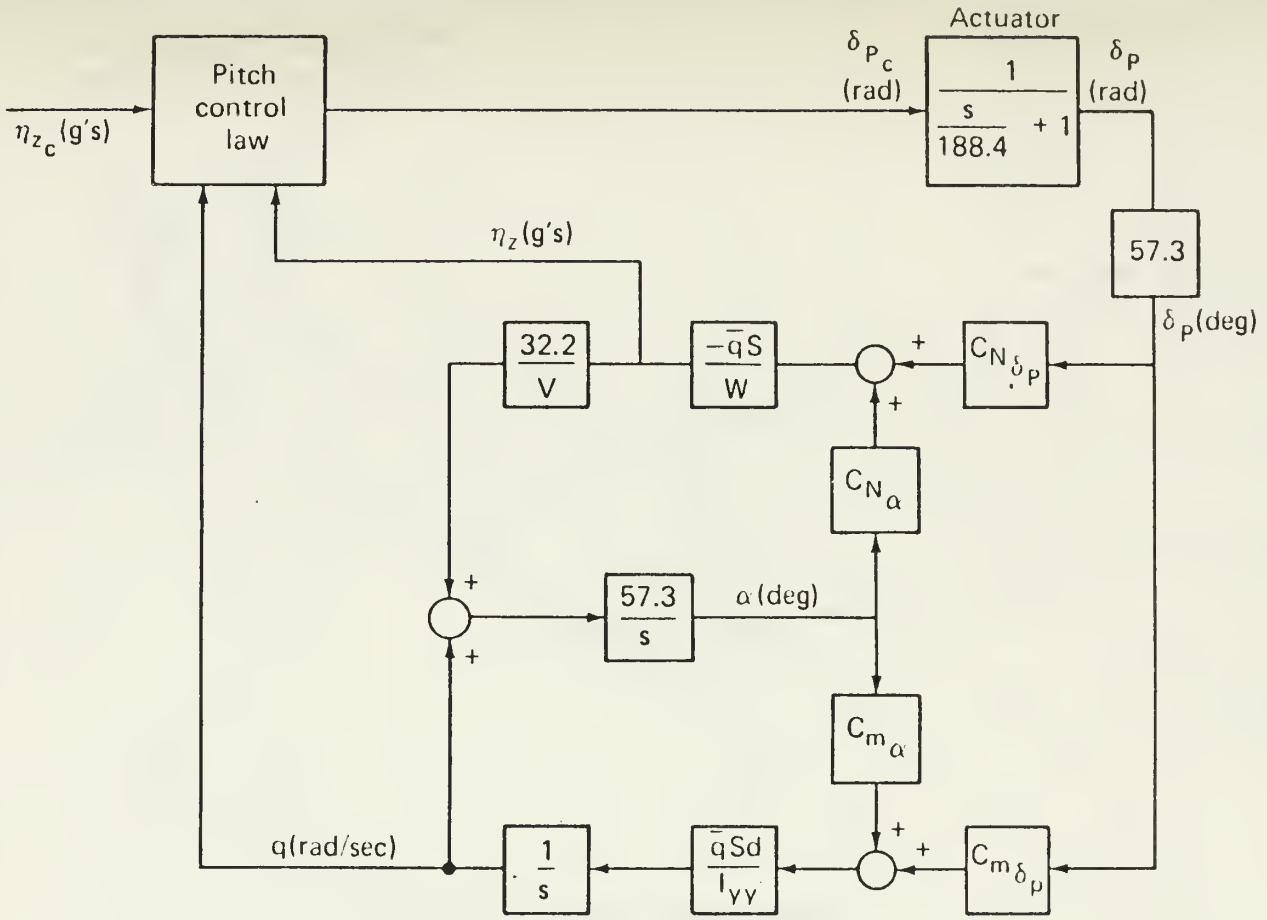

Figure 3.3 Uncoupled Pitch Channel Dynamic Model (Autopilot).

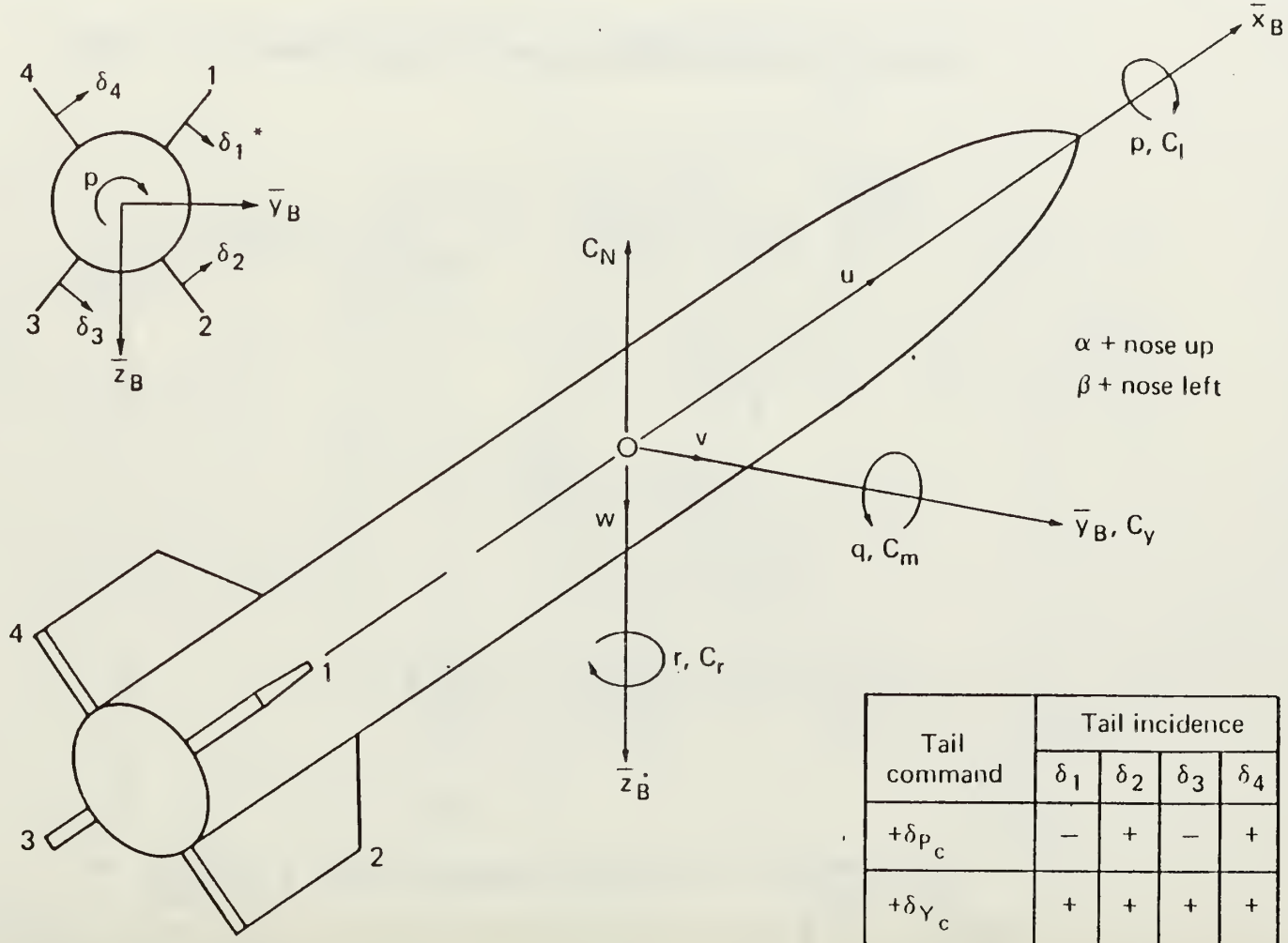

*Arrow indicates direction of positive leading edge deflection

Tail command	Tail incidence			
	δ_1	δ_2	δ_3	δ_4
$+\delta_{P_c}$	−	+	−	+
$+\delta_{Y_c}$	+	+	+	+
$+\delta_{R_c}$	+	−	−	+

Figure 3.4 Aerodynamic Sign Convention and Axes.

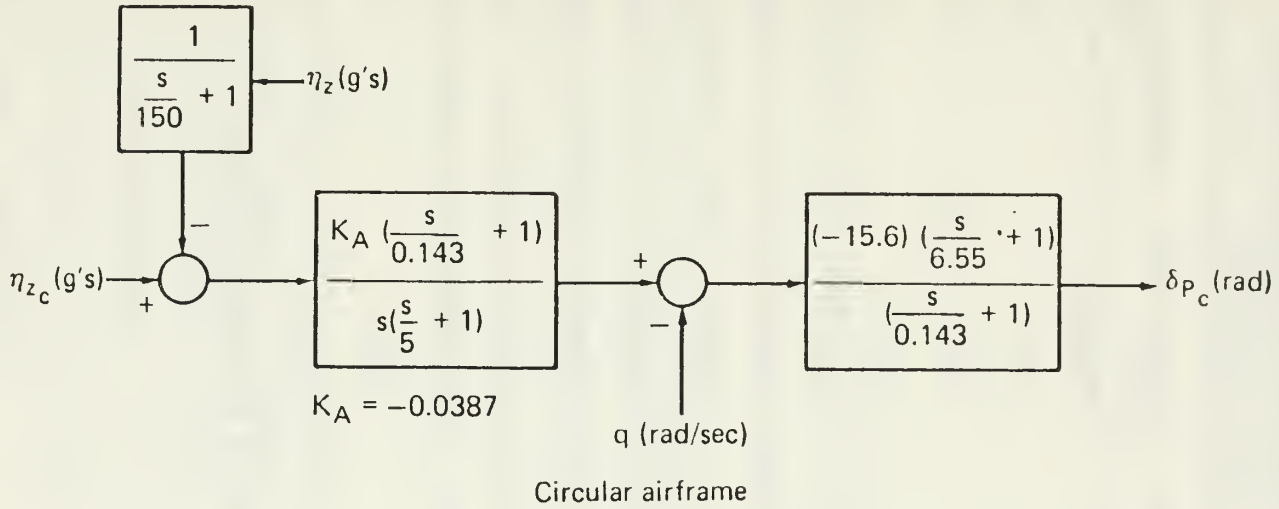

Figure 3.5 Pitch Control Low.

TABLE 3.1

LINEARIZED AERODYNAMIC DERIVATIVES (M=3.95)
FOR CIRCULAR AIRFRAME

	$\alpha=0^\circ$	$\alpha=10^\circ$	$\alpha=20^\circ$
$C_{Y\beta}$	-0.065	-0.082	-0.111
$C_{n\beta}$	-0.025	-0.019	-0.003
$C_{l\beta}$	0	-0.009	-0.020
$C_{Y\delta Y}$	0.021	0.022	0.028
$C_{n\delta Y}$	-0.050	-0.053	-0.062
$C_{l\delta Y}$	0	-0.016	-0.038
$C_{Y\delta R}$	0	-0.009	-0.022
$C_{n\delta R}$	0	0.018	0.044
$C_{l\delta R}$	0.031	0.035	0.044
$C_{N\alpha}$	0.15	0.17	0.22
$C_{N\delta P}$	0.04	0.04	0.05
$C_{m\alpha}$	-0.060	-0.065	-0.118
$C_{m\delta P}$	-0.080	-0.095	-0.115

Reference Center of Gravity (C.G) at 0.6 l

4. Analysis for Circular Airframe

The analysis of the uncoupled pitch channel autopilot is based on the time responses and Bode plots of maneuver plane acceleration, body angular rates and tail incidence angles, obtained by OPTSYS control program of Naval Postgraduate School (NPS), which requires the differential equations to be in the state-space variable format:

$$\dot{\mathbf{X}} = \mathbf{F}\,\mathbf{X} + \mathbf{G}\,\mathbf{U} \qquad \text{(III.B.4-1) to}$$

define the system. In this system the **F** matrix is the open loop dynamics matrix (system or plant) and the **G** matrix is the control matrix. The variable assignements are **X** as the state vector and **U** as the control input vector. It follows that $\dot{\mathbf{X}}$ is the time derivative of **X**.

Using state-space representation of a system, in which the forcing function involves derivatives, the following equations are derived and can be modeled as a tenth order system, for the uncoupled pitch channel :

$$\dot{X}_1 = -150\,X_1 + 150\,X_6 + 705.75\,\delta_p \qquad \text{(III.B.4-4)}$$

$$\dot{X}_2 = X_3 - 1.3531\,n_{zc} + 1.3531\,X_1 \qquad \text{(III.B.4-5)}$$

$$\dot{X}_3 = -5\,X_3 + 6.572\,n_{zc} - 6.572\,X_1 \qquad \text{(III.B.4-6)}$$

$$\dot{X}_4 = X_5 - 59.2637\,\delta_p \qquad \text{(III.B.4-7)}$$

$$\dot{X}_5 = -149.186 \times 10^{-3}\,X_5 - 44.3557\,X_4 + 1.7887\,\delta_p \qquad \text{(III.B.4-8)}$$

$$\dot{X}_6 = X_7 - 701.92 \times 10^{-3}\,\delta_p \qquad \text{(III.B.4-9)}$$

$$\dot{X}_7 = -149.186 \times 10^{-3}\,X_7 - 44.3557\,X_6 - 1043.36\,\delta_p \qquad \text{(III.B.4-10)}$$

$$\dot{\delta}_p = -188.4\,\delta_p + 188.4\,\delta_{pc} \qquad \text{(III.B.4-11)}$$

$$\dot{\delta}_{Pc} = -0.143\ \delta_{Pc} - 2.2308\ X_2 + 2.2308\ X_4 - 340.58\times10^{-3}\ X_3 + 460.839\times10^{-3}\ n_{zc} - 460.839\times10^{-3}\ X_1 + 340.58\times10^{-3}\ X_5 - 20.184\ \delta_p \qquad \text{(III.B.4-12)}$$

$$\dot{n}_z = -(\ X_7 - 887.124\ \delta_p + 886.422\ \delta_{Pc}\ ) \qquad \text{(III.B.4-13)}$$

where the state variables are:

- X_1, X_2 : pitch angular rate state variables
- X_6, X_7 : achived body acceleration state variables
- X_5 : output of acceleration filter
- δ_{Pc} : input command in actuator network
- δ_p : tail incidence angle

Expressing the above equations as a set of first order matrix in the format of (III.B.4-1) the plant and control matrices are:

$$F = \begin{bmatrix} -150 & 0 & 0 & 0 & 0 & 0 & 0 & 0 & 0 & 150 \\ 1.353 & 0 & 1 & 0 & 0 & 0 & 0 & 0 & 0 & 0 \\ -6.572 & 0 & -5 & 0 & 0 & 0 & 0 & 0 & 0 & 0 \\ 0 & 0 & 0 & 0 & 1 & 0 & 0 & -59.26 & 0 & 0 \\ 0 & 0 & 0 & -44.36 & -0.15 & 0 & 0 & 1.789 & 0 & 0 \\ 0 & 0 & 0 & 0 & 0 & 0 & 1 & -0.7019 & 0 & 0 \\ 0 & 0 & 0 & 0 & 0 & -44.36 & -0.1492 & -1043 & 0 & 0 \\ 0 & 0 & 0 & 0 & 0 & 0 & 0 & -188.4 & 188.4 & 0 \\ -0.461 & -2.231 & -0.3406 & 2.231 & 0.3406 & 0 & 0 & -20.18 & -0.143 & 0 \\ 0 & 0 & 0 & 0 & 0 & 0 & -1 & 887.1 & -886.4 & 0 \end{bmatrix}$$

(III.B.4-14)

The control matrix G is following:

$$G = \begin{bmatrix} 0 \\ -1.3531 \\ 6.572 \\ 0 \\ 0 \\ 0 \\ 0 \\ 0 \\ 0.4608 \\ 0 \end{bmatrix} \qquad \text{(III.B.4-15)}$$

where: $U = n_{z_c}$ as control input to the system. (III.B.4-16)

According to the [Ref. 1], using a step input function which represents the "1 gee Command" and a trim angle of attack a_e=0, the time response plots of the state-variables of interest were obtained from the OPTSYS program and are represented at the Figures 3.6, 3.7 and 3.8. Typical performance criteria used to characterize the transient response to the one gee unit step input include overshoot, delay time; rise time, and settling time. The above-mentioned criteria are defined with respect to the step response:

- *Maximum Overshot.* The maximum overshoot is defined as the largest deviation of the output over the step input during the transient state. The amount of maximum overshoot is also used as a measure of the relative stability of the system. The maximum overshoot is represented in this thesis as a percentage of the final value of the step response: that is,

$$\text{percent maximum overshoot} = \frac{\text{max. overshoot}}{\text{final value}} \times 100\% \qquad \text{(III.B.4-17)}$$

- *Delay time.* The delay time is defined as the time required for the step response to reach 50% of its final value.

- *Rise time.* The rise time is defined as the time required for the step response to rise from 10% to 90% of its final value. Frequently the rise time is also refered to as the time constant of the system.

- *Settling time.* The settling time is defined as the time required for the step response to decrease and stay within a specified percentage of its final value. For this thesis is specified arbitrarily at 0.01%.

The four quantities defined above give a direct measure of the transient characteristics of the system to the step input:

a. The pitch normal acceleration (n_z ro N_Z), Figure 3.6, g's vs. time which has:

(1) A 0.5 rise time or time constant.

(2) A minor 0.005 steady state error and 2.2% overshoot.

(3) A 0.28 sec delay time and 2 sec settling time.

b. The pitch angular rate (q or Q), Figure 3.7, rad/sec vs. time, which has:

(1) The maximum body angular rate (-0.17 rad/sec) occurs at 0.28 second when the tail incidence is at 0.02 rad angle of deflection.

(2) From the moment at 0.28 sec the rate increases and reaches at 2 sec its steady-state value (-0.01rad/sec).

(3) The -0.01 rad/sec steady-state constant rate is due to the fact that one has a type zero system and therefore has a finite error to a step input.

c. The pitch tail incidence (δ_p or DP), Figure 3.8, rad vs. time, which has:

(1) Actuator deflection angle 0.05 rad.

(2) Initially and within the 0.28 sec delay time a small transient occurs with an insignificant fluctuation.

(3) An overshoot 1.3% and a 2.0 sec settling time.

The above analysis has revealed that the perfomance of the system is according to the previous mentioned requirements.

Also should be mentioned here that according to the Eigenvalues found executing the OPTSYS program, the continuous open loop system is stable, since the s-plane poles are:

$s_1 = -159.724 + j18.9921$

$s_2 = -159.724 - j18.9921$

$s_3 = -8.29048 + j8.05932$

$s_4 = -8.29048 - j8.05932$

$s_5 = -3.75925 + j2.51463$

$s_6 = -3.75925 - j2.51463$

$s_7 = -0.14393 + j0$

$s_8 = -0.00000425 + j0$

$s_9 = -0.04593 + j6.65959$

$s_{10} = -0.04593 - j6.65959$

5. Design of the Modified Uncoupled Pitch Autopilot

To study reconfigurable flight controls the missile model should be capable of using the set of four available control surfaces to produce the required forces and moments.

To achieve this each control surface (δ_1, δ_2, δ_3, δ_4) is considered as an independent component.

The equations are then coupled so that a component of control surfaces used as a single or pair, will produce the appropriate moments. For example δ_1 deflected at an certain angle, while the other three remained at a zero angle, will produce primarily a rolling moment, and deflected together with δ_2 no roll effect is present, as we will see in Chapter V.

Taking under consideration the convention control surfaces theory of Chapter II., for the B.T.T. missiles, and for the configuration shown in the Figure 3.4, one can easily show, for the continuous pitch autopilot that the input command in the actuator network (δ_{Pc}) can be split up into independent components, using the following equation which compute the deflection inputs to Equation (III.B.4-12). (Also refer to Figures 2.2 and 3.4 which show the control surface positions and corresponding positive deflections).

$$+\delta_{Pc} = (-\delta_1 + \delta_2 - \delta_3 + \delta_4) / 2 \qquad \text{(III.B.5-1)}$$

Replacing the input vector in Equations (III.B.4-11), (III.B.4-12) and (III.B.4-13) with the above Equation and applying the superposition principle, gives the following modified airframe equations:

$$\dot{\delta}_P = -188.4\delta_P + 188.4 \frac{1}{2}(-\delta_1 + \delta_2 - \delta_3 + \delta_4) \qquad \text{(III.B.5-2)}$$

$$\frac{1}{2}(-\dot{\delta}_1 + \dot{\delta}_2 - \dot{\delta}_3 + \dot{\delta}_4) = -0.143 \frac{1}{2}(-\delta_1 + \delta_2 - \delta_3 + \delta_4) - 2.2308X_2 + 2.2308X_4 - 340.58\times10^{-3} X_3 + 460.839\times10^{-3}\eta_{Zc} - 460.839\times10^{-3}X_1 + 340.58\times10^{-3}X5 - 20.184\delta_P \qquad \text{(III.B.5-3)}$$

$$\dot{n}_{Zc} = -(X_7 - 887.124)\delta_p + 886.422\frac{1}{2}(-\delta_1 + \delta_2 - \delta_3 + \delta_4) \quad \text{(III.B.5-4)}$$

In Figure 3.6 the modification of the commanded tail incidence is presented.

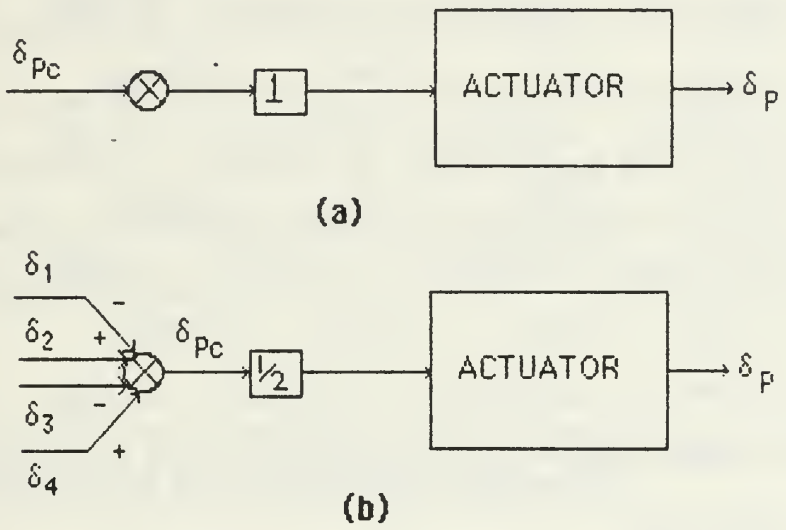

Figure 3.6 (a) Original System; (b) Modified System.

Rearranging the above equations and using the transfer functions of the system for the uncoupled pitch channel, Equations (III.B.4-4 to III.B.4-13), the following equations are derived and can be modeled in a thirteenth order system for the same channel:

$$\dot{X}_1 = -150X_1 + 150n_Z \quad \text{(III.B.5-5)}$$

$$\dot{X}_2 = X_3 - 1.3531n_{Zc} + 1.3531X_1 \quad \text{(III.B.5-6)}$$

$$\dot{X}_3 = -5X_3 + 6.572n_{Zc} - 6.572X_1 \quad \text{(III.B.5-7)}$$

$$\dot{X}_4 = X_5 - 59.2637\delta_p \qquad \text{(III.B.5-8)}$$

$$\dot{X}_5 = -149.186x10^{-3}X_5 - 44.3557X_4 + 1.7887\delta_p \qquad \text{(III.B.5-9)}$$

$$\dot{X}_6 = X_7 - 701.92x10^{-3}\delta_p \qquad \text{(III.B.5-10)}$$

$$\dot{X}_7 = -149.186x10^{-3}X_7 - 44.3557X_6 - 1043.36\delta_p \qquad \text{(III.B.5-11)}$$

$$\dot{\delta}_p = -188.4\delta_p - 94.2\delta_1 + 94.2\delta_2 - 94.2\delta_3 + 94.2\delta_4 \qquad \text{(III.B.5-12)}$$

$$\dot{\delta}_1 = -0.143\delta_1 + 1.1154X_2 - 1.1154X_4 + 0.17029X_3 - 0.23042n_{zc} + 0.23042X_1 - 0.17029X_5 + 10.029\delta_p \qquad \text{(III.B.5-13)}$$

$$\dot{\delta}_2 = -0.143\delta_2 - 1.1154X_2 + 1.1154X_4 - 0.17029X_3 + 0.23042n_{zc} - 0.23042X_2 + 0.17029X_5 - 10.092\delta_p \qquad \text{(III.B.5-14)}$$

$$\dot{\delta}_3 = -0.143\delta_1 + 1.1154X_2 - 1.1154X_4 + 0.17029X_3 - 0.23042n_{zc} + 0.23042X_1 - 0.17029X_5 + 10.029\delta_p \qquad \text{(III.B.5-15)}$$

$$\dot{\delta}_4 = -0.143\delta_4 - 1.1154X_2 + 1.1154X_4 - 0.17029X_3 + 0.23042n_{zc} - 0.23042X_1 + 0.17029X_5 - 10.029\delta_p \qquad \text{(III.B.5-16)}$$

$$\dot{n}_z = -X_7 + 887.124\delta_p + 443.211\delta_1 - 443.211\delta_2 + 443.211\delta_3 - 443.211\delta_4 \qquad \text{(III.B.5-17)}$$

We thus have a multiple-input-multiple-output (MIMO) system with the following order:

- $\dot{\mathbf{X}}$: 13x1, the time derivative of $\mathbf{X}$ matrix.
- $\mathbf{F}$: 13x13, the open loop dynamics matrix or plant.
- $\mathbf{X}$: 13x1, the variables assignements matrix.
- $\mathbf{G}$: 13x5, the control distribution matrix.
- $\mathbf{U}$: 5x1, the control input matrix.

The above plant control and output matrices are presented at the Appendix A of this thesis.

6. Analysis and Comparison with the Original System

Applying the same step input function as in section III.B.4, which represents the "1 gee command", and zero degrees deflection command for the four control surfaces (i.e., δ_{1C}, δ_{2C}, δ_{3C}, δ_{4C} = 0) the time response plots of the following state-variables of interest are obtained and presented in the Figures 3.10 through 3.13.

The performance of the system (N_z, q, δ_p) as shown in Figures 3.10 to 3.12 is the same as that shown in Figures 3.6 through 3.8.

In Figure 3.13 is shown the time response of the control surfaces deflection angle, for the input of an acceleration equal to 1 gee command.

Deflections (δ_1, δ_2, δ_3, δ_4 or D's), Figure 3.13, rad vs. time, which has:

(1) The δ_1 and δ_3 have the same sign (negative), as it was expected according to the sign convention of Figure 2.2.

(2) The δ_2 and δ_4, have the same response as above but with a positive sign.

(3) Insignificant overshoot.

(4) A 2 seconds settling time.

In the same Figure 3.13 the deflection of the control surfaces is illustrated. The presented deflection is the required position of each surface in order to achive the commanded one gee acceleration (downwards).

We procceed now to the analysis of the impaired control surfaces for the modified system.

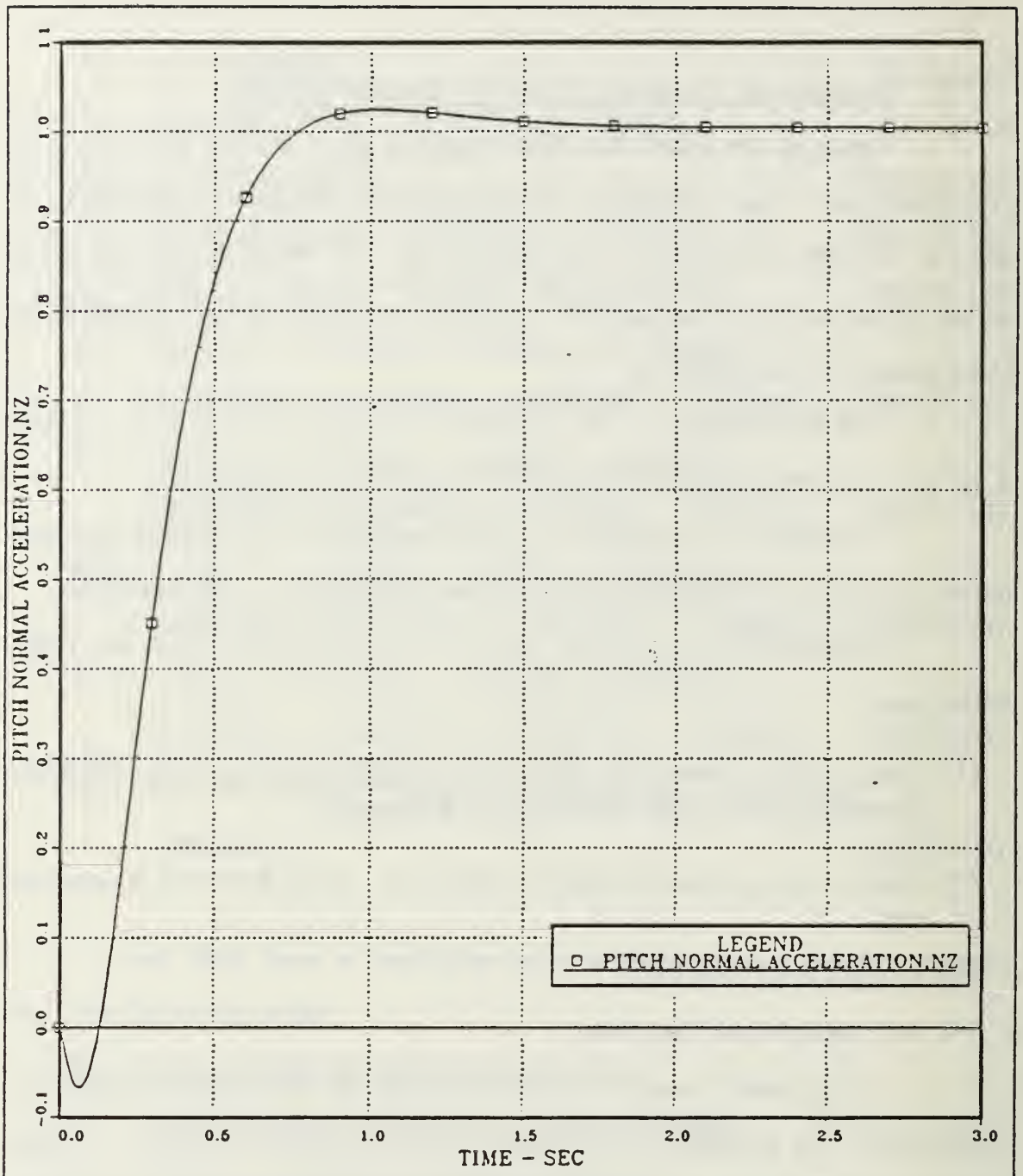

Figure 3.7 Pitch Normal Acceleration vs. Time; Uncoupled Pitch Channel; Continuous Open Loop System; a_e = 0; Step Input = 1 g's.

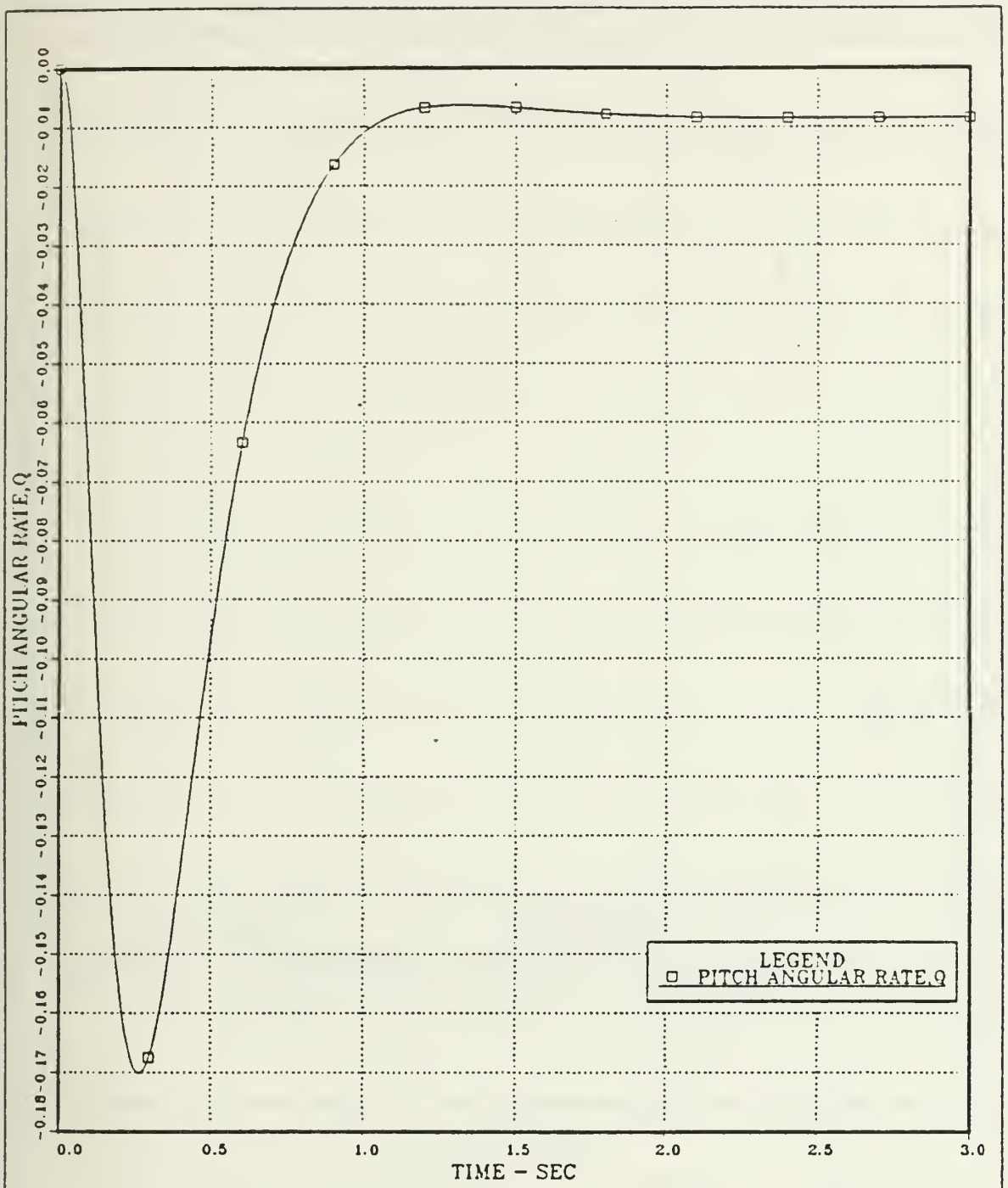

Figure 3.8 Pitch Angular Rate vs.Time; Uncoupled Pitch Channel; Continuous Open Loop System; a_e =0; Step Input = 1g's.

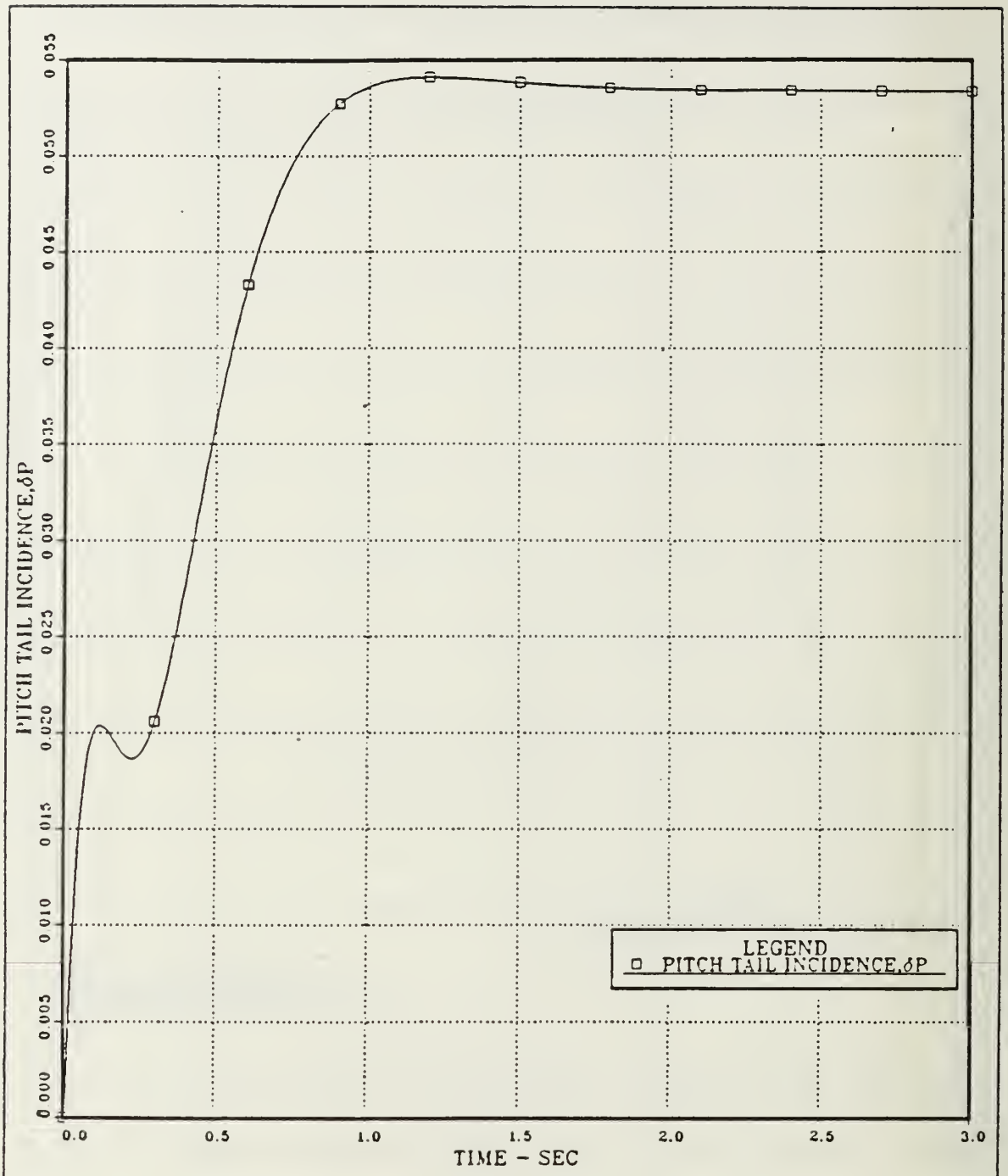

Figure 3.9 Pitch Tail Incidence vs. Time; Uncoupled Pitch Channel; Continuous Open Loop System; a_c=0; Step Input = 1 g's.

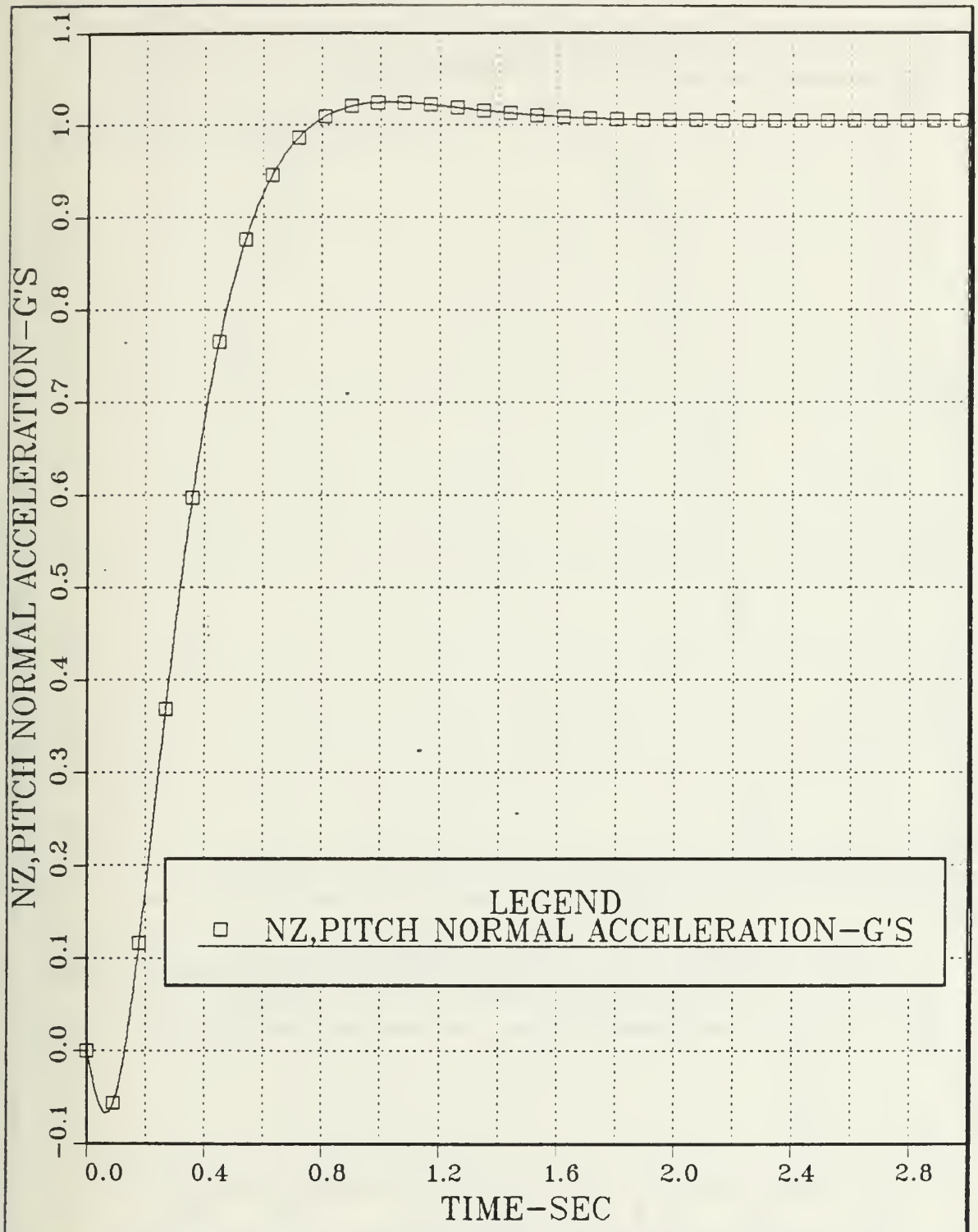

Figure 3.10 Pitch Normal Acceleration vs. Time; Uncoupled Pitch Channel; Unimpaired Open Loop System; a_e=0; Step Input: n_{zc}=1 g's and δ_{1C}, δ_{2C}, δ_{3C}, δ_{4C} = 0 degrees.

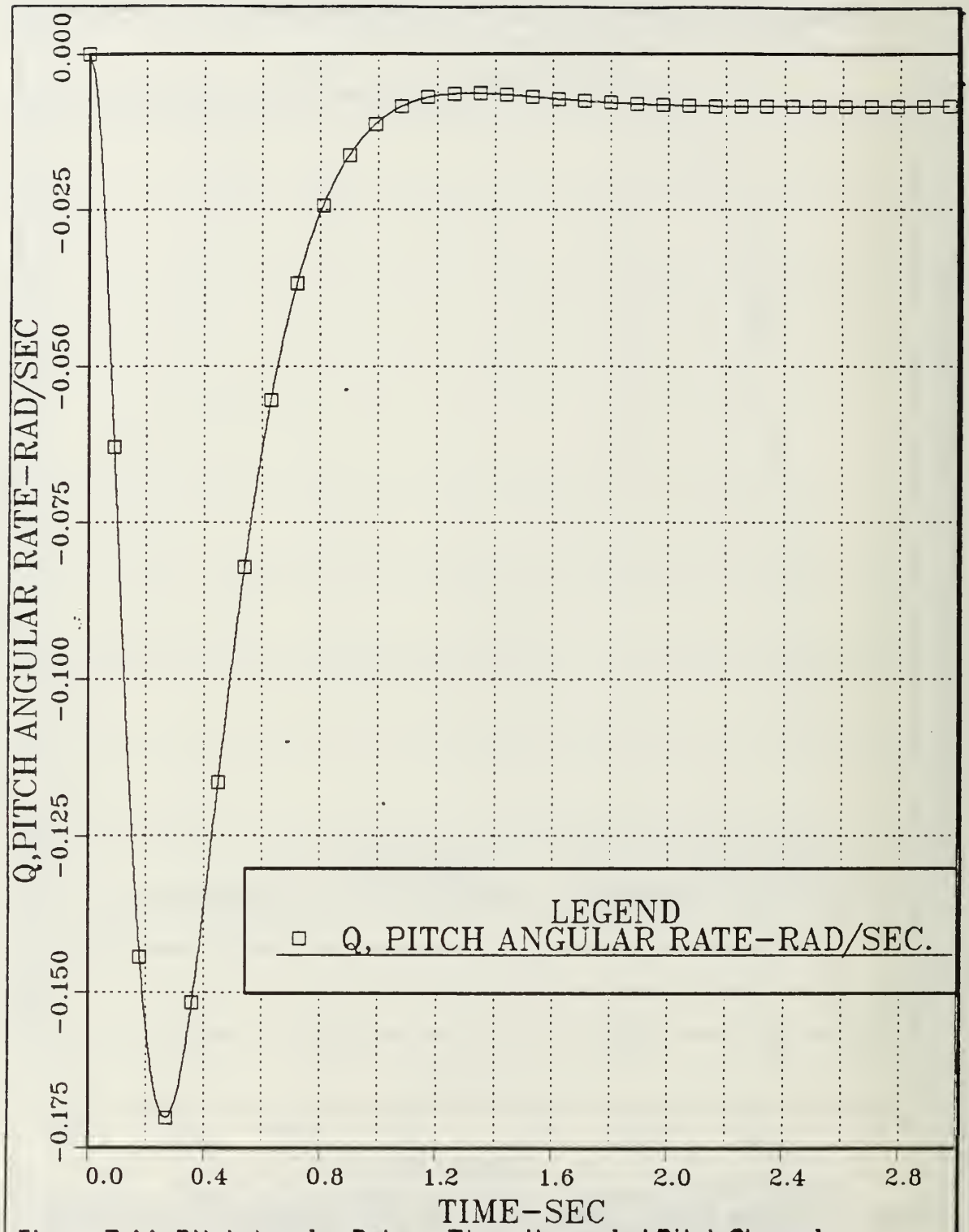

Figure 3.11 Pitch Angular Rate vs.Time; Uncoupled Pitch Channel; Unimpaired Open Loop System; a_e=0; Step Input: n_{zc}=1 g's and δ_{1c}, δ_{2c}, δ_{3c}, δ_{4c} = 0 degrees.

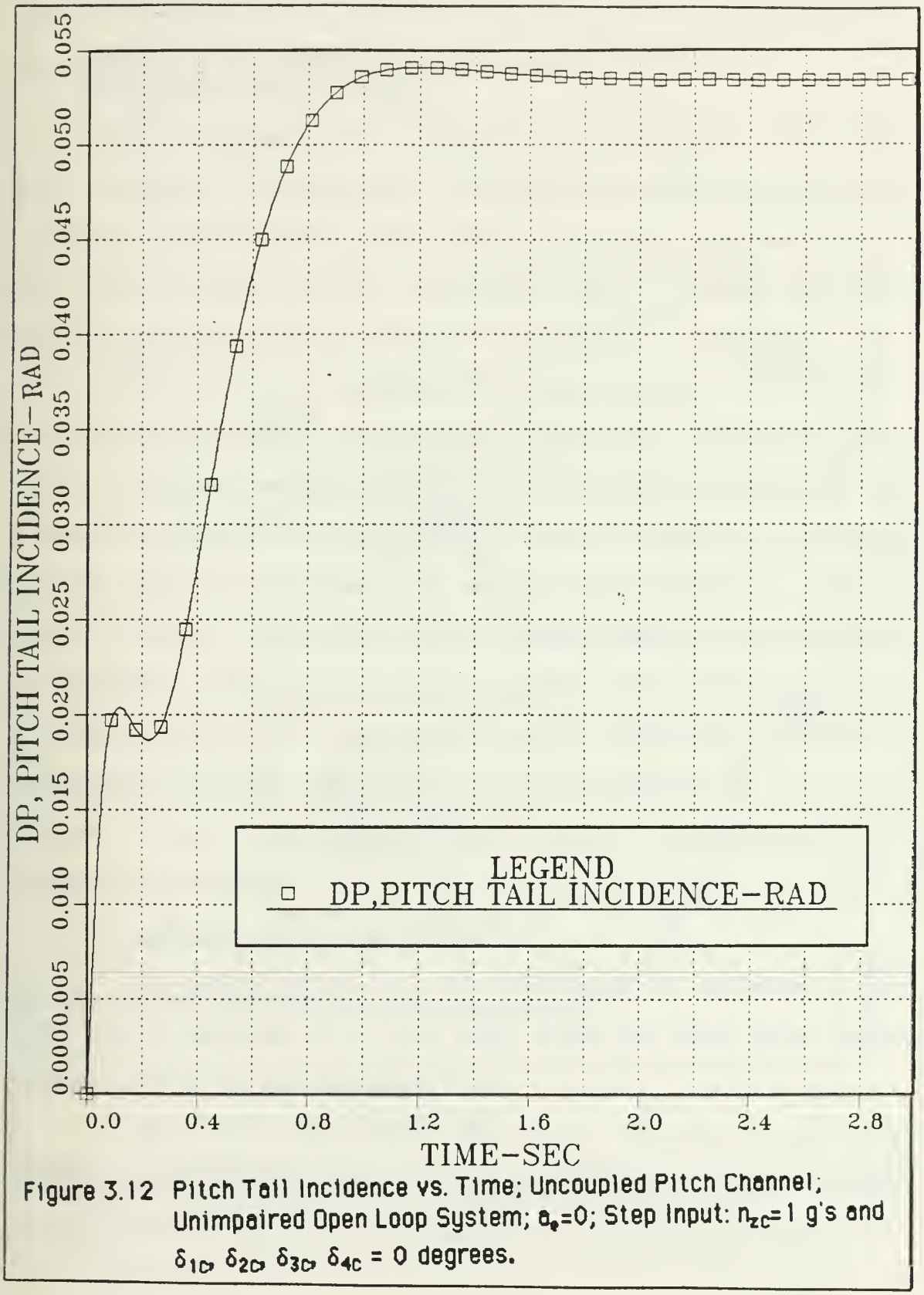

Figure 3.12 Pitch Tail Incidence vs. Time; Uncoupled Pitch Channel; Unimpaired Open Loop System; a_e=0; Step Input: n_{zc}= 1 g's and δ_{1c}, δ_{2c}, δ_{3c}, δ_{4c} = 0 degrees.

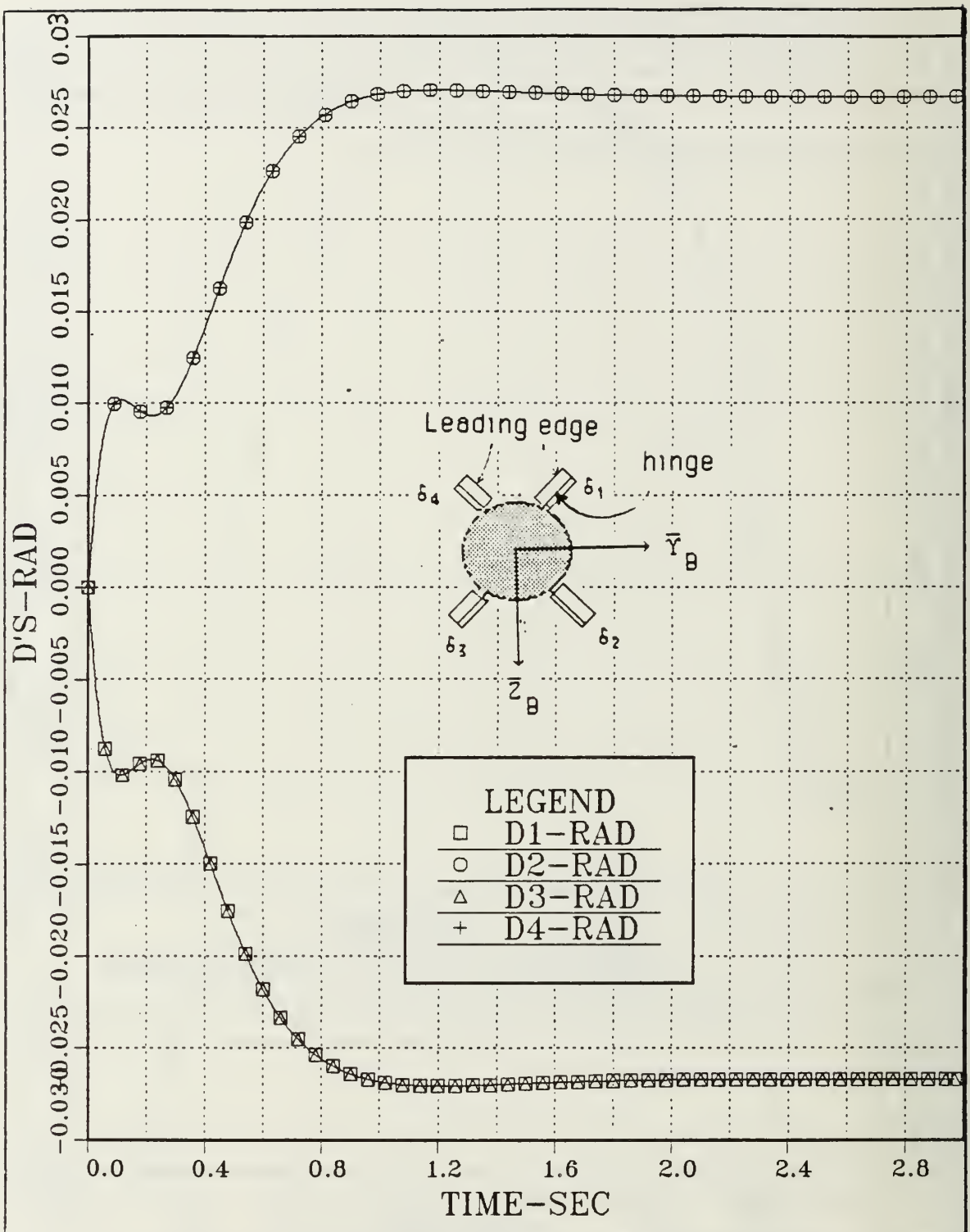

Figure 3.13 Control Surfaces Deflections vs. Time; Uncoupled Pitch Channel; Unimpaired Open Loop System; a_ϕ=0; Step Input: n_{zc}=1 g's and δ_{1c}, δ_{2c}, δ_{3c}, δ_{4c} = 0 degrees.

C. CONTROL EFFECTIVENESS DUE TO THE CONTROL SURFACES IMPAIRMENT AND COMPARISON

The time response plots of the system are obtained in this section for two types of damages. The first type is the locked or hard over surface at a small angle and the second type includes the inoperativity of one, two or three actuators. The second type of damage could also represent the destruction of the control surface(s), i.e., shot away.

Note that the first phase of the design approach for the CBTT autopilot was to design each channel independently with all coupling between channels removed. Sufficient high frequency attennuation was added for actuator and missile design so that the resulting missile body angular rates and control surfaces motion would represent a practical missile design. A relationship was established among the relative speeds of response of the uncoupled channels in order to meet CBTT requirements. The cross-coupling due to control surfaces impairment between the longitudinal and lateral motion of the missile is ignored when each control channel is treated independently. Cross-coupling of the controls is thus considered in Chapter V.

1. Hard Over One Control Surface

One control surface (δ_1), was selected to be deflected or hard over, i.e., it remained at a fixed angle while the other three control surfaces have a variable deflection angle.

The control input was a step input of one gee in the normal acceleration as in the original and unimpaired models. For the damaged control surface (δ_1) a hard over deflection of 0.2 rad was considered. The

time response plots of the state-variables of interest were obtained and analyzed with the performance criteria as defined in section (III.B.4):

a. Pitch normal acceleration (n_z or N_Z), Figure 3.14, g's vs. time, which has:

(1) Initially and with a fast response, the missile body tends to go upwards reaching a 0.6 gee acceleration. This is caused by the fact that at the beginning of the command the damaged surface was deflected at a +0.2 rad angle of deflection while the other three were at their steady position. Then the missile goes downwards until the -1.25 gee acceleration is achieved. This is due to the deflection of the unimpaired surfaces which are commaned in such a way as to counteract the damaged (δ_1) surface. From this point (0.2 sec) the acceleration rises constantly in order to achieve the one gee command.

(2) A rise time 0.75 seconds and a negligible overshoot.

(3) A delay time about 0.5 sec

(4) Steady-state error 0.005% which is insignificant.

b. The pitch angular rate (q or Q), Figure 3.15, rad/sec vs. time, which has:

(1) Initially and due to the fact that δ_1 is locked at a positive angle of 0.2 rad, to achieve the acceleration response, the required body angular rate the first tenth of the second increases very fast to 0.48 rad/sec. Then it begins to decrease crossing the zero rate at 0.2 sec, corresponding to the max decceleration (-1.25 gee's). Then it changes direction for the next 0.2 sec until the value of -0.38 rad/sec is achieved. From this point the rate is increased again until the constant value of -0.01 rad/sec is achieved at the settling time 1.4 sec.

(2) The initial increase of the rate is due to the produced pitch moment caused by the deflection of the damaged control surface while the other three are at their steady position.

c. Pitch tail incidence (δ_p or DP), Figure 3.16, rad vs. time which has:

(1) To achieve the acceleration response and due to the fact that δ_1 is locked at an angle of 0.2 rad, initally more control surface deflection is required (-0.13 rad). At 0.2 sec, when the acceleration begins to increase and the angular rate is zero, the tail incidence has the positive angle of 0.03 rad and a fluctuation begins before being stabilized at a constant angle of 0.06 rad.

(2) Settling time equal to 1.8 sec.

d. Deflections (δ_1, δ_2, δ_3, δ_4 or D's), Figure 3.17, rad vs. time.

This Figure illustrates the time response of the deflection of the four control surfaces,when one of them (δ_1) is locked at an angle of 0.2 rad, in order to achieve the acceleration response. Initially while δ_2, δ_3 and δ_4 control surfaces have zero angle of deflection, δ_1 is already at the 0.2 angle. Then δ_2 and δ_4 are deflected at a positive angle 0.17 rad and δ_3 at a negative 0.17 rad, according to the sign convention shown in Figure 2.2.

A comparison between Figure 3.17 and 3.13 of the unimpaired system, shows that to achieve the acceleration response the impaired system requires more control surface deflection.

Finally to cover completely this class of impairment, the case of a negative angle (-0.2 rad) at the δ_1 surface is examined. The time response of the same state variables are obtained and analyzed.

a. Pitch normal acceleration (n_z or N_Z), Figure 3.18, g's vs. time, which has:

(1) Initially and with a fast response, the missile body tends to go downwards reaching a 0.6 gee acceleration. This is caused by the

fact that at the beginning of the command the damaged surface was deflected at a -0.2 rad angle of deflection while the other three were at their steady position. Then the missile goes upwards until the +1.75 gee acceleration is achieved. The produced overshoot is due to the deflection of the unimpaired surfaces which are commanded in such a way as to counteract the damaged (δ_1) surface. From this point (0.3 sec) the acceleration deacreases constantly in order to achieve the one gee command.

(2) A small 0.18 second rise time (reason for the big overshoot).

(3) A delay time about 0.1 sec

(4) Steady-state error 0.005%.

b. The pitch angular rate (q or Q), Figure 3.19, rad/sec vs. time, which has:

(1) Initially and due to the fact that δ_1 is locked at a negative angle of -0.2 rad the required body angular rate the first tenth of the second decreases very fast to 0.68 rad/sec. Then it begins to increase crossing the zero rate at 0.3 sec, corresponding to the max decceleration (1.75 gee's), and it changes direction for the next 0.5 sec until the value of 0.13 rad/sec is achieved. From this point the rate is decreased again until the constant value of -0.01 rad/sec is achieved at 1.8 sec settling time .

(2) The big overshoot of the rate is due to the produced pitch moment caused by the deflection of the damaged control surface while the other three are at their steady position.

c. Pitch tail incidence (δ_p or DP), Figure 3.20, rad vs. time which has:

(1) To achieve the acceleration response and due to the fact that δ_1 is locked at a negative angle of -0.2 rad, initally more control surface deflection is required (about 0.16 rad). At 0.3 sec, when the acceleration begins to decrease and the angular rate is zero, the tail incidence has the positive angle of 0.01 rad. A fluctuation begins before the deflection being stabilized at a constant angle of 0.06 rad.

(2) Settling time equal to 1.8 sec.

d. Deflections (δ_1, δ_2, δ_3, δ_4 or D's), Figure 3.21, rad vs. time.

This Figure illustrates the time response of the deflection of the four control surfaces, when one of them (δ_1) is locked at a negative angle of -0.2 rad, in order to achieve the acceleration response. Initially and when the δ_2, δ_3 and δ_4 control surfaces have zero angle of deflection δ_1 is already at the -0.2 angle. Then δ_2 and δ_4 are deflected at a negative -0.09 rad angle and δ_3 at a positive 0.09 rad.

A comparison between Figure 3.21 and 3.17 indicates that when the surface δ_1 is hard over at a negative angle:

(1) The undamaged control surfaces in order to counteract the failure and achieve the commanded acceleration, are deflected at a smaller angle.

(2) The undamaged control surfaces are commanded to turn at angles with opposite sign comparing with those in Figure 3.17 (δ_1 positively hard over).

2. Damage One Control Surface

The δ_1 control surface was selected to simulate the inoperative actuator. The corresponding state variable δ_1 was therefore set equal to zero. The step input of one gee remained the same. The initial condition on the control surface was set at zero. This type of damage could also represent the distruction of the control surface.

For the above case the time response plots of the state variables of interest were obtained and analyzed according to the defined performanse criteria in Section (III.B.4). Later, in Section 5, a comparison

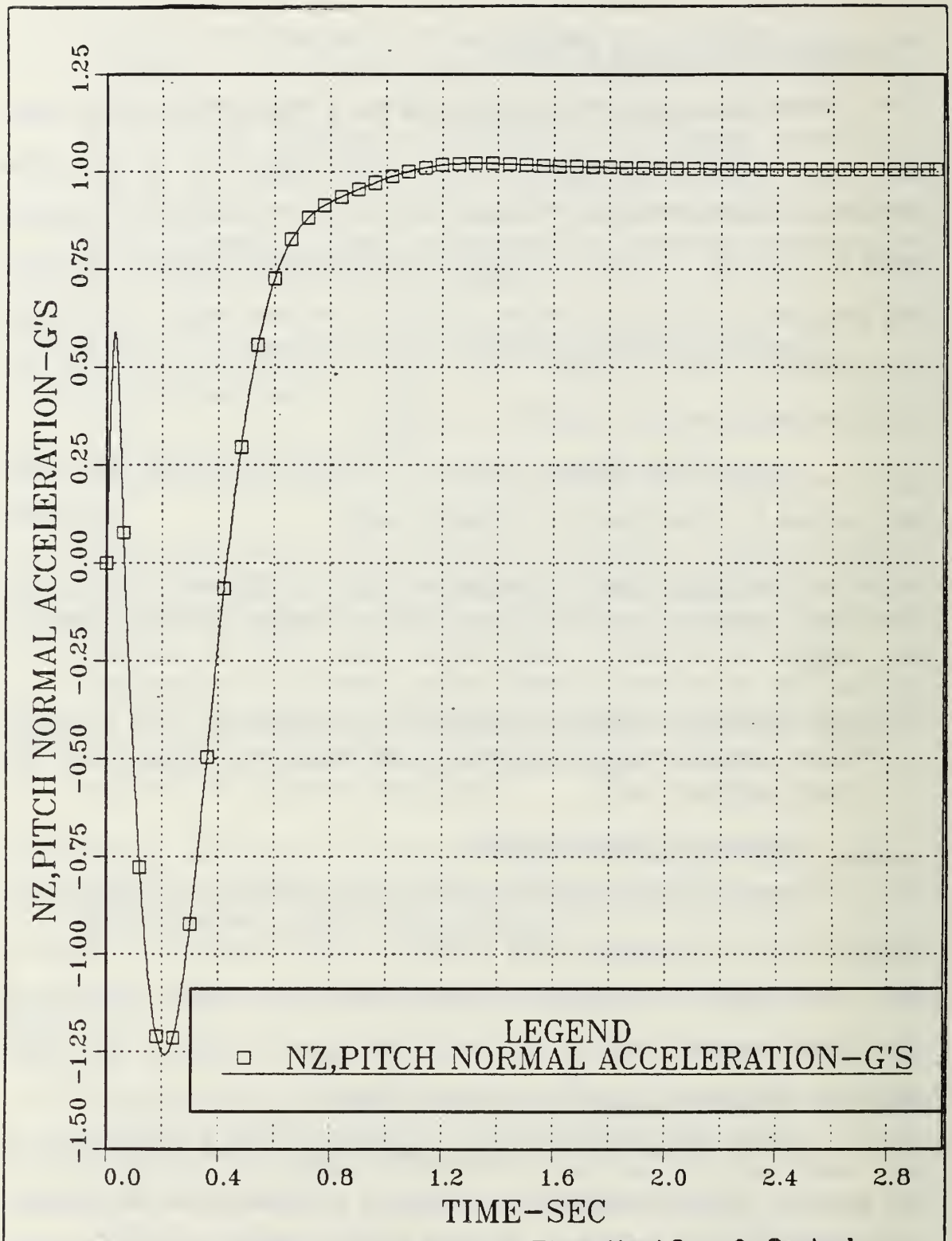

Figure 3.14 Pitch Normal Acceleration vs. Time; Hard Over δ_1 Control Surface; a_8=0; Step Input: n_{zc}= 1gee, δ_{1c}=0.2 rad, δ_{2c}, δ_{3c}, δ_{4c}=0.

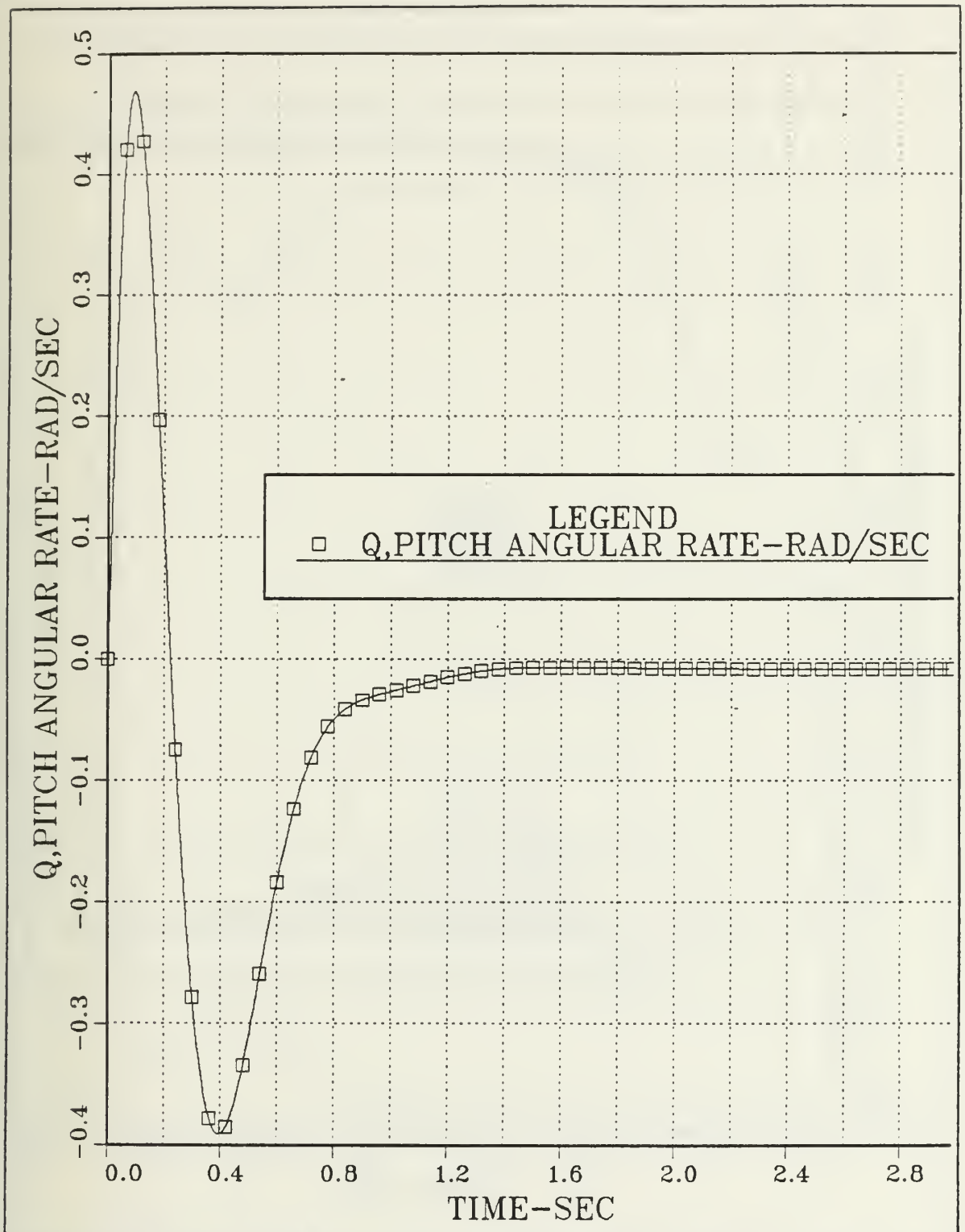

Figure 3.15 Pitch Angular Rate vs.Time; Hard Over δ_1 Control Surface; a_s=0; Step Input: n_{zc}=1 gee, δ_{1c}=0.2 rad, δ_{2c}, δ_{3c}, δ_{4c}=0.

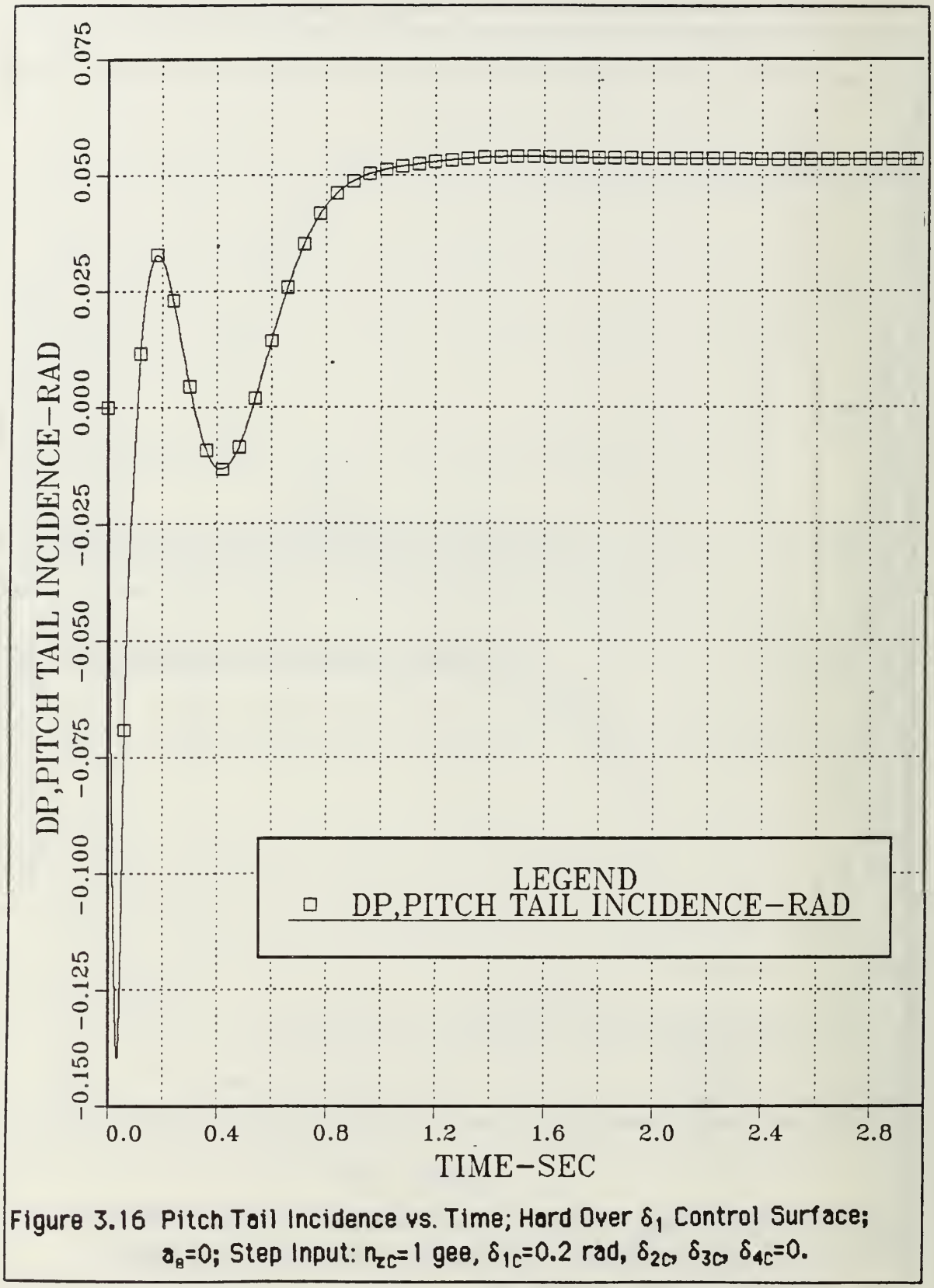

Figure 3.16 Pitch Tail Incidence vs. Time; Hard Over δ_1 Control Surface; a_s=0; Step Input: n_{zc}=1 gee, δ_{1c}=0.2 rad, δ_{2c}, δ_{3c}, δ_{4c}=0.

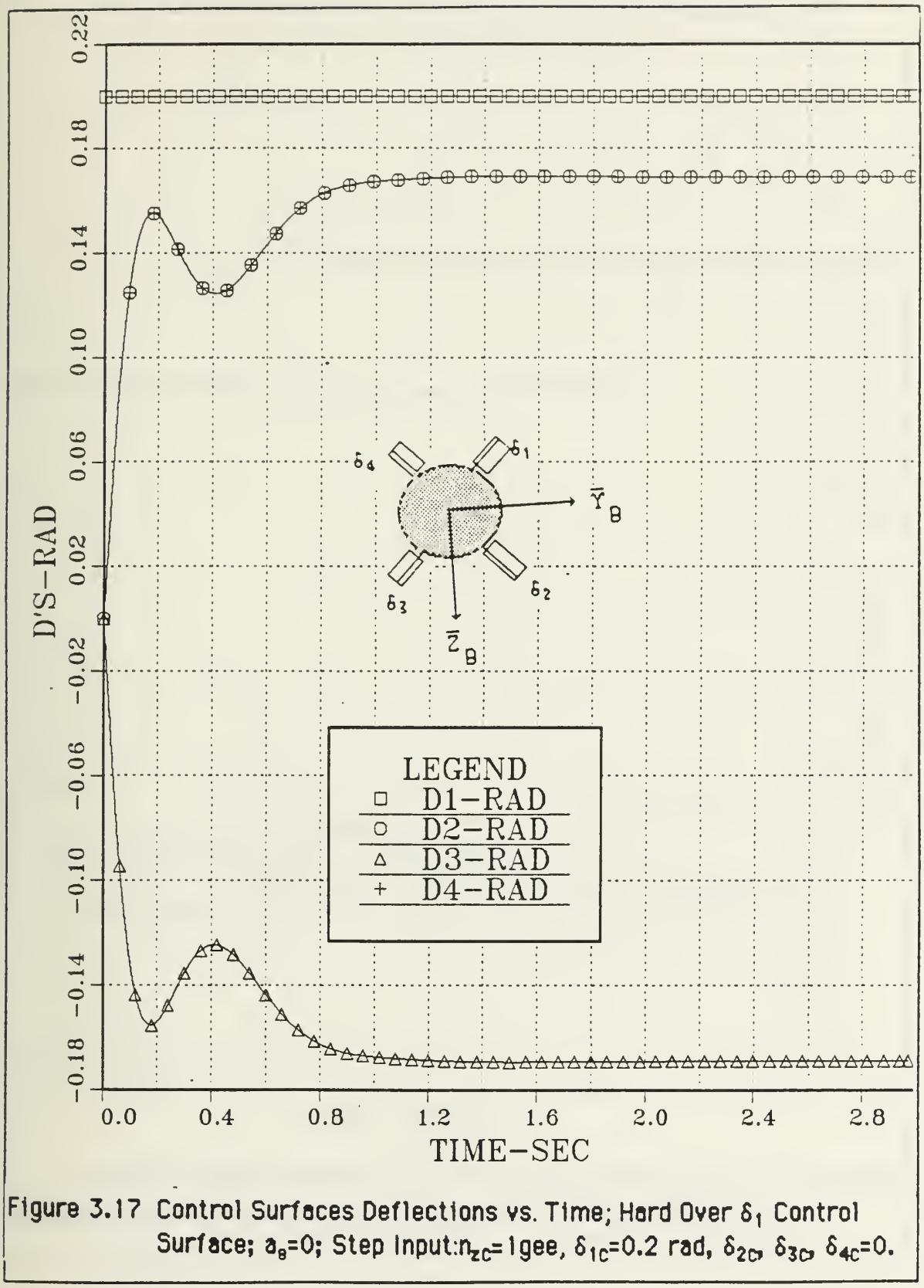

Figure 3.17 Control Surfaces Deflections vs. Time; Hard Over δ_1 Control Surface; a_θ=0; Step Input:n_{zc}= 1gee, δ_{1C}=0.2 rad, δ_{2C}, δ_{3C}, δ_{4C}=0.

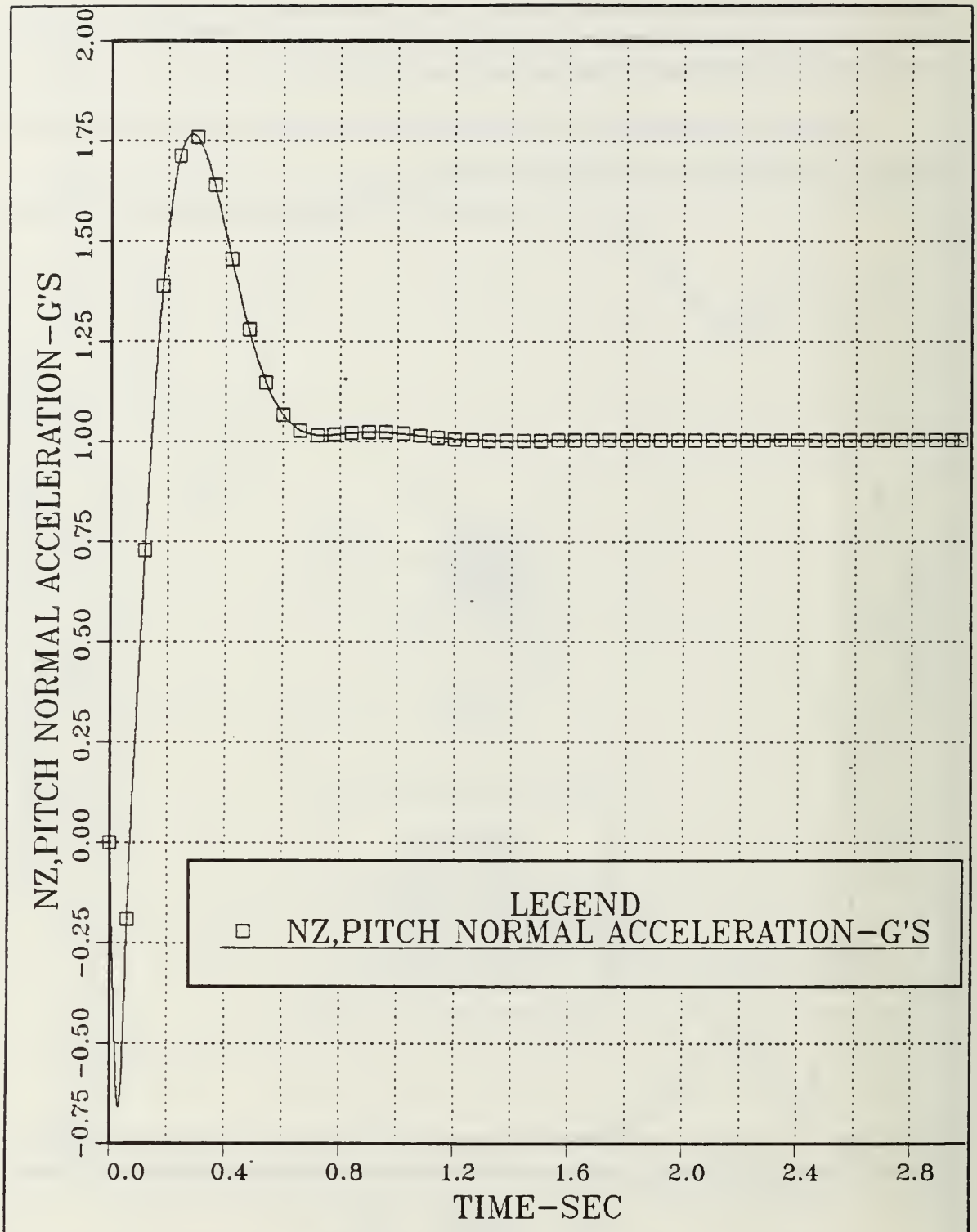

Figure 3.18 Pitch Normal Acceleration vs. Time; Hard Over δ_1 Control Surface; a_s=0; Step Input: n_{zc}=1 gee, δ_{1c}=-0.2 rad, δ_2, δ_3,δ_{4c}=0.

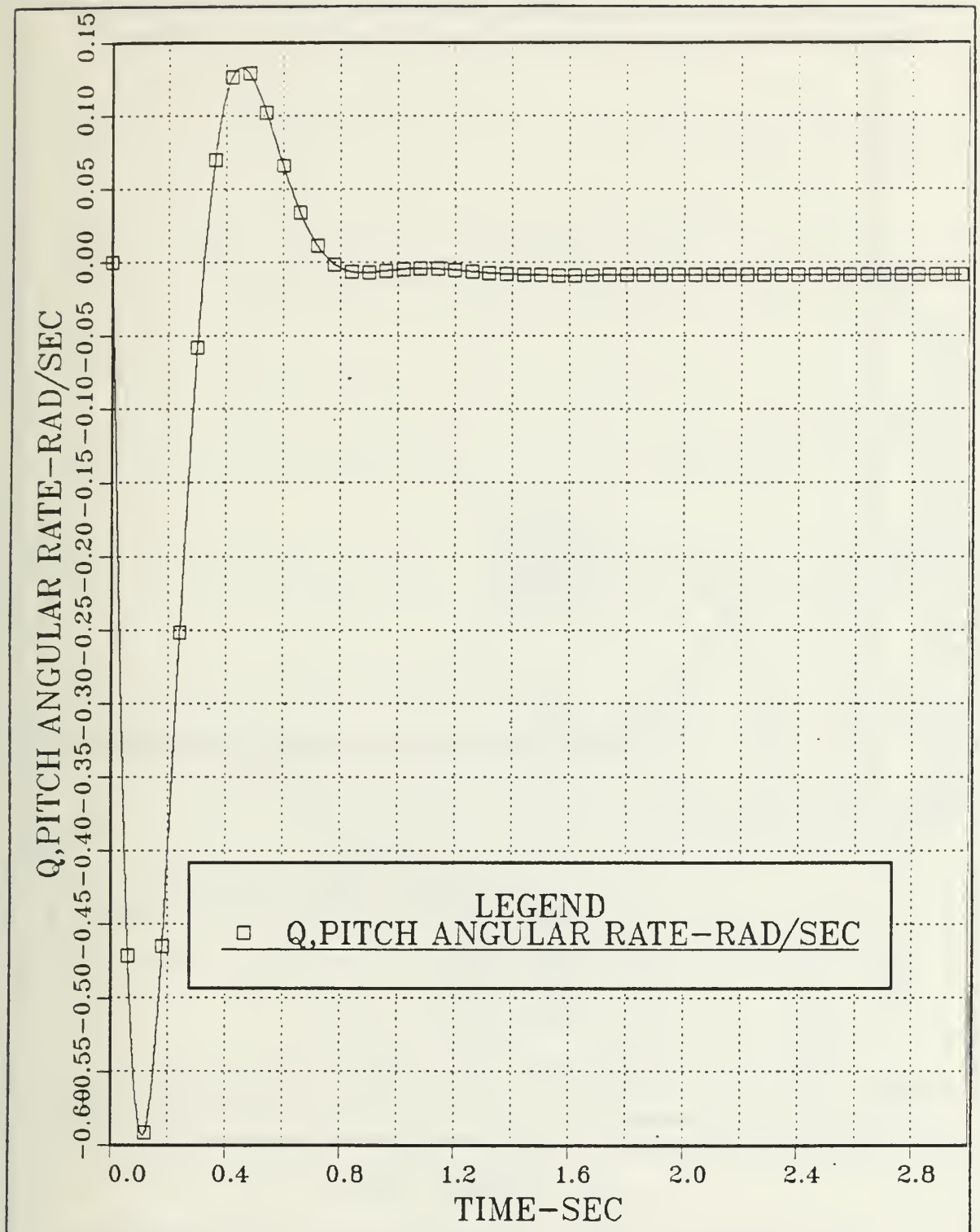

Figure 3.19 Pitch Angular Rate vs.Time; Hard Over δ_1 Control Surface; a_e=0; Step Input: n_{zc}=1 gee, δ_{1c}=-0.2 rad, δ_{2c}, δ_{3c}, δ_{4c}=0.

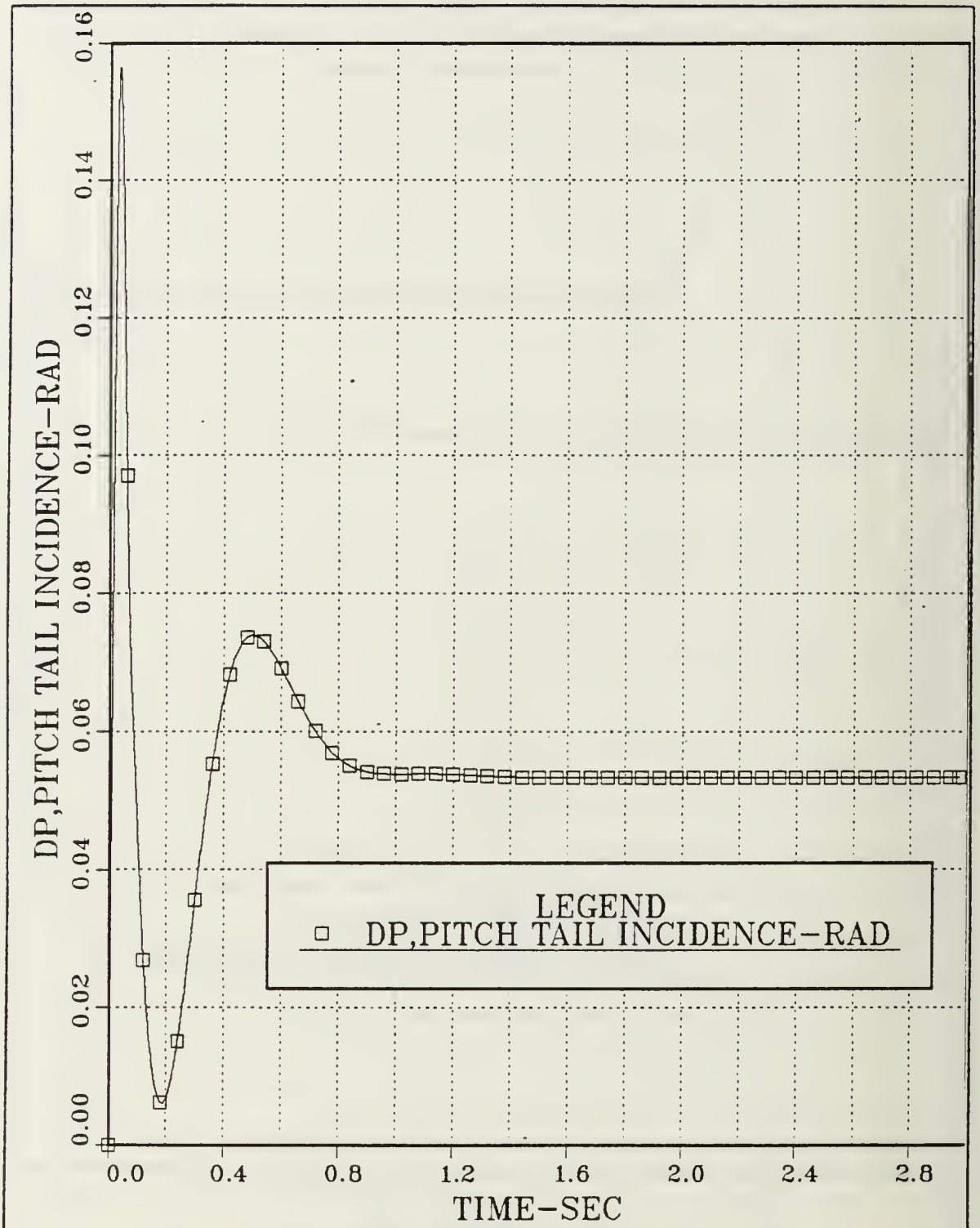

Figure 3.20 Pitch Tail Incidence vs. Time; Hard Over δ_1 Control Surface; a_s=0; Step Input: n_{zc}=1 gee, δ_{1c}=-0.2 rad, δ_{2c}, δ_{3c}, δ_{4c}=0.

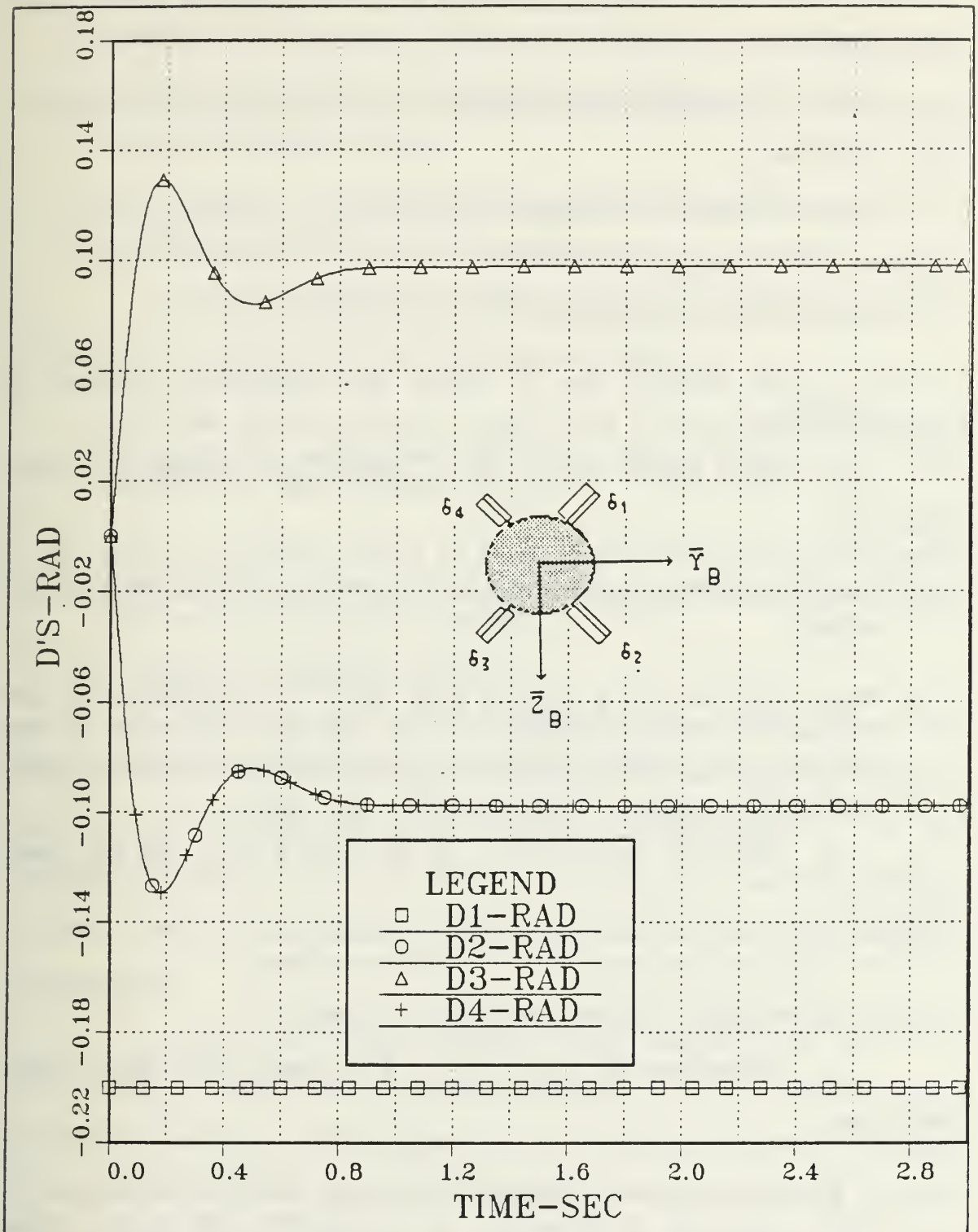

Figure 3.21 Control Surfaces Deflections vs. Time; Hard Over δ_1 Control Surface; a_s=0; Step Input: n_{zc}=1 gee, δ_{1C}=-0.2 rad, δ_2, δ_3, δ_4=0.

between the different types of damages and the unimpaired system was performed.

a. Pitch normal acceleration (n_Z or N_Z), Figure 3.22, g's vs. time, which has:

(1) Time constant or rise time 0.41 seconds.

(2) A 0.005% steady state error.

(3) Minor overshoot and delay time 0.35 sec and

(4) A 1.6 sec settling time at which the acceleration response is achieved.

b. Pitch angular rate (q or Q), Figure 3.23, rad/sec vs. time, which has:

(1) A maximum body angular rate of 0.17 rad/sec is achieved at 0.3 second.

(2) Minor overshoot and a settling time equal to 1.6 after which the angular rate remains constant at -0.01 rad/sec. This is due to the fact that the transfer function q/δ_P (Equation III.B.3-1) is a type zero system and has a finite error to a step input.

c. Pitch tail incidence (δ_P or DP), Figure 3.24, rad vs. time, which has:

(1) A 0.054 rad command from the actuator network.

(2) A 0.4 sec delay time and negligible overshoot.

d. Deflections (δ_1, δ_2, δ_3, δ_4 or D's), Figure 3.25, rad vs. time, which has:

(1) A positive deflection angle of 0.035 rad for the δ_2 and δ_4 actuators while the δ_3 is deflected at a negative and equal angle (-0.035 rad), and δ_1 as damaged remains constantly at zero.

(2) A 1.6 sec settling time for each of the unimpaired surfaces.

(3) A rise time equal to 0.7 sec and minor overshoot correspondingly for the undmaged surfaces.

(4) The deflection angle of the unimpaired control surfaces has a pitching moment effect on the system.

A comparison between the deflection angle in Figures 3.13, 3.17, 3.21, and 3.25 indicates that for the same step input:

(1) When one control surface is inoperative or shot away the system commands the undamaged surfaces at larger angles than those obtained with the unimpaired system.

(2) When one control surface is inoperative or shot away the system commands the undamaged surfaces at smaller angles (in comparison with the hard over type of damage).

3. Damage Two Control Surfaces

In this case two control surfaces, on the same side of the missile were considered damaged (δ_1 and δ_2). The two state variables δ_1 and δ_2 were therefore set equal to zero. The step input of one gee remained the same. The initial condition on the control surfaces was set at zero. Then the time response plots of the state variables were obtained and analyzed.

a. Pitch normal acceleration, Figure 3.26, which has a 0.6 rise time, 0.38 sec delay time and 0.005% steady state error. Note the faulty behavior at the start of the response (0 to 0.15 sec). Because the system is a nonminimum phase system (i.e., a zero lies in the right-half s plane) the transient response starts out in the opposite direction to the input i.e., there is an inherent delay in the transient response of the system.

b. Pitch angular rate, Figure 3.27, which has a maximum rate of -0.16 rad/sec at 0.3 sec. Then increases until the constant negative rate (-0.01 rad/sec) is achieved at 1.3 seconds.

c. Pitch tail incidence, Figure 3.28, which has a 0.8 sec rise time and 0.3 sec delay time. The command from the actuator network is 0.054 rad which is achieved at 1.6 sec settling time.

d. Deflections (δ_1, δ_2, δ_3, δ_4 or D's), Figure 3.29, in which the two damaged control surfaces (δ_1 and δ_2) remain always at zero (damaged) and the two others opposite deflected at the angle of 0.053 rad angle after a lapse time of 1.6 sec. Note that for this system with two impaired control surfaces more angle of deflection is required (in comparison with the system having one actuator shot away).

4. Damage Three Control Surfaces

In the last case three of the control surfaces δ_1, δ_2 and δ_3 were damaged or inoperative.

With a step input of one gee's for the commanded normal acceleration as in the unimpaired and other type damaged models, the plots of the state variables of interest were obtained and analyzed.

Figures 3.30 through 3.33 illustrate the response of the output variables. Figure 3.30 shows that the commanded one gee acceleration can still be achieved in the absense of three control surfaces (δ_1, δ_2, δ_3). However, some oscilation is evident into the response. The loss of the surfaces has produced a more lightly damped system as evidenced in Figures 3.30 through 3.33. The oscillatory and convergent behavior of the pitch rate and the undamaged surface (δ_4), shown in Figures 3.31 and 3.33,

illustrate how the surface attempt to "fill in" for the absence of the inoperative control surfaces. Specifically the response of the pitch normal acceleration (Figure 3.30) has:

(1) A 1.01 sec time constant.

(2) A 0.38 sec delay time and

(3) A 3.0 sec settling time at which the steady-state value of the commanded acceleration is achieved.

A comparison with the response of the corresponding deflection of the unimpaired system (Figure 3.13) and the other inoperative cases, Figures 3.21, 3.25 and 3.29, indicates that as the number of the inoperative control surfaces increases, the deflection of the undamaged actuator(s) also increases and more time is required to achieve the steady-state value.

5. Comparison with the Unimpaired System

In this section a performance comparison of each type of impairment with the undamaged system is performed and an analysis of their corresponding time response plots is presented.

In order to use the N.P.S. EASYPLOT program the state variables had to be input as data. This was accomplished by writing a computer program (Appendix D).

With the above data Figure 3.34 is obtained. This corresponds to pitch normal acceleration (n_z or NZ) for the unimpaired, hard over δ_1, and inoperative or shoot away one or more control surfaces, configurations.

The hard over case shows greater excursion in the normal acceleration with a peak value of -1.25 gee's at 0.2 sec being achieved.

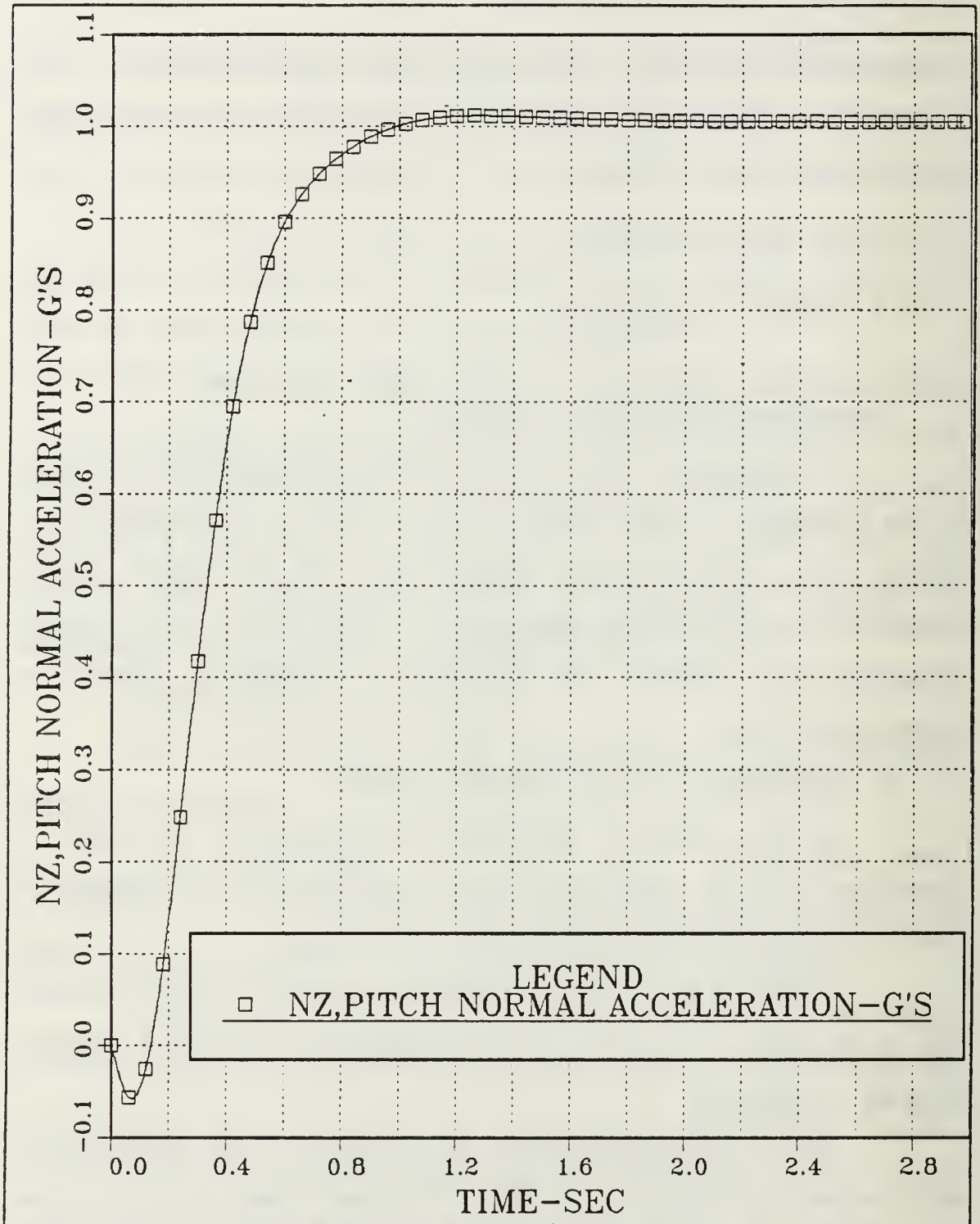

Figure 3.22 Pitch Normal Acceleration vs. Time;
Inoperative δ_1 Control Surface; a_e=0;
Step input: n_{Zc} =1 gee, δ_{1c} = 0.2, δ_{2c}, δ_{3c}, δ_{4c} = 0 rad.

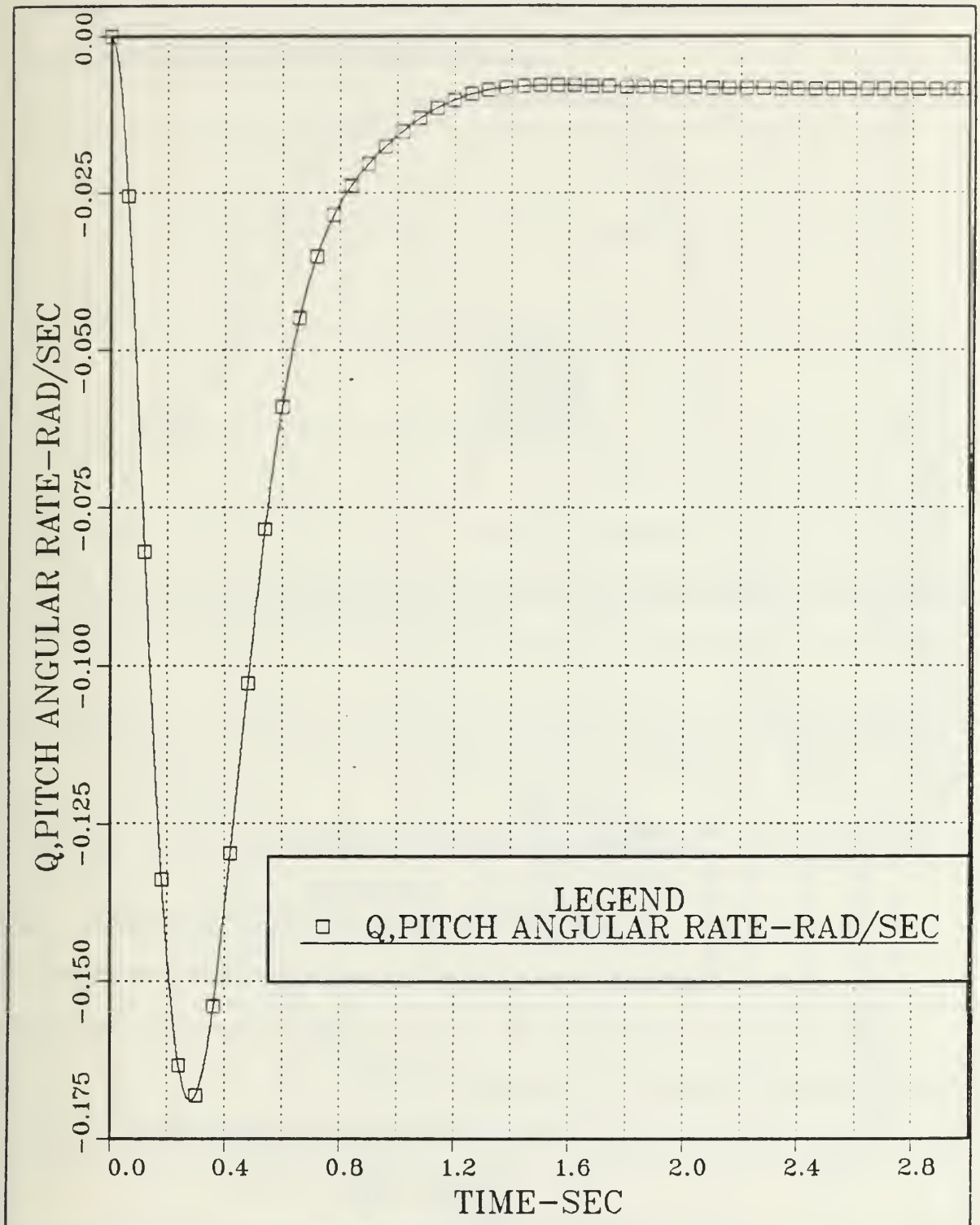

Figure 3.23 Pitch Angular Rate vs Time;
Inoperative δ_1 Control Surface; a_e=0;
Step input: n_{Zc} =1 gee, δ_{1c} = 0.2, δ_{2c}, δ_{3c}, δ_{4c} = 0 rad.

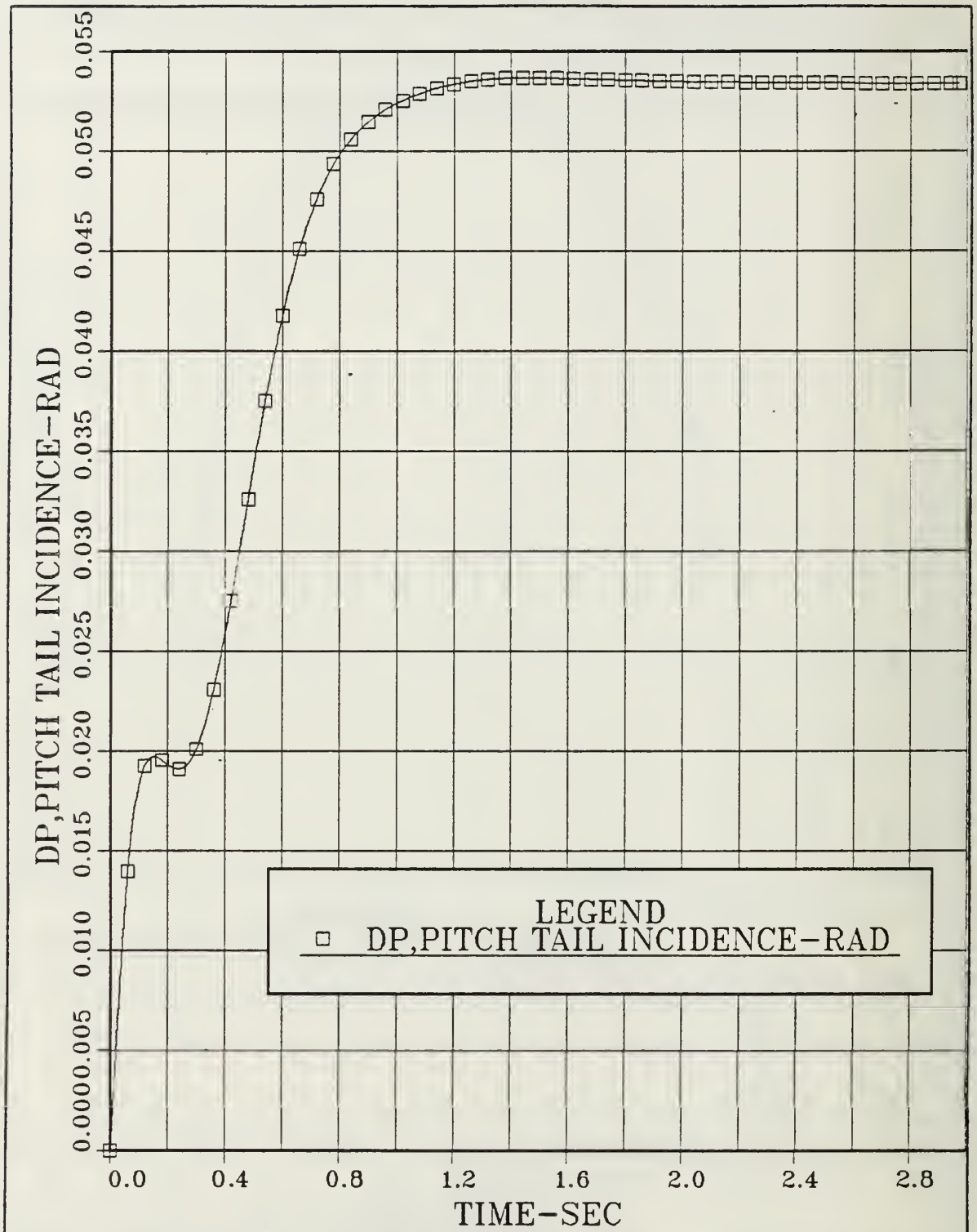

Figure 3.24 Pitch Tail Incidence vs Time;
Inoperative δ_1 Control Surface; a_e=0;
Step input: n_{Zc} =1 gee, δ_{1c} = 0.2, δ_{2c}, δ_{3c}, δ_{4c} = 0 rad.

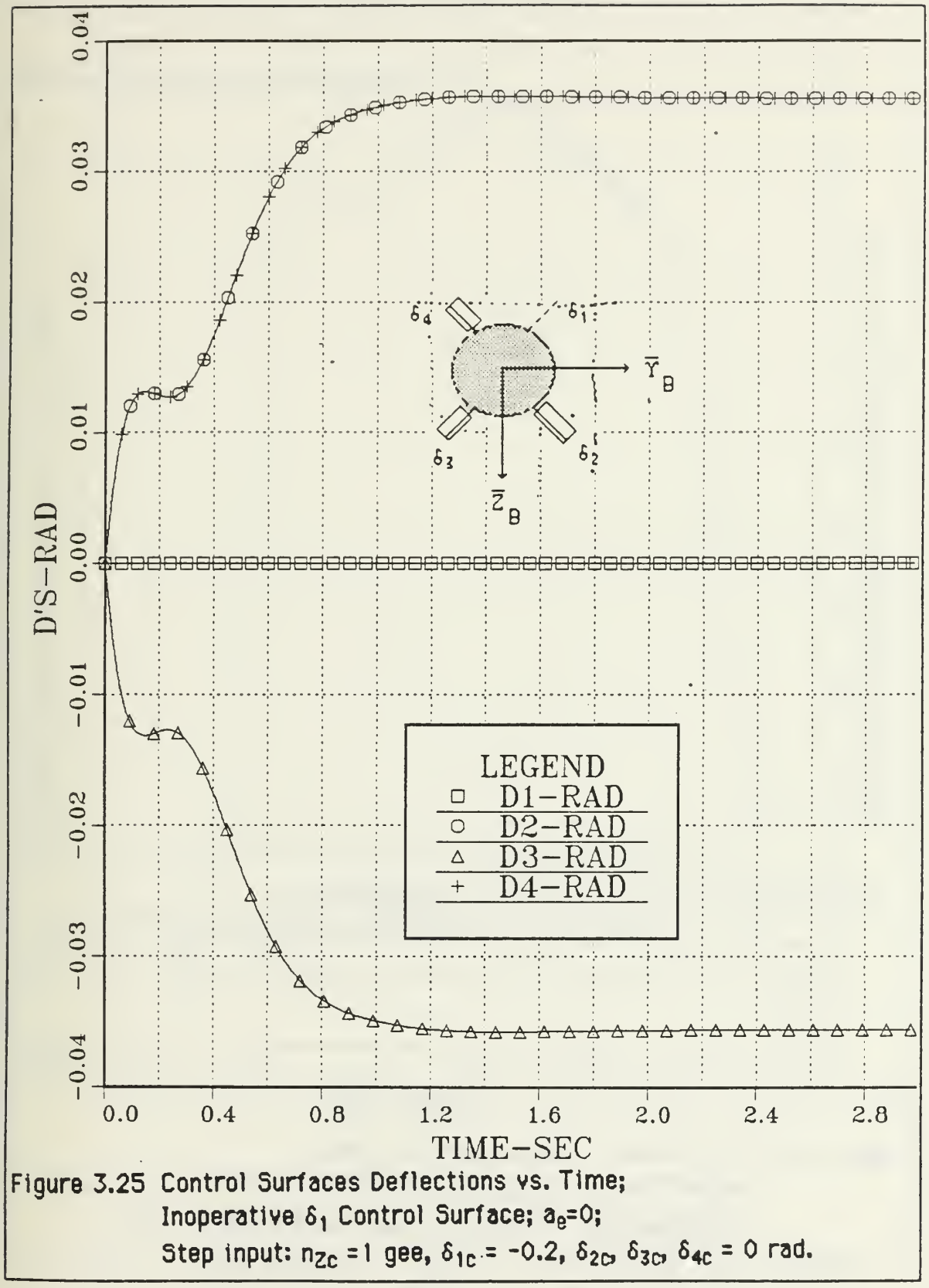

Figure 3.25 Control Surfaces Deflections vs. Time;
Inoperative δ_1 Control Surface; a_e=0;
Step input: n_{Zc} =1 gee, δ_{1c} = -0.2, δ_{2c}, δ_{3c}, δ_{4c} = 0 rad.

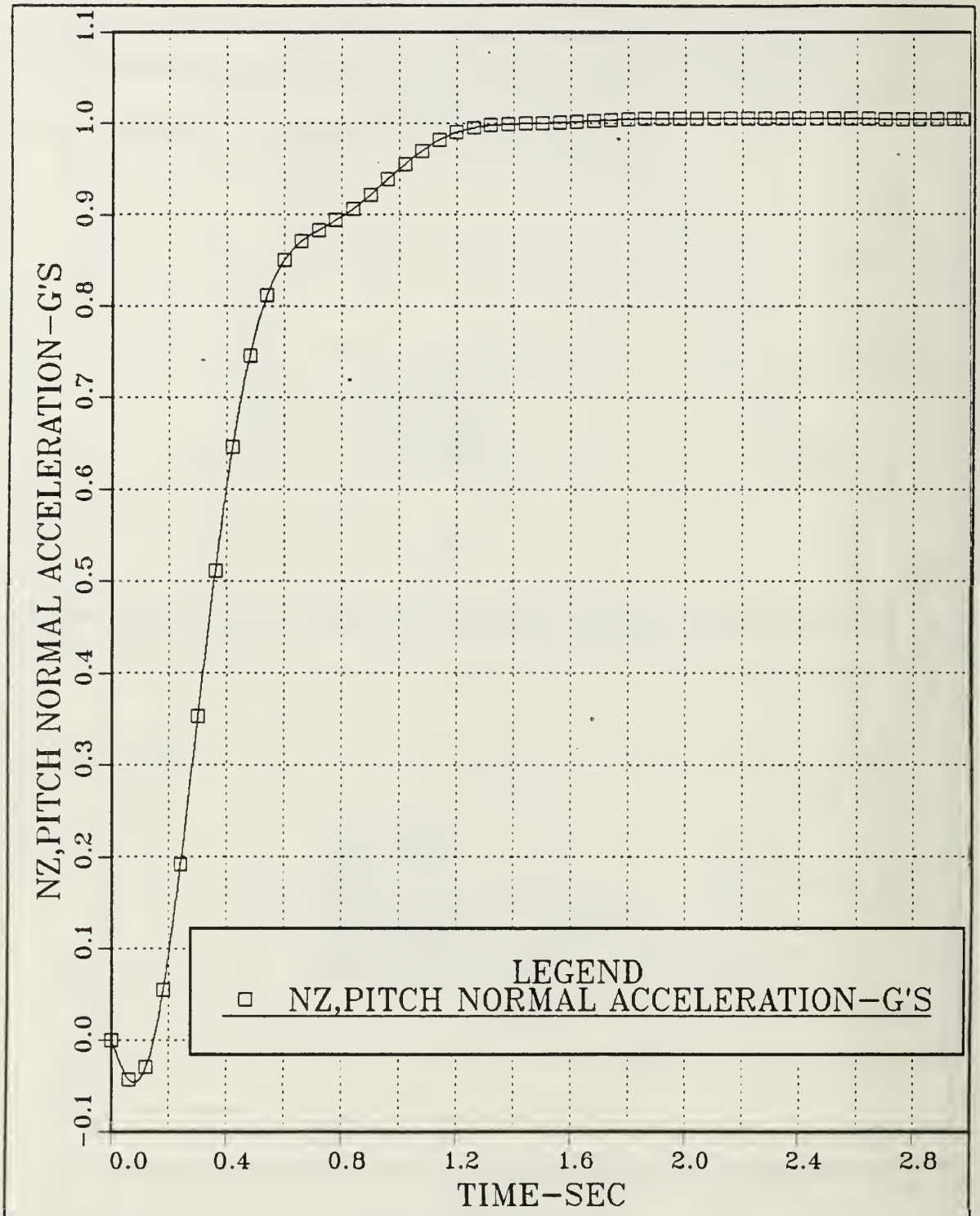

Figure 3.26 Pitch Normal Acceleration vs. Time;
Inoperative δ_1 and δ_2 Control Surfaces; a_e=0;
Step input: n_{Zc} =1 gee, δ_{1c} = 0.2, δ_{2c}, δ_{3c}, δ_{4c} = 0 rad.

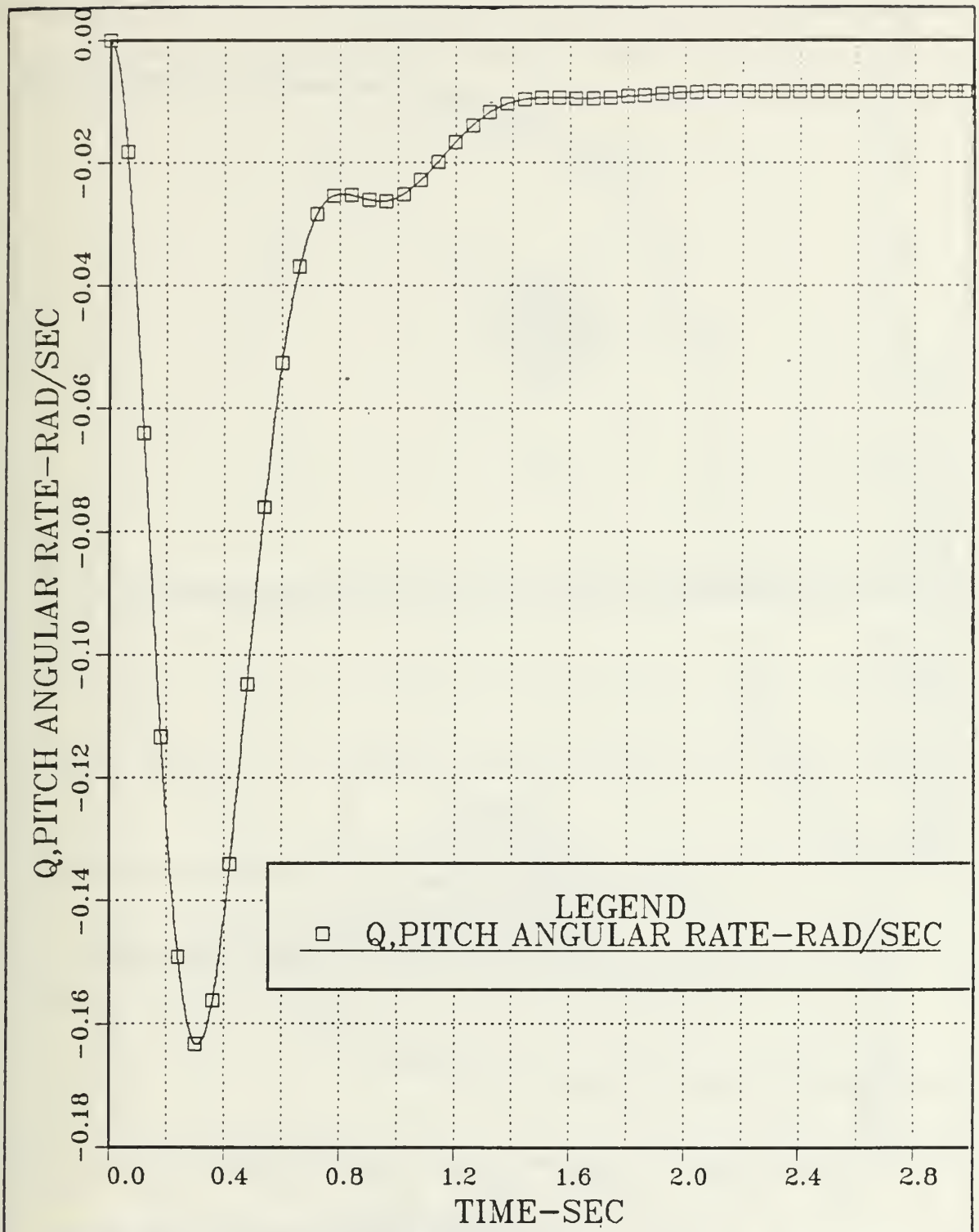

Figure 3.27 Pitch Angular Rate vs Time;
Inoperative δ_1 and δ_2 Control Surfaces; a_θ=0;
Step input: n_{Zc} =1 gee, δ_{1c} = 0.2, δ_{2c}, δ_{3c}, δ_{4c} = 0 rad.

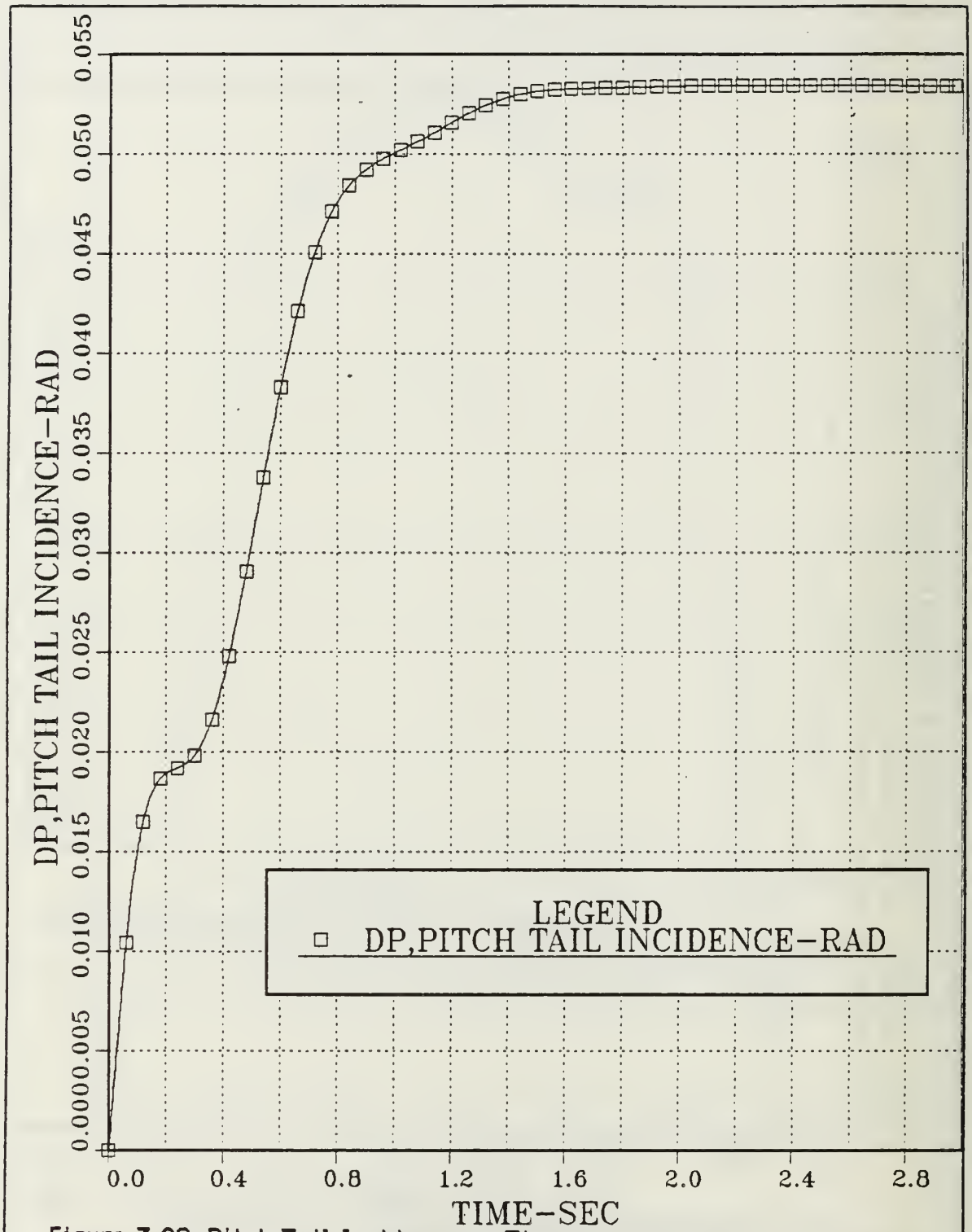

Figure 3.28 Pitch Tail Incidence vs Time;
Inoperative δ_1 and δ_2 Control Surfaces; a_e=0;
Step input: n_{Zc} =1 gee, δ_{1C} = 0.2, δ_{2C}, δ_{3C}, δ_{4C} = 0 rad.

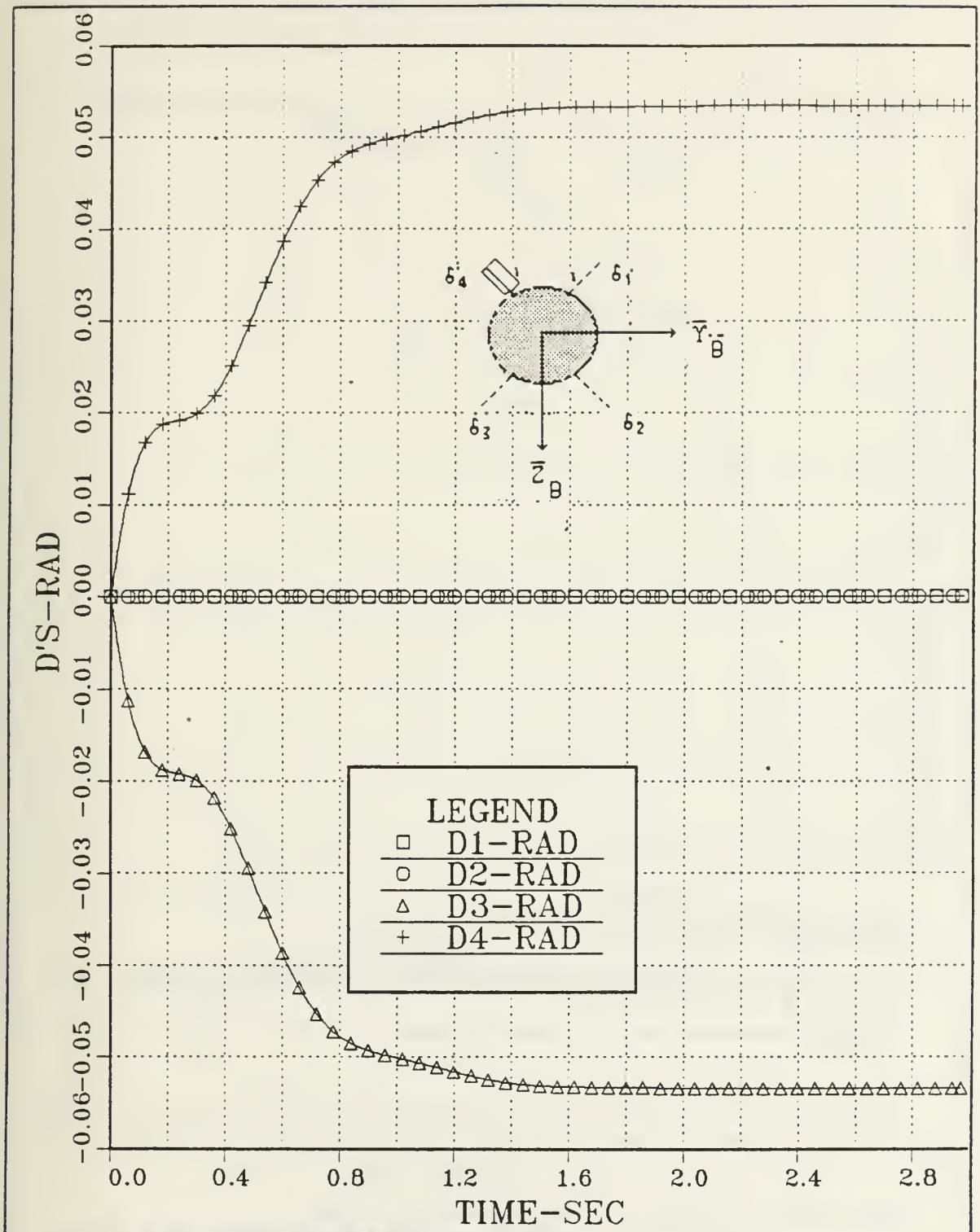

Figure 3.29 Control Surfaces Deflections vs. Time;
Inoperative δ_1 and δ_2 Control Surfaces; a_e=0;
Step input: n_{Zc} =1 gee, δ_{1c} = -0.2, δ_{2c}, δ_{3c}, δ_{4c} = 0 rad.

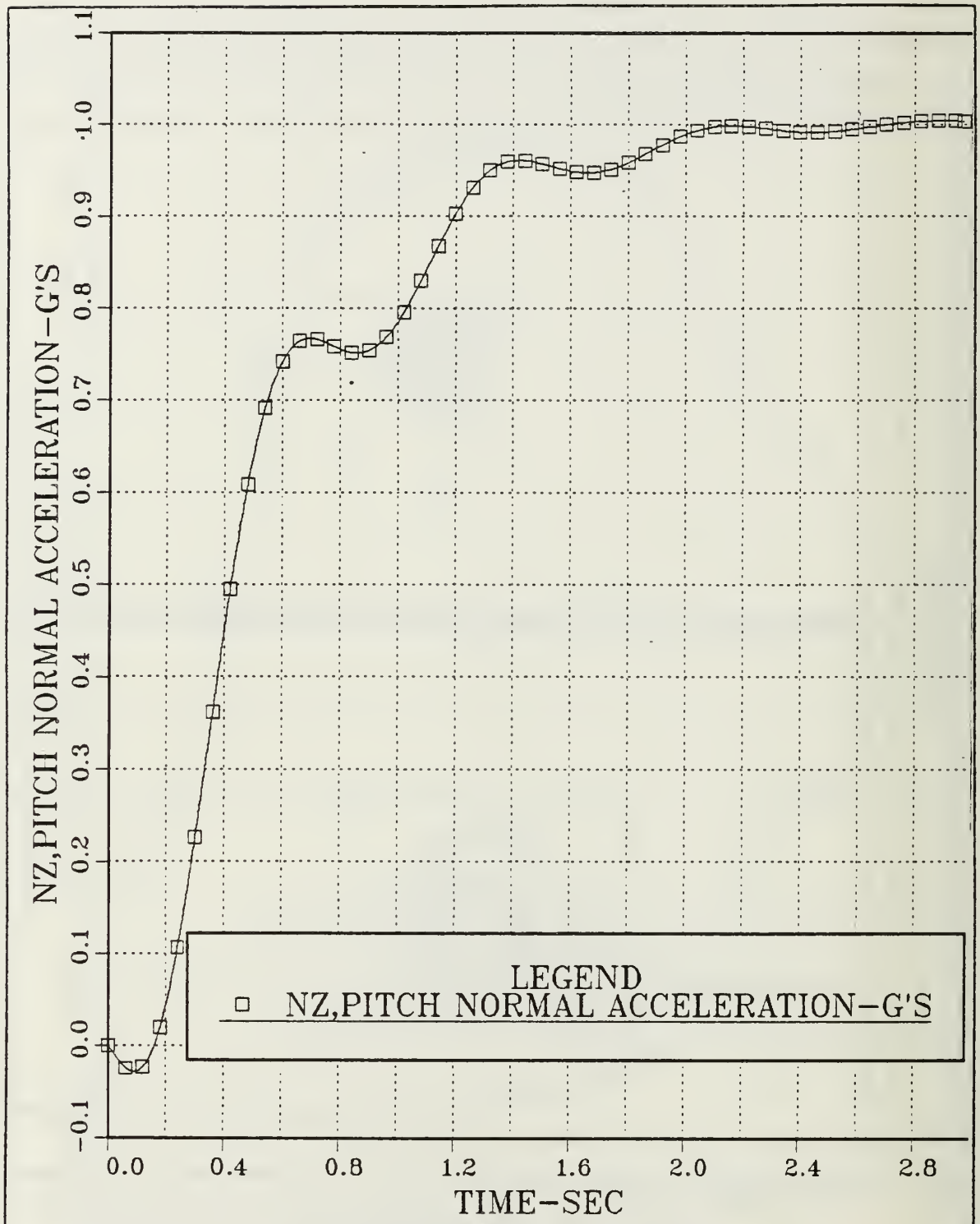

Figure 3.30 Pitch Normal Acceleration vs. Time;
Inoperative δ_1, δ_2 and δ_3 Control Surfaces; a_8=0;
Step input: n_{Zc} =1 gee, δ_{1c} = 0.2, δ_{2c}, δ_{3c}, δ_{4c} = 0 rad.

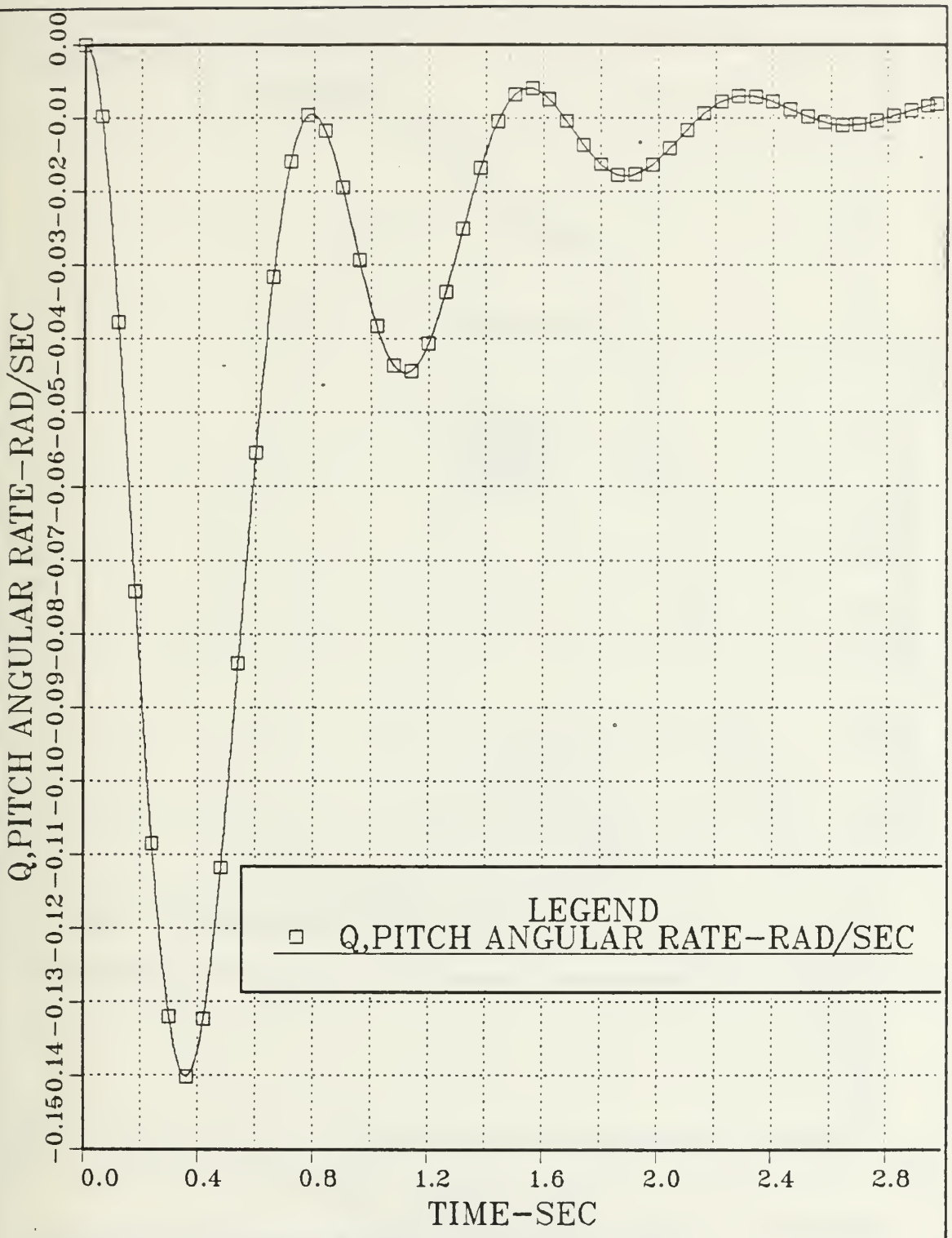

Figure 3.31 Pitch Angular Rate vs Time;
Inoperative δ_1, δ_2 and δ_3 Control Surfaces; a_e=0;
Step input: n_{Zc} =1 gee, δ_{1c} = 0.2, δ_{2c}, δ_{3c}, δ_{4c} = 0 rad.

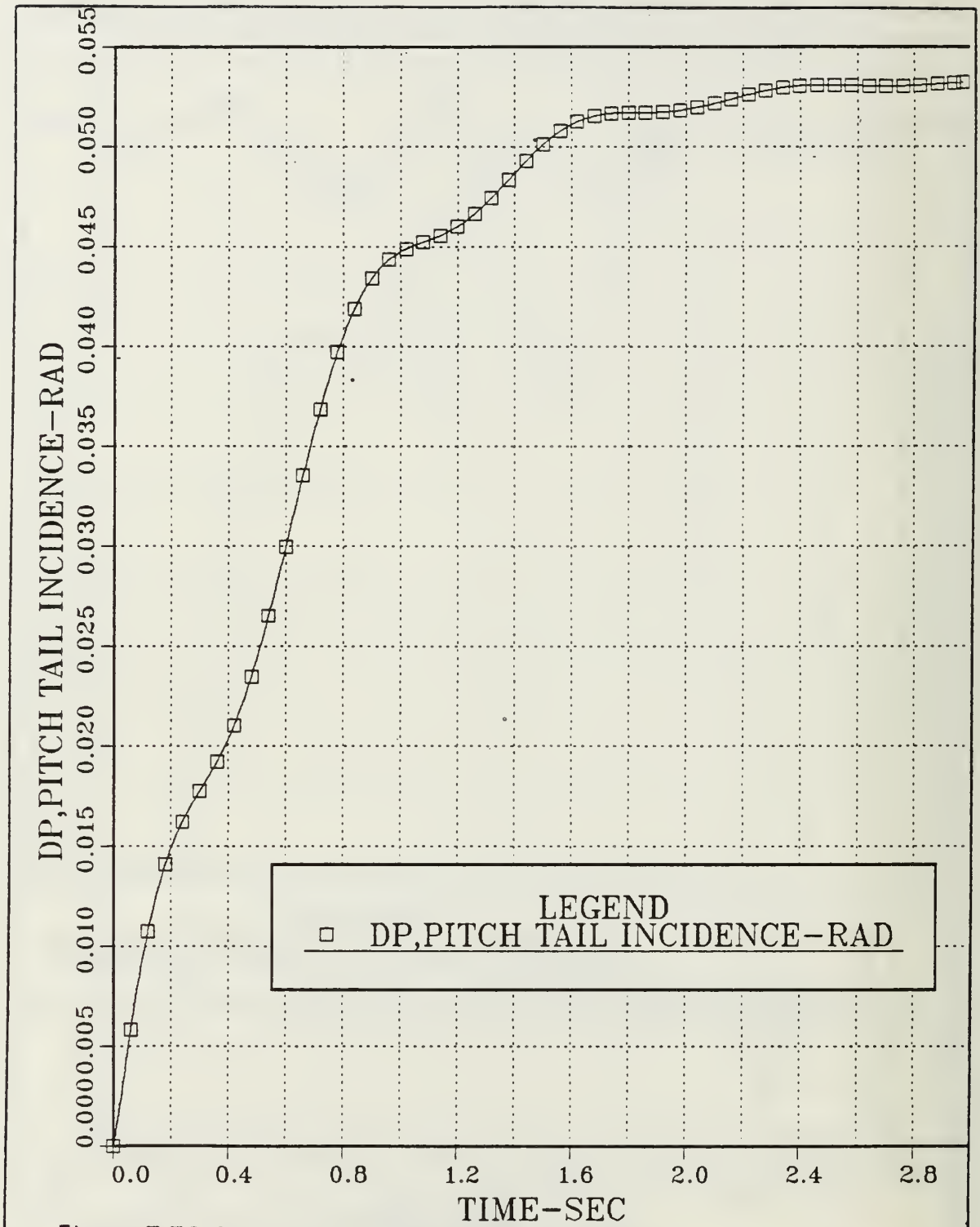

Figure 3.32 Pitch Tail Incidence vs Time;
Inoperative δ_1, δ_2 and δ_3 Control Surfaces; a_e=0;
Step input: n_{Zc} =1 gee, δ_{1c} = 0.2, δ_{2c}, δ_{3c}, δ_{4c} = 0 rad.

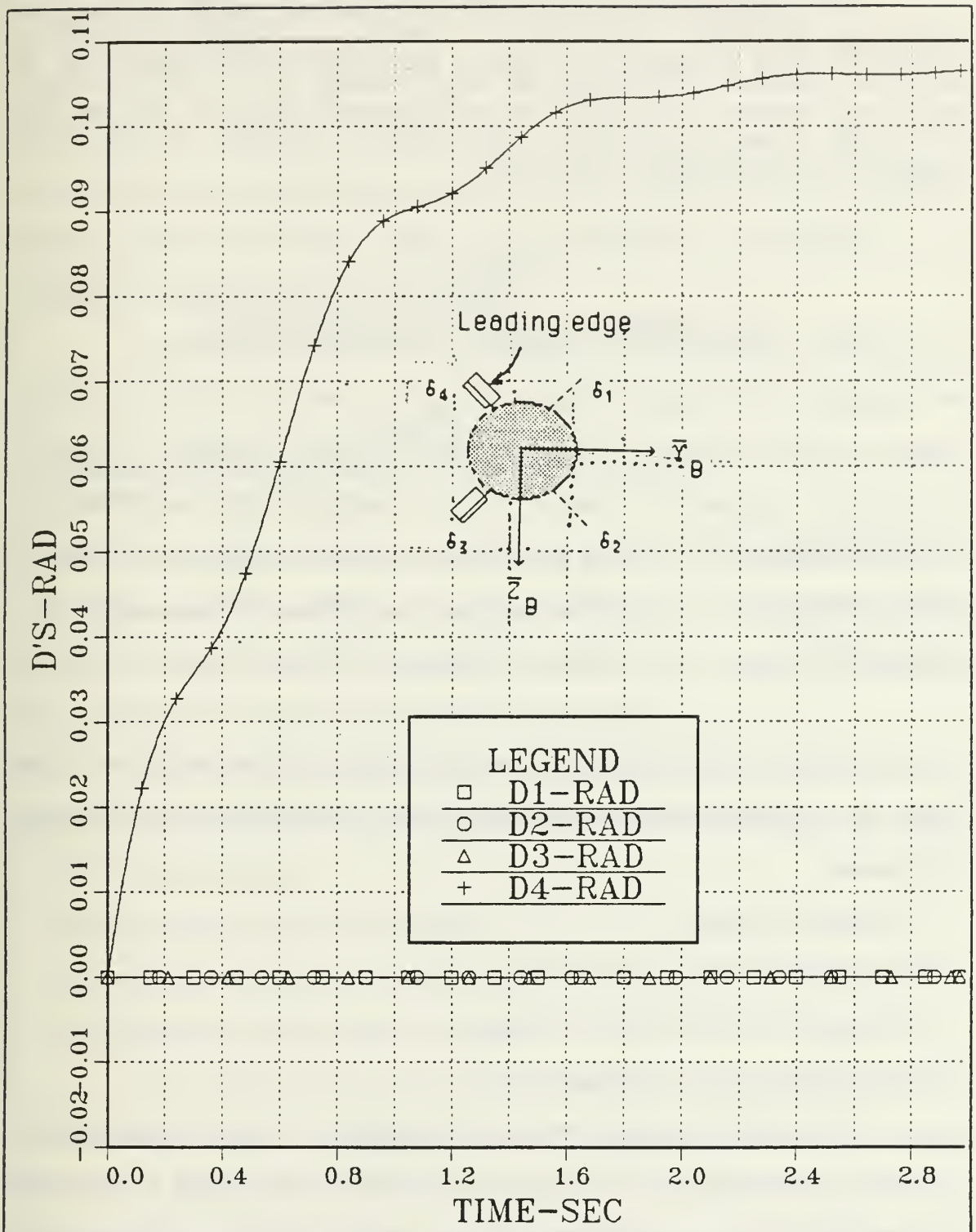

Figure 3.33 Control Surfaces Deflections vs. Time;
Inoperative δ_1, δ_2 and δ_3 Control Surfaces; a_e=0;
Step input: n_{Zc} = 1 gee, δ_{1c} = -0.2, δ_{2c}, δ_{3c}, δ_{4c} = 0 rad.

The inoperative cases are all quite similar except for the last case where only one control surface is available. In this latter case an oscillatory behavior is evident. The performance criteria to the one gee command are summarized in Table 3.2.

TABLE 3.2

PITCH NORMAL ACCELERATION PERFORMANCE

	System			
	Unimpaired- Hard Over- Inoperative Control Surfaces			
		One	Two	Three
Time Constant(sec):	0.50	0.41	0.60	0.60	1.01
Delay Time(sec):	0.28	0.5	0.35	0.38	0.40
Overshoot(%):	2.2%	0.01%	0.01%	0.01%	0.01%

Figure 3.35 compares the unimpaired system with the three cases of control surfaces impairments. The curves include the following four cases:

(1) Original system

(2) Inoperative one control surface

(3) Inoperative two control surfaces

(4) Inoperative three control surfaces

This Figure shows that as the number of the damaged control surfaces increases the delay time increases also from 0.28 sec for the unimpaired system to 0.41 sec for the system with three inoperative control surfaces. The increase also of the time constant from 0.5 sec

(unimpaired system) to about 1 sec (three inoperative actuators), indicates that as the number of the damaged control surfaces increases more time is required to achieve the steady-state value of the normal acceleration. Also observe the initially faulty response of the nonminimum phase system to the step input which decreases as the number of the inoperative control surfaces increases.

Figure 3.36, shows that to achieve the acceleration response the system with the hard over δ_1 type of damage, requires more angular rate (q or Q), compared with the unimpaired and the other three damaged system cases. The produced pitching moment is evident. Initially and because the δ_1 control surface is deflected at the 0.2 rad angle while the other three are at the zero position, the first tenth of the second the rate increases from zero to 0.45 rad/sec. The rate then begins to decrease very rapidily to a rate of -0.38 rad/sec at 0.4 sec.

Figure 3.37 compares the unimpaired system with three cases of control surfaces impairments. The curves include the following four cases:

(1) Original system

(2) Inoperative one control surface

(3) Inoperative two control surfaces

(4) Inoperative three control surfaces

This Figure shows that as the number of the damaged control surfaces increases, the angular rate of change is reduced, and more pronounced fluctuations occur, i.e., the system becomes more oscillatory. These fluctuations are connected with the pitching moment induced in the missile by the failed actuators.

Finally Figures 3.38 and 3.39 compare the unimpaired system with four cases of control surfaces impairments. The curves include the following five cases:

(1) Original system

(2) Hard over one control surface

(3) Inoperative one control surface

(4) Inoperative two control surfaces

(5) Inoperative three control surfaces

Figure 3.38 and 3.39 show that the required (steady-state) pitch tail incidence for the uncoupled longitudinal autopilot is 0.054 rad (unimpaired or damaged).

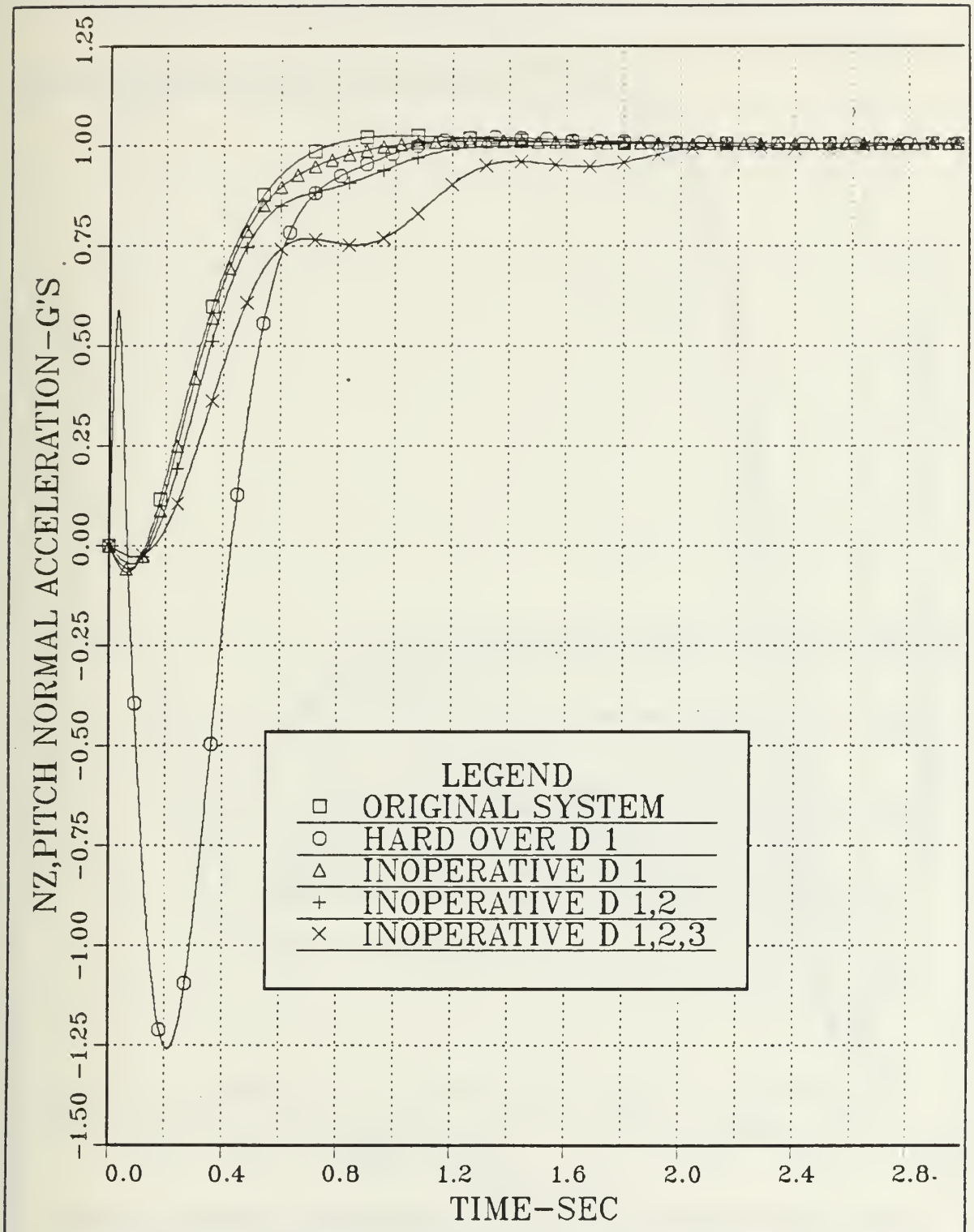

Figure 3.34 Comparison of the Pitch Normal Acceleration between the Unimpaired System and the Four Cases of Impairment.

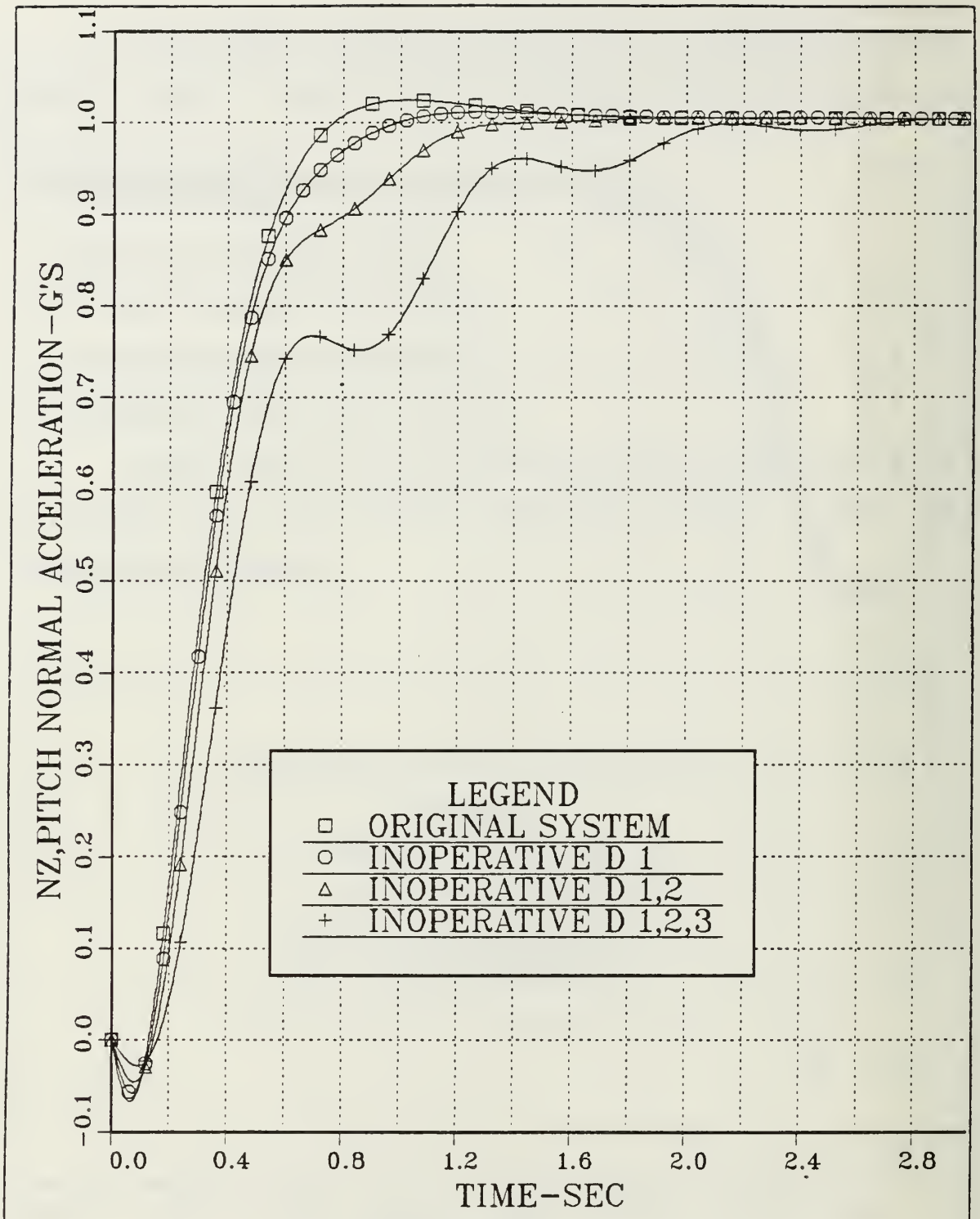

Figure 3.35 Pitch Normal Acceleration; Uncoupled open loop Channel: Unimpaired and Damaged Control Surfaces.

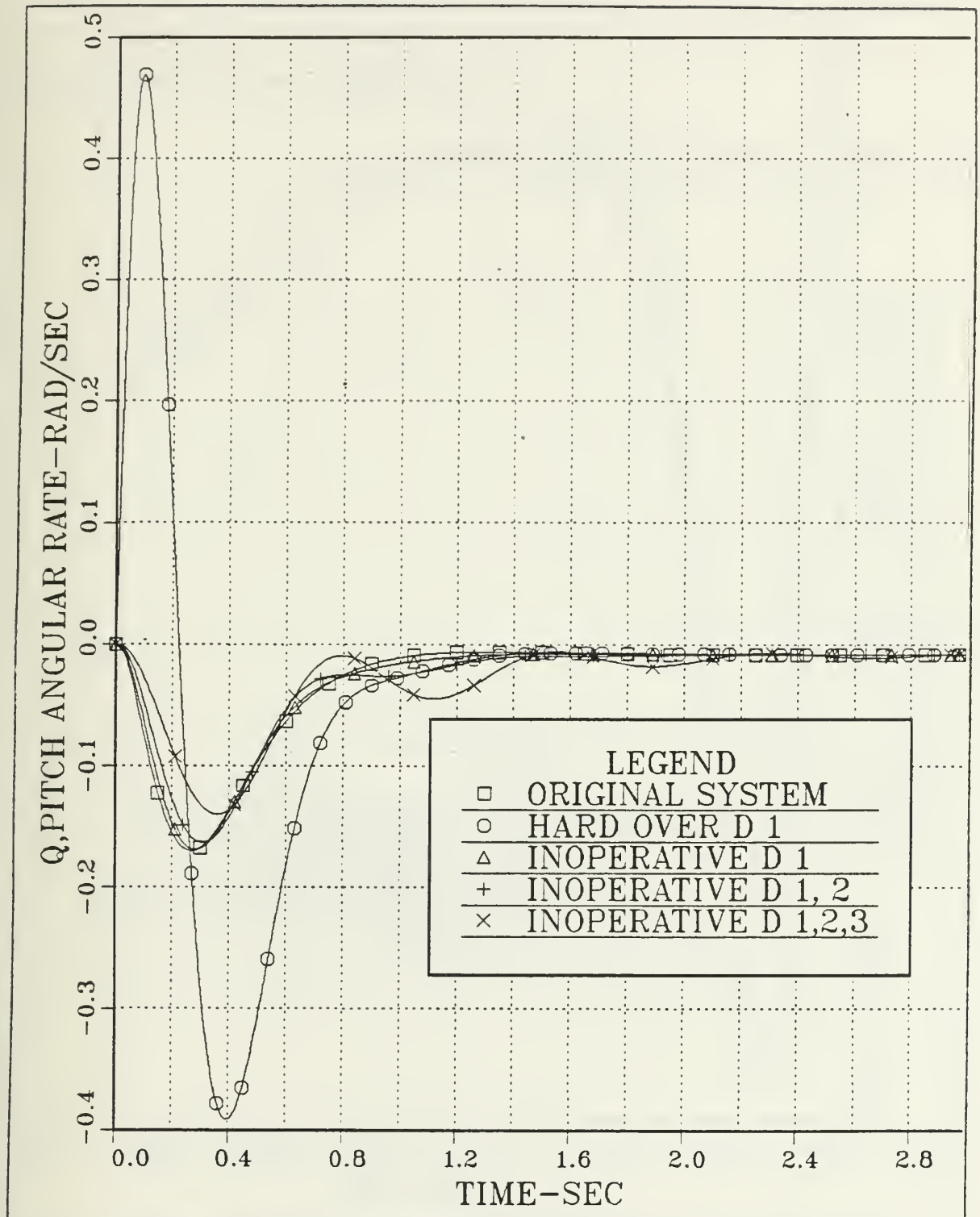

Figure 3.36 Comparison of the Pitch Angular Rate between the Unimpaired System and the Four Cases of Impairment.

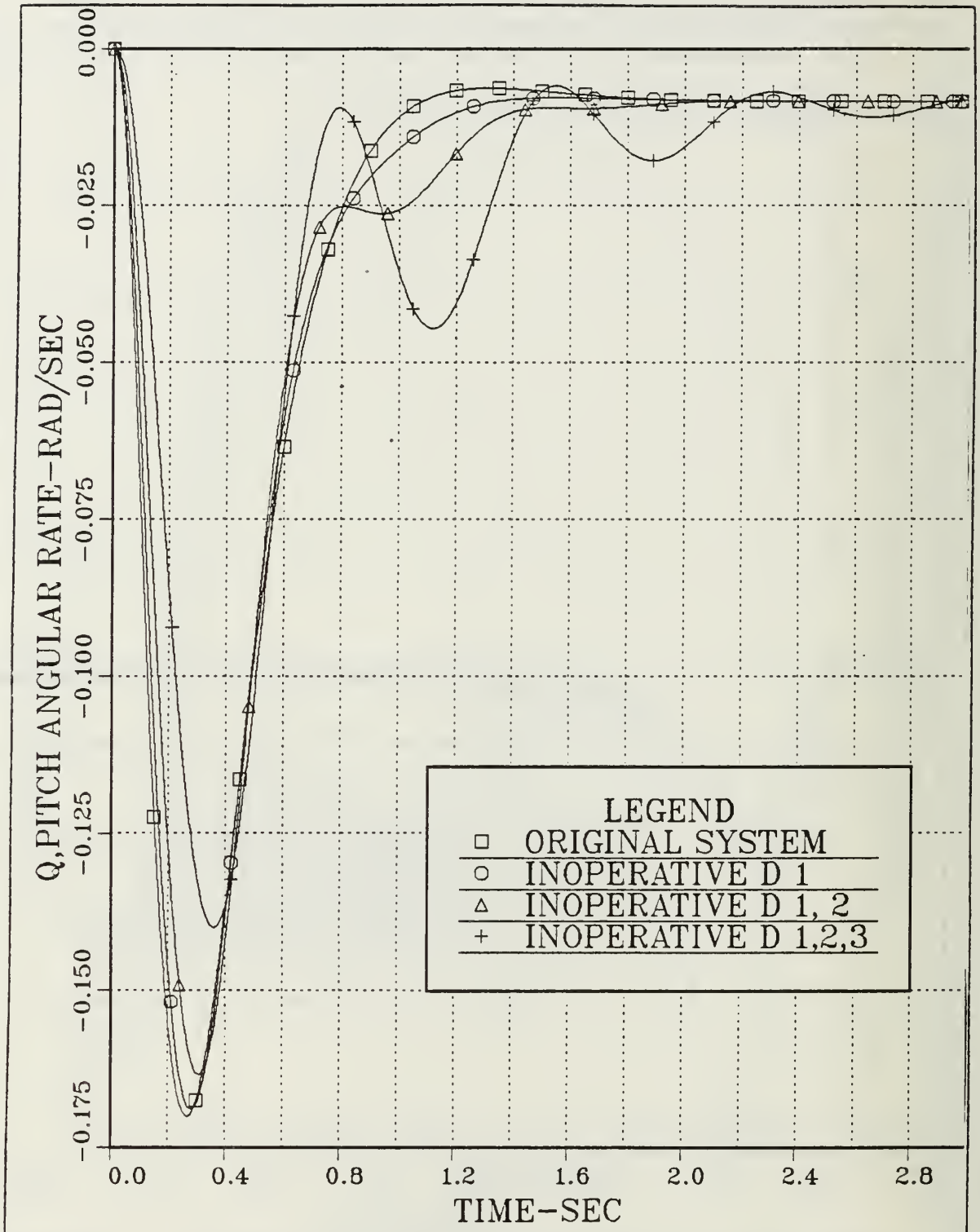

Figure 3.37 Pitch Angular Rate; Uncoupled open loop Channel: Unimpaired and Damaged Control Surfaces.

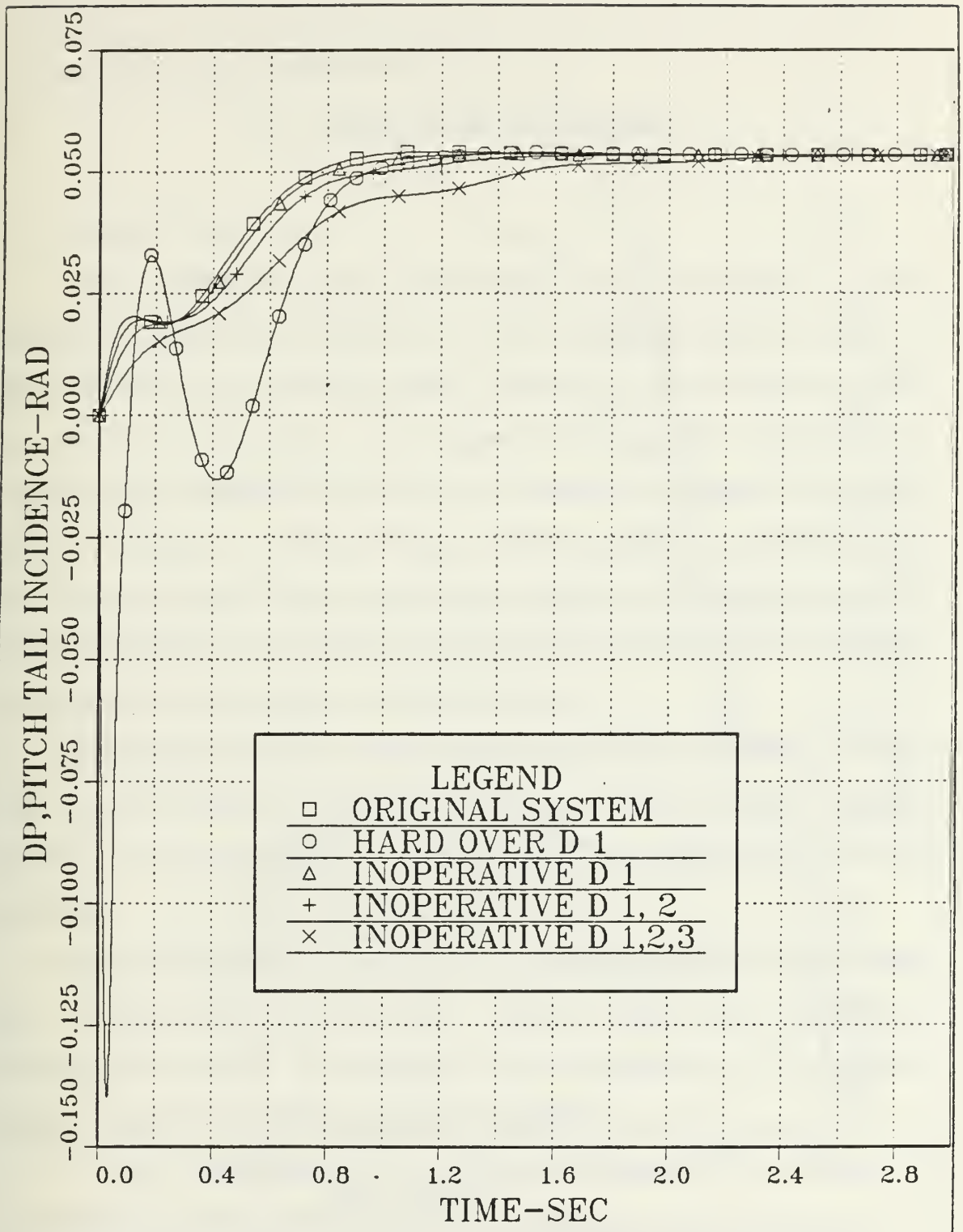

Figure 3.38 Comparison of the Pitch Tail Incidence between the Unimpaired System and the Four Cases of Impairment.

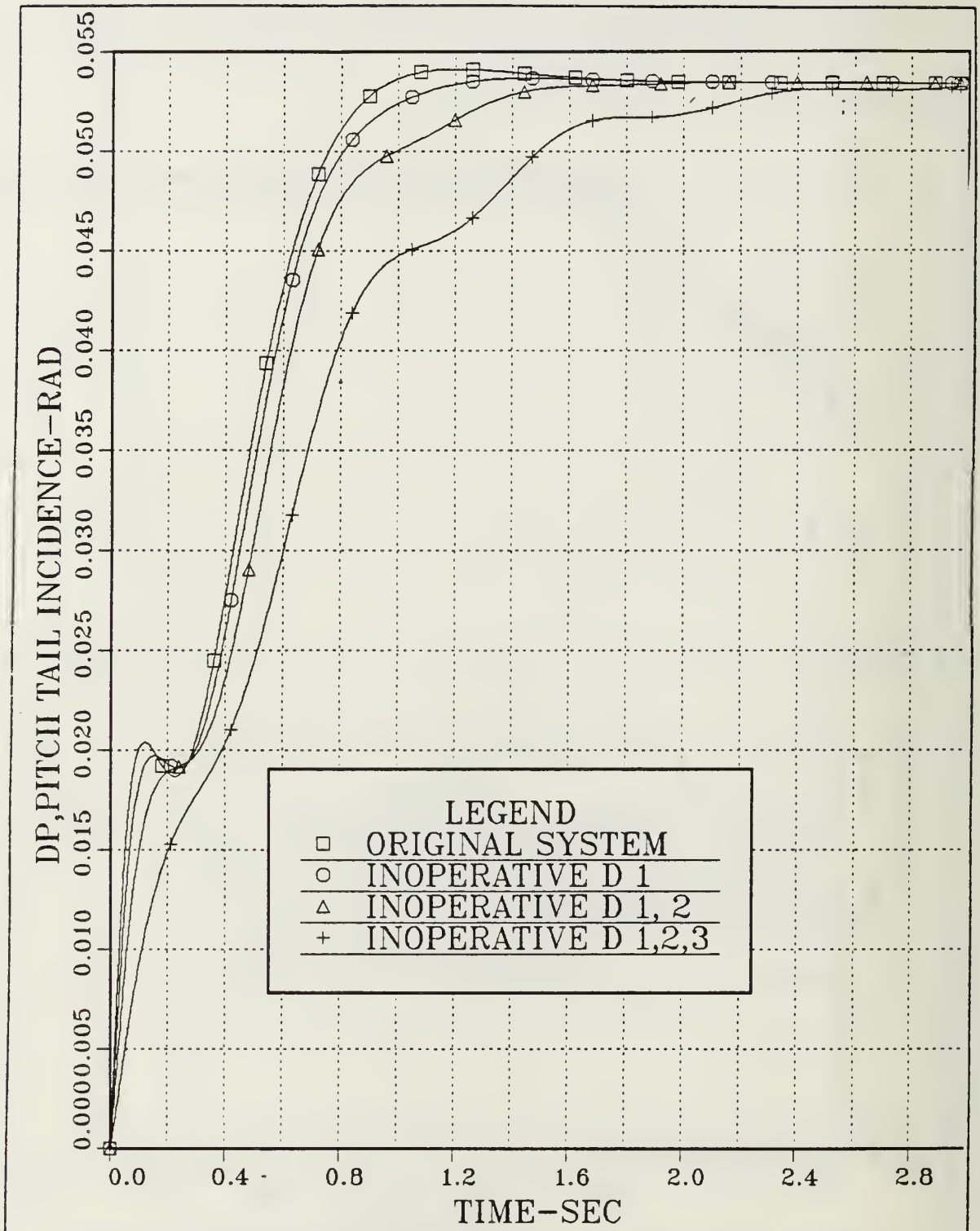

Figure 3.39 Pitch Tail Incidence; Uncoupled open loop Channel: Unimpaired and Damaged Control Surfaces.

IV. LATERAL MODEL METHODOLOGY

A. INTRODUCTION

In this chapter the design and analysis of the continuous uncoupled lateral (i.e., yaw and roll) channels of a B.T.T. autopilot derived in [Ref. 1 and 4] is reviewed. A modified lateral autopilot is then designed with the four control surfaces split into independent components. The model of elliptical (yaw channel) and circular (roll channels) configurations are both shown in Figure 4.1. Both airframes have the same cross sectional area distribution and specifically, the circular cross sectional body has a closure ratio Abase/Amax of 0.69 with Amax occuring at 68% missile body, whereas the elliptical airframe has a 3:1 cross section.

A comparison between the two systems (original and modified) shows that they are identical. The transient response plots and their analysis demonstrate the performance of the original and modified yaw and roll channels.

Having established the validity of the modified system one then uses the multiple-input/multiple-output control theory and state-space representation [Ref.3] to investigate the performance of the modified lateral autopilot for various classes of damages.

For the investigation of the lateral channel, two classes of impairments at the control surfaces are considered:

(1) Locked or hard over and

(2) Inoperative with the control surfaces centered or shot away.

The plots of the unimpaired modified yaw and roll autopilots are used as a basis for comparison. The impairment induced effects on roll angle, rate and tail incidence are assessed.

B. UNCOUPLED LINEAR YAW CHANNEL (ORIGINAL)

1. Aerodynamic Model, Airframe Configuration and Control Law

A general block diagram of a B.T.T. autopilot with all its channels is shown in Figure 3.2. Inertial acceleration commands are applied in polar coordinates, i.e., magnitude of the command (η_C) applied to pitch autopilot and the direction (ψ_C) is applied to the roll autopilot. The yaw autopilot is slaved to the roll autopilot in order to minimize sideslip angle by coordinating the missile yaw and roll motion. Achieved maneuver plane accelerations in rectangular coordinates, (η_Z) and (η_Y), were determined by resolving achieved body-fixed accelerations, (η_z) and (η_y) through the missile roll angle (ψ), i.e., the Euler angles θ and ψ are assumed to be sufficient small, so that the sideslip angle (β) is minimized and the motion between the yaw and roll channels is coordinated.

A general diagram of the uncoupled yaw channel where the aerodynamic and yaw control law are involved is shown in Figure 4.2. In Figure 4.3 [Ref. 1] the yaw control law is presented. The yaw normal acceleration (η_{YC}) is not used to command the coupled B.T.T. autopilot, although, it is used for the design and analysis of the uncoupled channel. The command used by the coupled system is shown in dashed lines and is a yaw angular rate command (r_C). The yaw control law is governed by missile body yaw angular rate (r) and yaw normal acceleration (η_Y).

The flight conditions are the same as was mentioned for the pitch channel, (i.e., 60 Kft altitude and Mack number 3.95). The yaw control law determines the required yaw tail incidence (δ_{Yc}) command to the actuator network which is approximated as a first-order lag at 30 Hz.

2. Requirements for the Classical Design

Requirements for the classical design approach are:

a. High frequency attenuation in actuator command branch ≥ 15 dB at 100 rad/sec and zero angles of attack and sideslip.

b. Relative stability: gain margins ≥ 6 dB, phase margins ≥30 deg with a goal of 12 dB and 50 degrees.

c. Acceleration time response:

(1) 63% time constant of approximately 0.4 sec for a step command of acceleration (n_Y) at flight conditions of interest and at α_e and β=0.

(2) Overshoot ≤ 10% for better sideslip control.

(3) Steady state error not necessarily zero.

3. Transfer Functions of Aerodynamic Model and Analysis

The aerodynamic transfer functions of the uncoupled yaw channel autopilot are according to Karadimas, C. thesis [Ref. 4]:

a. Transfer function of yaw angular rate:

$$\frac{r}{\delta_Y} = \frac{0.15\left\{\frac{1}{0.0748}s + 1\right\}}{\left\{\frac{1}{4.3}s + 1\right\}\left\{\frac{1}{-4.25}s + 1\right\}} \text{ (deg/sec/deg)} \qquad \text{(IV.B.3-1)}$$

b. Transfer function of Yaw Normal Acceleration:

$$\frac{\eta_Y}{\delta_Y} = \frac{17.76\{\frac{1}{11.48}s + 1\}\{\frac{1}{-11.48}s + 1\}}{\{\frac{1}{4.3}s + 1\}\{\frac{1}{-4.25}s + 1\}} \text{ (g's/deg)} \quad \text{(IV.B.3-2)}$$

Rearranging the above transfer functions in terms of the variable pairs (r,δ_Y) and (η_Y,δ_Y) respectively and applying the inverse Laplace transformation a set of linear differential equations can be obtained. Then, using rules of state-space representation, the following equations are obtained [Ref. 4]:

$$\dot{X}_1 = X_2 - 29.2321\,\delta_Y \quad \text{(IV.B.3-3)}$$

$$\dot{X}_2 = -16.7224X_1 - 0.0434X_2 + 0.2687\delta_Y \quad \text{(IV.B.3-4)}$$

$$\dot{Z}_1 = Z_2 - 0.0801\delta_Y \quad \text{(IV.B.3-5)}$$

$$\dot{Z}_2 = -16.7224_1 - 0.0435Z_2 - 150.7724\delta_Y \quad \text{(IV.B.3-6)}$$

$$\dot{Y} = 3.3574Z_1 - 4Y + 6.4341\delta_Y - 3.3574\eta_{Yc} \quad \text{(IV.B.3-7)}$$

$$\delta Yc = 6.06X_1 + 0.606X_2 + 2.0413Z_1 + 3.648Y - 13.8612 - 2.0413\eta_C \quad \text{(IV.B.3-8)}$$

$$\delta Y = 188.4\delta_{Yc} - 188.4\delta_Y \quad \text{(IV.B.3-9)}$$

Using state-space representation, the Equations (IV.B.3-3) through (IV.B.3-9) can be modeled in a seventh-order system of the form:

$$\dot{X} = FX + GU$$

with the continuous plant system F and control matrix G as follows:

$$\begin{bmatrix} \dot{X}_1 \\ \dot{X}_2 \\ \dot{Z}_1 \\ \dot{Z}_2 \\ \dot{Y} \\ \dot{\delta}_{Yc} \\ \dot{\delta}_Y \end{bmatrix} = \begin{bmatrix} 0 & 1 & 0 & 0 & 0 & 0 & -29.2321 \\ -16.722 & -0.0434 & 0 & 0 & 0 & 0 & 0.26870 \\ 0 & 0 & 0 & 1 & 0 & 0 & -0.08010 \\ 0 & 0 & -16.722 & -0.0435 & 0 & 0 & -150.772 \\ 0 & 0 & 3.357 & 0 & -4 & 0 & 6.434 \\ 6.06 & 0.606 & 2.041 & 0 & 3.648 & 0 & -13.86 \\ 0 & 0 & 0 & 0 & 0 & 188.4 & -188.4 \end{bmatrix} \begin{bmatrix} X_1 \\ X_2 \\ Z_1 \\ Z_2 \\ Y \\ \delta_{Yc} \\ \delta_Y \end{bmatrix}$$

$$+ \begin{bmatrix} 0 \\ 0 \\ 0 \\ 0 \\ -3.3574 \\ -2.0413 \\ 0 \end{bmatrix} \begin{bmatrix} n_{Yc} \\ \end{bmatrix}$$

where the state variables are:

- X_1, X_2 : yaw angular rates
- Z_1 , Z_2 : yaw normal acceleration
- Y : output of acceleration compansator
- δ_{Yc} : input command in the actuator
- δ_Y : yaw tail incidence

Using a step input function which represents the "1 gee command" at $a_e = 0$, the time response plots (Figure 4.4), the Yaw Normal Accelerarion (η_Y) (Figure 4.5), and the Yaw Angular Rate (R) and the Yaw

Tail Incidence (δ_Y) (in Figure 4.6) were obtained. The transient response satisfies the performance criteria and definitions given at Section (III.B.4), and are identical with the results presented in [Ref. 4].

In Figure 4.4 the Yaw Normal Acceleration is plotted which has:

(1) A 0.31 sec time constant.

(2) A 0.3 sec delay time and 6.4% overshoot.

(3) A 0.018 steady-state error.

(4) Note the faulty behavior at the start of the response (0 to 0.2 sec). Because the system is a nominimum phase system (i.e., a zero lies in the right-half s plane) the transient response starts out in the oppsite direction to the input i.e., this is a inherent delay in the transient response of the system.

In Figure 4.5 the Yaw Angular Rate is presented which has:

(1) A maximum body angular rate Of 0.6 rad/sec achieved at 0.3 second.

(2) A minor undershoot and 2.2 sec settling time after which the angular rate remains constant at 0.01 rad/sec. This is due to the fact that the transfer function r/δ_Y (Equation IV.B.3-1) is a type zero system and has a finite error to a step input.

Finally Figure 4.6 shows that a negative angle of deflection of -0.14 rad is required in order to achieve the commanded step input acceleration.

The above analysis has revealed that the performance of the system confirms to the previous mentioned requirements.

From the pole-zero plot in Figure 2.7 [Ref.4] we can see that the continuous open loop system is stable, since the s-plane poles are:

$$s_1 = -175.010 \quad -j0 \qquad \text{(IV.B.3-10)}$$

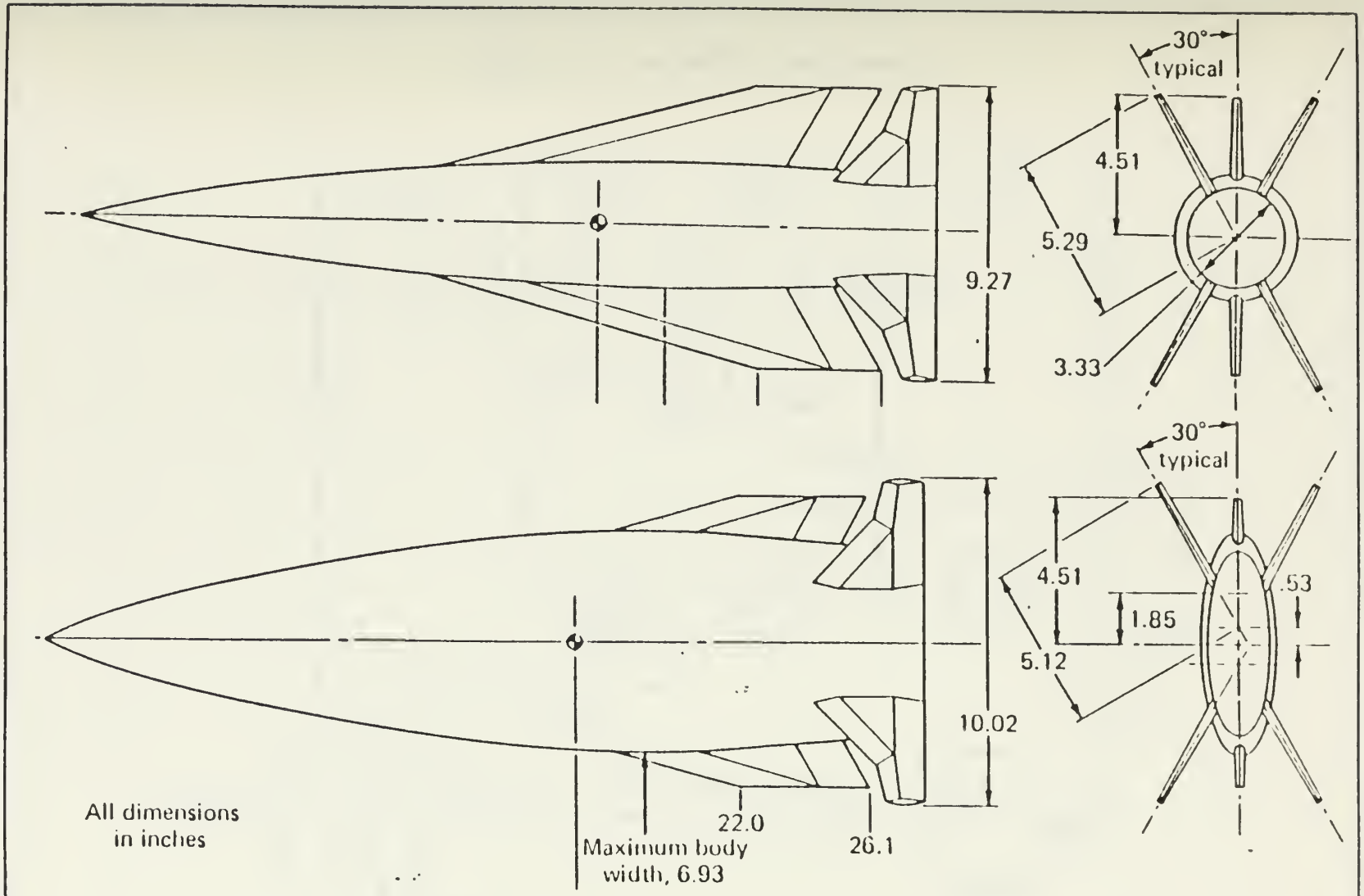

Figure 4.1 Models of Circular and Elliptical Airframes Configurations (1/6 scale)

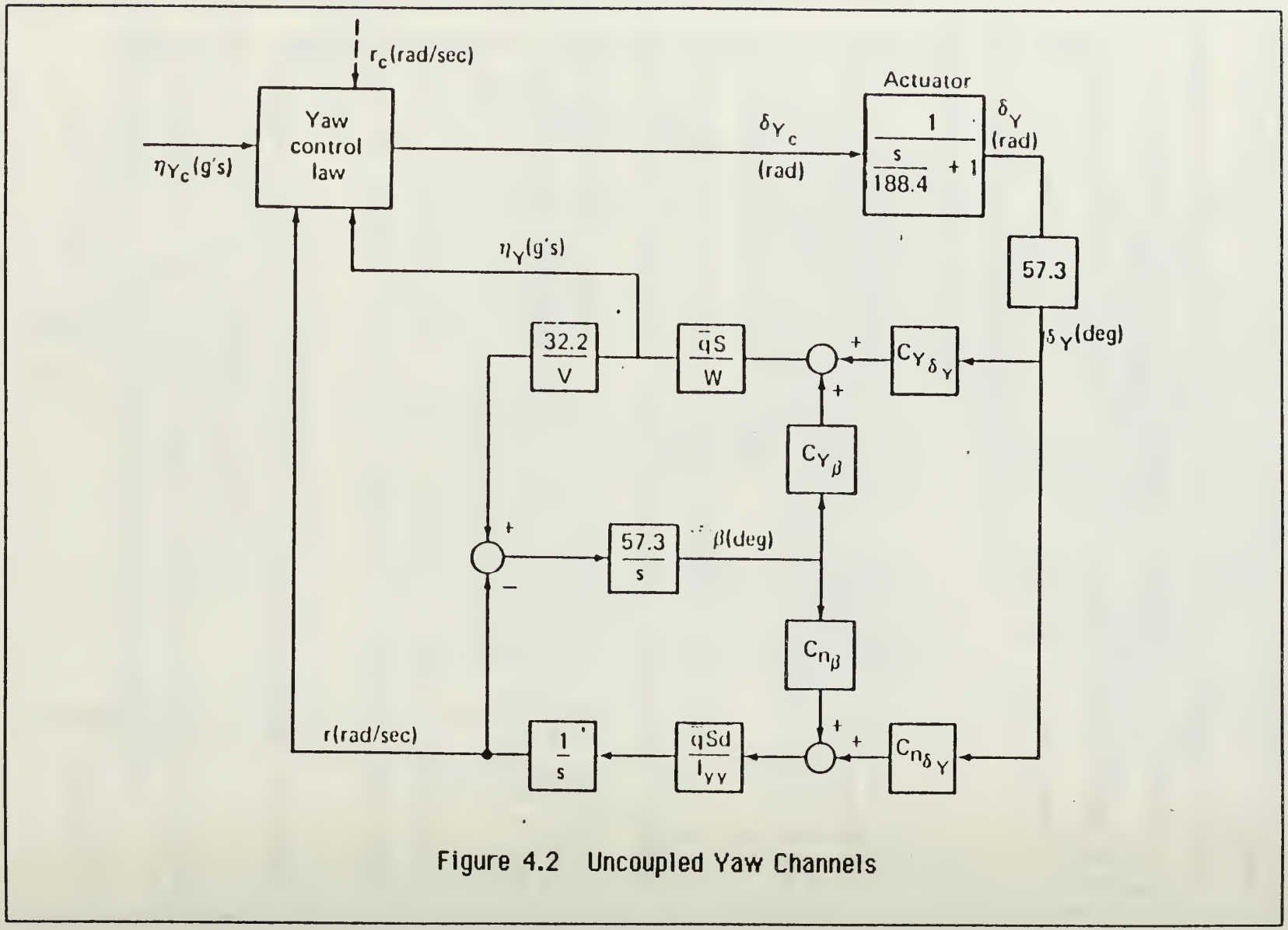

Figure 4.2 Uncoupled Yaw Channels

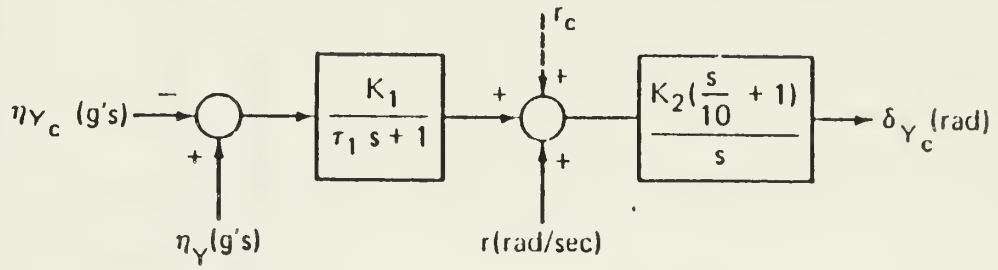

Airframe	K_1	τ_1	K_2
Circular	0.31946	0.2	4.85
Elliptical	0.83935	0.25	6.08

Figure 4.3 Yaw Control Law

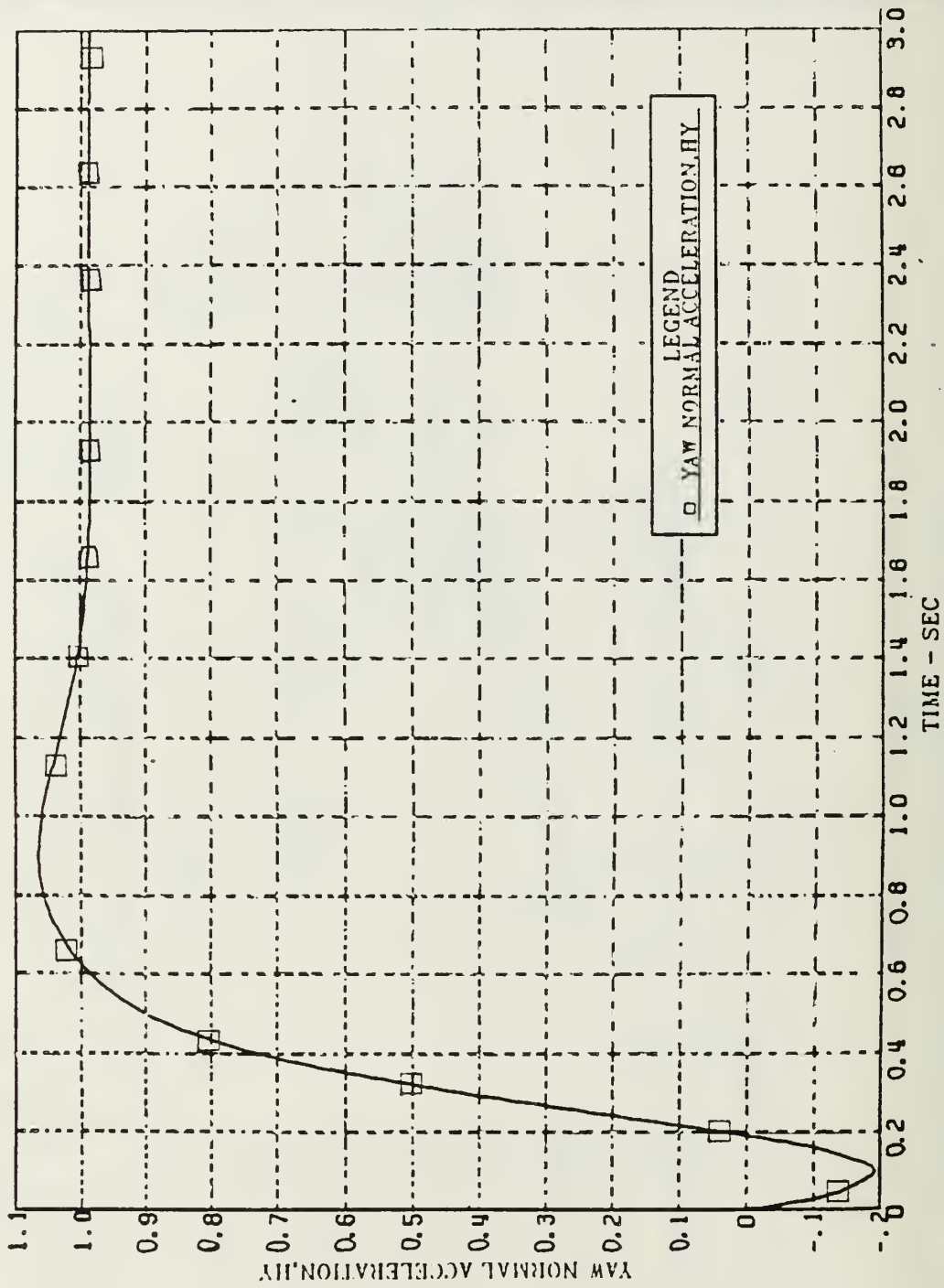

Figure 4.4 Yaw Normal Acceleration vs. Time; Uncoupled Yaw Channel Autopilot; Continuous Open Loop System; Elliptical Airframe; Step Input HY = 1 gee; $a_{\beta} = 0$.

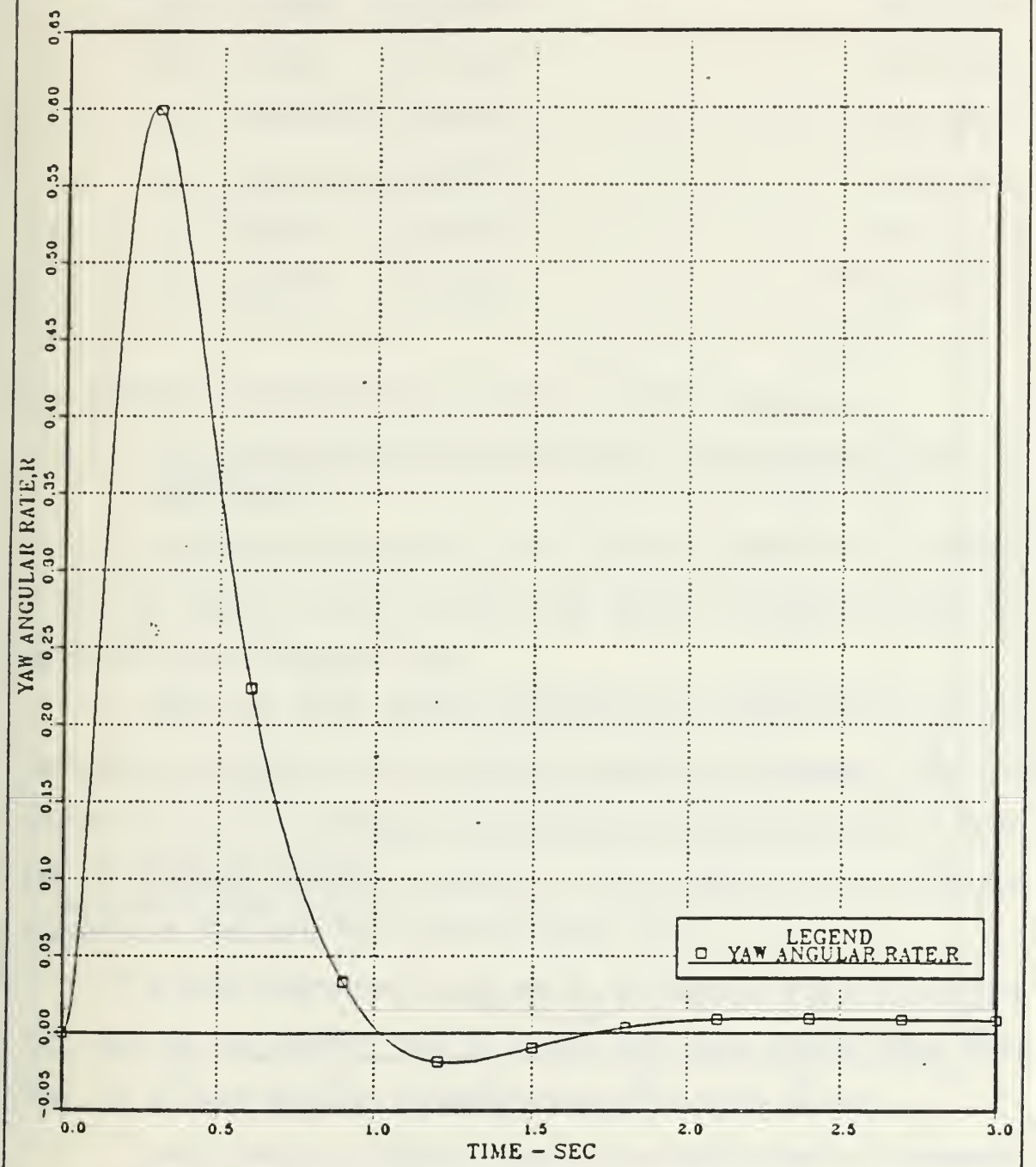

Figure 4.5 Yaw Angular Rate vs. Time; Uncoupled Yaw Channel Autopilot; Continuous Open Loop System; Elliptical Airframe; Step Input HY = 1 gee; $a_\beta = 0$.

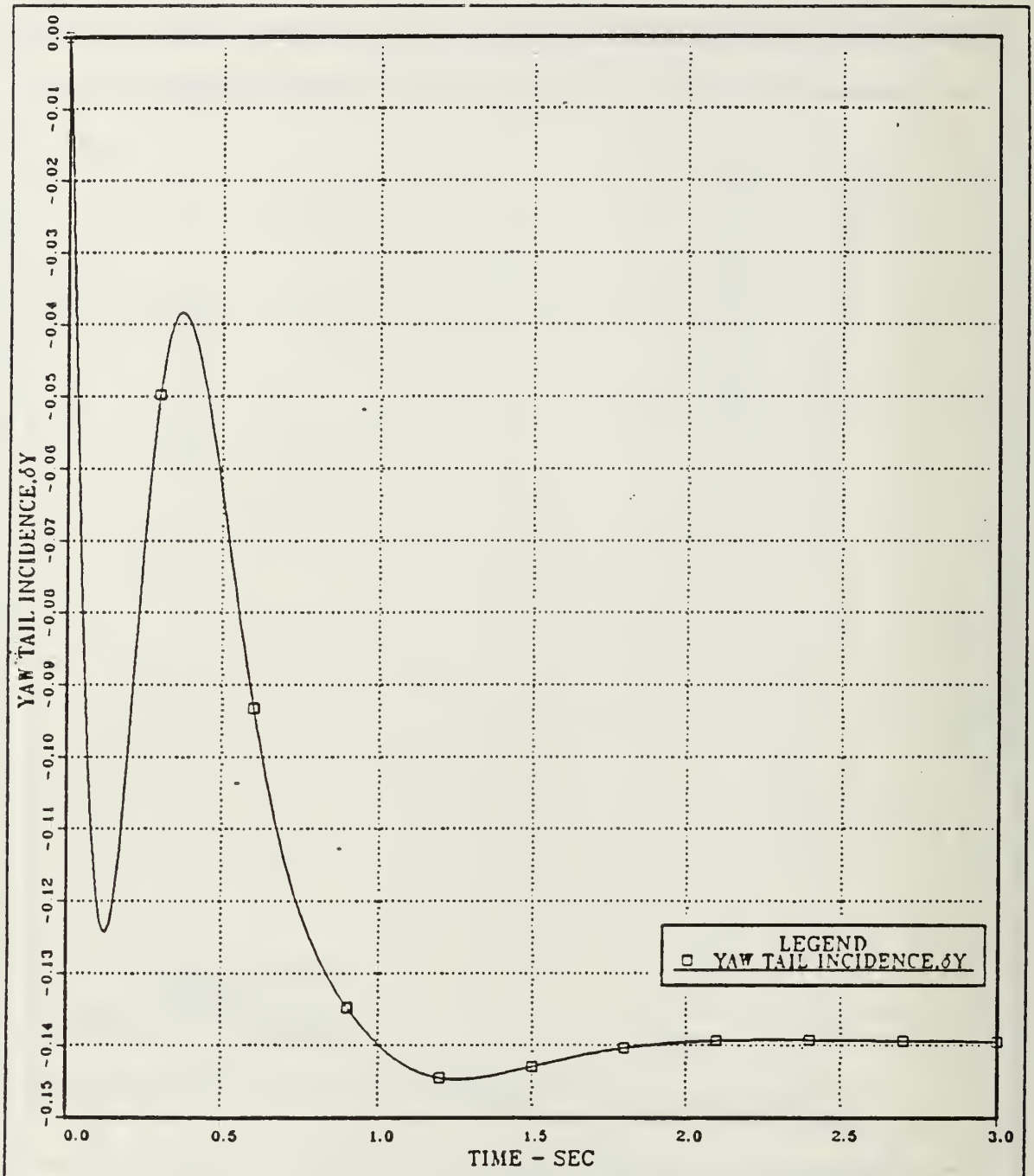

Figure 4.6 Yaw Tail Incidence vs. Time; Uncoupled Yaw Channel Autopilot; Continuous Open Loop System; Elliptical Airframe; Step Input HY = 1 gee; $a_B = 0$.

$s_2 = -5.7665 \quad +j10.4804$ (IV.B.3-11)

$s_3 = -5.7665 \quad -j10.4804$ (IV.B.3-12)

$s_4 = -0.0217473 \quad +j4.08919$ (IV.B.3-13)

$s_5 = -0.0217473 \quad -j4.08919$ (IV.B.3-14)

$s_6 = -2.9484 \quad +j2.99489$ (IV.B.3-15)

$s_7 = -2.9484 \quad -j2.99489$ (IV.B.3-16)

C. UNCOUPLED LINEAR OPEN LOOP ROLL CHANNEL (ORIGINAL)

1. The Aerodynamic Model, the Airframe Configuration and the Control Law

Generally, the purpose of a roll channel autopilot is to command a roll (φ) signal, in order to roll the missile through an angle (φ) measured from the vertical axis.

While the pitch channel acceleration is commanded to produce the total magnitude of the guidance acceleration command, the roll channel of the B.T.T. autopilot is commanded to roll the missile so as to put the prefered maneuver direction in the direction of the guidance acceleration command, as is shown in Figure 3.2.

A block diagram of the uncoupled roll channel is shown in Figure 4.7, and the roll control law in Figure 4.8 (both Figures taken from [Ref. 1]). In these diagrams the same aerodynamic model is used.

As is shown in Figures 4.7 and 4.8 the control law is commanded by a roll angle (φ_C), is governed by roll angular rate (P) and roll angle (φ) and determines the required command (δ_{Rc}) to an actuator. This is approximated as a first order lag at 188.4 rad/sec.

The circular airframe configuration is chosen for this channel and is shown in Figure 3.1. The flight conditions are the same as for the Yaw and Pitch channels, i.e. 60000 ft and Mack number 3.95.

2. Requirements for the Classical Design

Requirements for the classical design approach are:

a. High frequency attenuation in Actuator command branch ≥ 15 dB at 100 rad/sec and zero angle-of-attack. This requirement limits the speed of roll angle response.

b. Relative stability: gain margins ≥ 30^0 with a goal of 12 dB and 50^0, i.e. the same as for the yaw channel.

c. Acceleration time response :

(1) 63% time constant of 0.5 seconds for a step command of roll angle at the flight condition of interest and zero angle of attack.

(2) Overshoot ≤ 10%. This requirement is conservative and may be relaxed depending upon guidance results.

(3) Zero steady state roll angle error. If not zero, it will affect guidance.

3. Transfer Funcions of the Aerodynamic Model and Analysis

The aerodynamic transfer function of the uncoupled roll channel autopilot are [Ref. 4].

a. Transfer functions of the Roll Angular rate:

$$\dot{P} = (\bar{q} S d / I_{xx}) \times 57.3 \times C_{l\,\delta R}\ \delta_R \ (rad/sec^2)$$

where:

$\bar{q}$ = 1650 (lbs/ft^2)

S = 3. 14159 ft^2

d = 2 ft

I_{xx} =40 slug-ft^2

$C_{l\,\delta R}$ =0.031

$$\dot{P} = 8.0346\,\delta_R \qquad \text{(IV.C.3-1)}$$

b. Transfer function of Roll Angle:

$$\dot{\phi} = P \text{ (rad/sec)} \qquad \text{(IV.C.3-2)}$$

Rearranging the above equations along with those given in [Ref. 1] for the actuator and using rules of state-space representation, the following equations are obtained [Ref. 4] and verified:

$$\dot{P} = 8.03462\delta_R \qquad \text{(IV.C.3-3)}$$

$$\dot{\phi} = P \qquad \text{(IV.C.3-4)}$$

$$\dot{X} = -17.6\phi - 8X + 17.6\phi_c \qquad \text{(IV.C.3-5)}$$

$$\dot{Y} = -0.75325P - 0.8835\phi + 0.35165X - 5Y - 0.40334\delta_R + 0.88352\phi_c \qquad \text{(IV.C.3-6)}$$

$$\dot{X}_1 = -6X_1 + 0.6282291\delta_R \qquad \text{(IV.C.3-7)}$$

$$\dot{\delta}_{Rc} = -0.10271P - 0.12048\phi + 0.04795X + 14.3182Y - 14.18184X_1 - 15\delta_{Rc} \qquad \text{(IV.C.3-8)}$$

$$\dot{\delta}_R = 10795.32\delta_{Rc} - 188.4\delta_R \qquad \text{(IV.C.3-9)}$$

Utilizing state-state representation, the above Equations can be modeled as a seventh-order system in the format $\dot{X} = FX + GU$ with the continuous plant system F and control matrix G as shown in Table 4.1 and the state vector with the corresponding state variables as follows.

TABLE 4.1

PLANT SYSTEM AND INPUT MATRICES; UNCOUPLED ORIGINAL ROLL CHANNEL AUTOPILOT; CONTINUOUS OPEN LOOP SYSTEM CIRCULAR AIRFRAME

F MATRIX 7 ROWS 7 COLUMNS

0.0000000E+00	0.0000000E+00	0.0000000E+00	0.0000000E+00	0.0000000E+00	0.0000000E+00	8.0346200E+00
1.0000000E+00	0.0000000E+00	0.0000000E+00	0.0000000E+00	0.0000000E+00	0.0000000E+00	0.0000000E+00
0.0000000E+00	-1.7600000E+01	-8.0000000E+00	0.0000000E+00	0.0000000E+00	0.0000000E+00	0.0000000E+00
-7.5325000E-01	-9.9352000E-01	3.5165000E-01	-5.0000000E+00	0.0000000E+00	0.0000000E+00	-4.0334000E-01
0.0000000E+00	0.0000000E+00	0.0000000E+00	0.0000000E+00	-6.0000000E+00	0.0000000E+00	6.8291000E-01
-1.0271000E-01	-1.2048000E-01	4.7950000E-02	1.4318200E+01	-1.4181840E+01	-1.5000000E+01	-1.4067000E-01
0.0000000E+00	0.0000000E+00	0.0000000E+00	0.0000000E+00	0.0000000E+00	1.0725120E+04	-1.4840000E+02

G MATRIX 7 ROWS 1 COLUMNS

0.0000000E+00
0.0000000E+00
1.7600000E+01
9.9352000E-01
0.0000000E+00
1.2048000E-01
0.0000000E+00

P	Roll angular rate
φ	Roll angle
X	Output of roll angle compansator
Y	Output of roll rate compansator
X_1	Ouput of pseudodifferensiator
δ_{Rc}	Input command in the actuator
δ_R	Roll tail incidence

Executing the interactive implementation of the optimal systems control design program (OPTSYSX) using an input step function which represents "1 radian command" at zero trim angle of attack, the graphical time response plots were obtained for the state variables of interest.

Figure 4.9 shows the Roll Angular Rate (P) (rad/sec vs. time), Figure 4.10 the Roll Angle (φ) (rad vs. time), and Figure 4.11 the Roll Tail Incidence (δ_R) (deg. vs. time). A close observation in Figure 4.10 indicates that for the commanded input vector the time response plot of the roll angle has a 0.55 sec time constant, 5.3% overshoot and a steady-state error equal to zero. These results are in accordance with the requirements mentioned in the previous section.

From the pole-zero plot of Figure 2.23 [Ref.4] we can mention here that the continuous open loop system is stable, since the s-plane poles are:

$$s_1 = -174.785 \quad -j0 \qquad \text{(IV.C.3-10)}$$

$$s_2 = -9.2510 \quad +j28.4098 \qquad \text{(IV.C.3-11)}$$

$s_3 = -9.25097 \quad -j28.4098$ (IV.C.3-12)

$s_4 = -2.46608 \quad +j2.71152$ (IV.C.3-13)

$s_5 = -2.46608 \quad +j2.71152$ (IV.C.3-14)

$s_6 = -8.98209 \quad +j0$ (IV.C.3-15)

$s_7 = -5.19932 \quad +j0$ (IV.C.3-16)

4. Design Approach and Analysis of the Modified Model (Unimpaired)

To study reconfigurable flight controls the missile model should be capable of using the set of four available control surfaces to produce the required forces and moments.

To achieve this each control surface (δ_1, δ_2, δ_3, δ_4) was considered as an independent component.

The equations were then coupled so that a component of control surfaces used alone or in conjunction with another control surface, will produce the appropriate moments.

Taking under consideration the conventional control surface theory of Chapter II. for the Bank-to-Turn missiles, and for the circular configuration shown in Figure 3.4, one can easily show, for the continuous open loop roll autopilot that the input command in the actuator network (δ_{Rc}) can be split up into independent components, using the following equation which computes the deflection inputs to Equation (IV.C.3-8). Also refer to Figures 2.2 and 3.4 which show the control surface position and corresponding positive deflections.

$$+\delta_{Rc} = (\delta_1 - \delta_2 - \delta_3 + \delta_4) / 4 \qquad \text{(IV.C.4-1)}$$

Replacing the input vector in Equation (IV.C.3-8) and (IV.C.3-9) with the above Equation and applying the superposition principle, gives the following modified airframe equations:

$$\dot{\delta}_R = -188.4\delta_R + 10795.32\,(\delta_1 - \delta_2 - \delta_3 + \delta_4) / 4 \qquad \text{(IV.C.4-2)}$$

$$(\dot{\delta}_1 - \dot{\delta}_2 - \dot{\delta}_3 + \dot{\delta}_4) / 4 = -0.10271P - 0.12048\psi + 0.04795X + 14.318Y - 141818X_1 - 15/4\,(\delta_1 - \delta_2 - \delta_3 + \delta_4) - 0.14067\delta_R - 0.12048\psi_C \qquad \text{(IV.C.4-3)}$$

In Figure 4.6 the modification of the commanded tail incidence is presented.

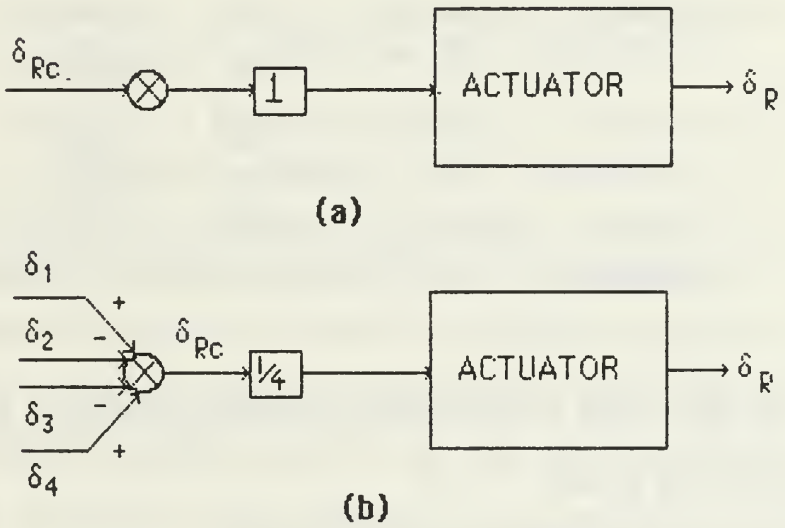

Figure 4.6 (a) Original System; (b) Modified System.

Rearranging the above equations and using the transfer functions of the system for the original uncoupled roll channel, Equations (IV.B.3-3)

through (IV.B.3-9), the following Equations were derived and can be modeled in a ten order system for the roll channel:

$$\dot{P}_1 = 8.03462\delta_R \qquad \text{(IV.C4-4)}$$

$$\dot{\psi} = P \qquad \text{(IV.C.4-5)}$$

$$\dot{X} = -17.6\psi - 8X + 17.6\psi_C \qquad \text{(IV.C.4-6)}$$

$$\dot{Y} = -0.75325P - 0.88352\psi + 0.35165X - 5Y - 0.40334\delta_R + 0.88352\psi_C \qquad \text{(IV.C.4-7)}$$

$$\dot{X}_1 = -6X_1 + 0.68291\delta_R \qquad \text{(IV.C.4-8)}$$

$$\dot{\delta}_1 = -0.10271P - 0.12048\psi + 0.04795X + 14.3182Y - 14.18184X_1 - 15\delta_1 - 0.14062\delta_R + 0.12048\psi_C \qquad \text{(IV.C.4-9)}$$

$$\dot{\delta}_2 = +0.10271P + 0.12048\psi - 0.04795X - 14.3182Y + 14.18184X_1 + 15\delta_1 + 0.14062\delta_R - 0.12048\psi_C \qquad \text{(IV.C.4-10)}$$

$$\dot{\delta}_3 = +0.10271P + 0.12048\psi - 0.04795X - 14.3182Y + 14.18184X_1 + 15\delta_1 + 0.14062\delta_R - 0.12048\psi_C \qquad \text{(IV.C.4-11)}$$

$$\dot{\delta}_4 = -0.10271P - 0.12048\psi + 0.04795X + 14.3182Y - 14.18184X_1 - 15\delta_1 - 0.14062\delta_R + 0.12048\psi_C \qquad \text{(IV.C.4-12)}$$

$$\dot{\delta}_R = 2698.83\delta_1 - 2698.83\delta_2 - 2698.83\delta_3 + 2698.83\delta_4 - 188.4\delta_R \qquad \text{(IV.C.4-13)}$$

We thus have a multiple-input-multiple-output (MIMO) system with the following order:

- $\dot{\mathbf{X}}$: 10×1, the time derivative of **X** matrix.
- **F** : 10×10, the open loop dynamic matrix or plant.
- **X** : 10×1, the variables assignments matrix.
- **G** : 10×5, the control distribution matrix.
- **U** : 5×1, the control input matrix.

The above control and output matrices of the Uncoupled Modified Unimpaired Roll Channel Autopilot are presented at the Appendix B.

The Eigenvalues found executing the OPTSYS Control Program, that is the DET(sI-F) values, show that the open loop system is stable, since the s-plane poles are:

S_1 = -185.057 + j0 (roll angular rate)

S_2 = -9.27462 + j29.2679 (roll angle)

S_3 = -9.27462 - j29.2679

S_4 = -2.35821 + j2.70296

S_5 = -2.35821 - j2.70296

S_6 = -8.89209 + j0 (input command in the actuator)

S_7 = -5.18517 + j0 (roll tail incidence)

S_8 = -15.000 + j0

S_9 = -15.000 + j0

S_{10}= -15.000 + j0

5. Analysis and Comparison with the Original System

Applying the same step input function as in Section IV.C.3 which represents the "1 radian command", and for zero rad deflection command for the four control surfaces (i.e, δ_{1C}, δ_{2C}, δ_{3C}, δ_{4C} = 0) the time response plots of the following state-variables of interest were obtained and presented in the Figure 4.12 through 4.15.

a. Roll Angle (ψ or F), Figure 4.12, rad vs. time which has:

(1) A time constant 0.6 seconds

(2) A 5.3% overshoot.

(3) Zero steady-state error and so the guidance will not be effected.

(4) Delay time 0.48 sec and settling time 2.2 sec when the steady state roll angle is achieved.

b. Roll Angular Rate (P or p), Figure 4.13, rad/sec vs. time, which has:

(1) A maximum body angular rate 1.58 rad/sec at 0.4 second.

(2) A 4.2% undershoot and a 2.4 sec settling time.

c. Roll Tail Incidence (δ_R or DR), Figure 4.14, degrees vs. time, which has:

(1) Initially and very fast, 0.1 sec, the maximum required deflection occurs, that is 1.17 degrees. Then changes direction to the opposite deflection angle in 0.6 sec to -0.32 deg. before stabilizing.

(2) A 2.6 sec settling time .

d. Deflections (δ_1, δ_2, δ_3, δ_4 or D's), Figure 4.15, rad vs. time, which has:

(1) The actuators δ_1 and δ_4 have the same sign (positive), as was expected according to the sign convention of Figure 2.2, and are first deflected to a 0.02 rad angle and then to -0.05 radians after 0.6 seconds. Finally the steady state zero angle of deflection is achieved at 2.6 seconds.

(2) The δ_2 and δ_3, have the same response sa above but with a negative sign.

As was shown the relative stability for zero-angle-of-attack is satisfactory for the modified unimpaired system.

A close observation of Figures 4.12 throught 4.15 and the above analysis, indicates that the corresponding obtained responses are identical, with those of the original roll channel, Figures 4.9, 4.10 and

4.11. So, the performance of the designed system meets the perviously mentioned requirements.

In table 4.2 a summary of the stability margins is presented, obtained from the frequency response plots calculated up to 100 rad/sec.

TABLE 4.2

PHASE CROSSOVER FREQUENCIES AND GAIN MARGINS;
UNCOUPLED MODIFIED ROLL CHANNEL(UNIMPAIRED);
CIRCULAR AIRFRAME

	PHASE CROSSOVER FREQUENCY(RAD/SEC)	GAIN MARGIN(DB)
ROLL ANGLE (φ)	10.0461	60.2165
ROLL ANGULAR RATE (P)	10.0461	60.2165
ROLL TAIL INCIDENCE (δ_p)	10.0461	42.1172

We procceed now to the analysis of the impaired control surfaces for the modified system.

D. CONTROL EFFECTIVENESS DUE TO THE CONTROL SURFACES IMPAIRMENT AND COMPARISON

The time response plots for the system are obtained in this section for two types of damages. The first type is the locked or hard over actuator at a small angle and the second type includes the centered or inoperative one, two and three control surfaces.

Note that the first phase of the design approash for the CBTT autopilot was to design each channel independently with all coupling

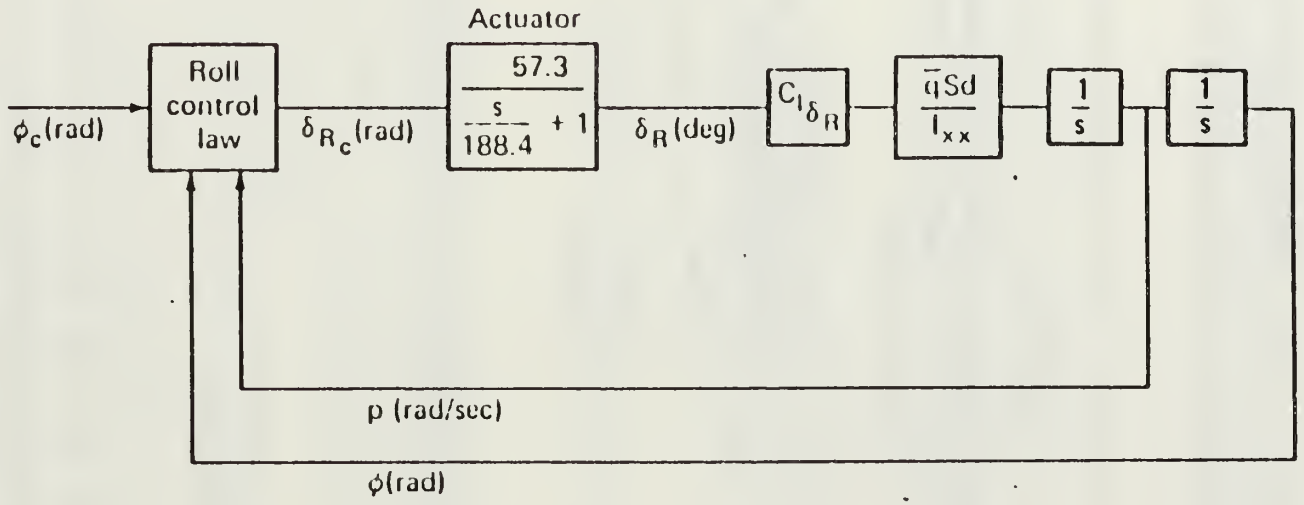

Figure 4.7 Uncoupled Roll Channel.

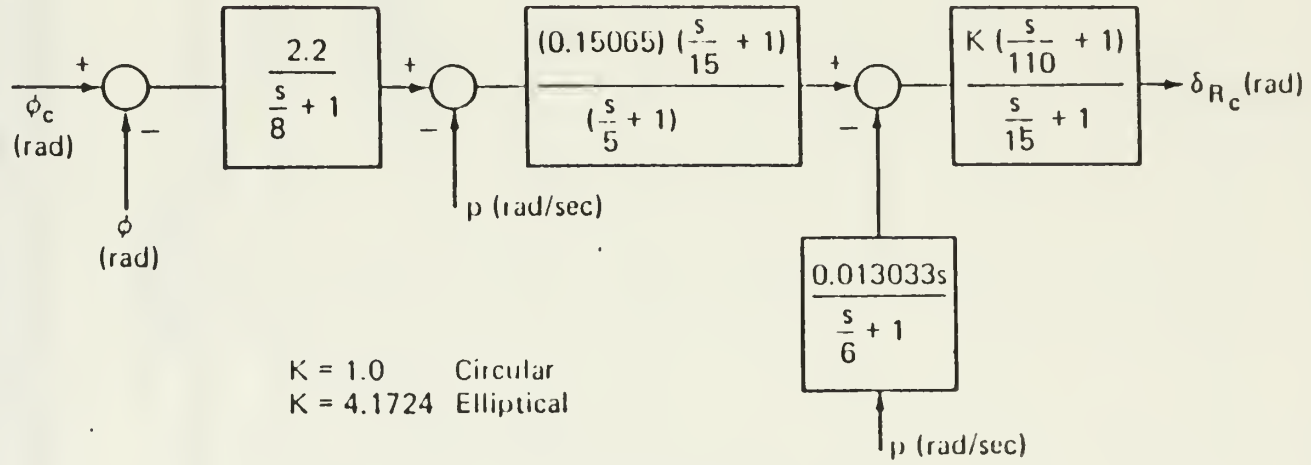

Figure 4.8 Roll Control Law.

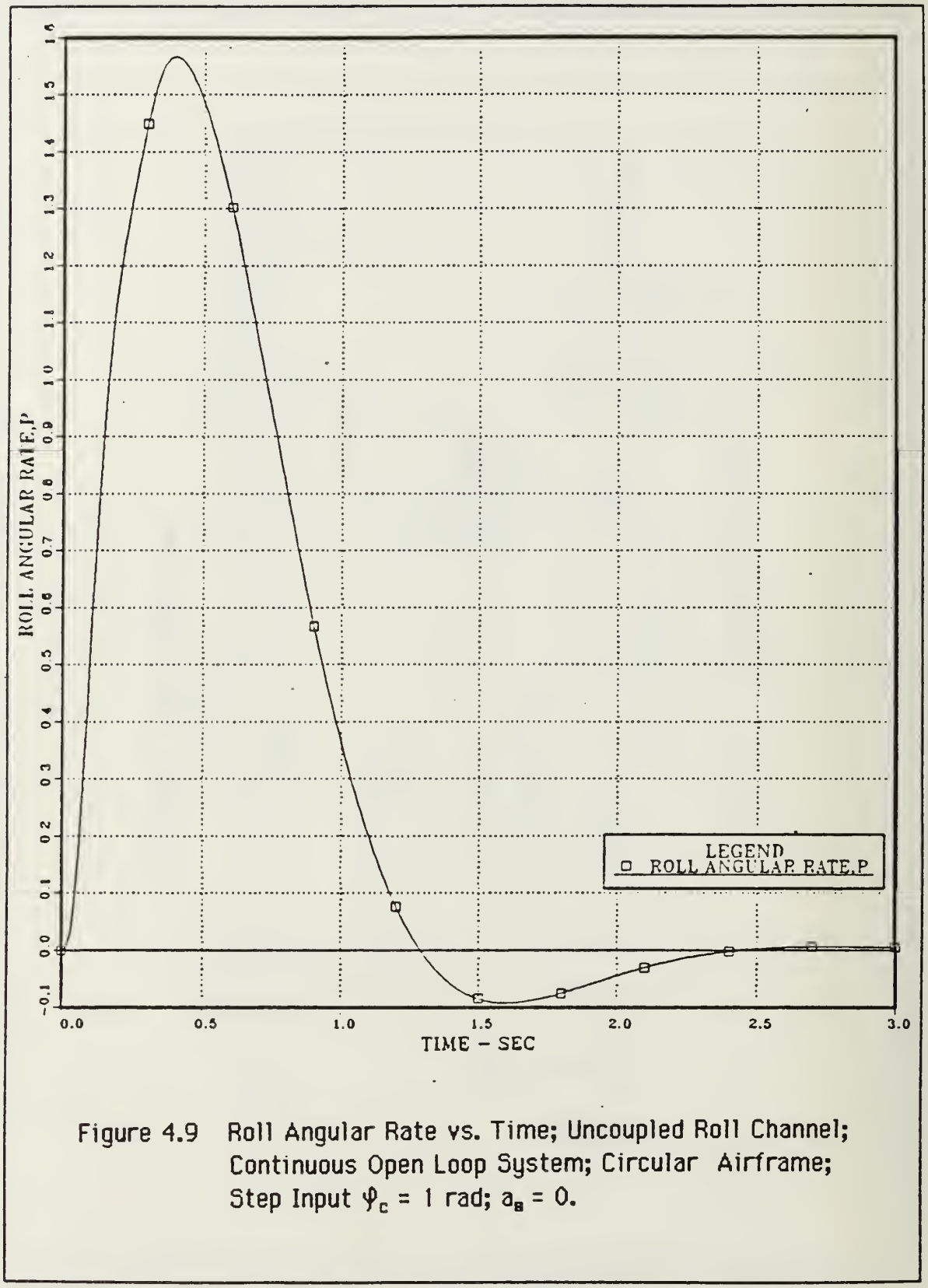

Figure 4.9 Roll Angular Rate vs. Time; Uncoupled Roll Channel; Continuous Open Loop System; Circular Airframe; Step Input φ_c = 1 rad; a_s = 0.

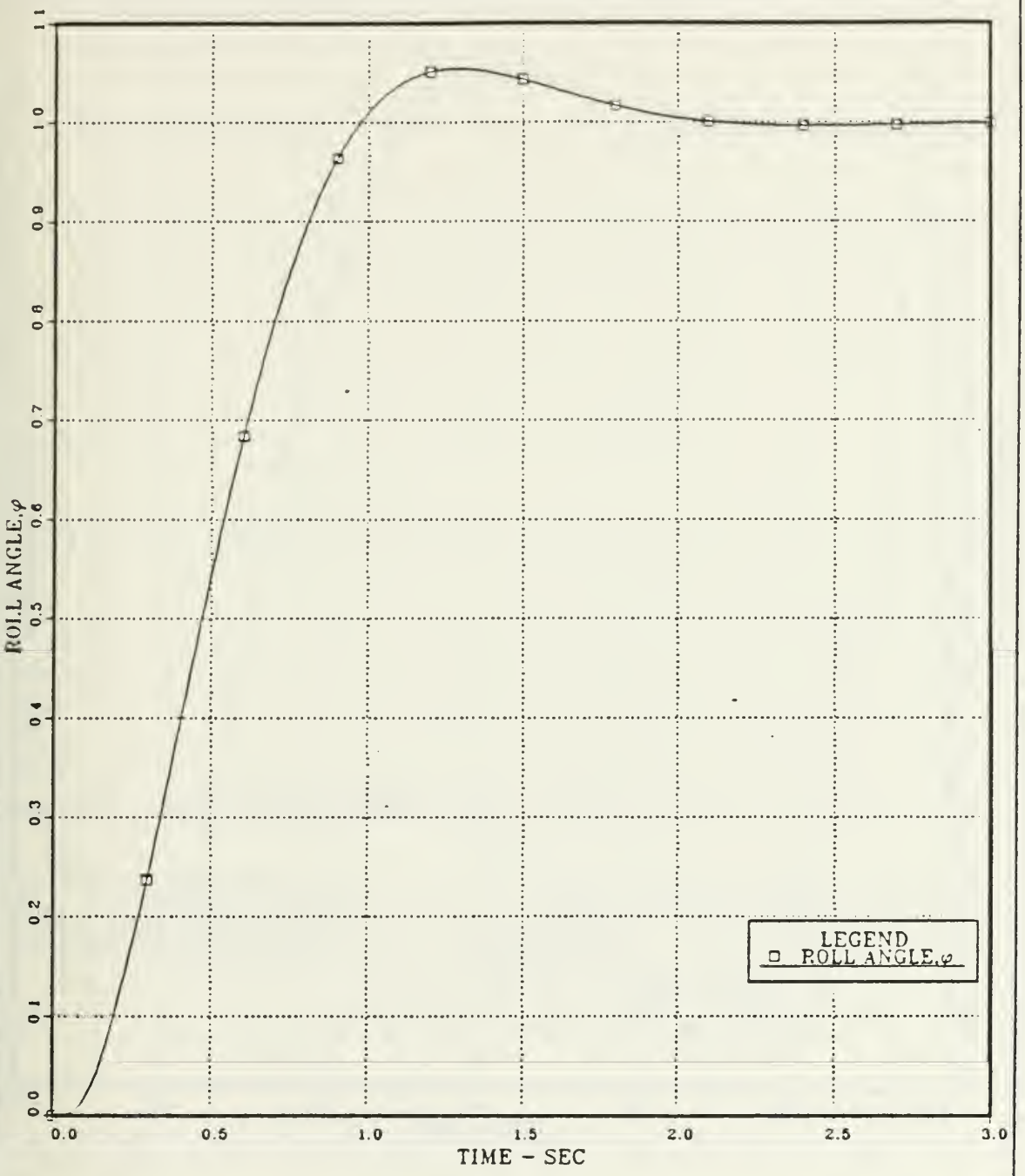

Figure 4.10 Roll Angle vs. Time; Uncoupled Roll Channel; Continuous Open Loop System; Circular Airframe; Step Input ψ_c = 1 rad; a_β = 0.

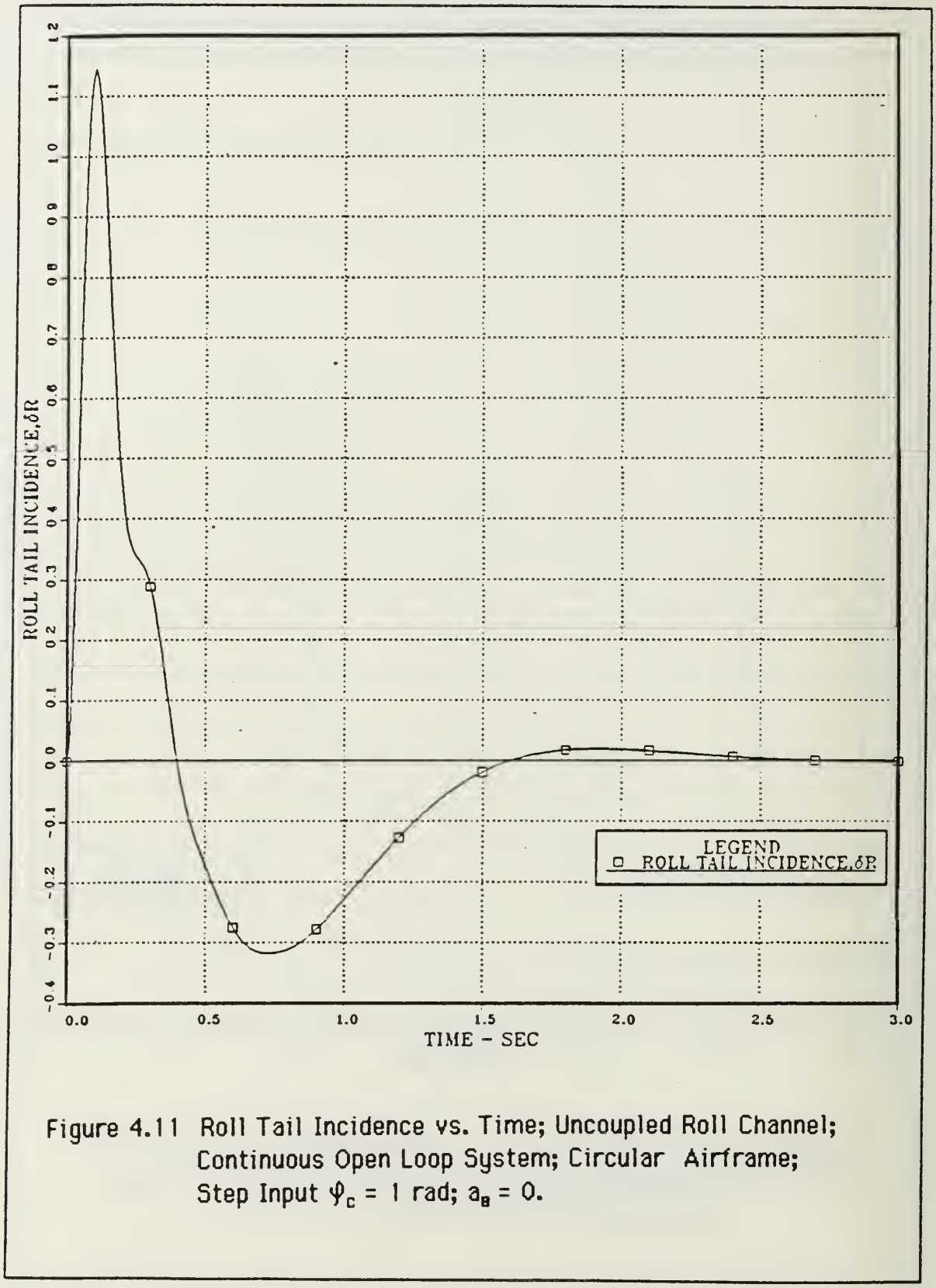

Figure 4.11 Roll Tail Incidence vs. Time; Uncoupled Roll Channel; Continuous Open Loop System; Circular Airframe; Step Input φ_c = 1 rad; a_B = 0.

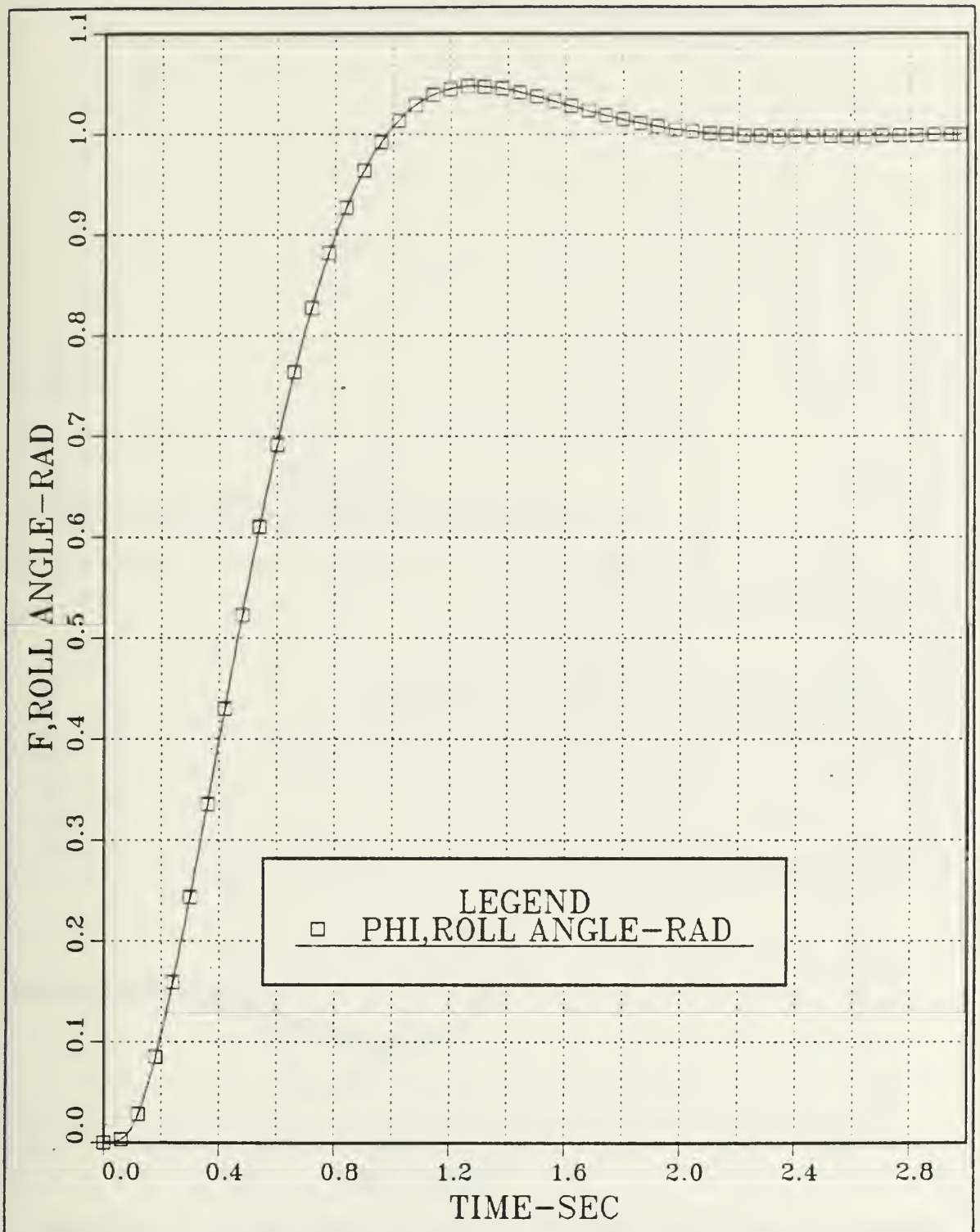

Figure 4.12 Roll Angle vs. Time; Uncoupled Modified Unimpaired Channel; Continuous Open Loop system; Step Input : $\varphi_c = 1$ and $\delta_{1c}, \delta_{2c}, \delta_{3c}, \delta_{4c} = 0$; $a_\theta = 0$.

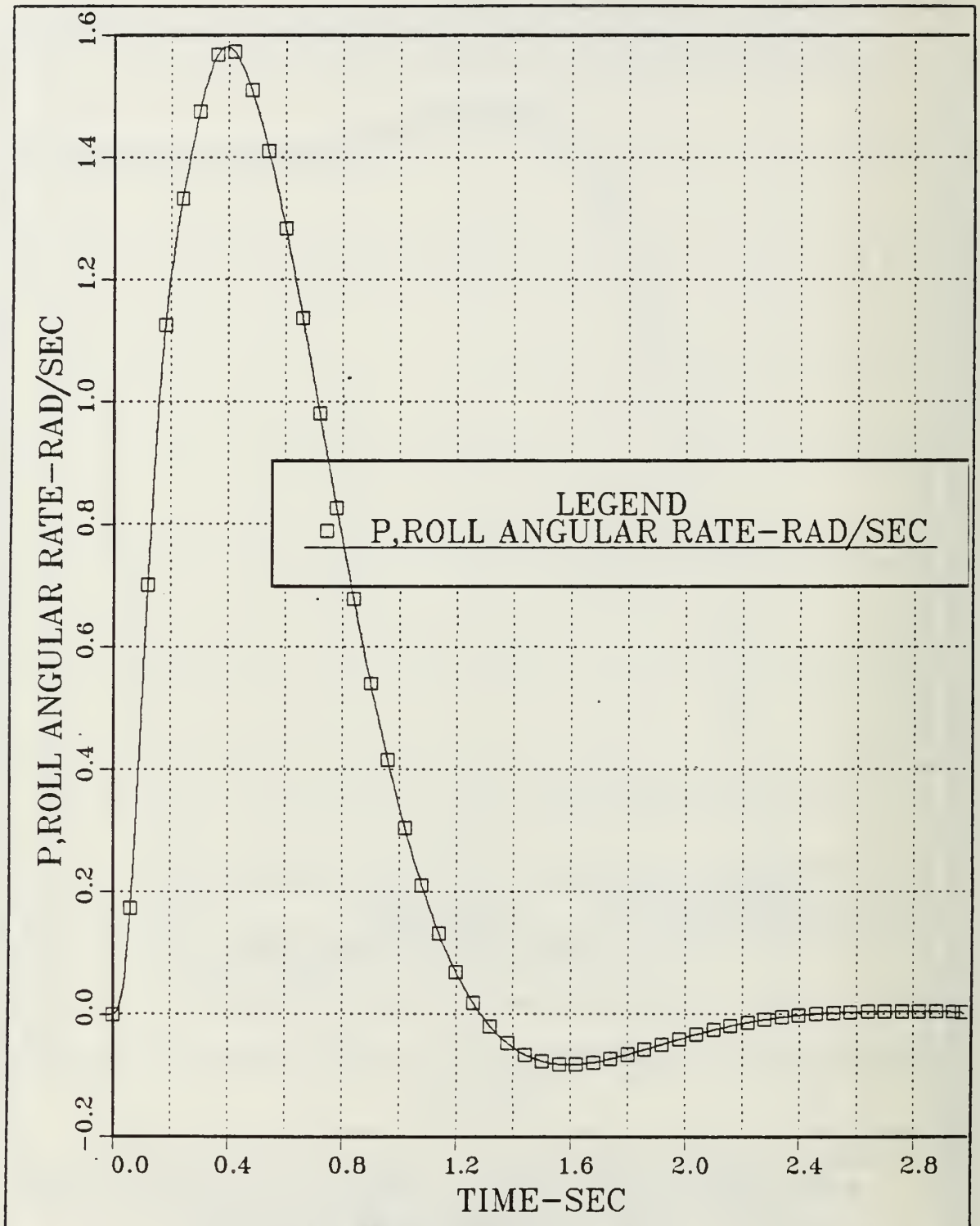

Figure 4.13 Roll Angular Rate vs. Time; Uncoupled Modified Unimpaired Channel; Continuous Open Loop system; Step Input : Ψ_c = 1 and δ_{1c}, δ_{2c}, δ_{3c}, δ_{4c} = 0 ; a_e = 0.

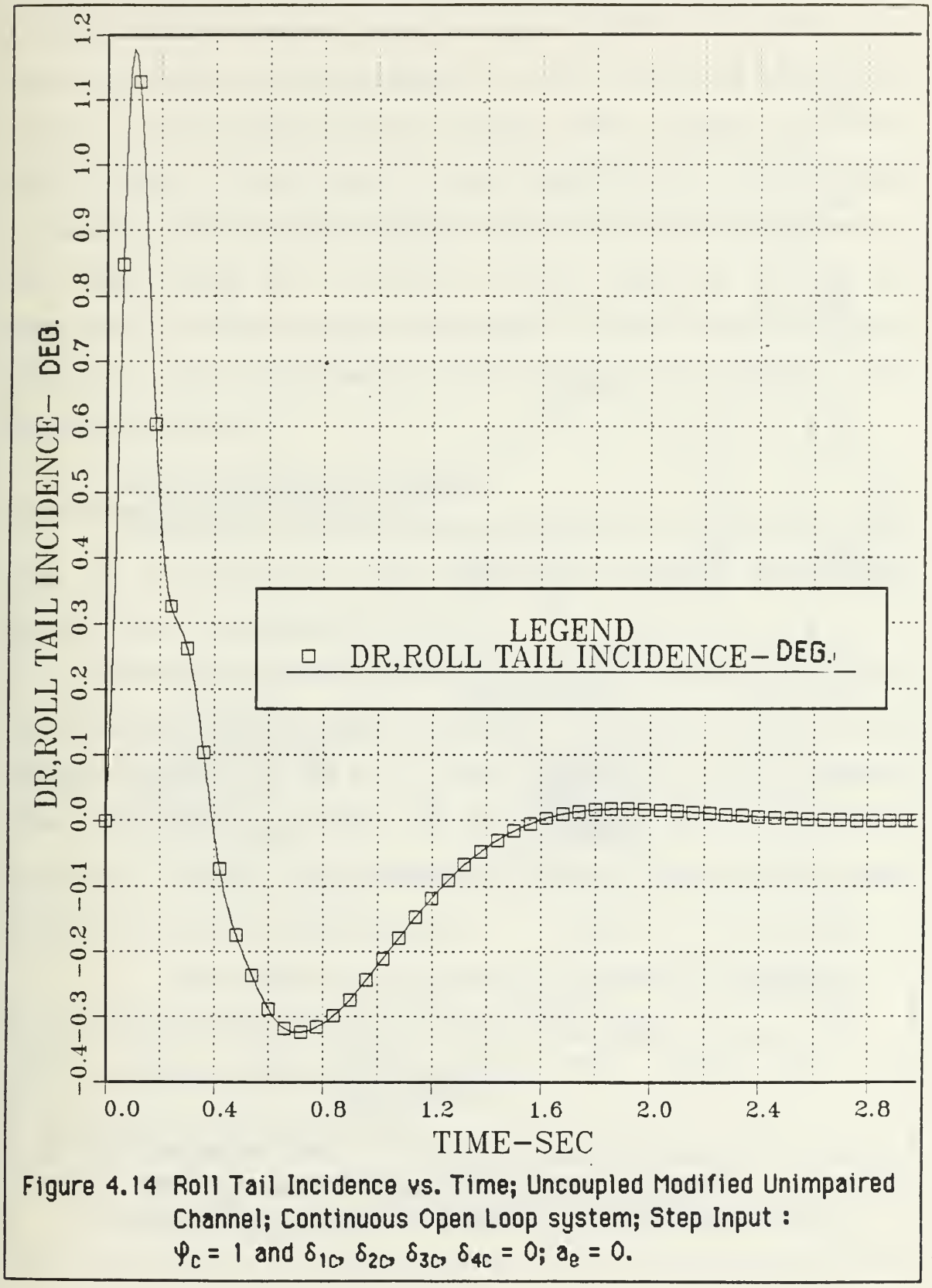

Figure 4.14 Roll Tail Incidence vs. Time; Uncoupled Modified Unimpaired Channel; Continuous Open Loop system; Step Input : $\psi_c = 1$ and $\delta_{1c}, \delta_{2c}, \delta_{3c}, \delta_{4c} = 0$; $a_e = 0$.

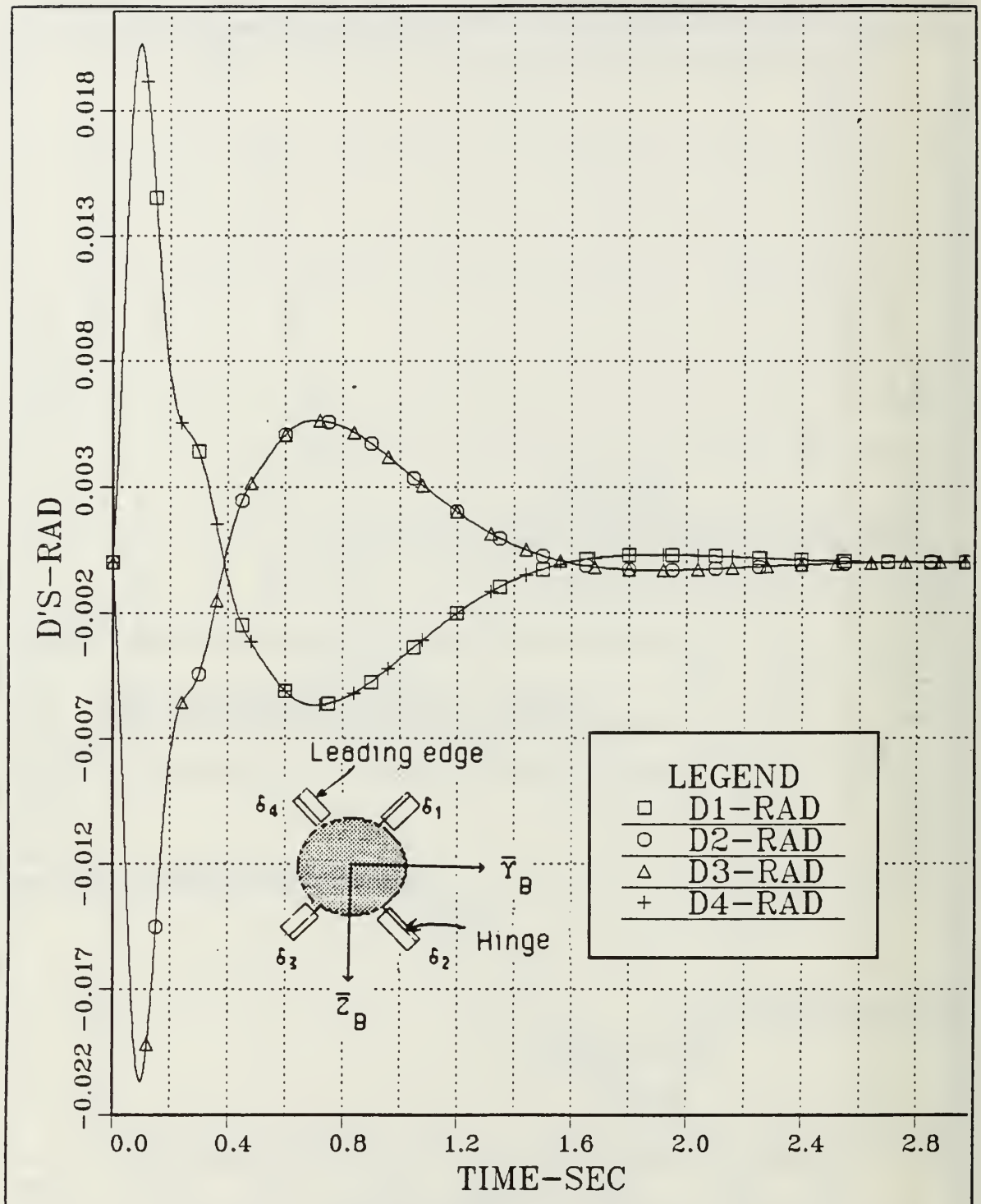

Figure 4.15 Control Surfaces Deflections vs. Time; Uncoupled Modified Unimpaired Channel; Continuous Open Loop system; Step Input : $\psi_C = 1$ and $\delta_{1C}, \delta_{2C}, \delta_{3C}, \delta_{4C} = 0$; $a_e = 0$.

between channels removed. Sufficient high frequency attennuation was added for actuator and missile design so that the resulting missile body angular rates and control surfaces motion would represent a practical missile design. A relationship was established among the relative speeds of response of the uncoupled channels in order to meet CBTT requirements. The cross-coupling due to control surfaces impairment between the longitudinal and lateral motion of the missile is ignored when each control channel is treated independently. Cross-coupling of the controls is thus considered in Chapter V.

1. Hard Over One Control Surface

One control surface (δ_1), was selected to be deflected or hard over, i.e. it remained at a fixed angle while the other three control surfaces had a variable deflection angle.

Using a step input 1 radian for the commanded roll angle (φ_C) (as in the original and unimpaired models); an angle of 0.2 rad for the damaged surface (δ_{1C}); and a zero angle of deflection, for the remaining other three (δ_{2C}, δ_{3C}, andδ_{4C}). The time response plots of the state variables of interest were obtained and analyzed with the performance criteria as defined in section (III.B.4).

a. Roll Angle (φ or F), Figure 4.16, (radians vs. time) has:

(1) A time constant 0.6 sec and 0.3 sec delay time .

(2) A constant 0.4 rad steady state error.

(3) A 5.8% overshoot at 1.2 sec.

(4) The roll angle is stabilized at an incorrect angle of 1.4 rad instead of the commanded 1 radian due to the impairment of δ_1 surface.

b. Roll Angular Rate (P), Figure 4.17 (radians/sec vs. time) which has:

(1) Initially and due to the fact that δ_1 is locked at a positive angle of 0.2 rad, to achieve the the roll command, the angular rate increases very fast the first tenth of the second to a 2.1 rad/sec rate. Then, a pronounced oscillation occurs until the 0.4 sec when the rate begins to decrease crossing the zero rate at 1.2 sec corresponding to the max roll angle (1.5 rad).

(2) The initial increase of the rate is due to the induced rolling moment caused by the deflection of the damaged control surface while the other three are at their steady position.

(3) A 6.6% undershoot at 1.5 sec and settling time 2.5 sec.

c. Roll Tail Incidence (δ_R or DR), Figure 4.18 (deg. vs. time) which has:

(1) At time equal to 0.1 sec the actuator is commanded to an angle 4.75 degrees. This is is due to the fact that δ_1 is hard over at the 0.2 rad angle while the other three remain have a zero initial condition. Then the tail incidence is stabilized after a 2 second period during which a fluctuation occurs.

(2) A zero steady-state error and 2.2 sec settling time.

d. Control Surface Deflections (δ_1, δ_2, δ_3,δ_4 or D's), Figure 4.19, rad vs. time, which has:

(1) The actuator δ_1, is deflected at the angle of 0.2 rad, from zero sec up to 3 seconds.

(2) The commanded input vector now causes the two surfaces δ_2 and δ_3 to turn in a positive angle of 0.13 rad, instead of a negative angle as when no impairment existed.

(3) A 1.6 seconds settling time to achieve this angle.

(4) The fourth surface δ_4 is commanded to turn at an angle of equal amount but with an opposite sign, for the same reasons.

A comparison between Figure 4.19 and 4.15 of the unimpaired system, shows that to achieve the roll response the impaired sustem requires more control surfaces deflection and more time.

2. Damage One Control Surface

The δ_1 control surface was selected to simulate the inoperative actuator. The corresponding state variable δ_1 was therefore set equal to zero. The step input of one radian remained the same. The initial condition on the control surface was set at zero. This type of damage could also represent the dedtruction of the control surface.

For the above case the time response plots of the state variables of interest were obtained and analyzed. Later in Section 5, a comparison between the different type of damages and the unimpaired system is performed.

a. Roll Angle (φ or F), Figure 4.20, rad vs time, which has:

(1) A 0.6 second time constant.

(2) An overshoot equal to 5.6% and

(3) Zero Steady state error.

(4) Delay time 0.5 sec and 2.1 sec settling time at which the the roll response is achieved.

b. Roll Angular Rate (P), Figure 4.21, radian/sec vs. time, which has:

(1) A maximum body angular rate 1.58 rad/sec at 0.4 sec.

(2) A 6.3% undershoot.

(3) A 2.5 sec settling time at which the zero steady state value is achived.

c. Roll Tail Incidence (δ_R or DR), Figure 4.22, deg. vs. time, which has:

(1) At the very beginning of the response, 0.1 sec, the maximum deflection occurs, that is 1.1 degrees, to change then to the opposite deflection angle in 0.7 sec to -0.32 deg.

(2) A zero steady state error and settling time 2.6 sec.

d. Control surfaces deflection (δ_R or DR), Figure 4.23, deg. vs. time which has:

(1) The surface δ_1 as damaged remains constantly at zero angle of deflection.

(2) The actuators δ_2 and δ_3 are deflected at a negative angle 0.026 rad and are stabilized after 2.4 seconds.

(3) The actuator δ_4 is deflected at an equal but opposite angle as it was expected according to the selected sign convention.

A comparison between the deflection angle in Figures 4.15, 4.19 and 4.23 indicates that for the same step input:

(1) When one control surface is inoperative or shot away the system commands the undamaged surfaces at larger angles (in comparison with the unimpaired system).

(2) When one control surface is inoperative or shot away the system commands the undamaged surfaces at smaller angles than obtained with the hard over type of damage.

(3) The required time that the undamaged control surfaces need to achieve the zero steady state value is the same (in comparison with the unimpaired system).

3. Damage Two Control Surfaces

In this case two control surfaces, on the same side of the missile were considered damaged (δ_1 and δ_2). The two state variables δ_1 and δ_2 were therefore set equal to zero. The step input of one radian remained the same. The initial condition of the control surfaces was set at zero. Then the time response plots of the state variables were obtained and analyzed.

a. Roll Angle ($\dot{\varphi}$ or F), Figure 4.24, rad vs. time, which has:

(1) Time constant 0.59 seconds

(2) An overshoot 6.8% at 1.25 sec and an undershoot of 0.003% at 2.2 seconds.

(3) A zero steady-state error and a 0.5 sec delay time.

(4) The commanded roll angle is achieved after 2.8 seconds.

b. Roll Angular Rate (P), Figure 4.25, radian/sec vs. time, which has:

(1) The peak body angular rate 1.61 rad/sec is achieved at 0.41 sec.

(2) An 8.2% undershoot at 1.6 sec and

(3) A 2.6 sec settling time.

c. Roll Tail Incidence (δ_C or DR), Figure 4.26, deg. vs. time, which has:

(1) The peak angle is 1.01 degrees at 0.1 sec and then in 0.6 seconds a negative angle (-0.35 deg) is commanded.

(2) A second 6.3% overshoot at 1.8 sec and

(3) Zero steady state error (settling time 2.6 sec).

d. Control surface deflection (δ_1, δ_2, δ_3, δ_4 or D's), Figure 4.27, rad vs. time, which has:

(1) The two inoperative or shot away control surfaces δ_1 and δ_2 remain always at zero angle of deflection.

(2) The two remaining actuators δ_3 and δ_4 moving at opposite directions, as expected, with a peak value of ±0.35 radians.

(3) The impairment of δ_1 and δ_2 has produced a more overshoot lags system as evidenced in Figure 4.27.

(4) The convergent and oscillatory behavior of the two unimpaired control surfaces which attempt to "fill in" for the damaged surfaces is shown in the same Figure. Also note that for this system with two impaired control surfaces more angle of deflection is required (incomparison with the system having one actuator shot away).

4. Damage Three Control Surfaces

In the last case three of the control surfaces δ_1, δ_2 and δ_3 were damaged or inoperative.

With a step input of one radian for the commanded roll angle (φ_c) as in the unimpaired and other type damaged models, the plots of the state variables of interest were obtained and analyzed.

Figures 4.28 through 4.31 illustrate the response of the output variables. Figure 3.30 shows that the commanded one radian roll angle can still be achieved in the absence of three control surfaces (δ_1, δ_2, δ_3). However, some oscilation is evident in the response. The loss of the surfaces has produced a more lightly damped system as evidenced in Figures 4.28 through 4.31. The oscillatory and convergent behavior of the roll rate and the undamaged surface (δ_4), shown in Figures 4.29 and 4.31, illustrate how the surface attempt to "fill in" for the absence of the

inoperative control surfaces. Specifically the response of the roll angle (Figure 4.28) has:

(1) A 0.55 sec time constant.

(2) A max. 10.5% overshoot at 1.2 sec and a 0.5% undersoot at 2.2 sec.

(3) The commanded roll angle is achieved after 2.8 sec.

(4) A 0.51 sec delay time .

A comparison with the response of the corresponding deflection of the unimpaired system (Figure 4.15) and the other inoperative cases, Figures 4.19, 4.23 and 4.31, indicates that as the number of the inoperative control surfaces increases, the deflection of the undamaged actuator(s) also increases and more time is required to acheive th steady-state value.

5. Comparison with the Unimpaired System

In this section a performance comparison of each type of impairment with the unimpaired system, was performed and an analysis of their corresponding time plots is presented.

For the above purposes, a computer program was written (Appendix D) to create a data file, for the state variables of interest, to be used as input data in the use of the EASYPLOT program of the NPS computer.

For the decoupled roll channel the first plots are for the roll angle and are presented in Figures 4.32 and 4.33

In Figure 4.32 which compares the two types of impairments with the original (unimpaired) system it is quite obvious that the worst case is the hard over case because when the autopilot is commanded at a

roll angle (φ_c) equal to 1 radian, the missile turns at a roll angle (φ) of 1.4 rad instead of 1 rad as for the unimpaired autopilot.

Other characteristic point is that for the hard over case, the roll angle reaches its final value of 1.4 rad (80.2^0) in approximately 2 seconds with a 5.8% overshoot, without any steady state error.

Figure 4.33 compares the roll angle of the unimpaired system with the three cases of control surfaces impairments. The curves include the following four cases:

(1) Original system

(2) Inoperative one control surface

(3) Inoperative two control surfaces

(4) Inoperative three control surfaces

This Figure shows that as the number of the damaged control surfaces increases the overshoot and the settling time icrease.

Figures 4.34 and 4.35 compare the roll angular rate of the unimpaired system with four cases of control surfaces impairments. The curves include the following five cases:

(1) Original system

(2) Hard over one control surface

(3) Inoperative one control surface

(4) Inoperative two control surfaces

(5) Inoperative three control surfaces

In Figure 4.34 it is shown that the hard over case induce greater excursion in the roll rate with a peak value of 2.2 rad/sec at 0.38 sec being achieved. Due to the fact that δ_1 control surface is deflected at the

0.2 rad the initial rolling moment in the first tenth of the second increases from zero to 2.1 rad/sec. The other control surfaces have zero as an initial condition.

Figure 4.35 compares the unimpaired system with three cases of control surfaces impairments (inoperative one, two and three actuators). In this is shown that the inoperative cases are all quite similar except for the last case where only one control surface is available. In this last case a larger delay time, overshoot and undershoot are evident.

Finally in Figures 4.36 and 4.37 the roll tail incidence is compared and include the following cases:

(1) Original system

(2) Hard over one control surface

(3) Inoperative one control surface

(4) Inoperative two control surfaces

(5) Inoperative three control surfaces

Figure 4.36 shows that the required roll incidence for the hard over case is larger in comparison with the unimpaired system and with the other three cases of control surfaces impairment. In Figure 4.37 the maximum peak overshoot decreases with the number of control surfaces that are impaired.

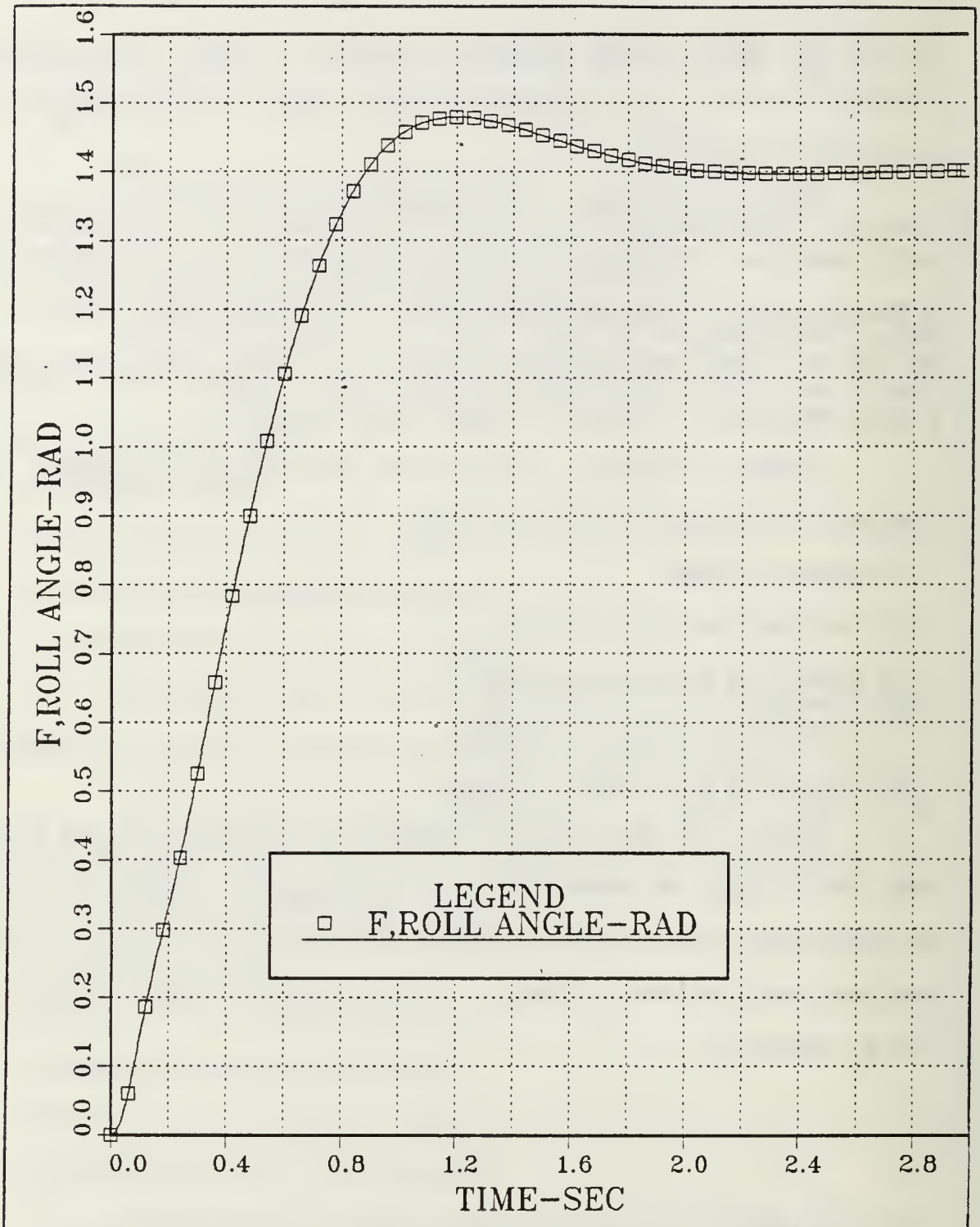

Figure 4.16 Roll Angle vs. Time; Uncoupled Modified Roll Channel with δ_1 Hard Over; Continuous Open Loop System; Step Input: ψ_c = 1 and δ_{1c}=0.2 rad; δ_{2c},δ_{3c},δ_{4c}=0; a_e = 0.

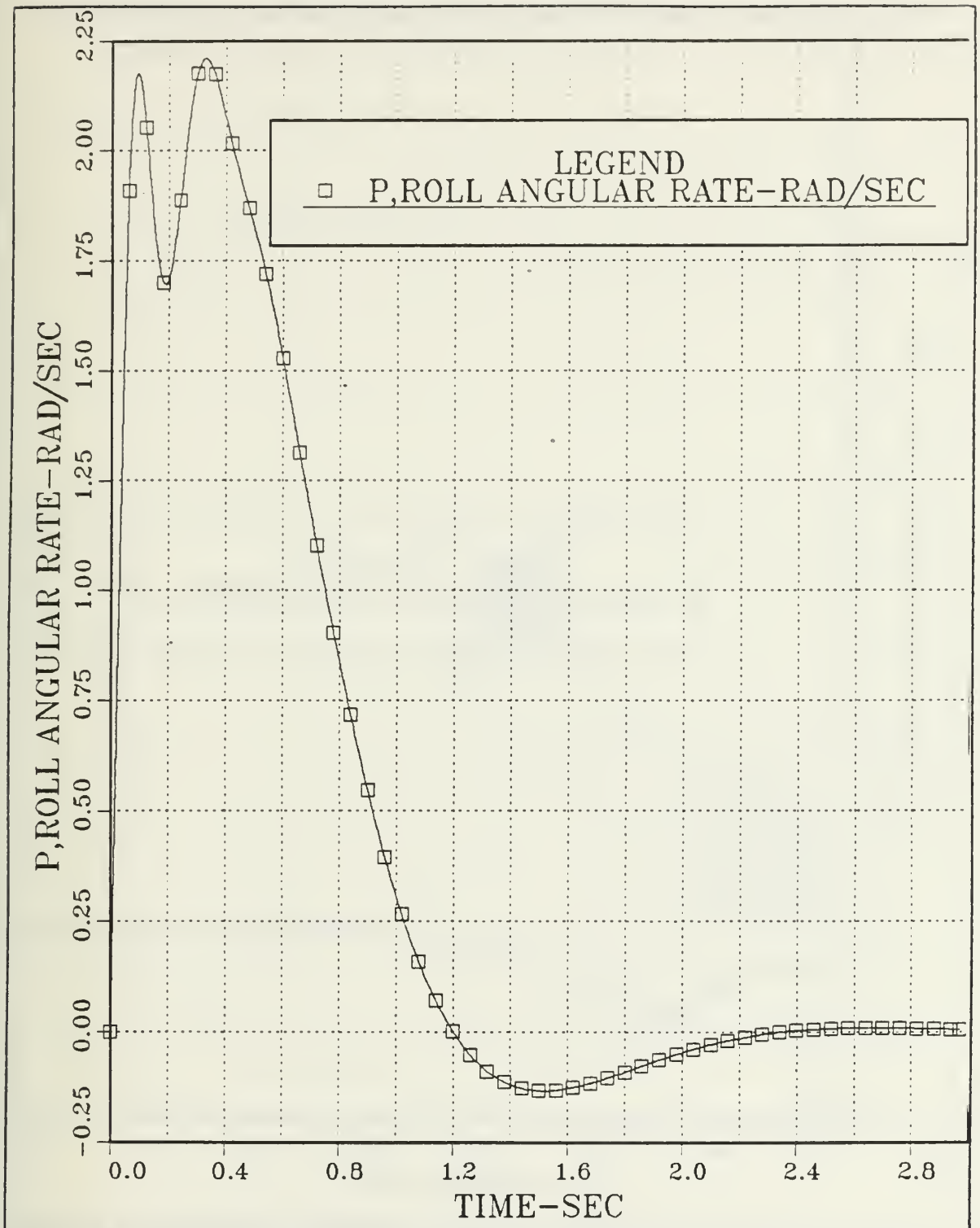

Figure 4.17 Roll Angular Rate vs. Time; Uncoupled Modified Roll Channel with δ_1 Hard Over ; Continuous Open Loop System; Step Inputs: δ_1=0.2 rad; $\delta_2,\delta_3,\delta_4$=0; ψ_C=1 rad and a_B = 0.

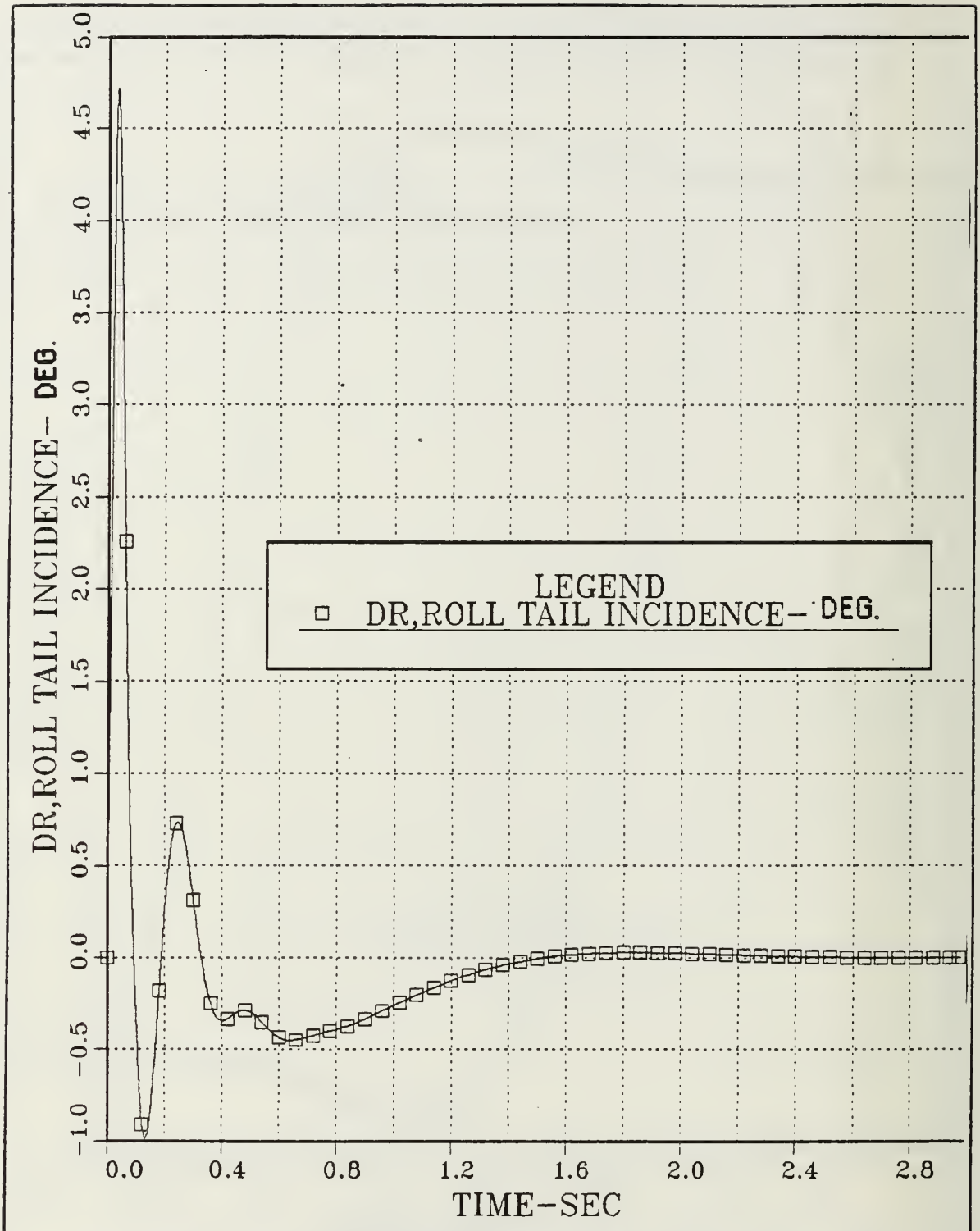

Figure 4.18 Roll Tail Incidence vs. Time; Uncoupled Modified Roll Channel with δ_1 Hard Over ; Continuous Open Loop System; Step Inputs: δ_1=0.2 rad; $\delta_2,\delta_3,\delta_4$=0; Ψ_C=1 rad and a_β = 0.

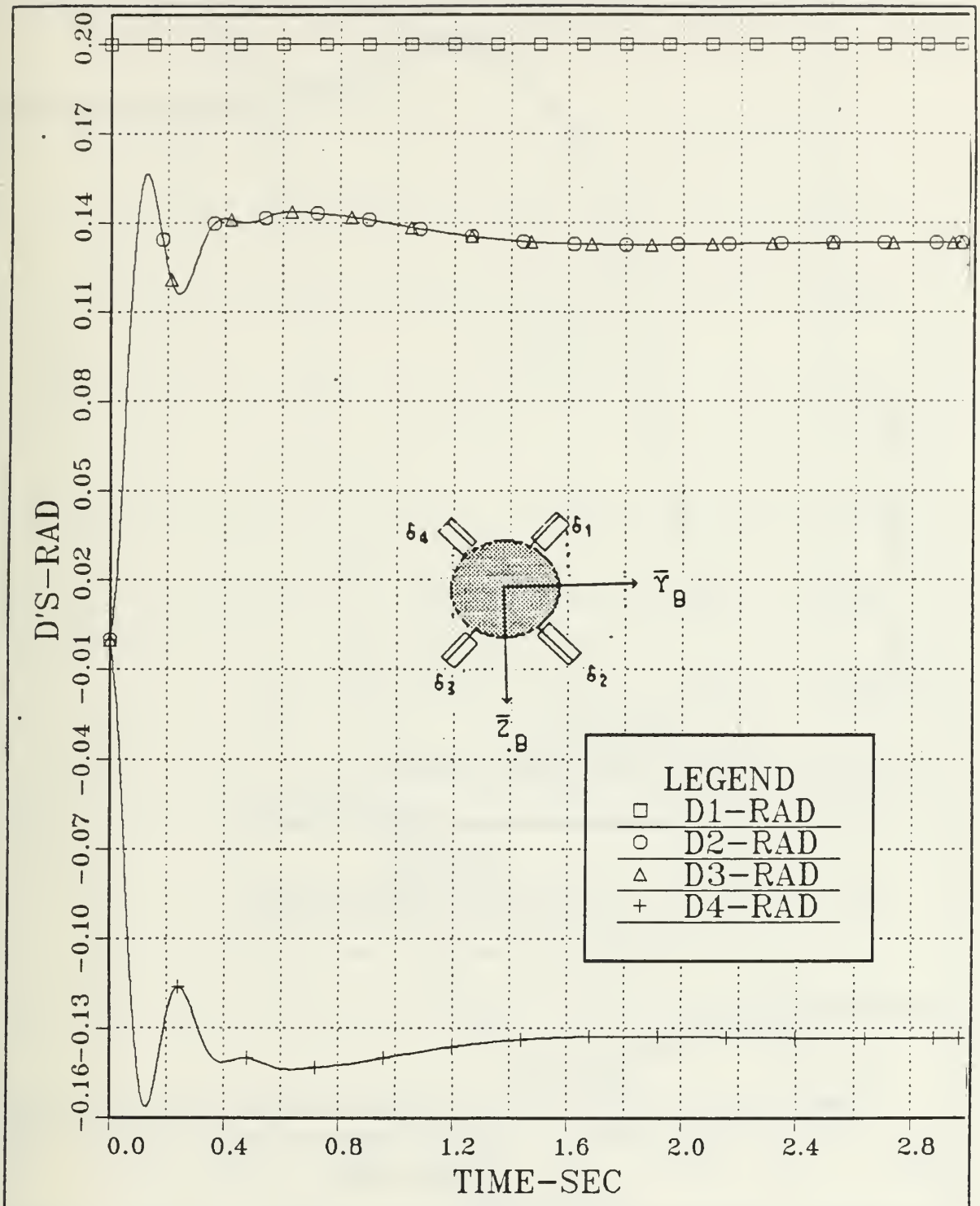

Figure 4.19 Control Surfaces deflections vs.time; Uncoupled Modified Roll Channel with δ_1 Hard Over ; Continuous Open Loop System; Step Inputs: δ_1=0.2 rad; $\delta_2,\delta_3,\delta_4$=0; Ψ_C=1 rad and a_β = 0.

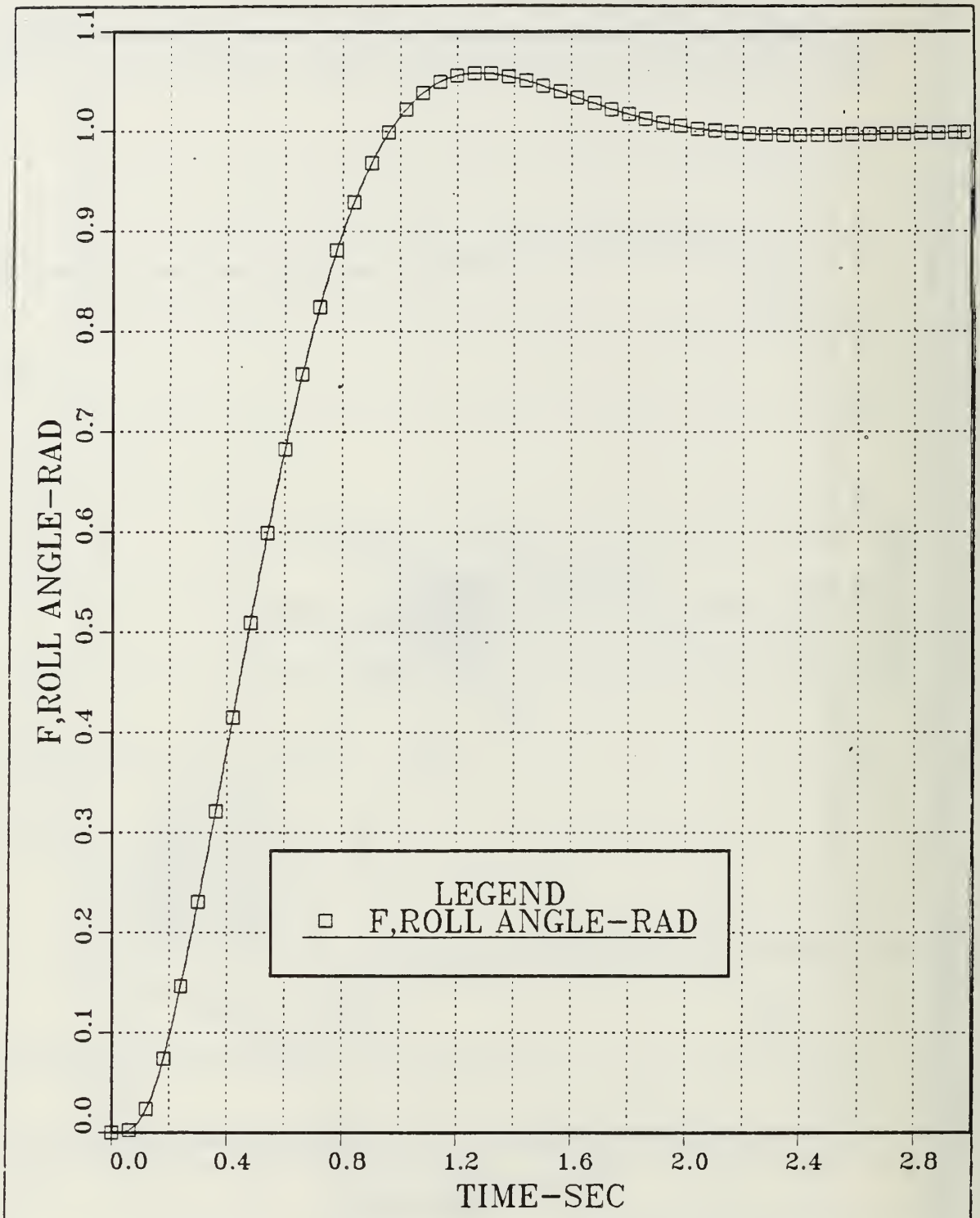

Figure 4.20 Roll Angle vs. Time; Uncoupled Modified Roll Channel with δ_1 Centered; Continuous Open Loop System;
Step Input: ψ_C=1 rad and δ_{1C}, δ_{2C},δ_{3C},δ_{4C}=0; a_e = 0.

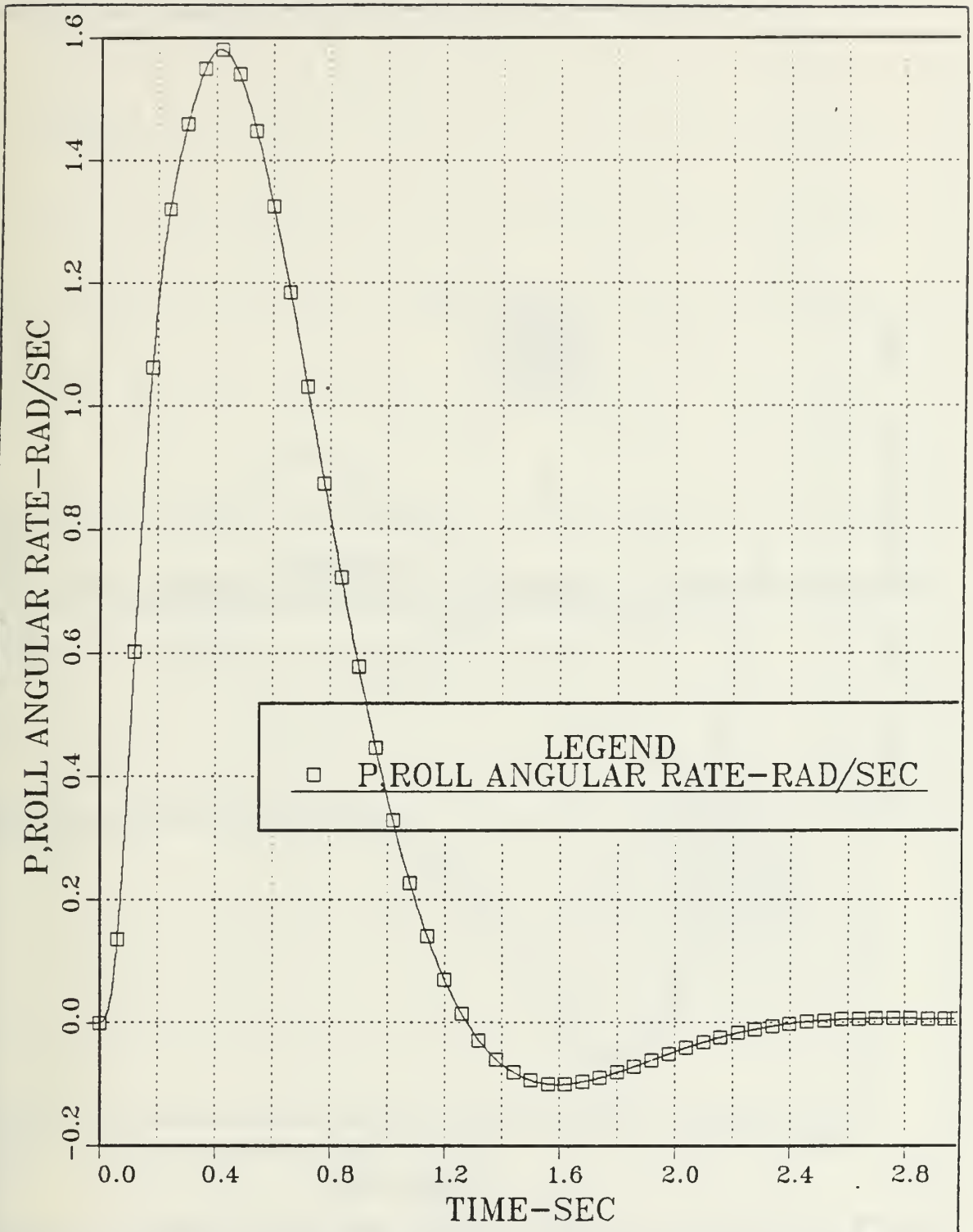

Figure 4.21 Roll Angular Rate vs. Time; Uncoupled Modified Roll Channel with δ_1 Centered; Continuous Open Loop System; Step Input: ψ_C=1 rad and δ_{1C},δ_{2C},δ_{3C},δ_{4C}=0; a_e = 0.

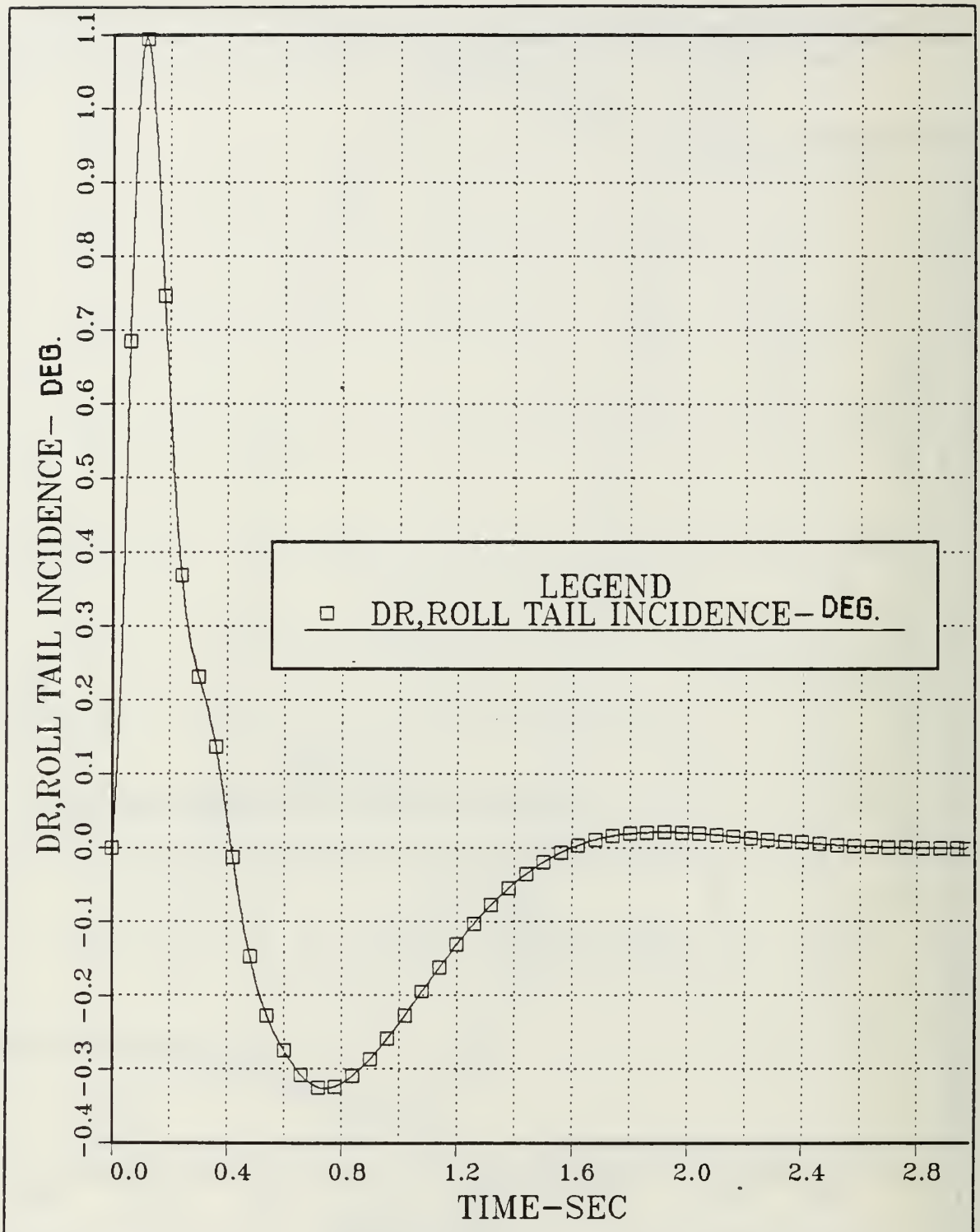

Figure 4.22 Roll Tail Incidence vs. Time; Uncoupled Modified Roll Channel with δ_1 Centered; Continuous Open Loop System; Step Input: ψ_C=1 rad and $\delta_{1C}, \delta_{2C}, \delta_{3C}, \delta_{4C}$=0; a_e = 0.

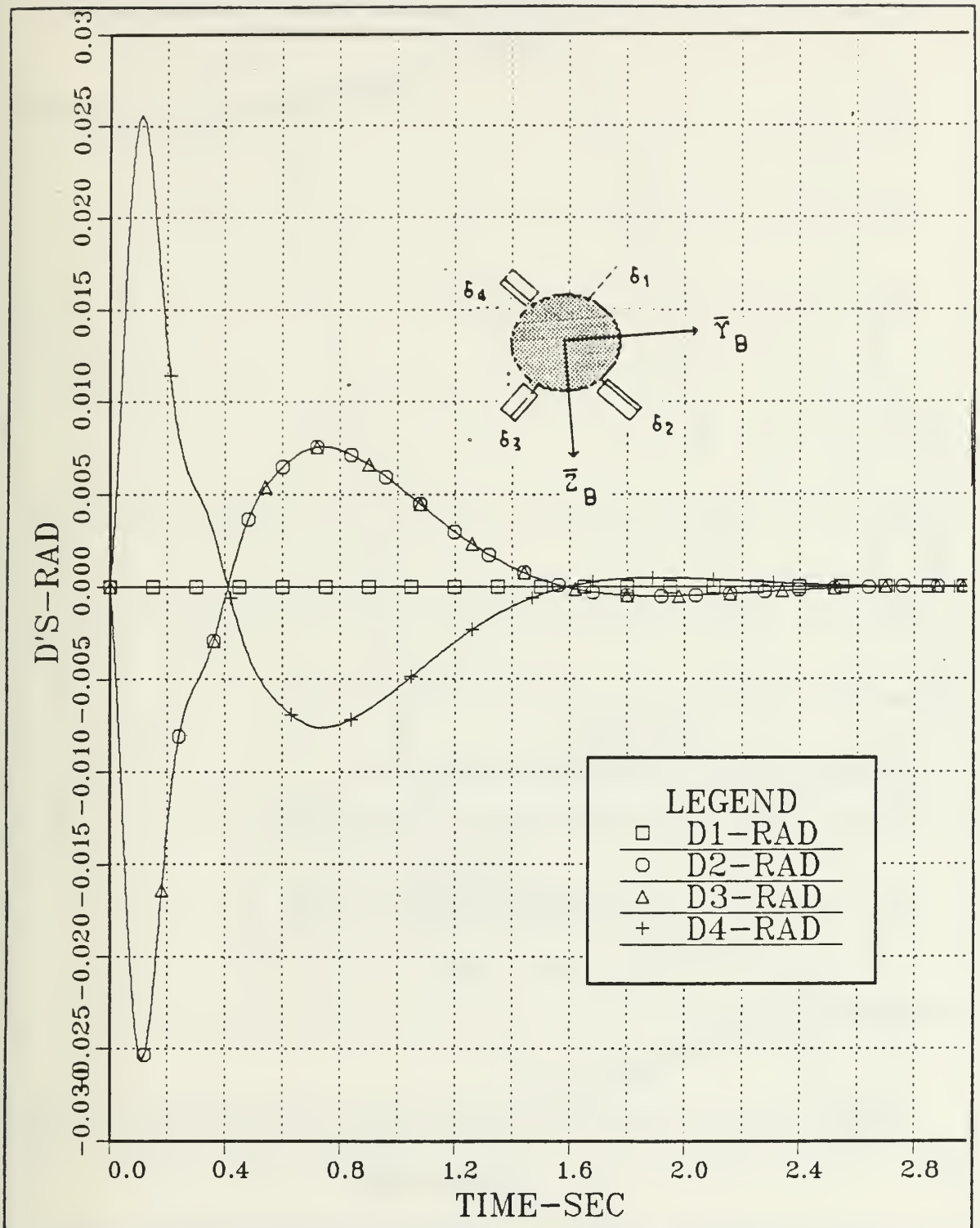

Figure 4.23 Control Surfaces deflections vs. Time; Uncoupled Modified Roll Channel with δ_1 centered; Continuous Open Loop System; Step Input: ψ_C=1 rad and δ_{1C}=,δ_{2C},δ_{3C},δ_{4C}=0; a_e = 0.

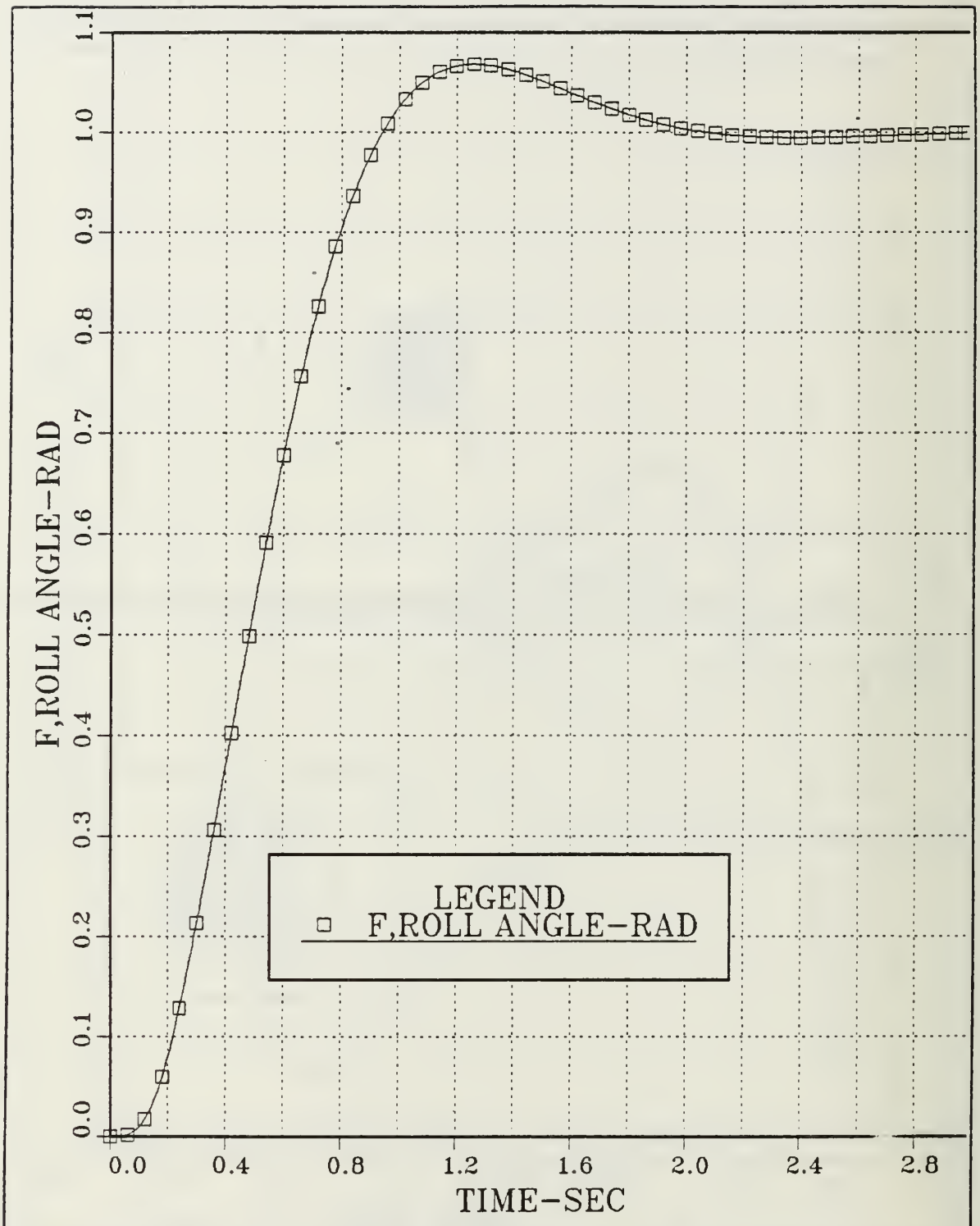

Figure 4.24 Roll Angle vs. Time; Uncoupled Modified Roll Channel with δ_1 and δ_2 Centered; Continuous Open Loop System; Step Input: ψ_C=1 rad and $\delta_{1C}, \delta_{2C}, \delta_{3C}, \delta_{4C}$=0; a_e = 0.

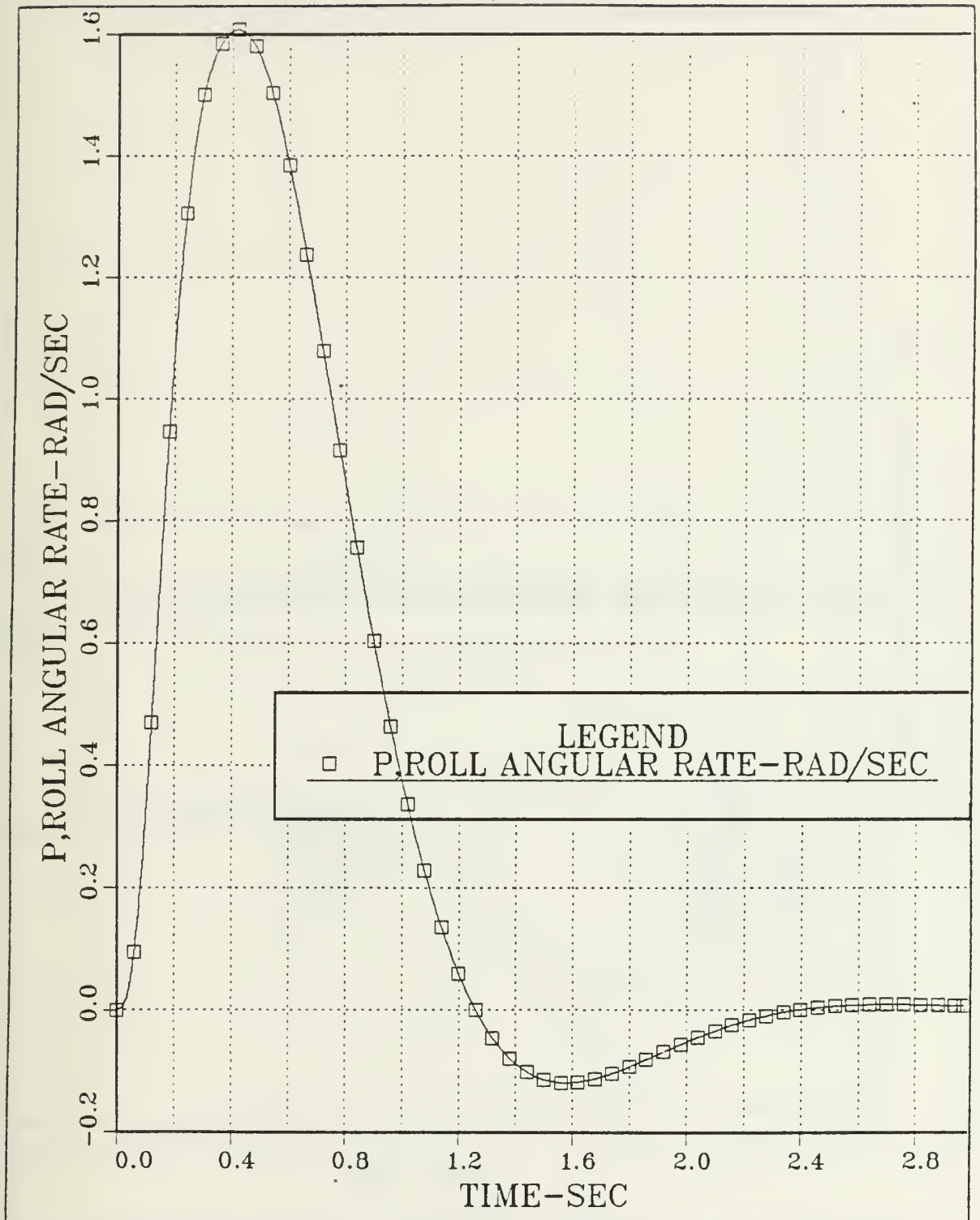

Figure 4.25 Roll Angular Rate vs. Time; Uncoupled Modified Roll Channel with δ_1 and δ_2 Centered; Continuous Open Loop System; Step Input: ψ_C=1 rad and $\delta_{1C}, \delta_{2C}, \delta_{3C}, \delta_{4C}$=0; a_e = 0.

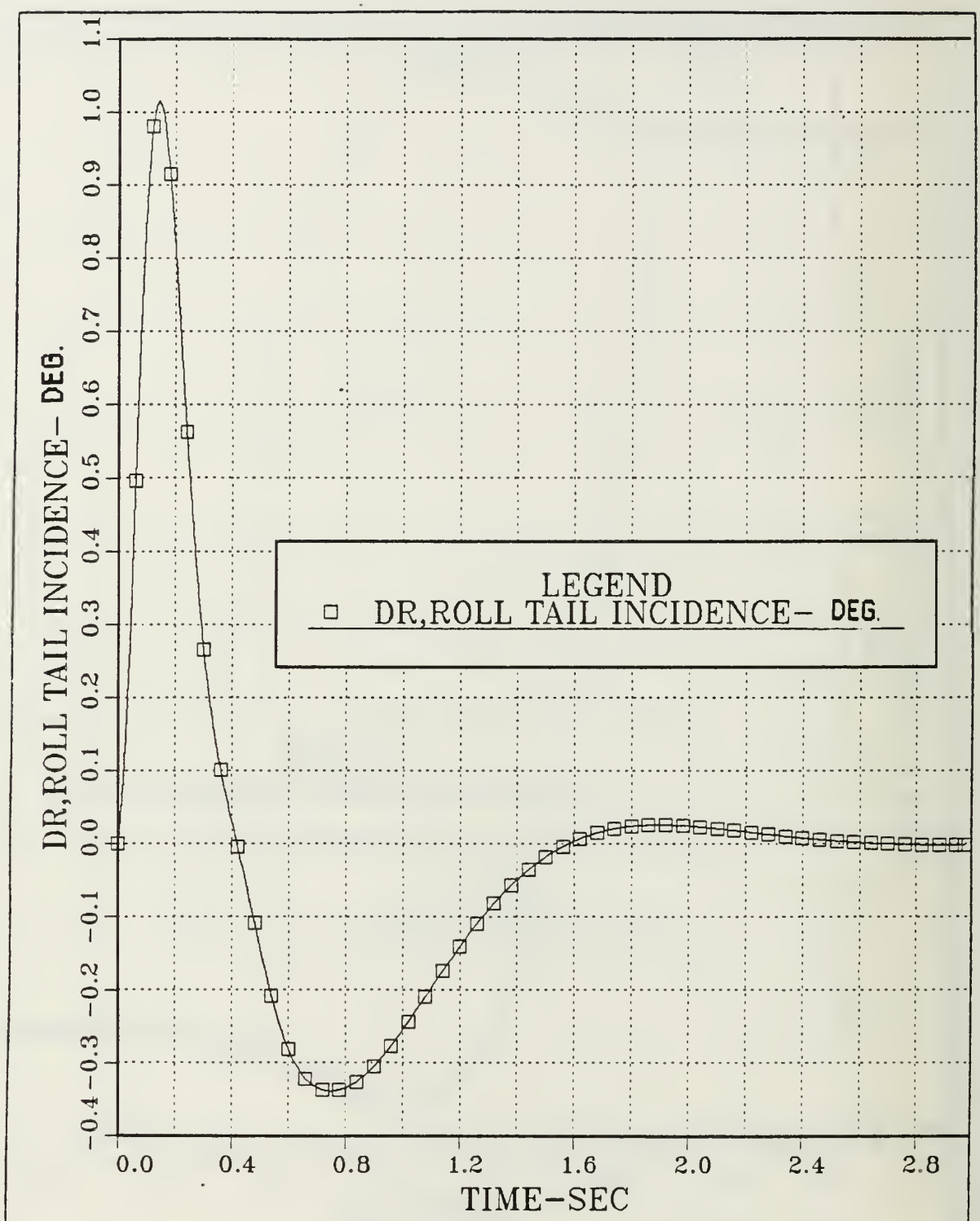

Figure 4.26 Roll Tail Incidence vs. Time; Uncoupled Modified Roll Channel with δ_1 and δ_2 Centered; Continuous Open Loop System; Step Input: ψ_C=1 rad and $\delta_{1C}, \delta_{2C}, \delta_{3C}, \delta_{4C}$=0; a_e = 0.

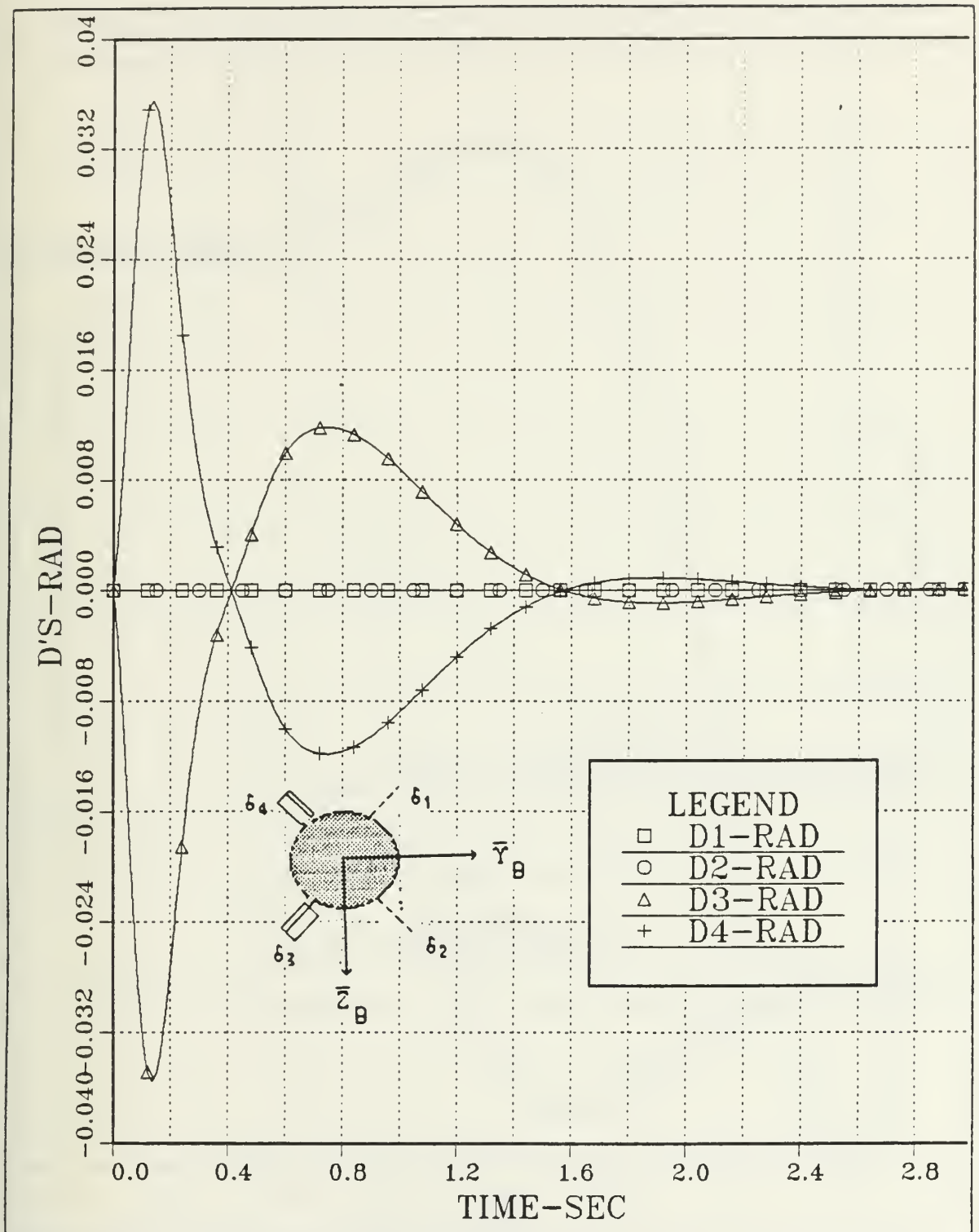

Figure 4.27 Control Surfaces deflections vs. Time; Uncoupled Modified Roll Channel with δ_1,δ_2 centered; ContinuousOpen Loop System; Step Input: ψ_C=1 rad and$\delta_{1C},\delta_{2C},\delta_{3C},\delta_{4C}$=0; a_e = 0.

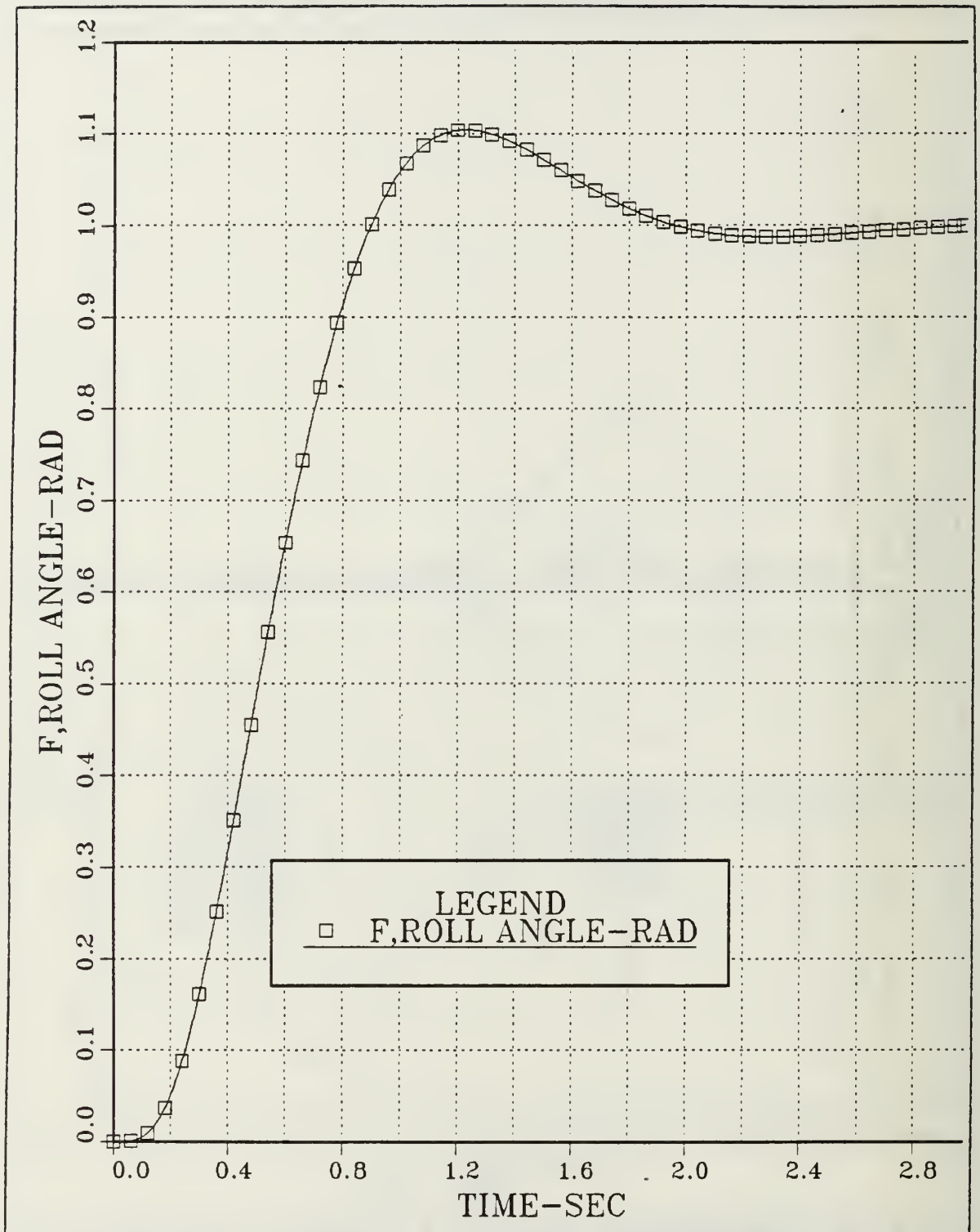

Figure 4.28 Roll Angle vs. Time; Uncoupled Modified Roll Channel with δ_1, δ_2 and δ_3 Centered; Continuous Open Loop System; Step Input: ψ_C=1 rad and δ_{1C},δ_{2C},δ_{3C},δ_{4C}=0; a_e = 0.

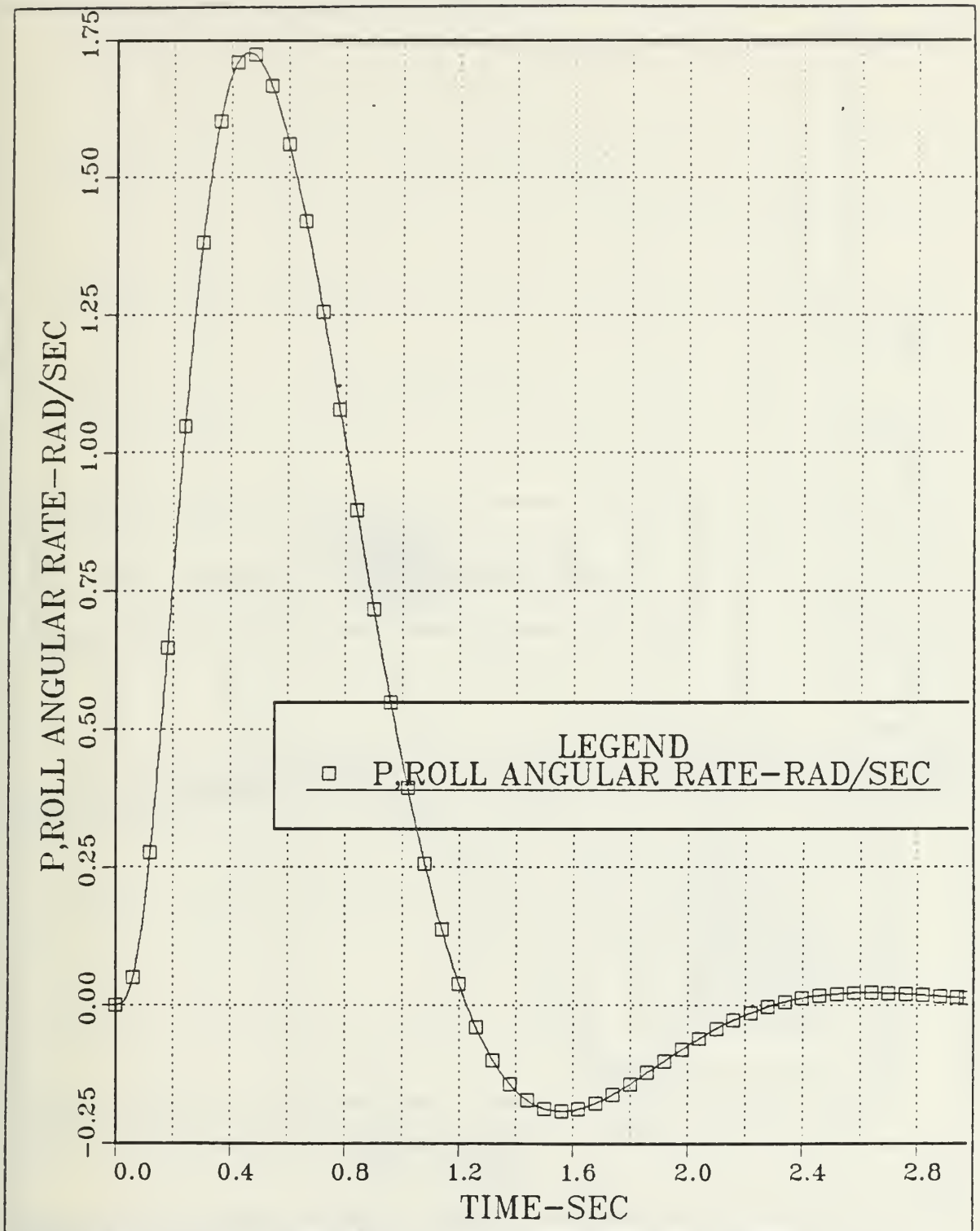

Figure 4.29 Roll Angular Rate vs. Time; Uncoupled Modified Roll Channel with δ_1,δ_2 and δ_3 Centered; Continuous Open Loop System; Step Input: ψ_C=1 rad and δ_{1C},δ_{2C},δ_{3C},δ_{4C}=0;a_e = 0.

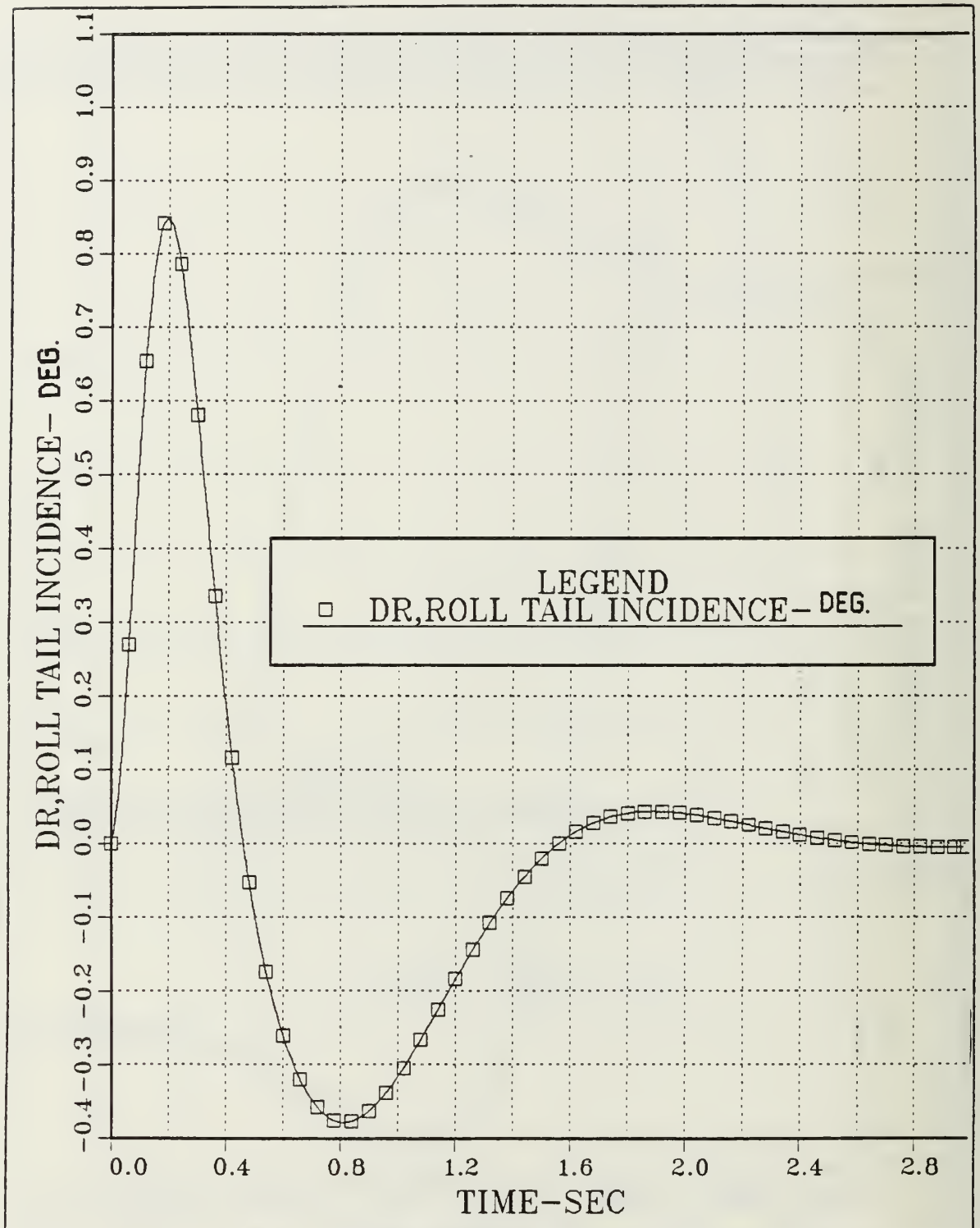

Figure 4.30 Roll Tail Incidence vs. Time; Uncoupled Modified Roll Channel with δ_1, δ_2 and δ_3 Centered; Continuous Open Loop System; Step Input: ψ_C=1 rad and δ_{1C},δ_{2C},δ_{3C},δ_{4C}=0; a_e = 0.

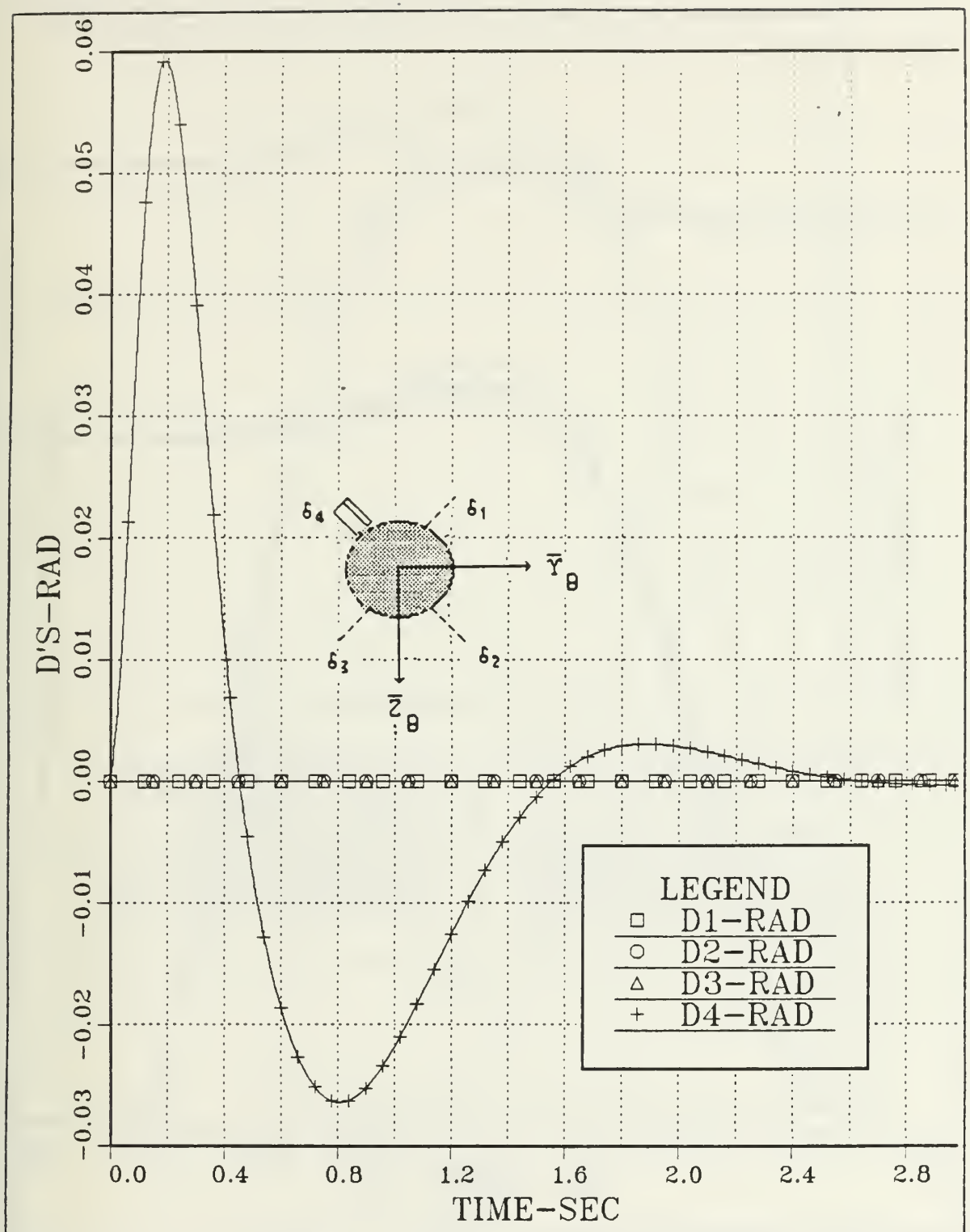

Figure 4.31 Control Surfaces deflections vs. Time; Uncoupled Modified Roll Channel : $\delta_1,\delta_2,\delta_3$ Centered; Continuous OpenLoop System; Step Input: ψ_C=1 rad and $\delta_{1C},\delta_{2C},\delta_{3C},\delta_{4C}$=0; a_e = 0.

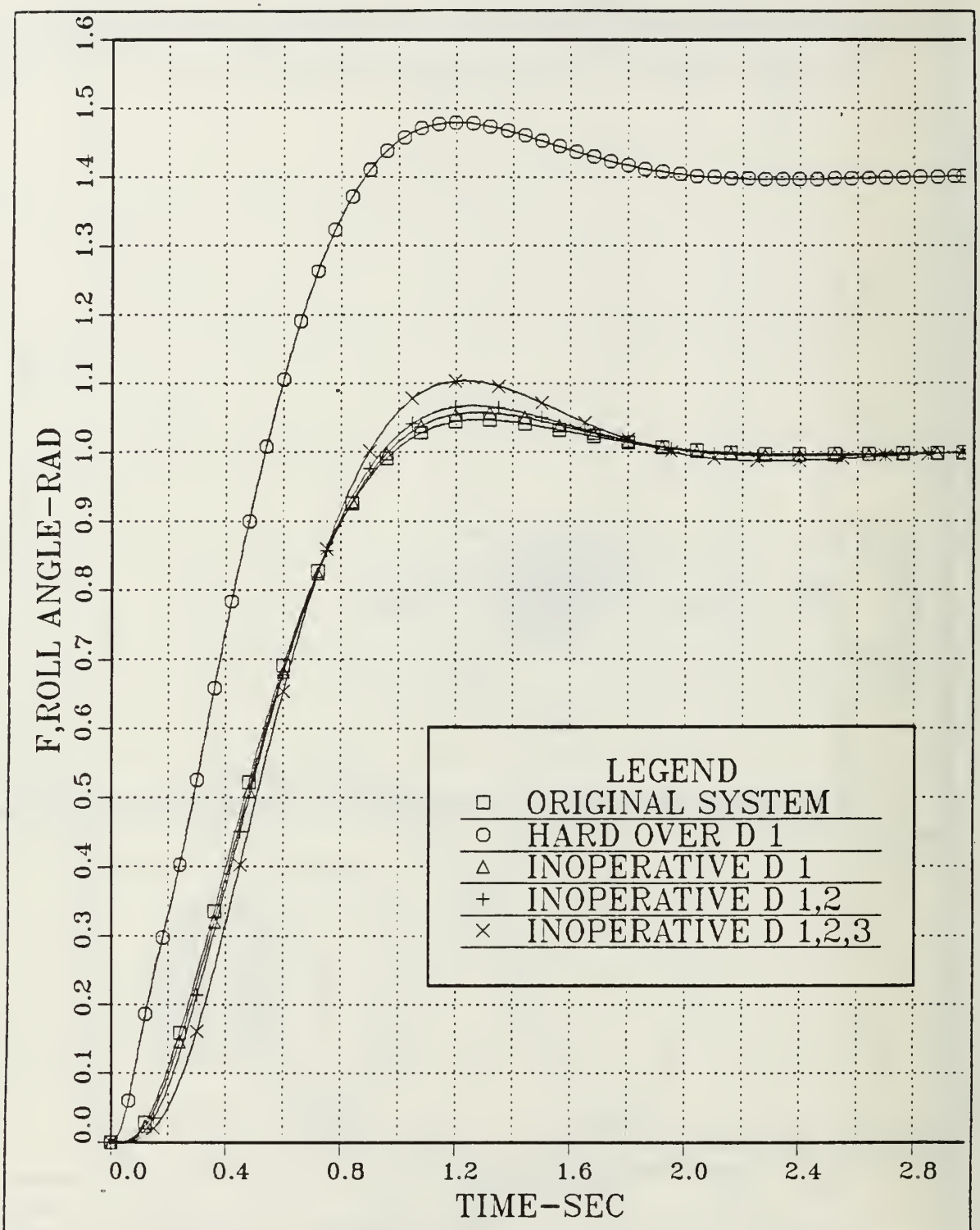

Figure 4.32 Comparison of the Roll Angle between the Unimpaired System and the Four Cases of Impairment.

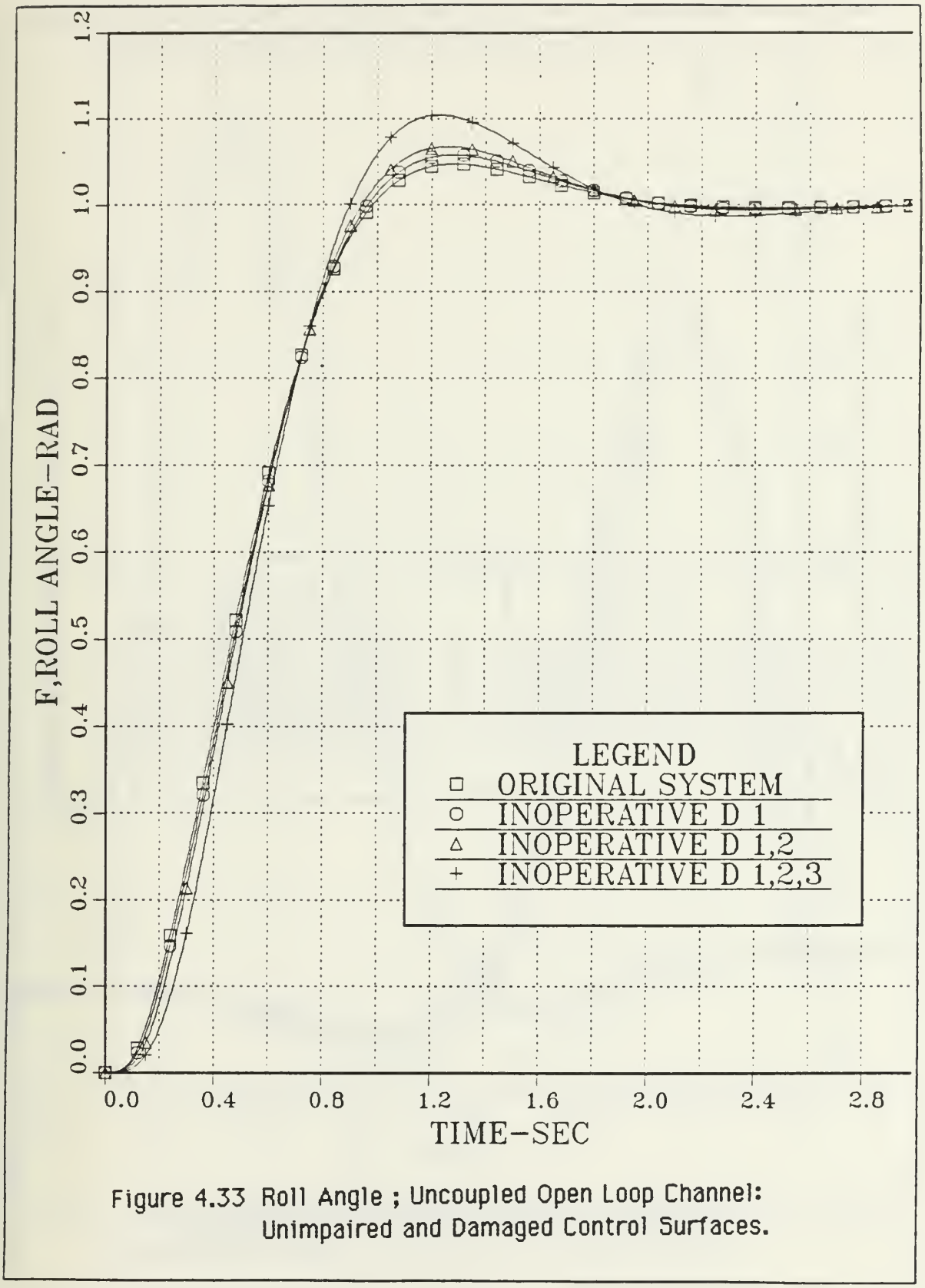

Figure 4.33 Roll Angle ; Uncoupled Open Loop Channel:
Unimpaired and Damaged Control Surfaces.

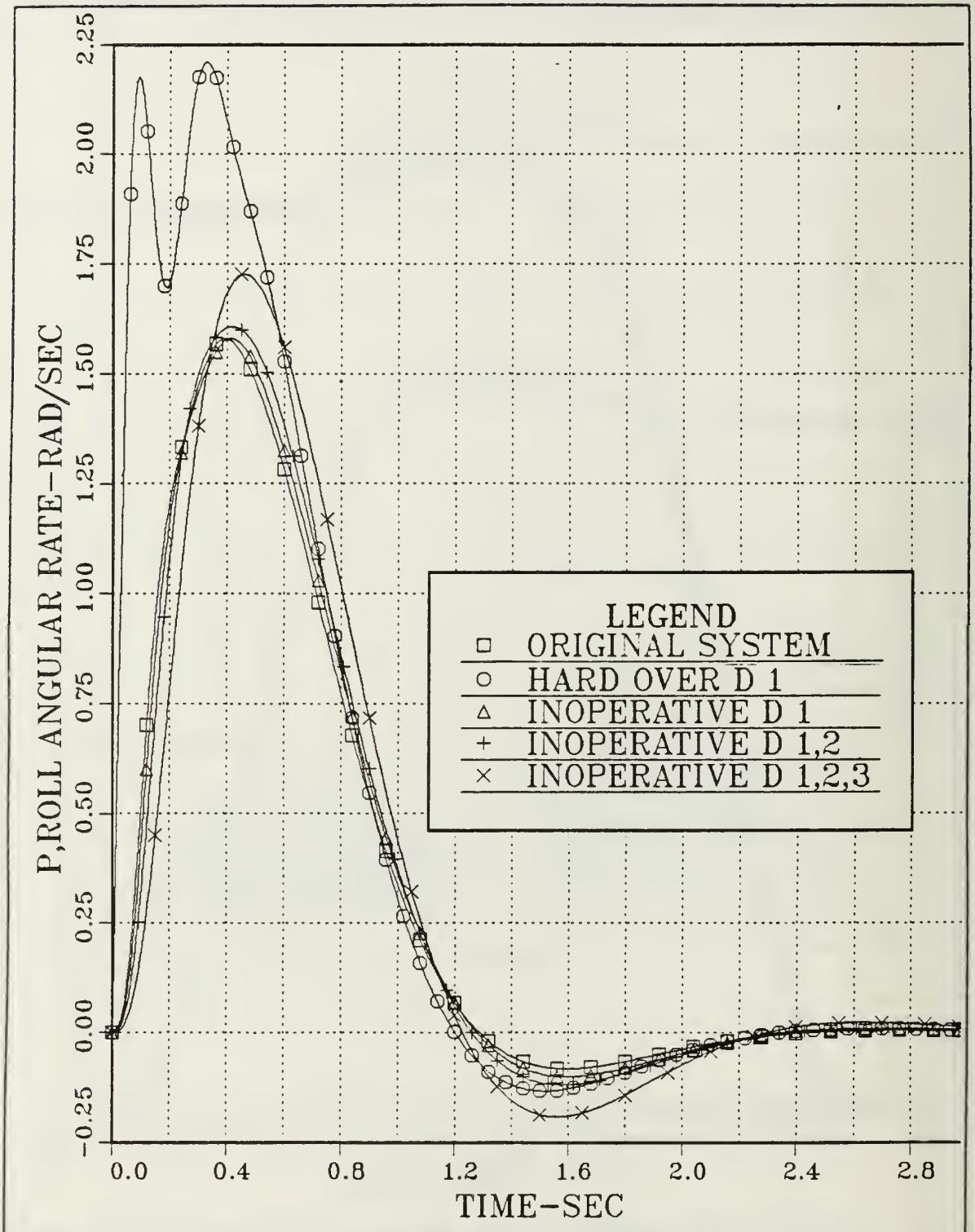

Figure 4.34 Comparison of the Roll Angular Rate between the Unimpaired System and the Four Cases of Impairment.

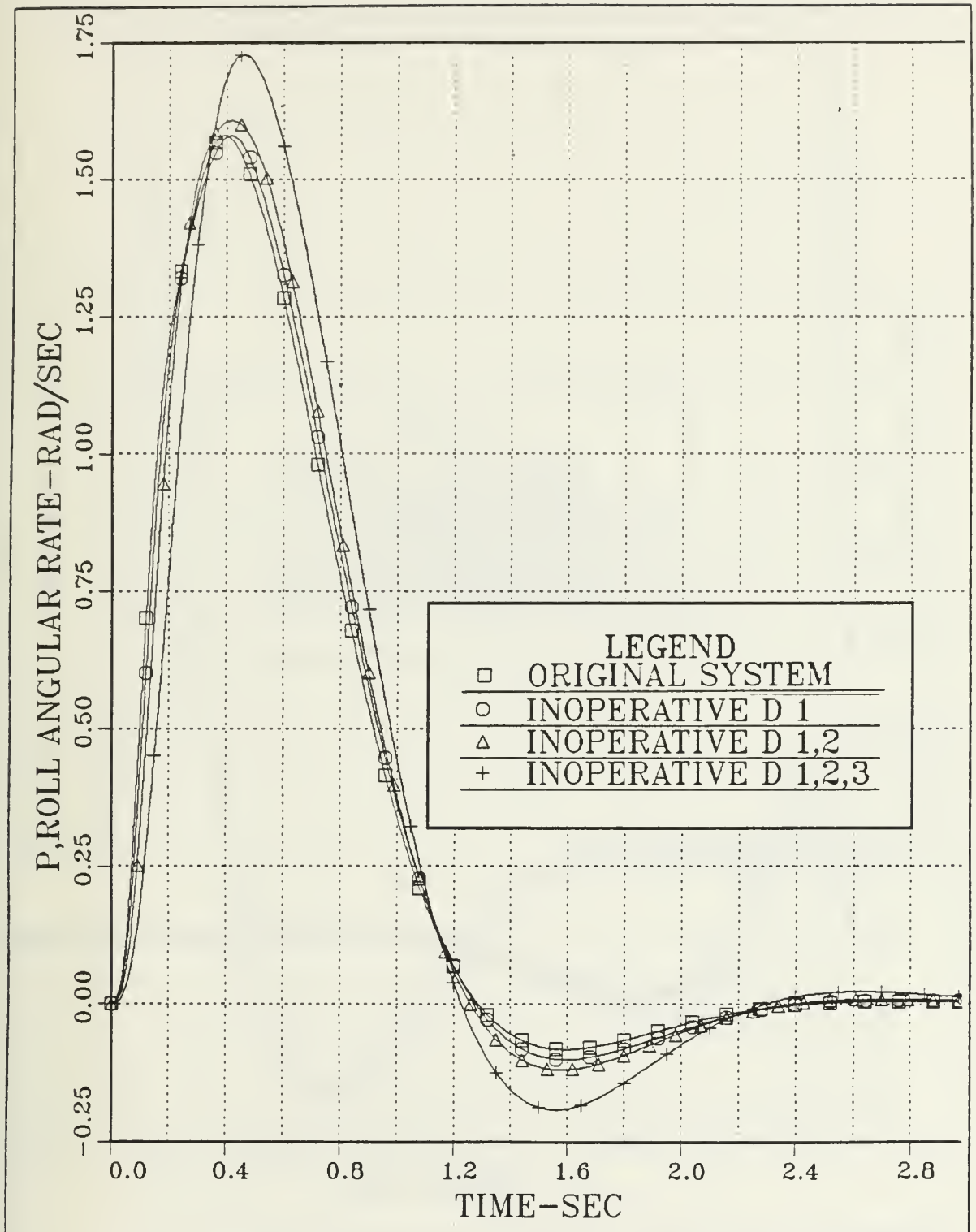

Figure 4.35 Roll Angular Rate; Uncoupled Open Loop Channel: Unimpaired and Damaged Control Surfaces.

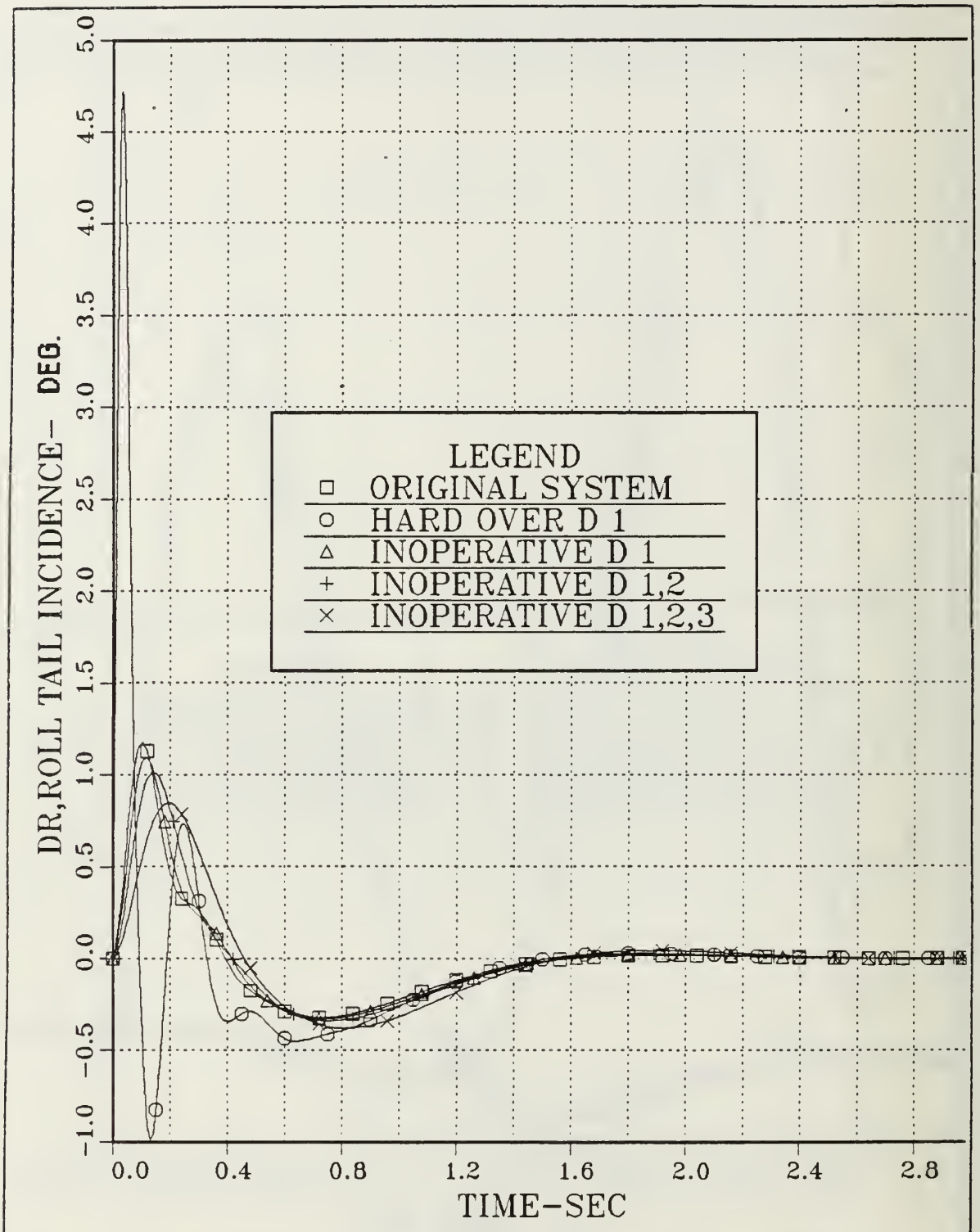

Figure 4.36 Comparison of the Roll Tail Incidence between the Unimpaired System and the Four Cases of Impairment.

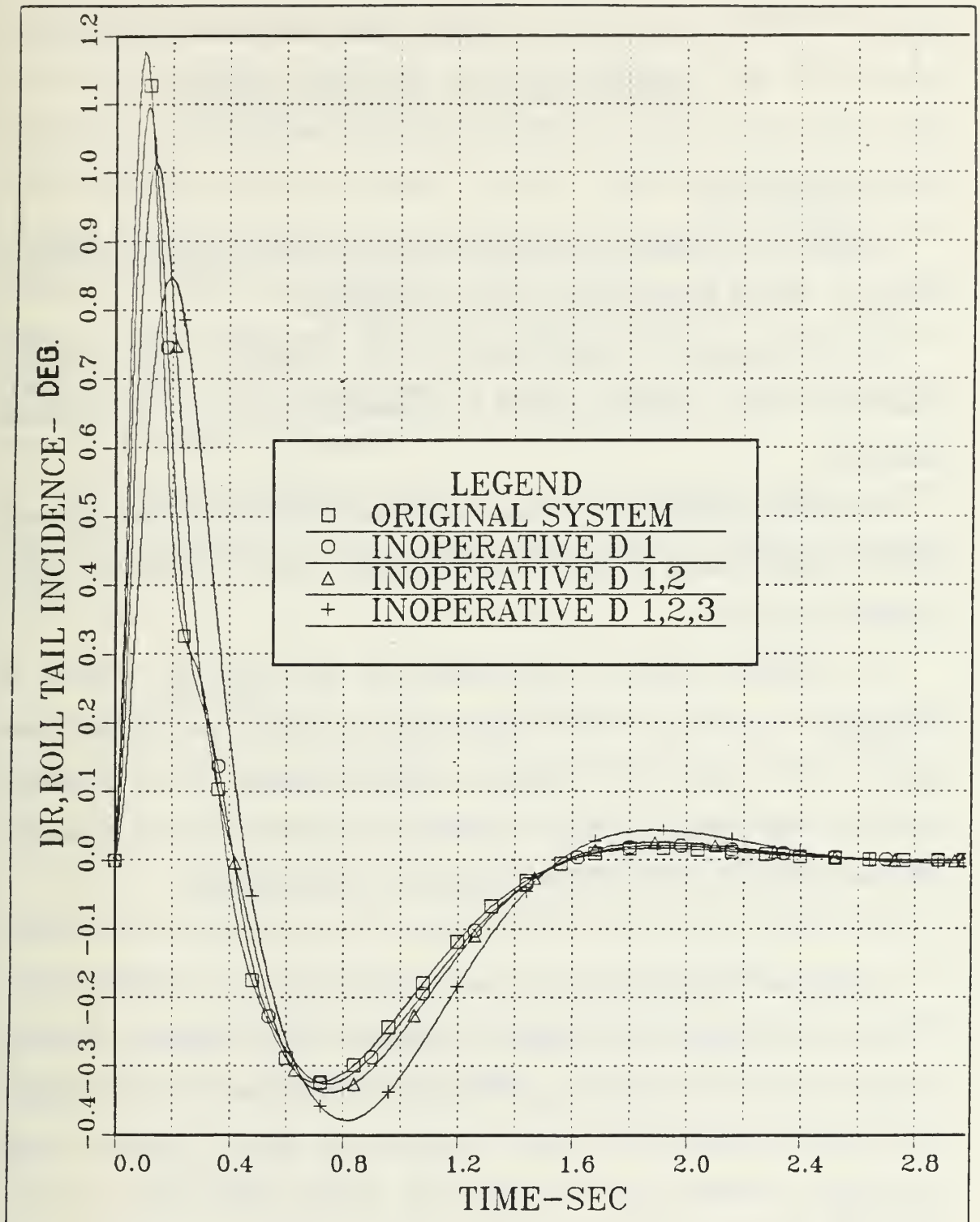

Figure 4.37 Roll Tail Incidence; Uncoupled Open Loop Channel: Unimpaired and Damaged Control Surfaces.

V. COUPLED LINEAR PITCH AND ROLL CHANNELS

A. INTRODUCTION

Separate longitudinal and lateral autopilots were designed in Chapters III and IV, for the Modified Linear Open Loop system.

In this Chapter the longitudinal and roll autopilots were combined, resulting in a new autopilot capable of commanding pitch, roll or combined maneuvers.

The time responses to an input vector are identical to that obtained when the same input is put into the separate pitch and roll autopilots of the unimpaired system.

The response plots of this system are then used as a basis to investigate the effect of the damaged control surfaces on the combined system. In this section the hard over type of damage for the combined system is investigated. Corrective actions are then developed and presented and the robustness of the complete system is finally analyzed.

B. DESIGN APPROACH, ANALYSIS AND PERFORMANSE OF THE SYSTEM

For the design of the combined system of the circular airframe configuration, the requirements and assumptions mentioned in the design of the separate autopilots are used. To achieve the desired maneuver plane acceleration response for the unimpaired system, both pitch and roll uncoupled autopilots were designed to have the desired maneuver plane speed of response. In paticular, the goal for maneuver plane acceleration

response was a 0.5 second time constant for the flight condition of interest (i.e., 60 Kft altitude, Mach 3.95. In the next phase of the linear design technique the longitudinal and lateral autopilot channels are coupled using the aerodynamic model of Chapter III. Both channels are cross-coupled through the control surfaces (i.e., a command to the control surface of one channel will affect the parameters of the other and vice versa). The pitch and roll state Equations (III.B.5-5) through (III.B.5-17) and (IV.C.4-4) through (IV.C.4-13) are combined to yield a twenty-three order system which is presented in Appendix C.

The Open Loop dynamic matrix is a 23 x 23 matrix. This composite system is formed by two block diagonal matrices as is stated in Equation (V.B-1):

$$F = \begin{bmatrix} F_1\,(13\times13) & 0 \\ 0 & F_2\,(10\times10) \end{bmatrix} \qquad \text{(V.B.1-1)}$$

That is, the upper block composed of the 13x13 F matrix from the pitch channel and the lower block composed of the 10x10 F matrix from the roll channel.

The control distribution matrix **G**, folowing the same pattern, is given by a 23x10 matrix, of the form and order:

$$G = \begin{bmatrix} G_1\,(13\times5) & 0 \\ 0 & G_2\,(10\times5) \end{bmatrix} \qquad \text{(V.B.1-2)}$$

Finally the state vector **X** and the control input vector **U** matrices are of the form and order:

$$\mathbf{X} = [\,23 \times 1\,] \qquad \text{(V.B.1-3)}$$

$$\mathbf{U} = [\,10 \times 1\,] \qquad \text{(V.B.1-4)}$$

Because of this form, any input to the stated combined system, has a time response identical to that resulting from the same input into the pitch and roll channels separately. An example of this is shown in Figure 5.1 where the same input vector used for the vertical translation maneuver longitudinally and the rolling translation maneuver laterally are combined and serve as inputs to the combined system resulting in a response identical to those achieved separately in Figures 3.9 through 3.12 and 4.12 through 4.15.

The combined autopilot designed in this thesis and the simulations made to test the different step input commands are accomplished using the interactive, multivariable design program called OPTSYS.

In addition, in order to compare different control surface impairment configurations a computer program was developed (Appendix D). This program creates data files to be used as input files at the EASYPLOT program by changing the format of the OPTPLOT data into a fixed format data file. This Format is 80 characters in length with space between the values.

Three different command inputs are examined for the Modified Unimpaired system and are discussed below.

Test 1: For this test, both a pitch normal acceleration and a roll angle were commanded (i.e., N_{Zc} = 1 gee, φ_c = 1 rad and δ_{1c}, δ_{2c}, δ_{3c}, δ_{4c} = 0 rad). In Figure 5.1 the time response plots of the normal acceleration and the roll angle are presented. As was expected, both curves are identical to the corresponding plots obtained when separate autopilots were used.

Figures 5.2 through 5.4 illustrate the performance of the other state variables. Figure 5.4 shows the control surface deflections for only two control surfaces from each channel. The remaining four coincide or are the mirror image of the obtained results. In the same Figure the configuration of the control surfaces for each channel is provided and the distinction is also provided in the legend.

Test 2: For this test, only a pitch command in acceleration was applied (i.e., N_{Zc} = 1 gee), while , φ_c = 0 rad and δ_{1c}, δ_{2c}, δ_{3c}, δ_{4c} = 0 rad. Figures 5.5 through 5.8 show the performance of the system. Observe that no roll angle or any roll rate is present, as was expected, while a downwards maneuver is performed according to the command input vector (downward maneuver is the positive one). Figure 5.8 shows the response of the control surfaces for both channels. The control surfaces of the longitudinal channel are deflected at a ±0.025 radian angle and of the lateral channel remained at the initial zero position while only a downward maneuver was commanded.

Test 3: In the last test, only a roll command is applied (i.e., φ_c = 1 rad), while N_{Zc} = 0 gee and δ_{1c}, δ_{2c}, δ_{3c}, δ_{4c} = 0 rad. Figures 5.9 through 5.12 illustrate the effectiveness of input vector on the state variables of interest. In Figure 5.12 only the two control surfaces δ_1 and δ_2 of the roll channel are plotted while the corresponding surfaces in the pitch channel

remain at zero. The other four coincide with the obtained results. The control surfaces of the roll channel are deflected at a ±0.022 radian angle and of the longitudinal channel remained at the initial zero position while only a rolling maneuver was commanded.

It should be mentioned here that according to the pole-zero plot for the designed combined system, the combined continuous open loop system is also stable, since the s-plane poles are:

$s_1 = -159.724 + j18.9922$ (V.B-5)

$s_2 = -159.724 - j18.9922$ (V.B-6)

$s_3 = -8.29043 + j0.05911$ (V.B-7)

$s_4 = -8.29043 - j0.05911$ (pitch angular rate) (V.B-8)

$s_5 = -3.75933 + j2.51441$ (V.B-9)

$s_6 = -3.75933 - j2.51441$ (V.B-10)

$s_7 = -0.14393 + j0$ (V.B-11)

$s_8 = -0.00005 + j0$ (pitch tail incidence) (V.B-12)

$s_9 = -0.07460 + j0.66599$ (V.B-13)

$s_{10} = -0.07460 - j0.66599$ (pitch normal acceleration) (V.B-14)

$s_{11} = -0.14300 + j0$ (V.B-15)

$s_{12} = -0.14300 + j0$ (V.B-16)

$s_{13} = -0.14300 + j0$ (V.B-17)

$s_{14} = -0.01850 + j0$ (roll angular rate) (V.B-18)

$s_{15} = -9.27462 + j29.2679$ (roll angle) (V.B-19)

$s_{16} = -9.27462 - j29.2679$ (V.B-20)

$s_{17} = -2.35821 + j2.70296$ (V.B-21)

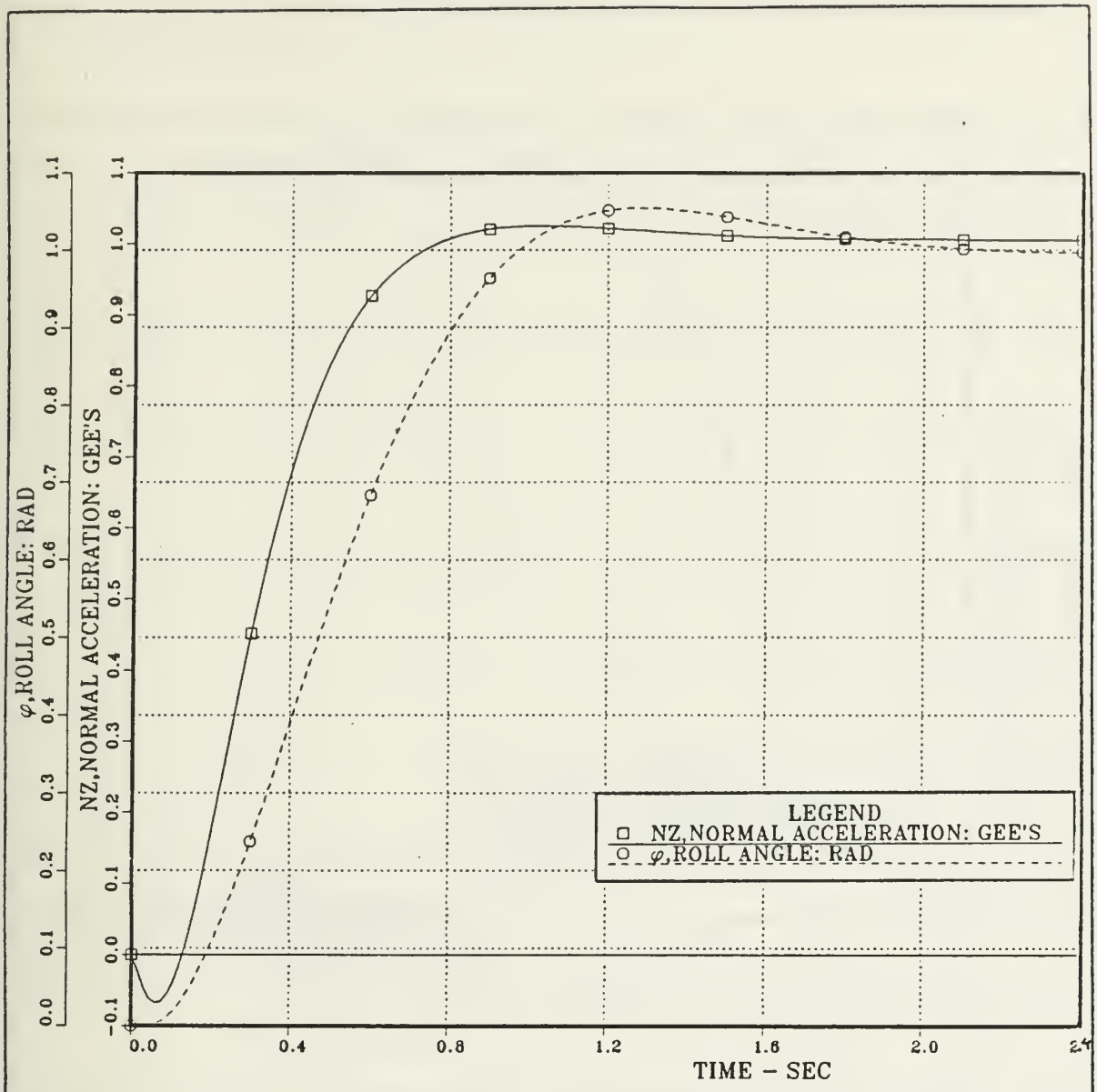

Figure 5.1 Normal Acceleration and Roll Angle vs. Time; Combined Pitch and Roll Channels; Continuous Open Loop System; Step Inputs: δ_{1c}, δ_{2c}, δ_{3c}, δ_{4c} = 0 and N_{zc} = 1 gee, φ_c = 1 rad; a_e = 0.

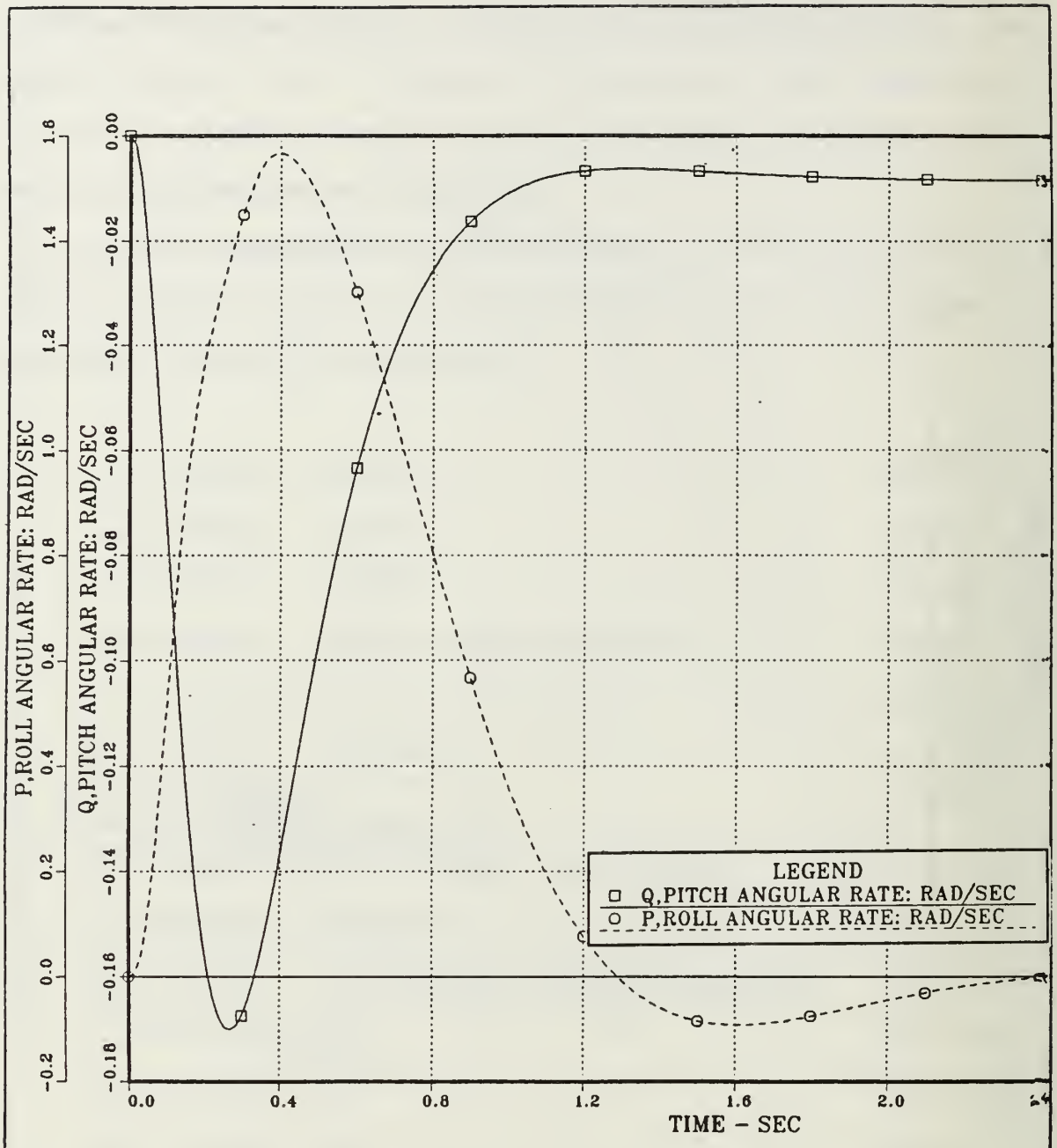

Figure 5.2 Pitch and Roll Angular Rate vs. Time; Combined Pitch and Roll Channels; Continuous Open Loop System; Step Inputs: δ_{1c}, δ_{2c}, δ_{3c}, δ_{4c} = 0 and N_{zc} = 1 gee. Ψ_c = 1 rad; a_θ = 0.

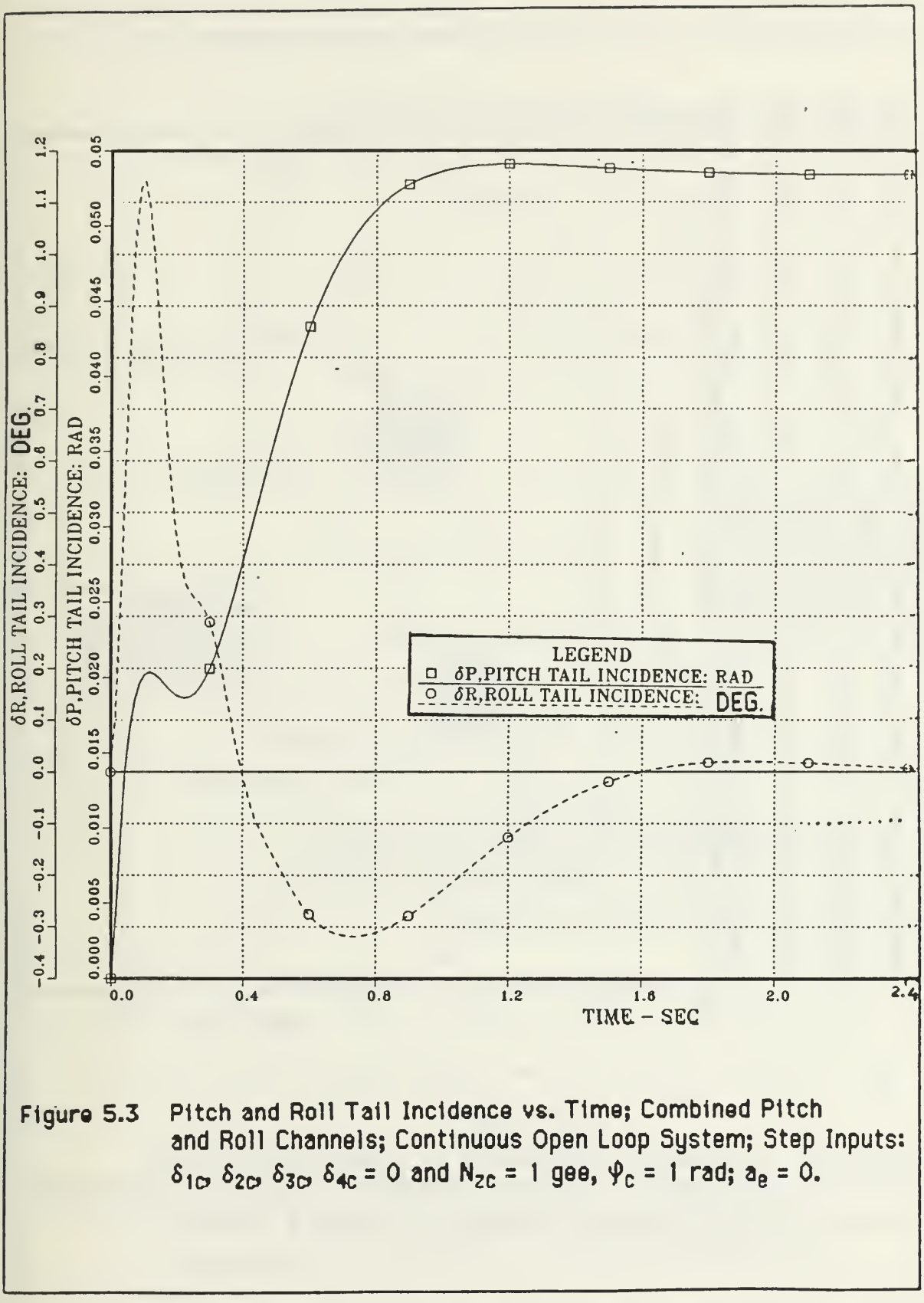

Figure 5.3 Pitch and Roll Tail Incidence vs. Time; Combined Pitch and Roll Channels; Continuous Open Loop System; Step Inputs: δ_{1c}, δ_{2c}, δ_{3c}, δ_{4c} = 0 and N_{zc} = 1 gee, ψ_c = 1 rad; a_e = 0.

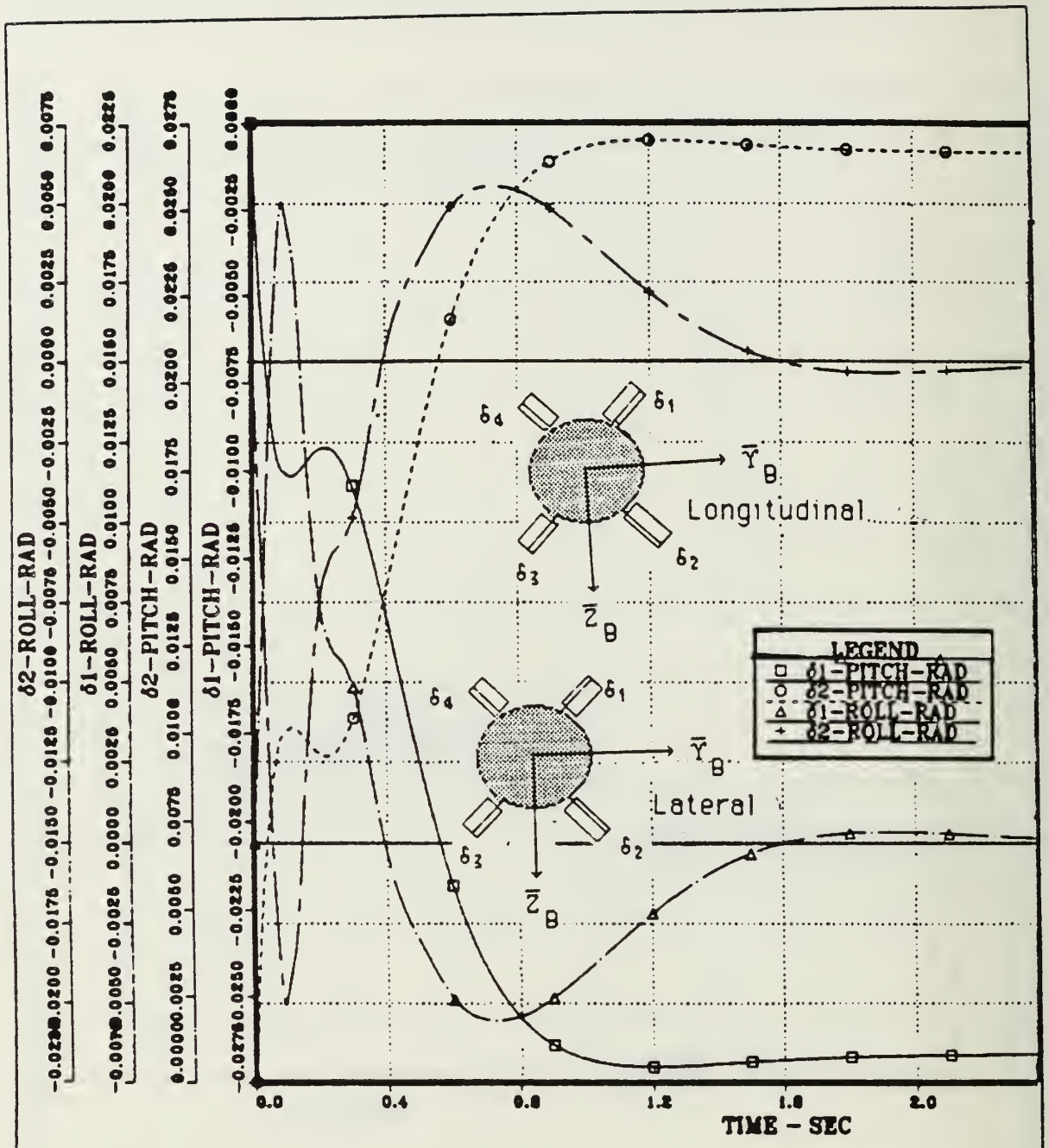

Figure 5.4 Pitch and Roll Deflections vs. Time; Combined Pitch and Roll Channels; Continuous Open Loop System; Step Inputs: δ_{1C}, δ_{2C}, δ_{3C}, δ_{4C} = 0 and N_{ZC} = 1 gee, ψ_C = 1 rad; a_B = 0.

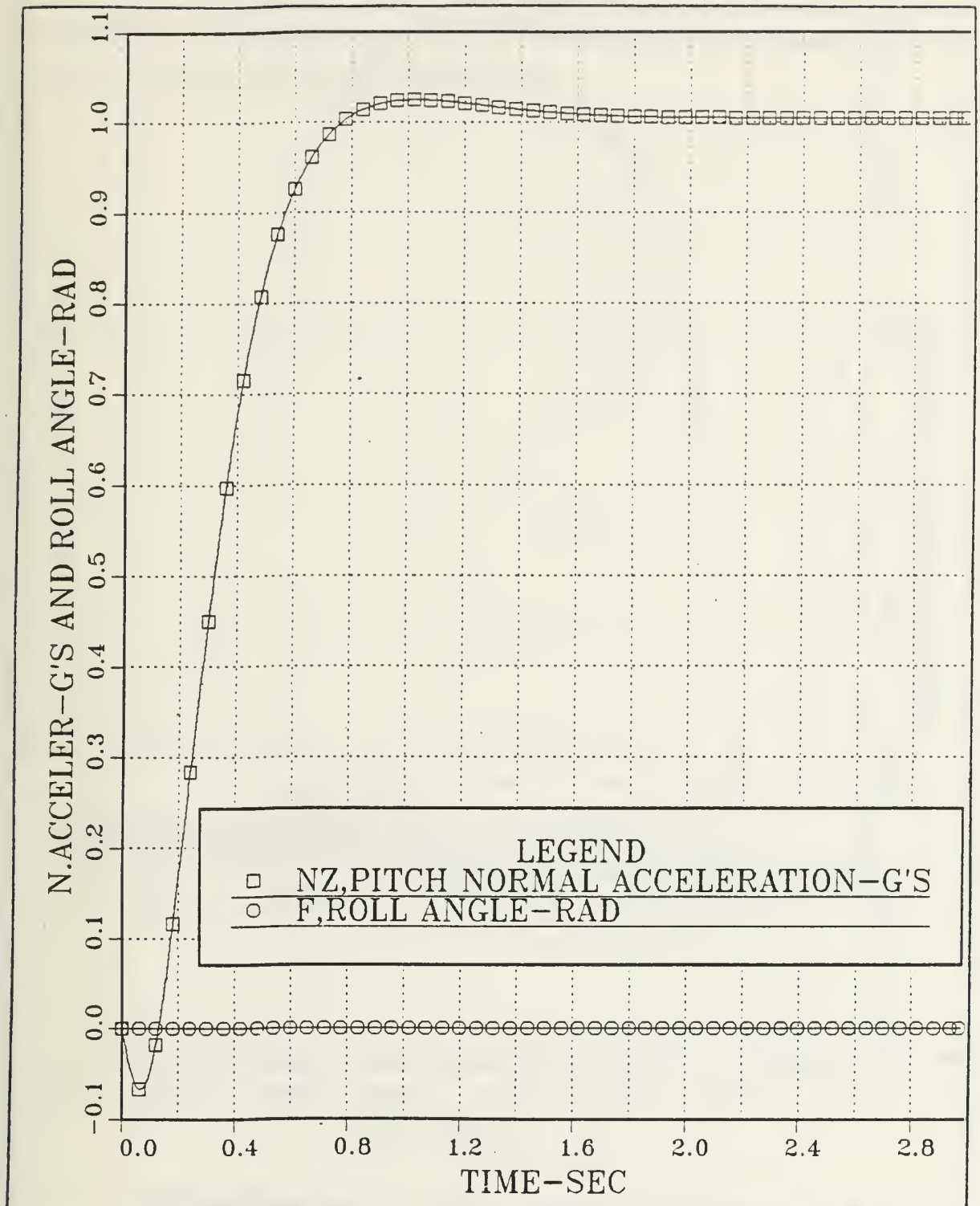

Figure 5.5 Normal Acceleration and Roll Angle vs. Time; Combined Pitch and Roll Channels; Continuous Open Loop System; Step Inputs: δ_{1C}, δ_{2C}, δ_{3C}, δ_{4C} = 0 and N_{ZC} = 1 gee, ψ_C = 0 rad; a_e = 0.

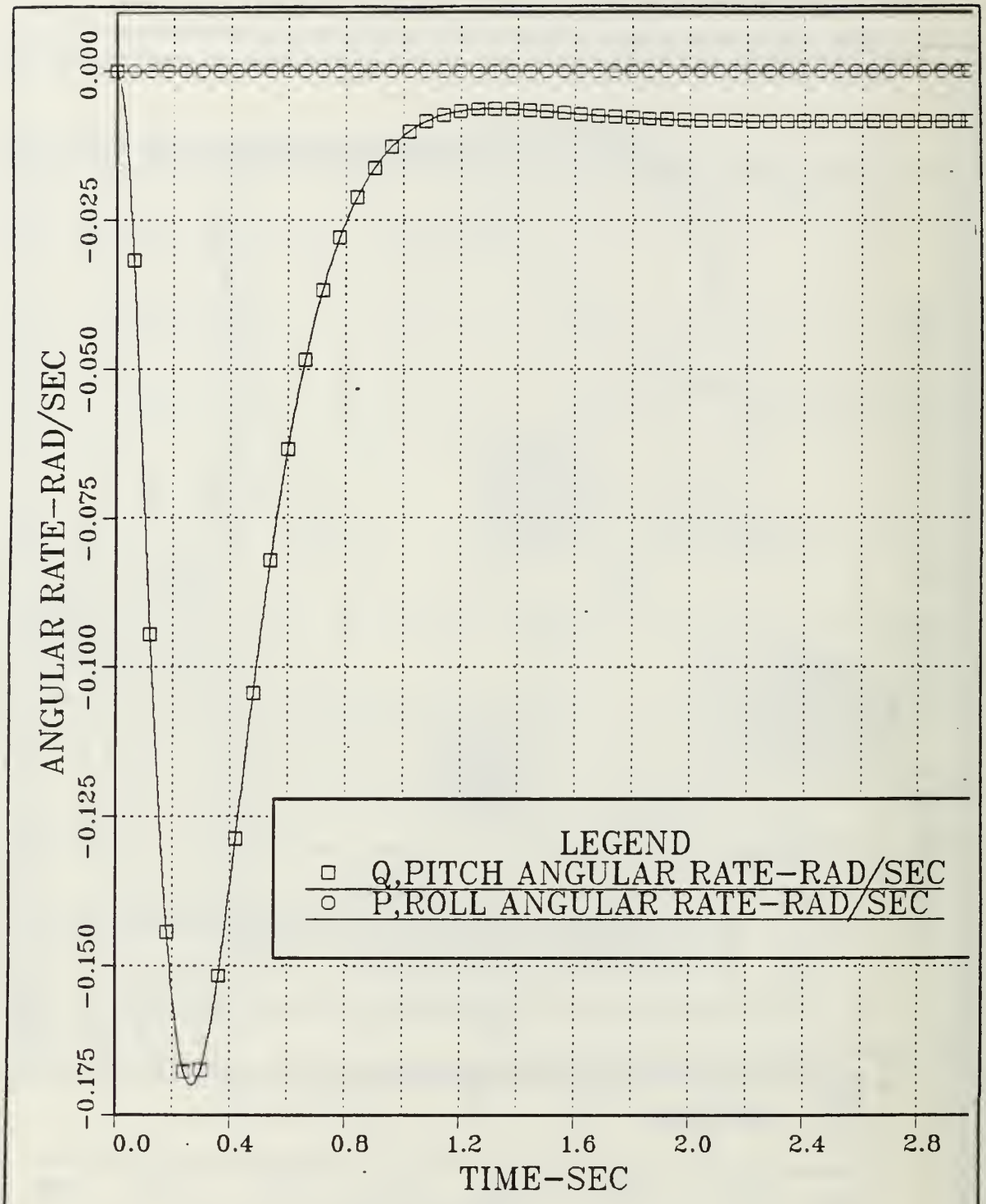

Figure 5.6 Pitch and Roll Angular Rate vs. Time; Combined Pitch and Roll Channels; Continuous Open Loop System; Step Inputs: δ_{1c}, δ_{2c}, δ_{3c}, δ_{4c} = 0 and N_{zc} = 1 gee, ψ_c = 0 rad; a_e = 0.

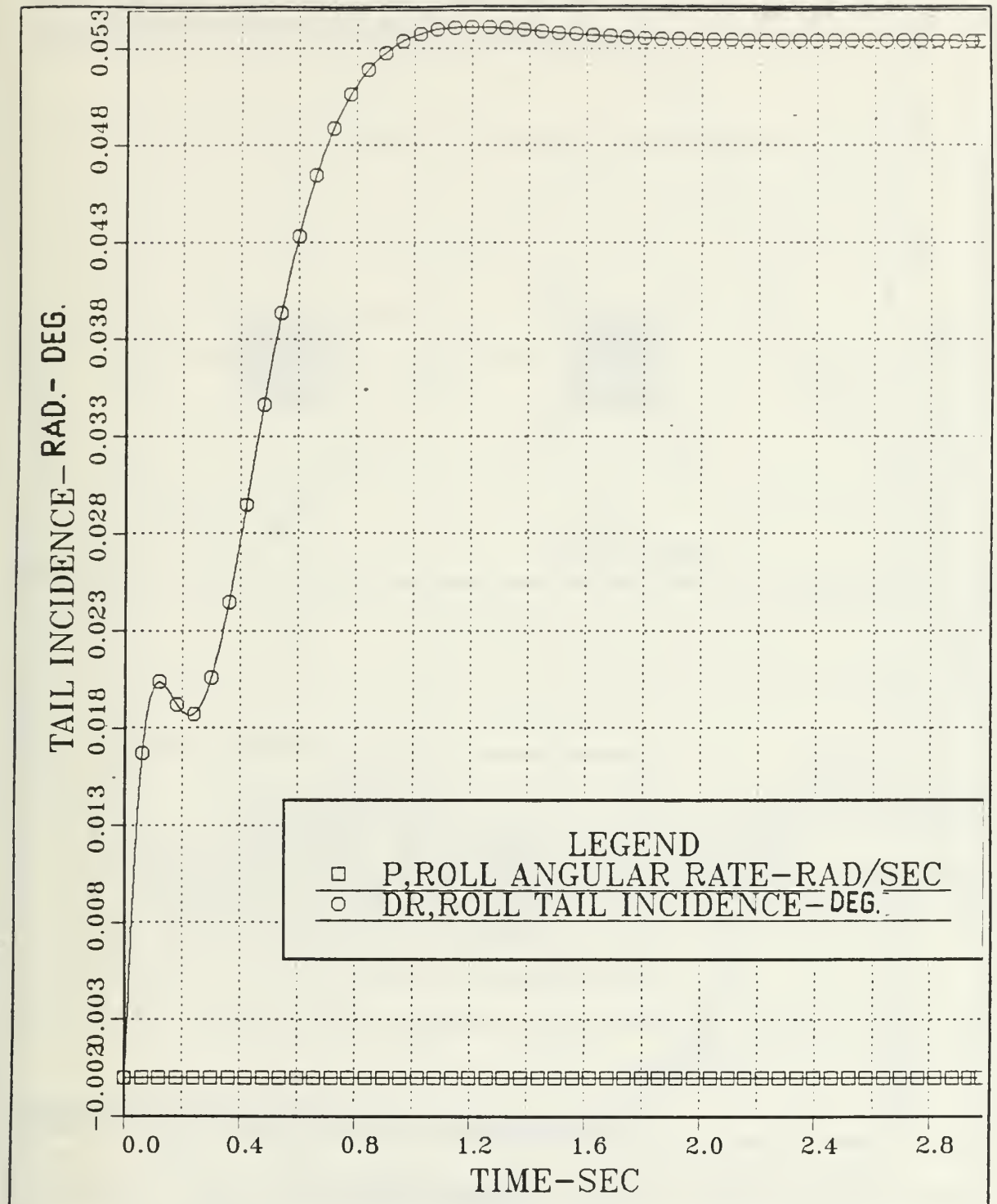

Figure 5.7 Pitch and Roll Tail Incidence vs. Time; Combined Pitch and Roll Channels; Continuous Open Loop System; Step Inputs: δ_{1C}, δ_{2C}, δ_{3C}, δ_{4C} = 0 and N_{ZC} = 1 gee, ψ_C = 0 rad; a_β = 0.

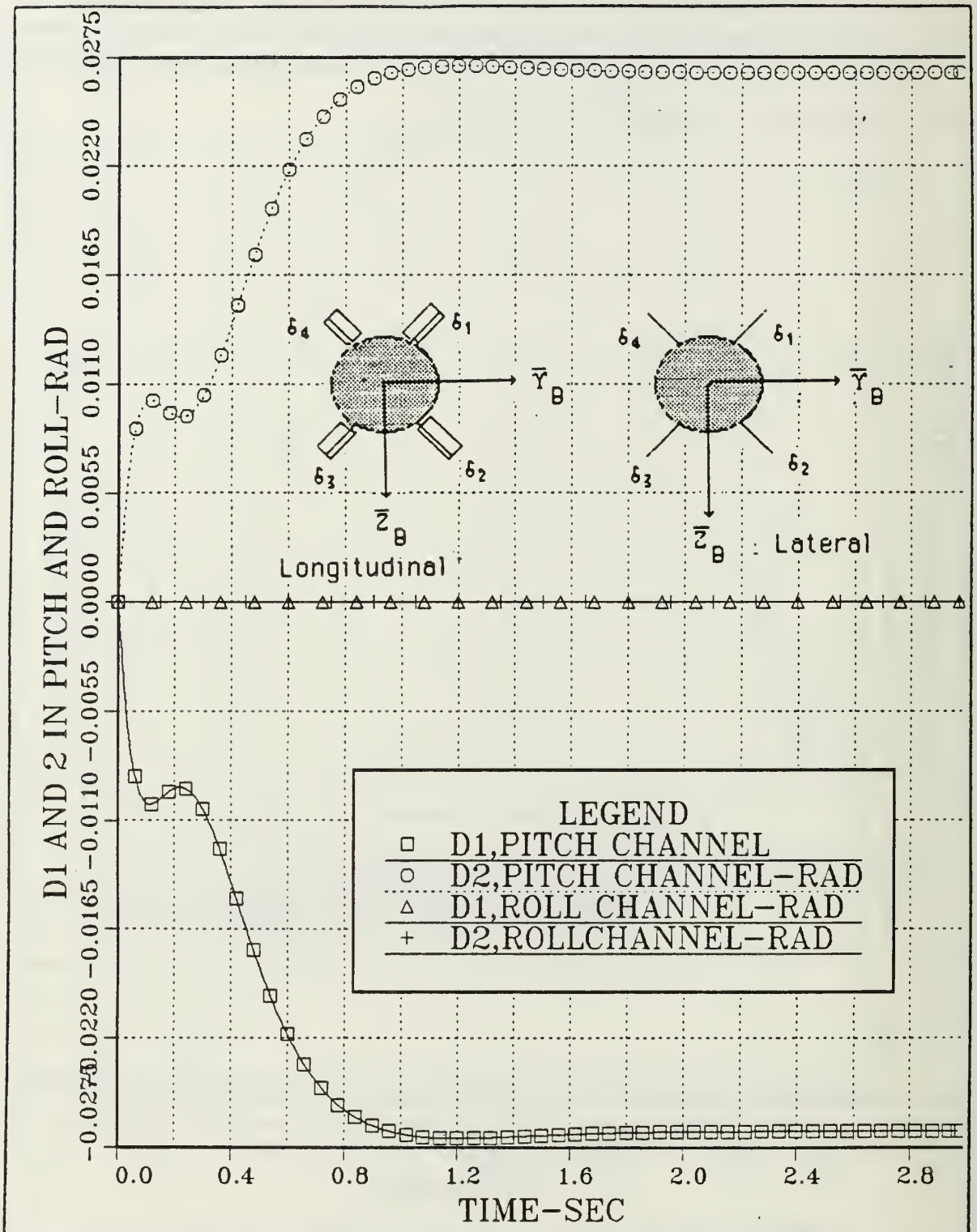

Figure 5.8 Pitch and Roll Deflections vs. Time; Combined Pitch and Roll Channels; Continuous Open Loop System; Step Inputs: δ_{1C}, δ_{2C}, δ_{3C}, δ_{4C} = 0 and N_{ZC} = 1 gee, ψ_C = 0 rad; a_θ = 0.

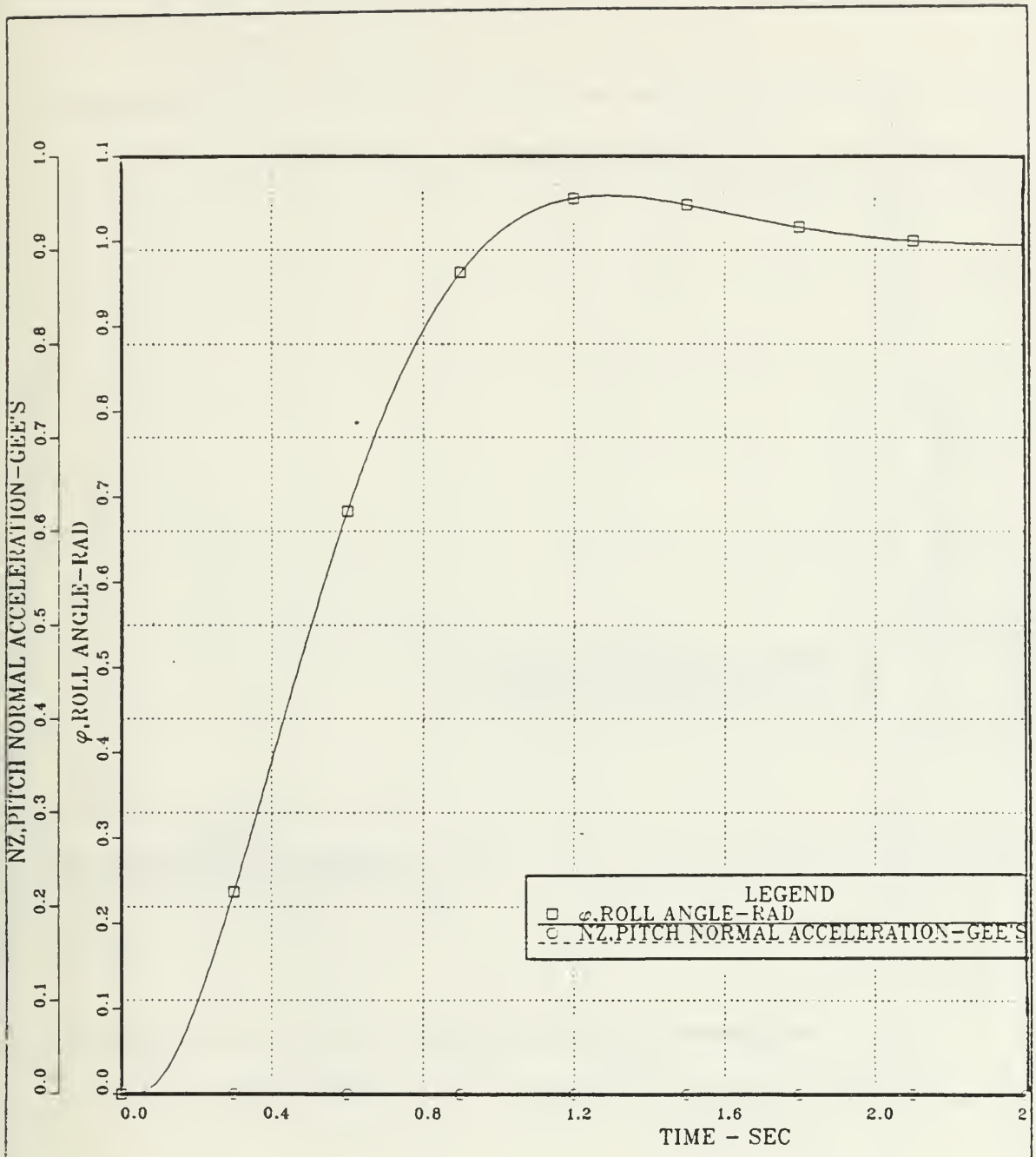

Figure 5.9 Normal Acceleration and Roll Angle vs. Time; Combined Pitch and Roll Channels; Continuous Open Loop System; Step Inputs: δ_{1C}, δ_{2C}, δ_{3C}, δ_{4C} = 0 and N_{ZC} = 0 gee, ψ_C = 1 rad; a_e = 0.

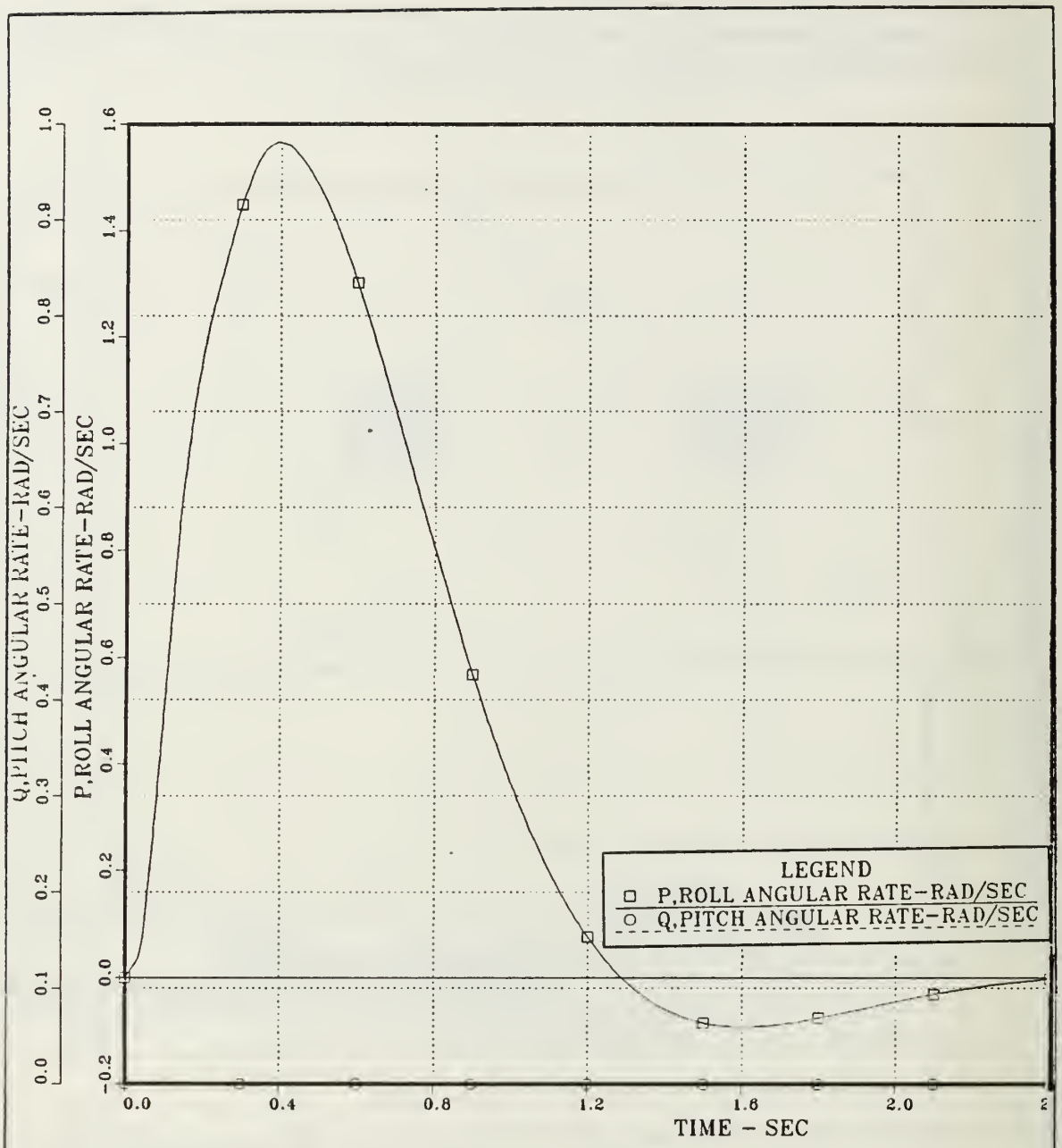

Figure 5.10 Pitch and Roll Angular Rate vs. Time; Combined Pitch and Roll Channels; Continuous Open Loop System; Step Inputs: δ_{1C}, δ_{2C}, δ_{3C}, δ_{4C} = 0 and N_{ZC} = 0 gee, ψ_C = 1 rad; a_e = 0.

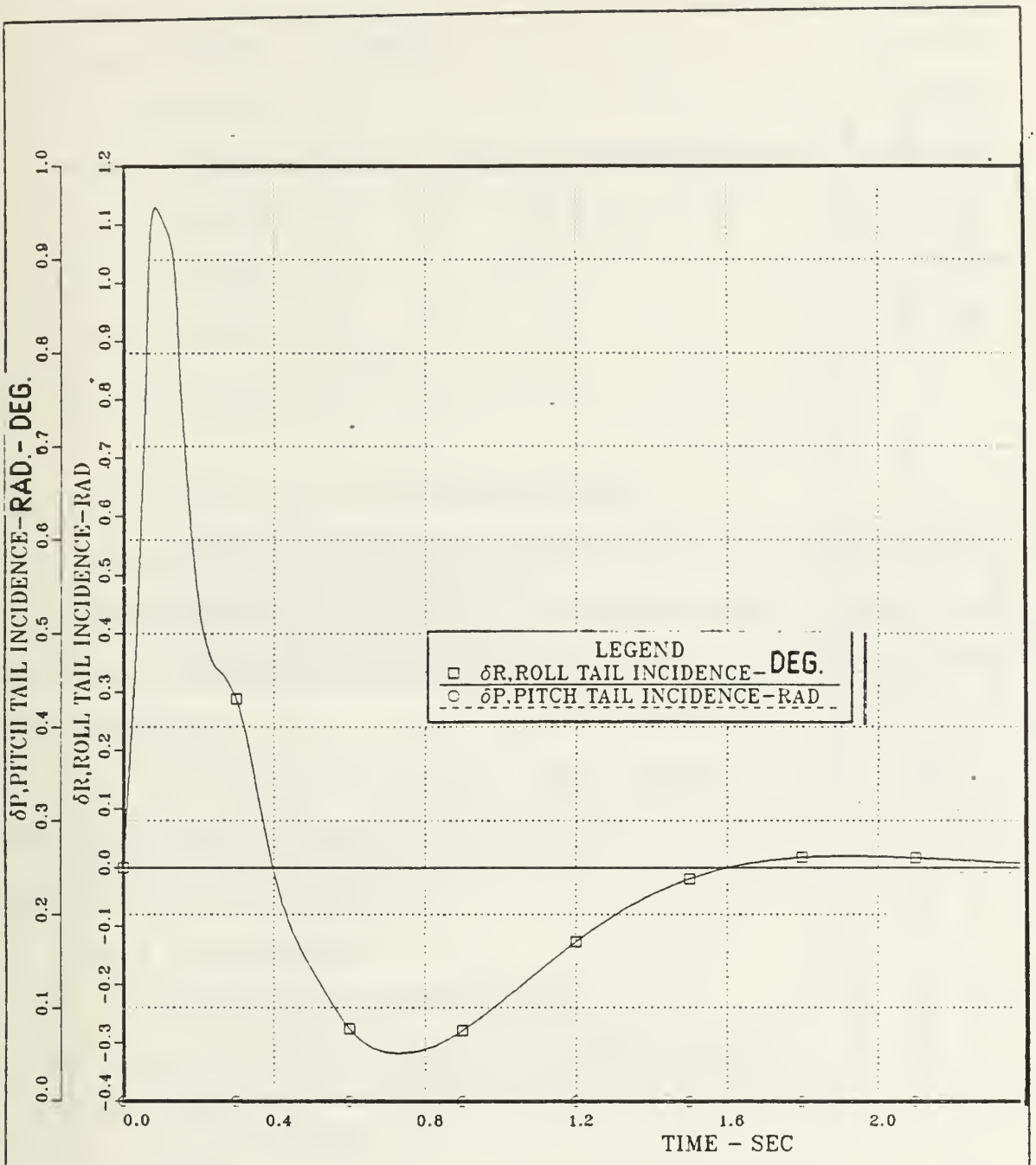

Figure 5.11 Pitch and Roll Tail Incidence vs. Time; Combined Pitch and Roll Channels; Continuous Open Loop System; Step Inputs: δ_{1c}, δ_{2c}, δ_{3c}, δ_{4c} = 0 and N_{zc} = 0 gee, ψ_c = 1 rad; a_e = 0.

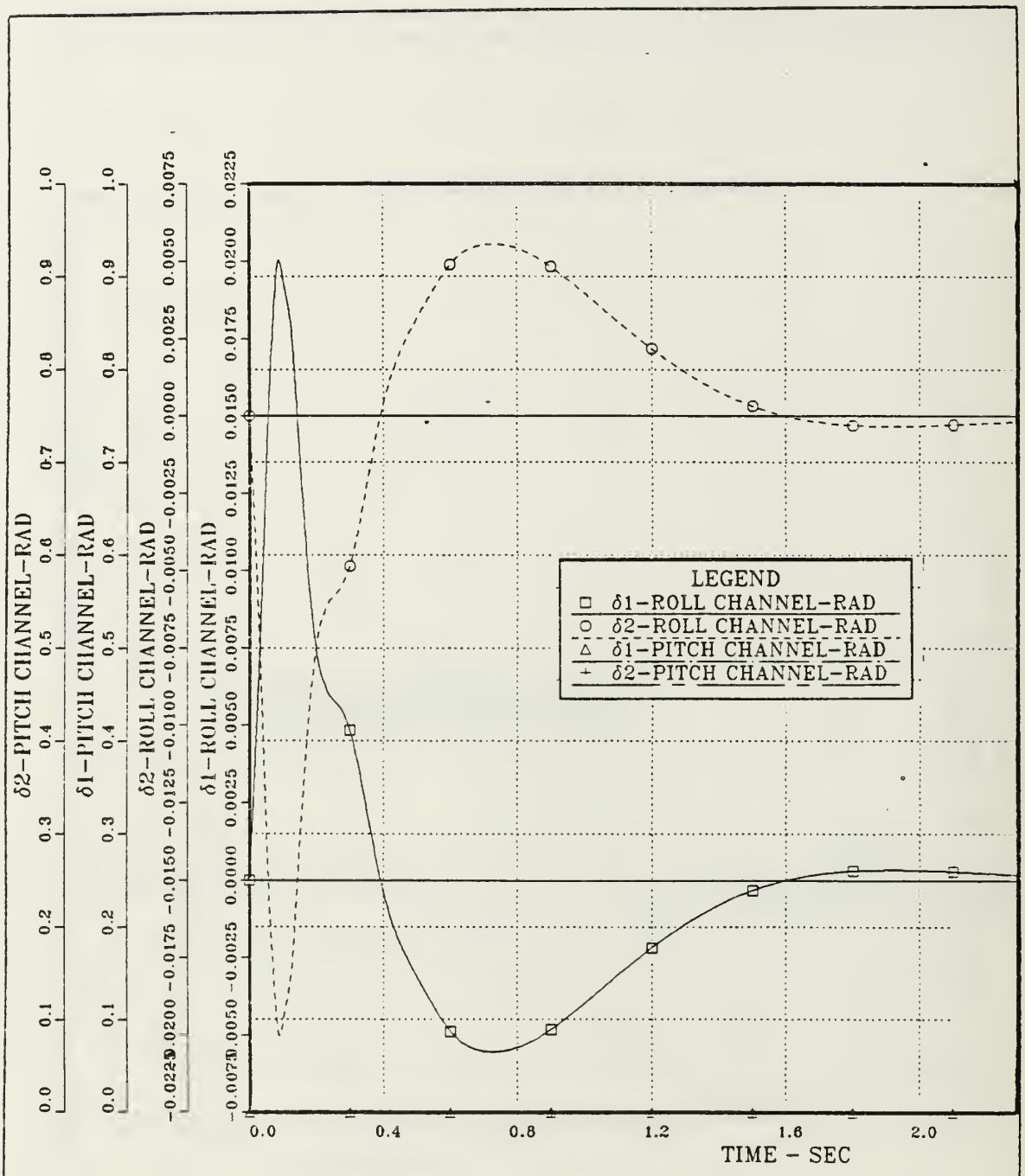

Figure 5.12 Pitch and Roll Deflections vs. Time; Combined Pitch and Roll Channels; Continuous Open Loop System; Step Inputs: δ_{1c}, δ_{2c}, δ_{3c}, δ_{4c} = 0 and N_{2c} = 0 gee, ψ_c = 1 rad; a_e = 0.

$$s_{18} = -2.35821 - j2.70296 \quad \text{(V.B-22)}$$

$$s_{19} = -8.89209 + j0 \quad \text{(V.B-23)}$$

$$s_{20} = -5.18517 + j0 \quad \text{(roll tail incidence)} \quad \text{(V.B-24)}$$

$$s_{21} = -15.0000 + j0 \quad \text{(V.B-25)}$$

$$s_{22} = -15.0000 + j0 \quad \text{(V.B-26)}$$

$$s_{23} = -15.0000 + j0 \quad \text{(V.B-27)}$$

C. THE EFFECTS DUE TO ACTUATOR IMPAIRMENT

In this section the effects on the system due to a damaged actuator was investigated. One control surface (δ_1) was considered damaged. It was locked at a fixed angle while the other three control surfaces had a variable deflection angle.

Two different control inputs were examined for this type of impairment and are discussed below. For each test, corrective actions were then developed and presented.

Test 1. Command Input:

(1) δ_1 for both channels locked at 0.2 rad

(2) δ_2, δ_3, δ_4 for both channels have variable deflections

(3) $N_{Zc} = 1$ gee

(4) $\psi c = 0$ rad

Using the above control input the time response plots of the system were obtained, analyzed and presented in Figures 5.13 through 5.16. In Figure 5.13 the pitch normal acceleration and the roll angle are presented. Commanding a downward maneuver (i.e., $N_Z = 1$ gee and $\psi = 0$) the missile

body the first tenth of the second moves downward and then upward with its pitch axis directed at the velocity vector until it reaches the desired maneuver level. This is due to the induced pitching moment effect of the locked δ_1 control surface and the undamaged control surfaces (δ_2, δ_3, δ_4) which try to counteract the impairment of δ_1. Allthough no roll motion is required to maintain cordination for this maneuver, as is shown in Figure 5.13 a roll angle (0.4 rad) is present. In Figure 5.14 the pitch and roll angular rates are also presented in which the 1.9 rad/sec roll rate is achieved. In Figure 5.16 two control control surfaces from each channel are presented. The other two are the mirror images of the obtained results. The δ_1 (of pitch and roll channels) respond properly to the command input. The δ_2 for the pitch channel is deflected 0.174 radians and for the roll channel 0.130 radians. Both are stabilized after 1.4 seconds.

Corrective actions: The roll effect of the damaged control surface on the performance of the combined autopilot was examined here and corrective actions to overcome this problem were studied and presented.

Figure 5.13 shows the roll angle (φ) reaching its final value of 0.40 rad (23°) in approximately 1.4 seconds with a 7% overshoot. The first try to overcome the roll effect was to command the opposite surface (δ_3) in an equal angle of deflection 0.2 radian. The obtained time response of the pitch normal acceleration and the roll angle are presented in Figure 5.17. For comparison, Figure 5.17 presents three configurations. It shows that the produced roll angle due to the δ_1 control surface impairment is eliminated. But, there is a penalty in the pitch normal acceleration which reaches approximately 4 gee and a oscillatory behavior is evident before the steady

state value of 1 gee command being achieved. So, another test was performed by commanding the δ_3 surface at an opposite angle of deflection (-0.2 rad). By this action, shown in Figure 5.18, the normal acceleration responds very well but the roll angle is increased at 1.18 radians (68°) after 1.75 seconds, as might be expected. The next test was performed using the second control surface (δ_2). In Figure 5.19 the time response of the same variables of the system are obtained and presented. The control surface δ_2 is commanded at the same angle of deflection i.e., 0.2 radians. As is illusrtated in Figure 5.19 commanding a downward maneuver the missile body reaches the desired maneuver level without any roll motion (i.e., $N_Z = 1$ gee and $\varphi = 0$).

At the end of this Chapter a transition reconfiguration strategy is proposed addressing the topics of failure detection and isolation, and implementation. That is, one. pssible strategy for transitioning from the normal control laws for a missile with all control surfaces operative, to one set of reconfigured control laws for a missile with a failed surface.

Test 2. Command Input:

(1) δ_1 for both channels locked at 0.2 rad.

(2) δ_2, δ_3, δ_4 for both channels have variable deflections.

(3) $N_{Zc} = 0$ gee.

(4) $\varphi_c = 1$ rad.

Using the above step input vector the time response plots of the system were obtained and presented in Figures 5.20 through 5.23.

In Figure 5.20 the time response of the pitch normal acceleration and the roll angle of the combined system are illustrated. Due to the fact that

the two channel autopilots were cross-coupled through the four control surfaces (δ_1, δ_2, δ_3, δ_4), a damage in any actuator(s) will affect the performance of both channels. The locked control surface δ_1 at the one rad angle affects the combined autopilot. A constant incorrect level was achived in the response of the roll angle (i.e., ϕ = 1.4 rad instead of the commanded one rad). In addition, due to the induced pitching moment effect by the damaged control surface, a down and upward maneuver was commanded by the pitch channel during the first second of the response of the normal acceleration.

A change of the other state variables was obvious as is shown in Figures 5.21 through 5.23. Figure 5.23, which represents the time response of two control surfaces from each channel, i.e., δ_1 and δ_2, indicates the commanded (simulated) failure of 0.2 radian at δ_1 and the deflection angle of 0.13 radians (7.5°) for the other three control surfaces. The control surfaces not presented in this plot are the mirror images of the obtained ones.

Corrective actions: The roll and pitch effects caused by the damaged control surface δ_1 on the combined autopilot performance was examined and corrective actions to overcome this failure were studied and presented.

In Figure 5.20 the undesirable rolling and pitching effect caused by the damaged δ_1 control surface is obvious. The missile rolls about its velocity vector with a 1.4 radians roll angle (80°) (instead of the commanded 1 radian). Also observe the effect on the pitch normal acceleration which should be constant at zero since no down or upward maneuver was commanded.

To overcome these failures several runs of the Controls Program OPTSYS were performed to find an appropriate corrective action for the control system. The most interesting cases are illustrated in Figures 5.24 and 5.25.

In Figure 5.24 the roll angle (φ) and the pitch normal acceleration (n_z) were obtained and presented for three cases to compare their responses. A comparison was performed between the original system, the impaired system with the δ_1 effector locked at an angle of 0.2 radians, and the system with the δ_2 control surface commanded at an angle equal but opposite (-0.2) to the defective surface. As is illustrated in Figure 5.24, if such an input was commanded, the missile body rolls even more at a 2.2 radians (126º) angle as might be expected. Also, the pitch normal acceleration increases and achieves the large value of -4.2 gee's before stabilizing after 1.4 seconds.

In Figure 5.25 the roll angle (φ) and the pitch normal acceleration (n_z) were obtained and presented but now the second control surface δ_2 was commanded to be deflected at the same angle as the δ_1, (0.2 radians). As is illustrated in Figure 5.25, both effects, on the roll angle and the pitch normal acceleration, were eliminated and their time response plots indicates that the missile body performed according to the command input.

In comparing output time responses, as was done by these two tests, it is apparent that the impaired missile was able to track the unimpaired missile as long as there was another control surface to provide the appropriate corrective action and control power of the failed surface.

In the case where one or more control surfaces are inoperative or shot away and are not considered here, similar effects are expected. This is due to the fact that as far as all the control surfaces are operative, are commanded by the system such that one will counteract the induced moment effect of the other. But when one control surface is inoperative or shot away undesirable roll, pitch or combined effects will be present.

D. PROPOSED RECONFIGURATION STRATEGY

1. Introduction

This section presents one possible strategy for transitioning from the control laws for a missile with all surfaces operative, to a set of reconfigured control laws for an missile with a failed surface. The discussion begins with a definition of reconfiguration and why it is important. A transition stategy is then proposed, addressing the topics of failure detection, isolation, and implementation.

2. Reconfiguration

Reconfiguration is a technique which shows promise in restoring missile stability and a degraded level of controllability in the event a control surface becomes inoperative. This technique implies that the control laws governing missile motion compensate for the failed surface by using the remaining surfaces to maintain control. The control laws of Chapter III, IV and the corrective actions of Chapter V provide the independent control of each surface necessary to implement reconfiguration which deals with the coupled aerodynamics.

3. Transition Strategy

The development of reconfigurable control laws, such as those developed in this thesis, must include a method of failure identification and implementation of a revised control law. For a given failure it thus necessary to determine when the new laws should be used and how to switch to them from from normal control laws. A failure detection and isolation scheme must be developed to determine when and which surface has failed. The proposed failure detection and isolation system would use a set of redundant sensors and an estimator, to determine if the actuators are still operative. Should an actuator fail to move a control surface, the sensors notify a control surface monitor. The monitor validates the fail signal and determines which control surface is inoperative.

The control surface monitor is the heart of the reconfigurable flight control system. When notified of a failure, the monitor informs the flight control computers of the problem and provides the necessary information concerning which set of new control laws (corrective actions) should be used to calculate the appropriate surface deflections. The off-line flight control computer is programmed with the new control laws and then signals the on-line system that it is ready to assume control of the missile. Thus the autopilot is again ready to control a stable missile with some degree of control capability.

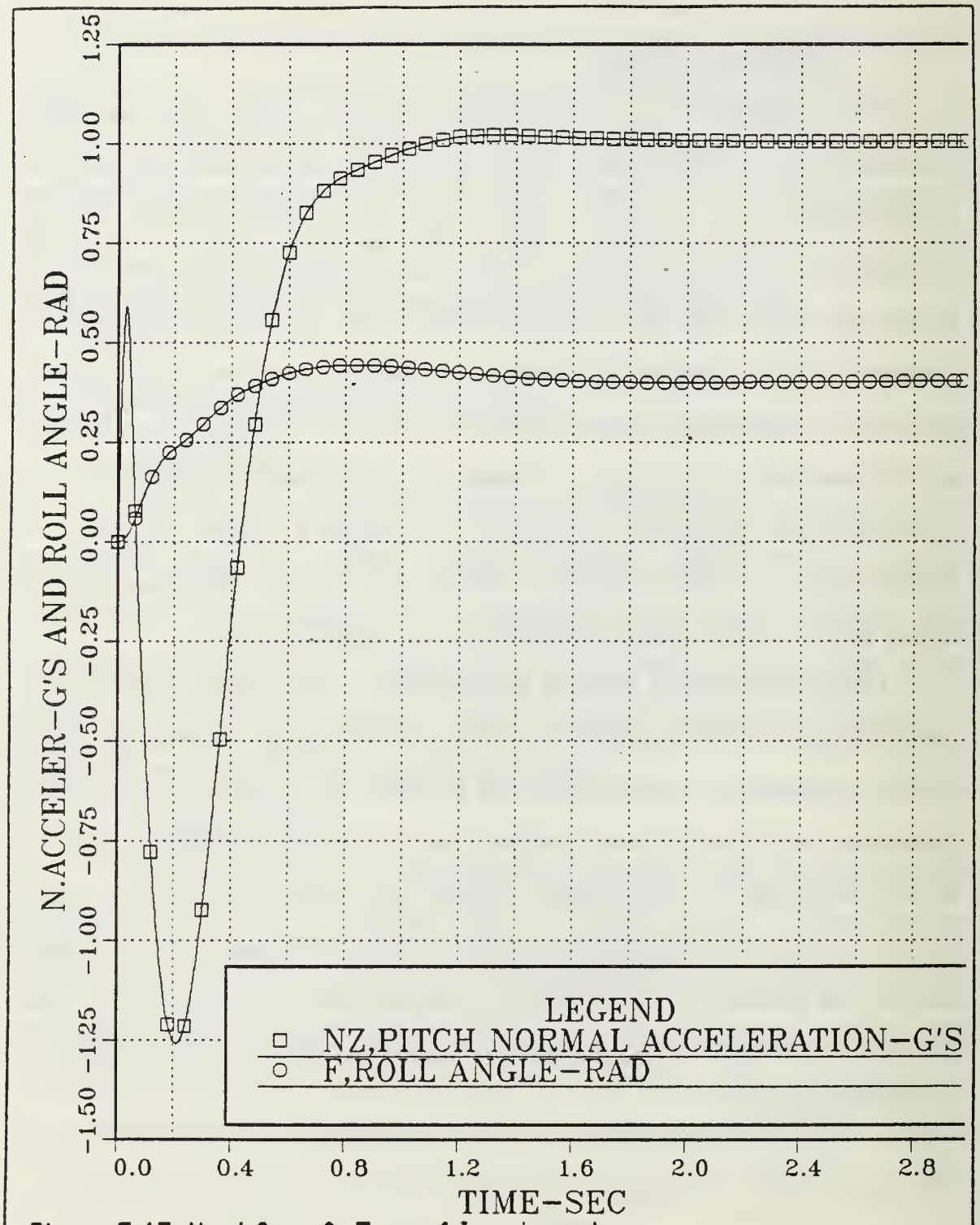

Figure 5.13 Hard Over δ_1 Type of Impairment: Normal Acceleration and Roll Angle vs. Time; Combined Pitch and Roll Channels; Continuous Open Loop System; Step Inputs: δ_{1C}=0.2rad, δ_{2C}, δ_{3C}, δ_{4C} = 0 and N_{ZC} = 1 gee, ψ_C = 0 rad; a_e = 0.

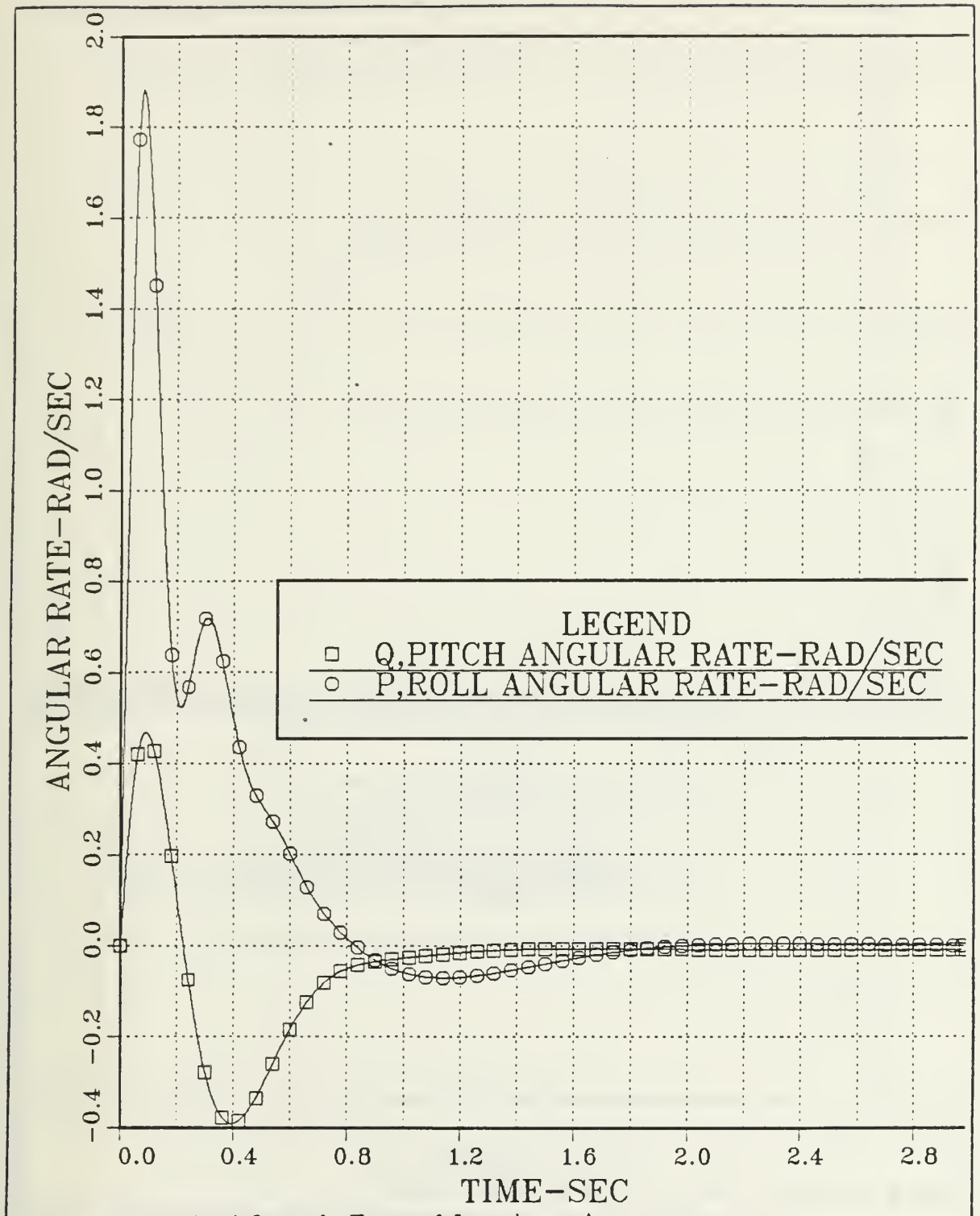

Figure 5.14 Hard Over δ_1 Type of Impairment: Pitch and Roll Angular Rate vs. Time; Combined Pitch and Roll Channels; Continuous Open Loop System; Step Inputs: δ_{1c}=0.2rad. δ_{2c}, δ_{3c}, δ_{4c} = 0 and N_{zc} = 1 gee, ψ_c = 1 rad; a_e = 0.

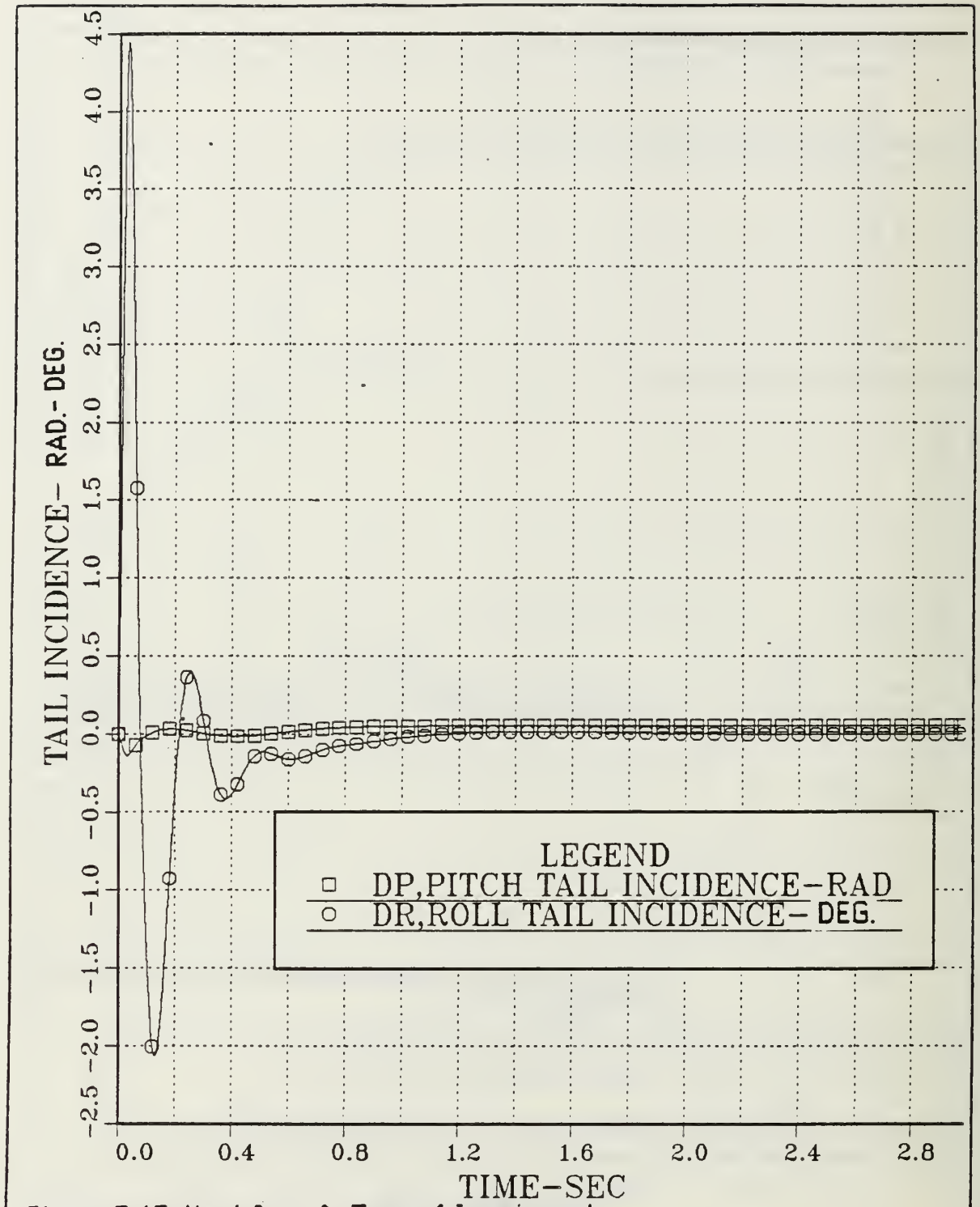

Figure 5.15 Hard Over δ_1 Type of Impairment:
Pitch and Roll Tail Incidence vs. Time; Combined Pitch and Roll Channels; Continuous Open Loop System; Step Inputs: δ_{1C}=0.2rad, δ_{2C}, δ_{3C}, δ_{4C} = 0 and N_{ZC} = 1 gee, ψ_C = 0 rad; a_β = 0.

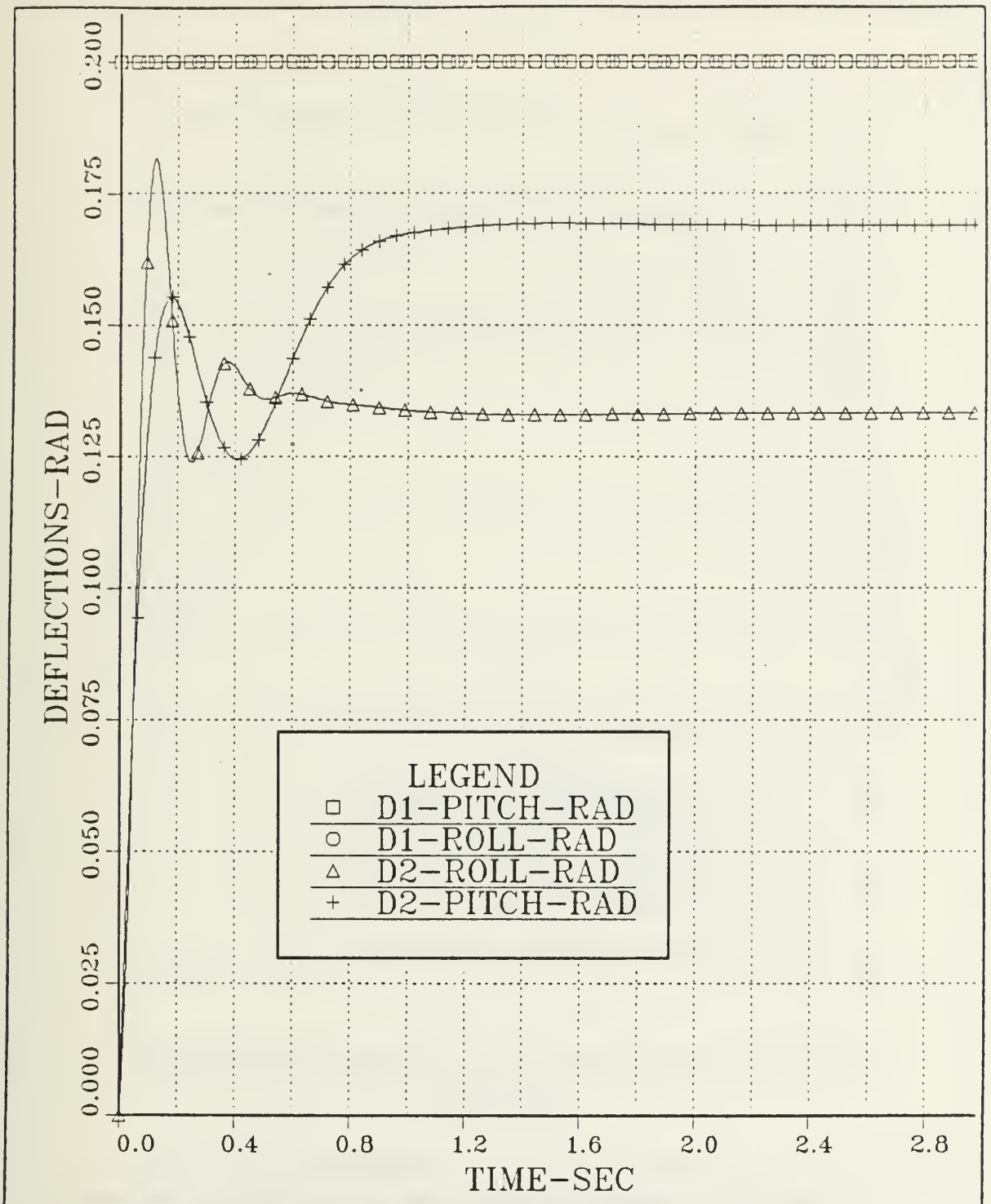

Figure 5.16 Hard Over δ_1 Type of Impairment: Pitch and Roll Deflections vs. Time; Combined Pitch and Roll Channels; Continuous Open Loop System; Step Inputs: δ_{1C}=0.2rad, δ_{2C}, δ_{3C}, δ_{4C} = 0 and N_{ZC} = 1 gee, ψ_C = 0 rad; a_e = 0.

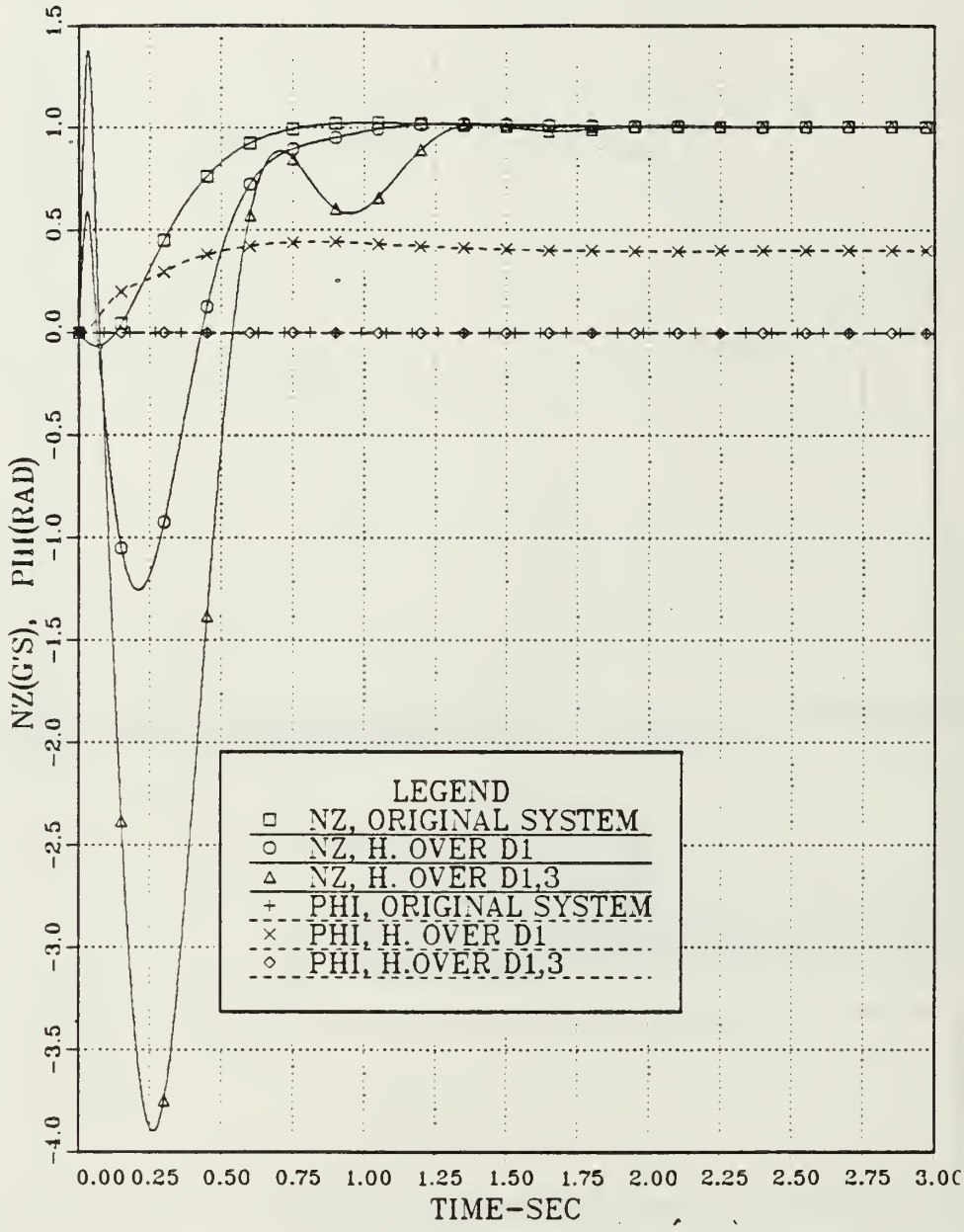

Figure 5.17 First Corrective Action and Comparison of the Pitch Normal Acceleration (Nz) and the Roll Angle (φ), between Three Different Effectors Configuration.

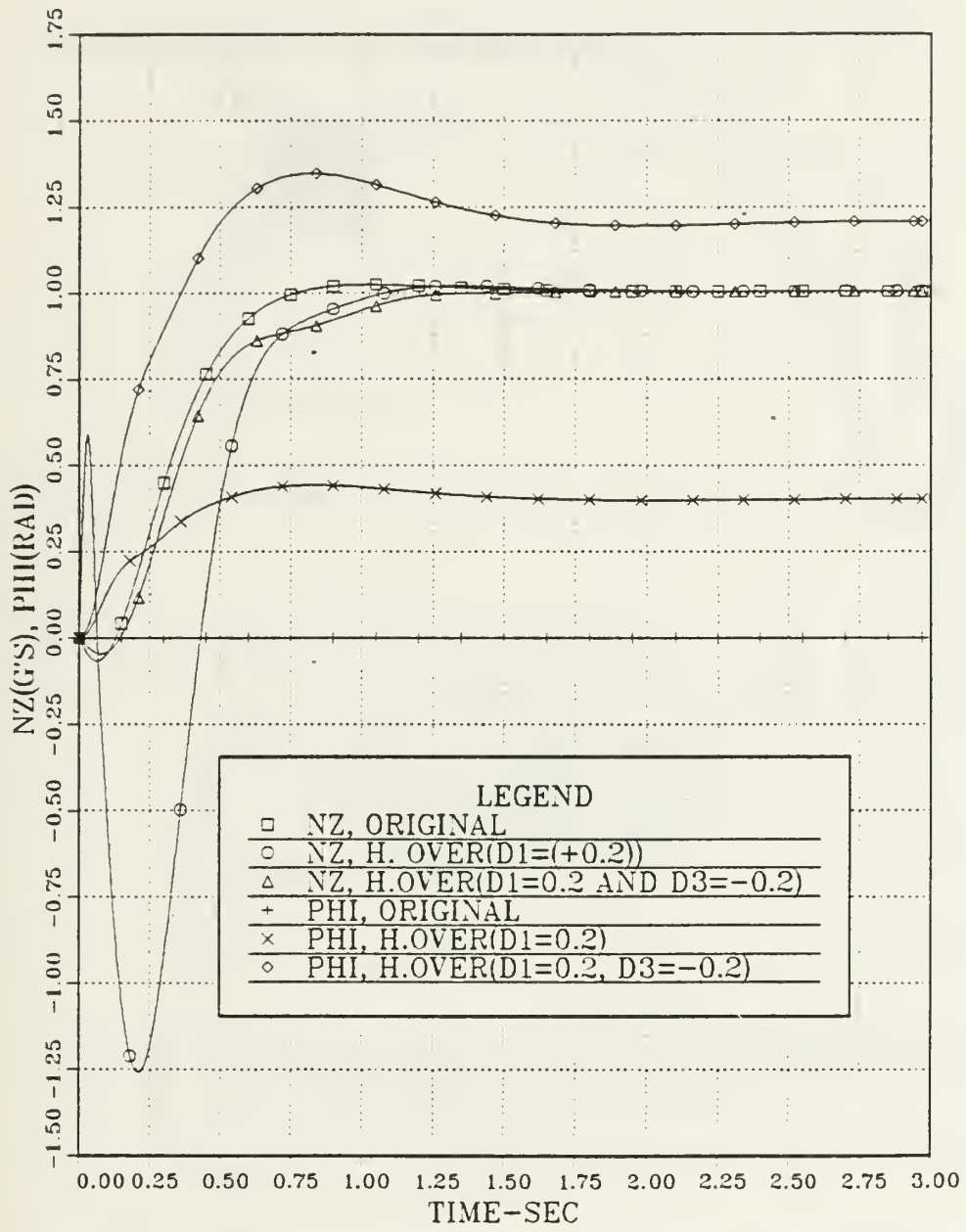

Figure 5.18 Second Corrective Action and Comparison of the Pitch Normal Acceleration (Nz) and the Roll Angle (φ), between Three Different Effectors Configuration.

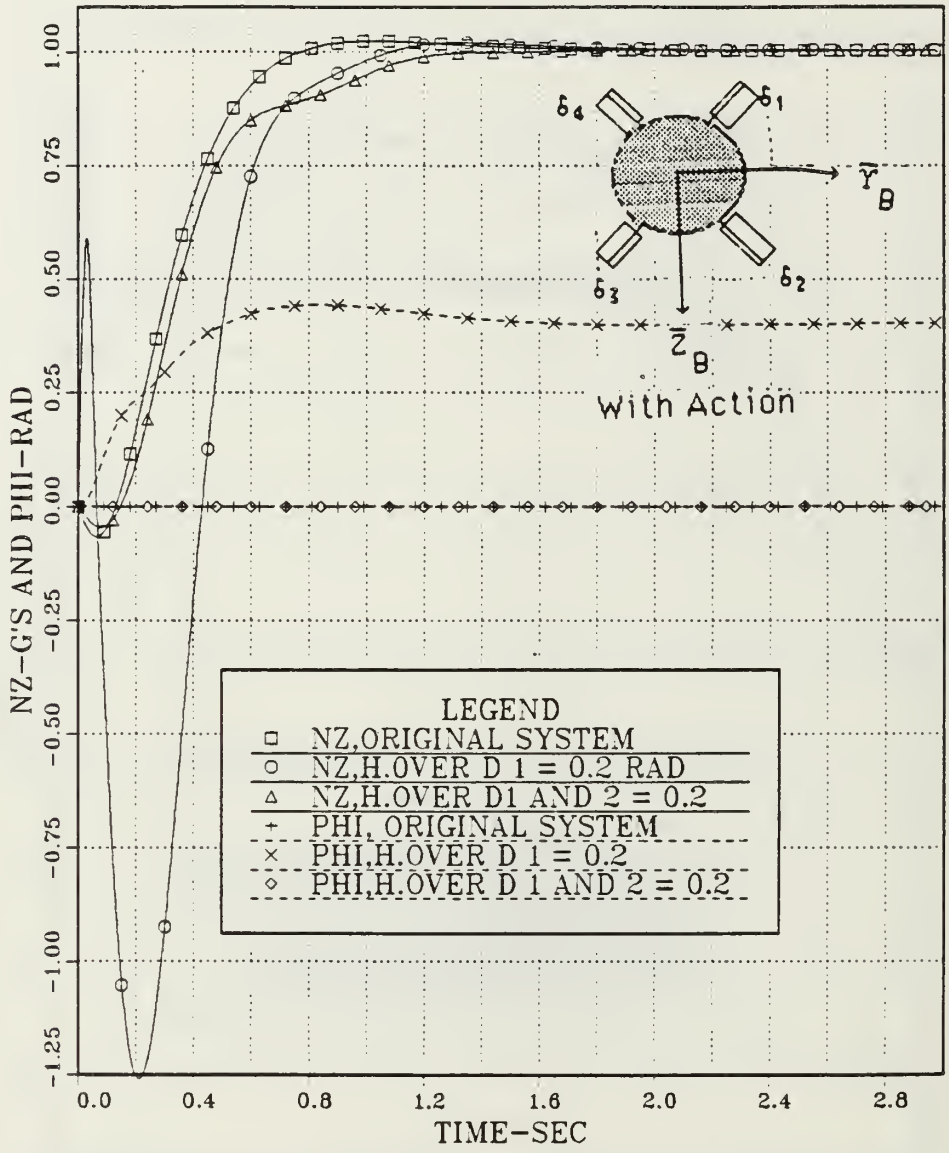

Figure 5.19 Final Corrective Action and Comparison of the Pitch Normal Acceleration (Nz) and the Roll Angle (φ), between Three Different Effectors Configuration.

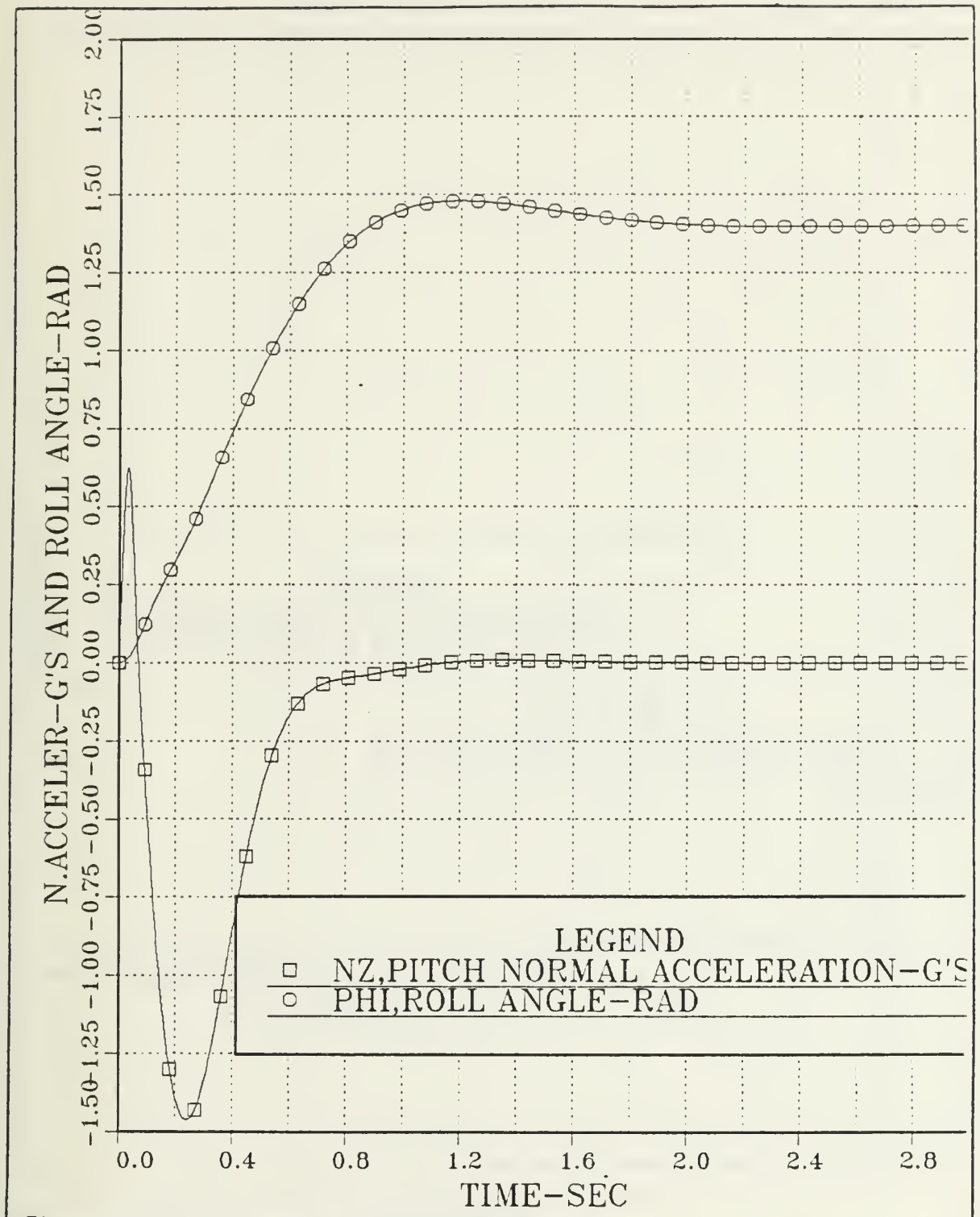

Figure 5.20 Hard Over δ_1 Type of Impairment:
Normal Acceleration and Roll Angle vs. Time; Combined Pitch and Roll Channels; Continuous Open Loop System; Step Inputs: δ_{1C}=0.2rad, δ_{2C}, δ_{3C}, δ_{4C} = 0 and N_{ZC} = 0 gee, φ_C = 1 rad; a_e = 0.

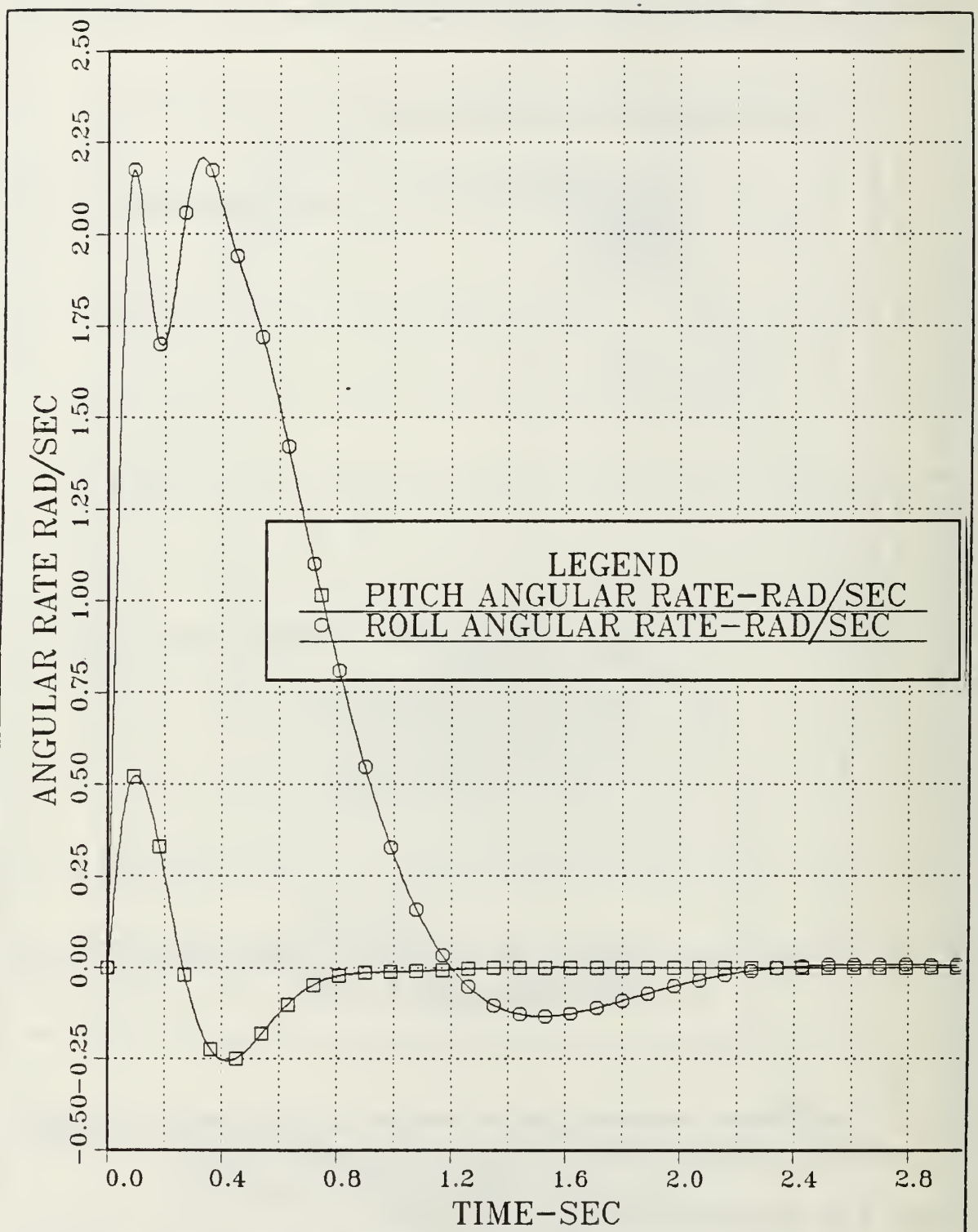

Figure 5.21 Hard Over δ_1 Type of Impairment: Pitch and Roll Angular Rate vs. Time; Combined Pitch and Roll Channels; Continuous Open Loop System; Step Inputs: δ_{1c}=0.2rad, δ_{2c}, δ_{3c}, δ_{4c} = 0 and N_{zc} = 0 gee, ψ_c = 1 rad; a_e = 0.

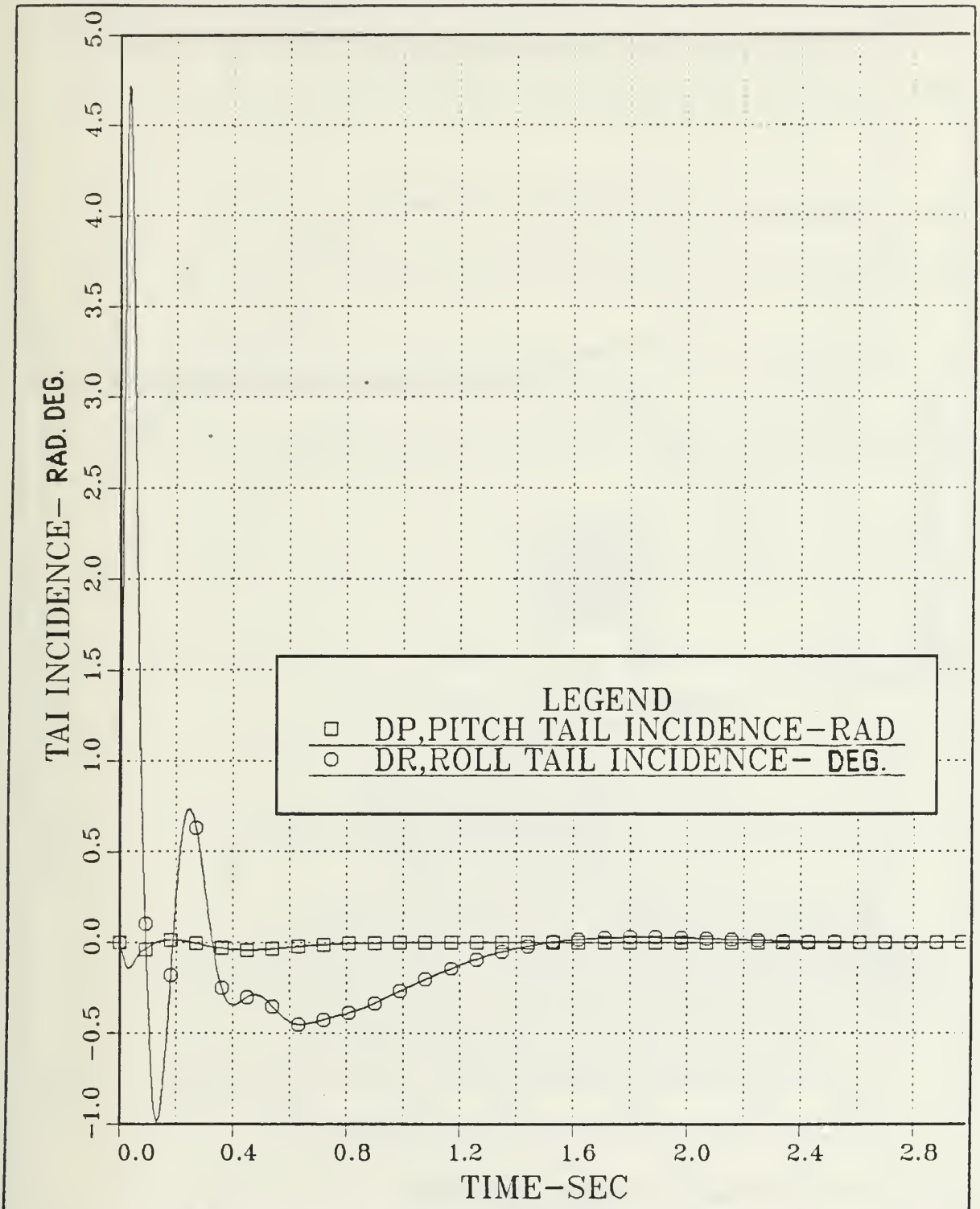

Figure 5.22 Hard Over δ_1 Type of Impairment:
Pitch and Roll Tail Incidence vs. Time; Combined Pitch and Roll Channels; Continuous Open Loop System; Step Inputs: δ_{1C}=0.2rad, δ_{2C}, δ_{3C}, δ_{4C} = 0 and N_{ZC} = 0 gee, ψ_C = 1 rad; a_e = 0.

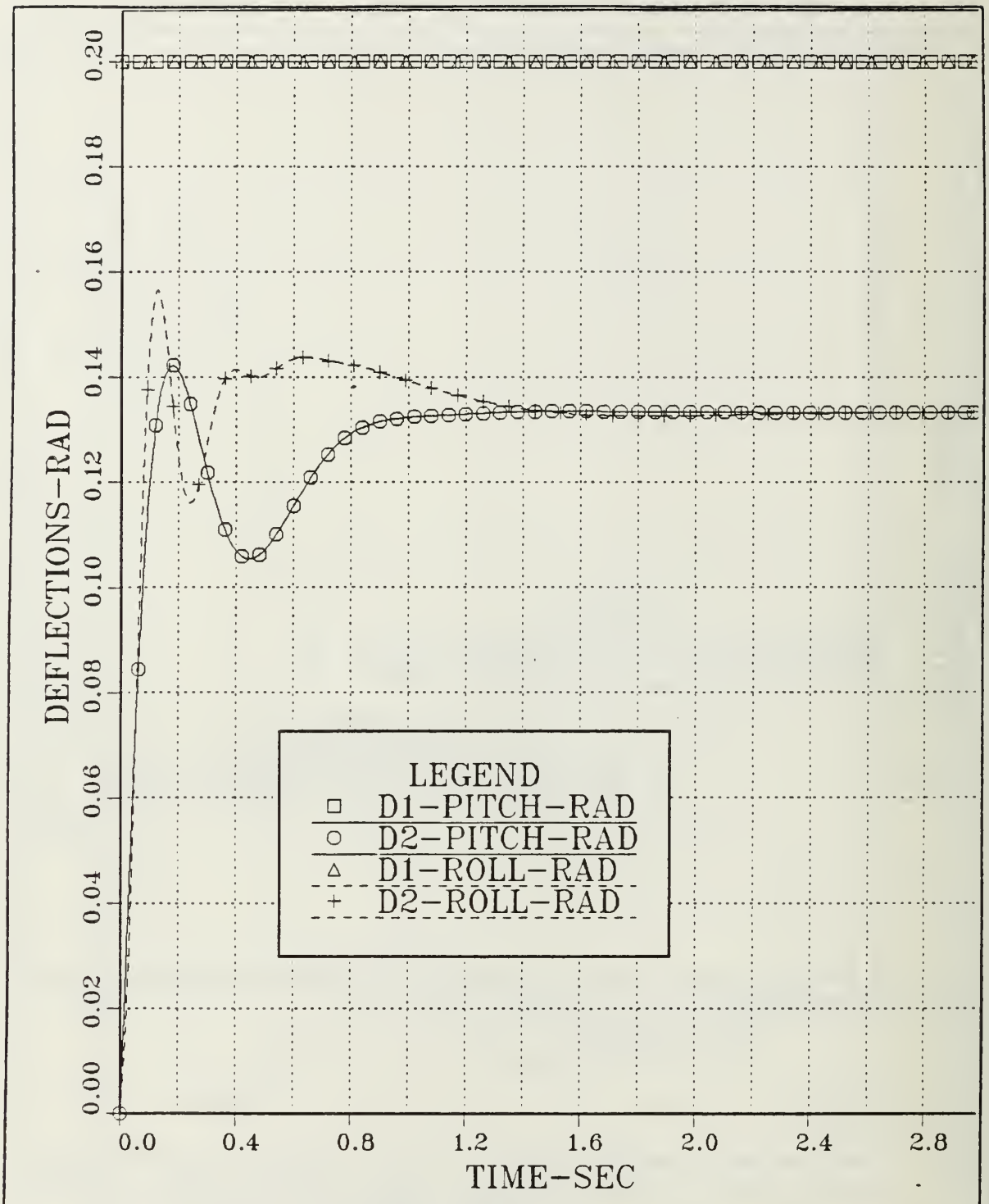

Figure 5.23 Hard Over δ_1 Type of Impairment:
Pitch and Roll Deflections vs. Time; Combined Pitch
and Roll Channels; Continuous Open Loop System; Step Inputs:
δ_{1C}=0.2rad, δ_{2C}, δ_{3C}, δ_{4C} = 0 and N_{ZC} = 0 gee, ψ_C = 1 rad; a_e = 0.

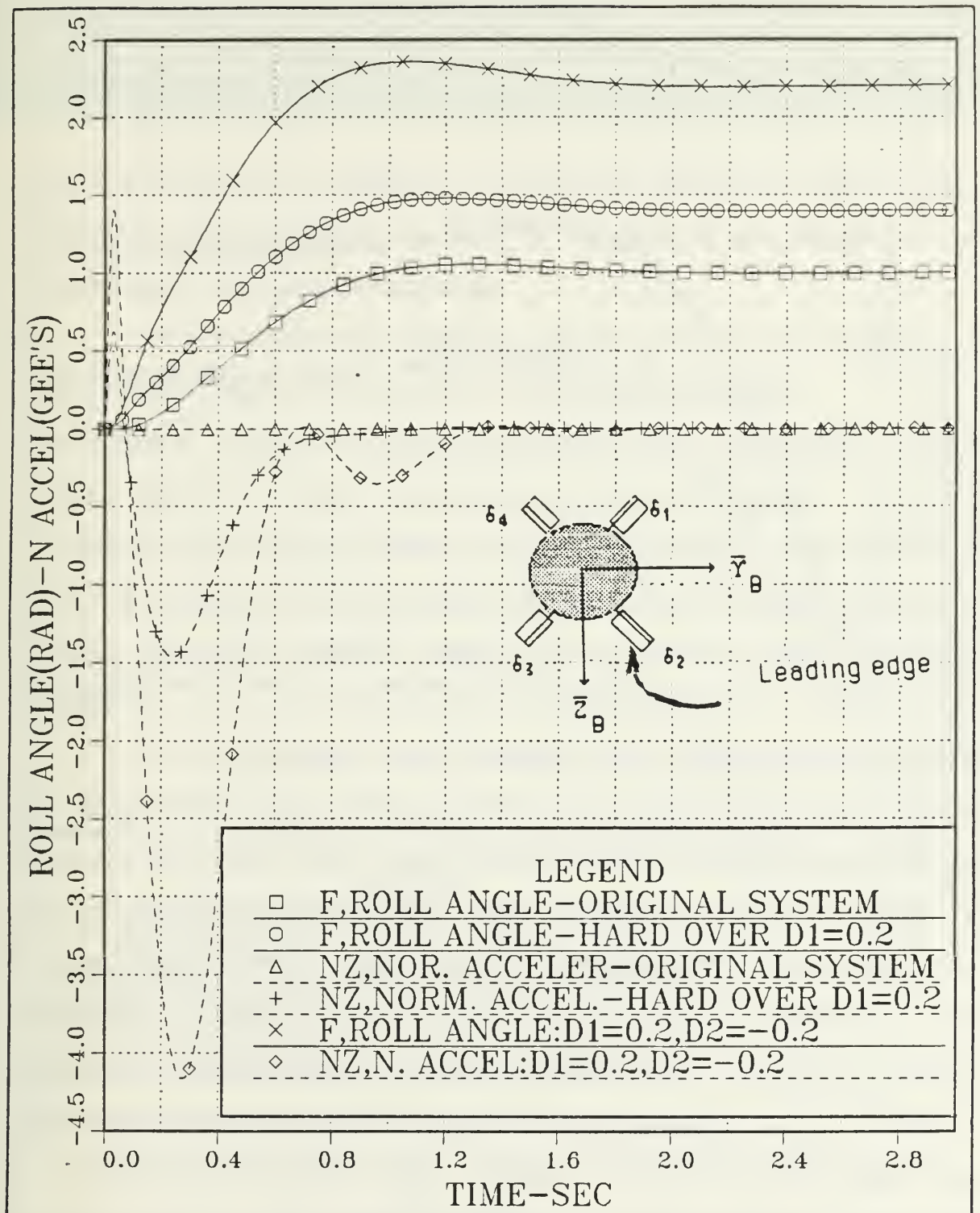

Figure 5.24 First Corrective Action and Comparison of the Pitch Normal Acceleration (Nz) and the Roll Angle (φ), between Three Different Effectors Configuration.

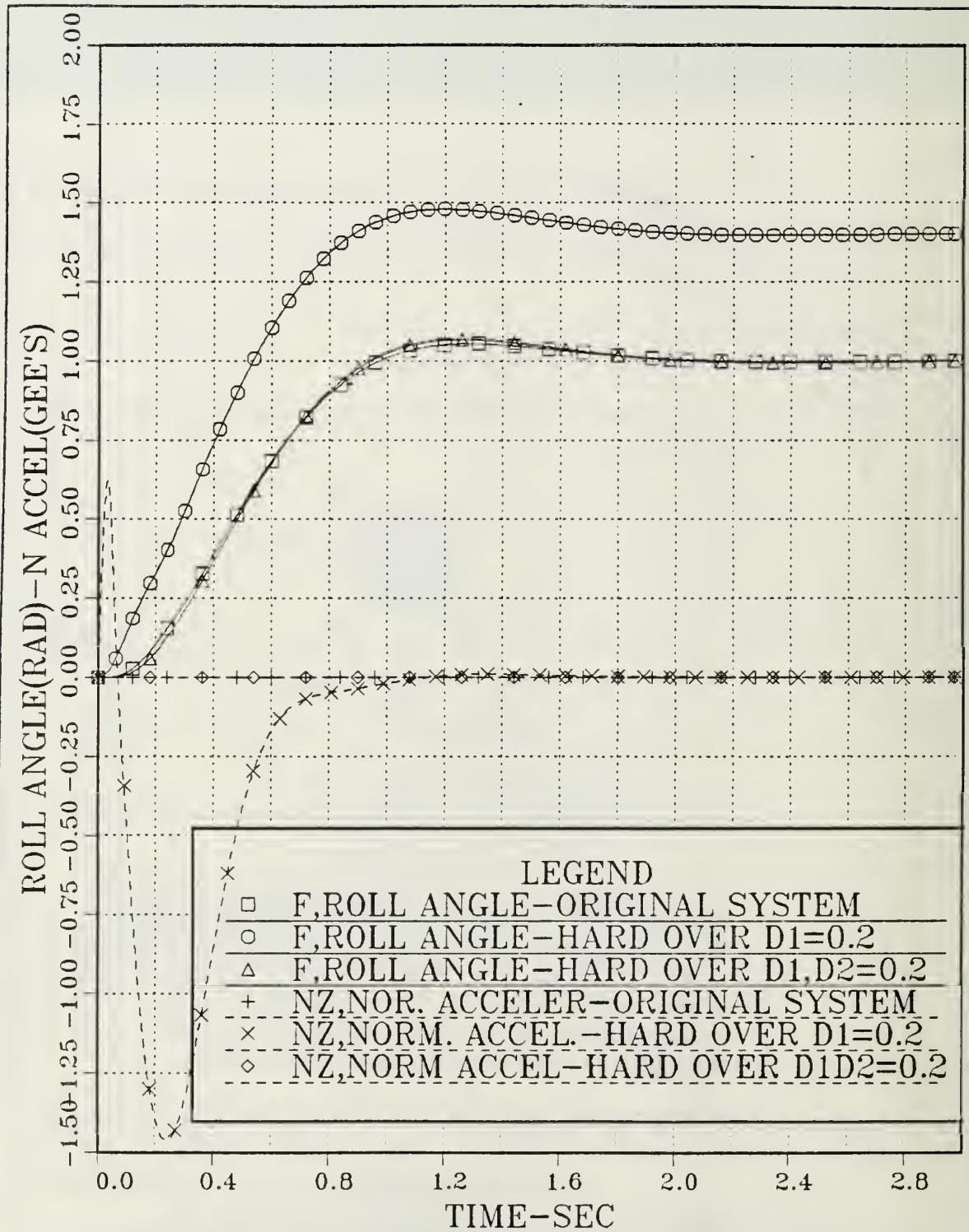

Figure 5.25 Second Corrective Action and Comparison of the Pitch Normal Acceleration (Nz) and the Roll Angle (φ), between Three Different Effectors Configuration.

E. ROBUSTNESS OF THE UNIMPAIRED SYSTEM

1. Introduction

Up to this point the continuous open loop system was investigated and it was found to be stable, as is indicated by Equations (V.B-5) through (V.B-27). In this section the concept of feedback is introduced and the robustness of the system is examined.

Design criteria for feedback control systems can be lumped into three broad categories: performance, stability, and robustness.
Performance criteria are generally specified as a requirement for the control system to follow commands or reject disturbances. The most commonly used stability criteria are stability margins which generally refer to the amount of gain or phase variations from a design condition a system employing feedback control can experience before becoming unstable.

In early feedback control applications, reducing sensitivity was the only control design criteria, particularly reducing sensitivity to noise. Over the last several years, sensitivity issues have attracted new attention and have generated a new requirement, robustness. A control system is robust (insensitive) if performance is maintained in the presence of variations in the plant from the design model. These variations can be modeling approximations, modeling uncertainties, failures of control elements (sensors, actuators), noise, non-linearities, etc.

These criteria are not mutually exclusive. Good stability characteristics in well designed systems are usually accompanied by good

performance. Robustness must be considered relative to the variations from the design model that the control system will experience.

2. The Benefits of Feedback and the Singular Value Design Technique

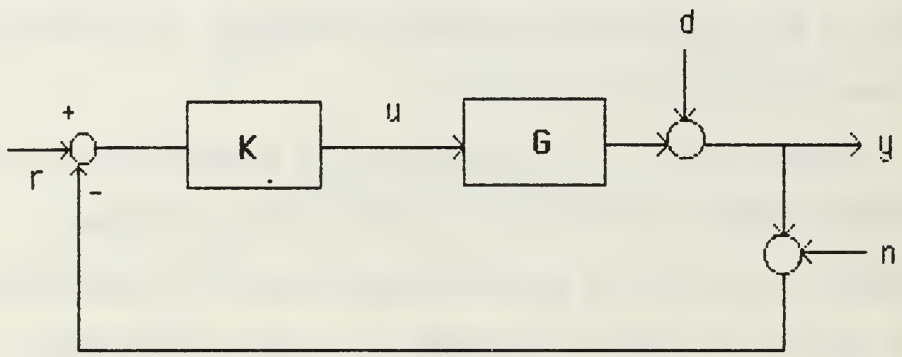

Figure 5.26 Standard Feedback Configuration

We deal with the standard feedback configuration illustrated in Figure 5.26. It consists of the interconnected plant (G) and controller (K) forced by commands (r), measurement noise (n), and disturbances (d).

The noise in this case is assumed to be zero. The disturbances are assumed to be reflected to the measured output (y).

All signals are multivariable, in general, and both nominal mathematical models for G and K are finite dimensional linear time invariant systems with transfer functions matrices G(s) and K(s). Then it is well known that the configuration, if it is stable, has the following major properties:

a. Input-output behavior

$$y = G K (I + G K)^{-1} (r - n) + (I + G K)^{-1} d \qquad \text{(V.E.2-1)}$$

$$e = r - y$$
$$= (I + G K)^{-1} (r - d) + G K (I + G K)^{-1} n \qquad \text{(V.E.2-2)}$$

b. System sensitivity

$$\Delta H_{cl} = (I + G' K)^{-1} \Delta H_{ol} \qquad \text{(V.E.2-3)}$$

In Equation (V.E.2-3), ΔH_{cl} and ΔH_{ol} denote changes in the closed loop system and changes in a nominally equivalent open loop system, respectively, caused by changes in the plant G, i.e., $G' = G + \Delta G$.

Equations (V.E.2-1) through (V.E.2-3) summarize the fundamental benefits and design objectives inherent in feedback loops. Specifically, Equation (V.E.2-2) shows that the loop's errors in the presence of commands and disturbances can be made "small" by making the sensitivity operator, $(I + G K)^{-1}$, "small". Equation (V.E.2-3) shows that loop sensitivity is improved under these same conditions, provided ΔG is not too large from G.

With the increased interest in MIMO systems numerous methods of design have been employed to obtain suitable system performance and robustness with varying degrees of success. One primary method of design is to keep the plant as decoupled as possible throughout the design so that each individual element may be controlled independently and designed essentially as a single loop system. In another procedure the multiloop system is modified into a system that has diagonal elements that are much larger than any off-diagonal elements. This diagonally dominant system is

then in a form where conventional Nyquist type techniques can be employed in the analysis. A third common MIMO design method is that of the Linear Quadratic (LQ) method. This method uses a quadratic cost functional and optimization principles to allow the designer to design for various performance levels by adjusting the matrix weighting terms used in the cost function. The major difficulty with all of the above methods is that they are not necessarily robust. This is especially true for cross-coupling terms between loops.

As was mentioned before, a simple interpretation of robustness is the ability of the system to tolerate design pertubations. These perturbations could be in the form of actuator failures, plant parameter uncertainty, unmodeled dynamic or nonlinear terms, or any one of many other perturbations to the nominal design of the system.

The analysis of the robustness of the system was obtained using the Pole Placement and Robustness Design Program (POPLAR) developed by Gordon, V.C. [Ref. 5].

Utilizing the above program and using the data file shown in Appendix E for the state-feedback autopilot, the unimpaired system was found to be robust. The standard full state-feedback design was carried out using the N.P.S. program OPTSYS.

Figures 5.27 and 5.28 show the Minimum Additive Output Singular Value (SVADMO) vs. frequency, and the Minimum Additive Input Singular Value (MIN.ADD.IN.SV) vs. frequency respectively for the state-feedback designed autopilot. It is noted that for 0.1 to 100 db frequency the output

F*G singular value is too low (0.03 rad) but the input transfer function G*F input minimum singular value is above the 0.5 rad region.

Therefore the closed loop unimpaired system is robust (at least in the input). Further analysis would be needed if robustness were required in both the input and output case simultaneously.

In the case of state-feedback autopilot and for a singular value of 0.5 rad the pole placement and robustness design routine places the poles as follows:

Ordered (input)		Computed (output)	
-1706.00000	j0.00000	-1706.58980	j0.00000
-285.39990	j0.00000	-285.42944	j0.00000
-219.48999	j0.00000	-158.78516	j0.00000
-117.77000	j0.00000	-49.74738	j0.00000
-56.00000	j0.00000	-49.74738	j0.00000
-21.84399	j0.00000	-27.69325	j0.00000
-7.05800	-j1.59000	-27.59982	j0.00000
-7.05800	j1.59000	-8.57168	-j2.58016
-4.97000	j0.00000	-8.57168	j2.58016
-4.97000	j0.00000	-6.42040	j0.00000
-4.88000	j2.59000	-6.35900	-j5.27725
-4.88000	j2.59000	-6.35900	j5.27725
-2.90000	j0.00000	-5.99561	j0.00000
-0.77000	j0.00000	-4.27422	j0.00000
-0.47000	j0.00000	-2.33516	j0.00000
-0.47000	j0.00000	-0.98429	j0.00000

-0.47000	j0.00000	-0.47444	j0.00000
-0.40000	j0.00000	-0.47427	j0.00000
-0.10000	j0.00000	-0.47415	j0.00000
-0.07000	-j6.60000	-0.14287	j0.00000
-0.07000	j6.60000	-0.07482	-j6.66396
-0.00001	j0.00000	-0.07482	j6.66396
-4.97000	j0.00000	-0.00153	j0.00000

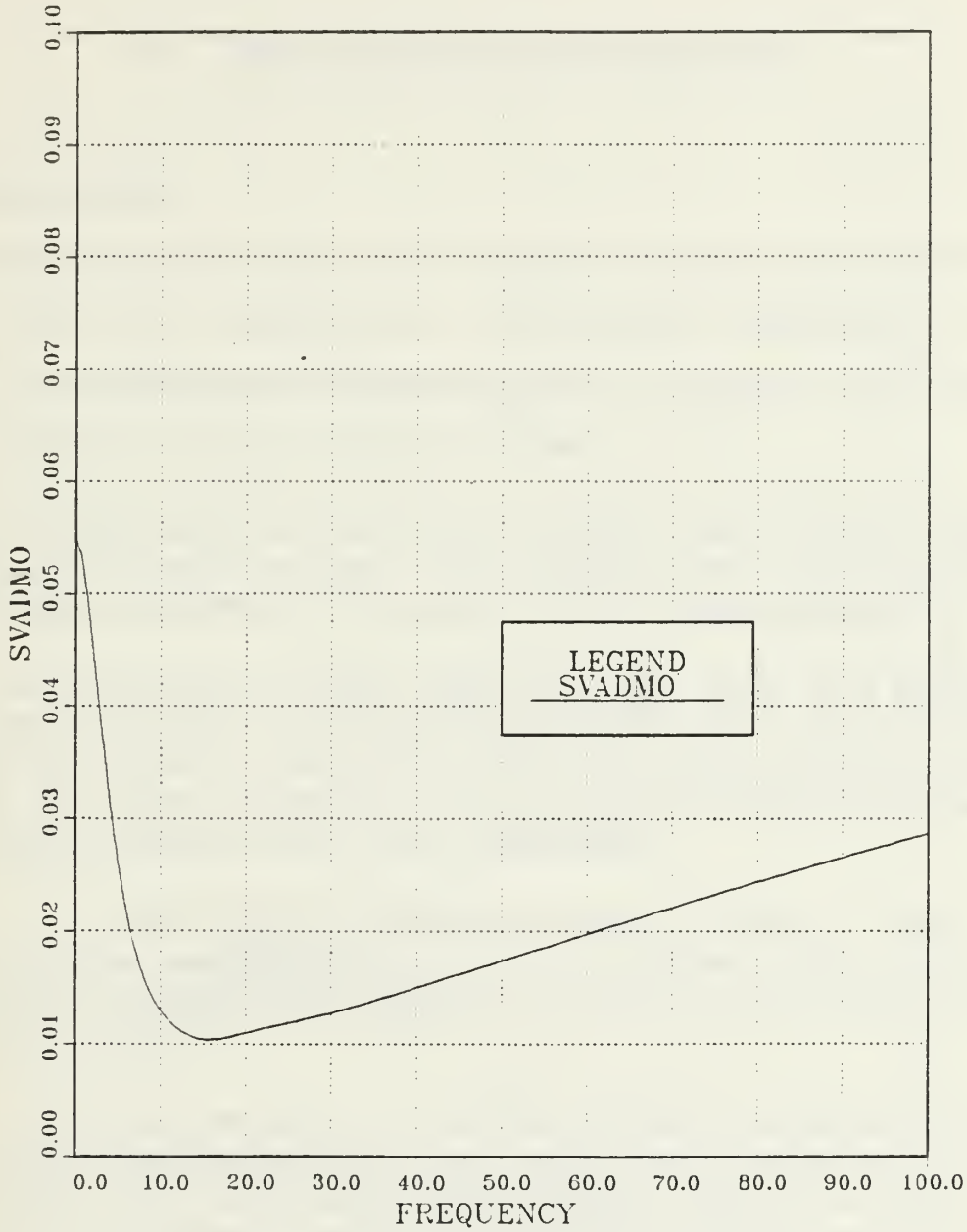

Figure 5.27 SVADMO vs. Frequency; Copled Pitch and Roll Channel Autopilot; State-Feedback Design; Continuous Closed Loop Unimpaired System; Circular Airfram.

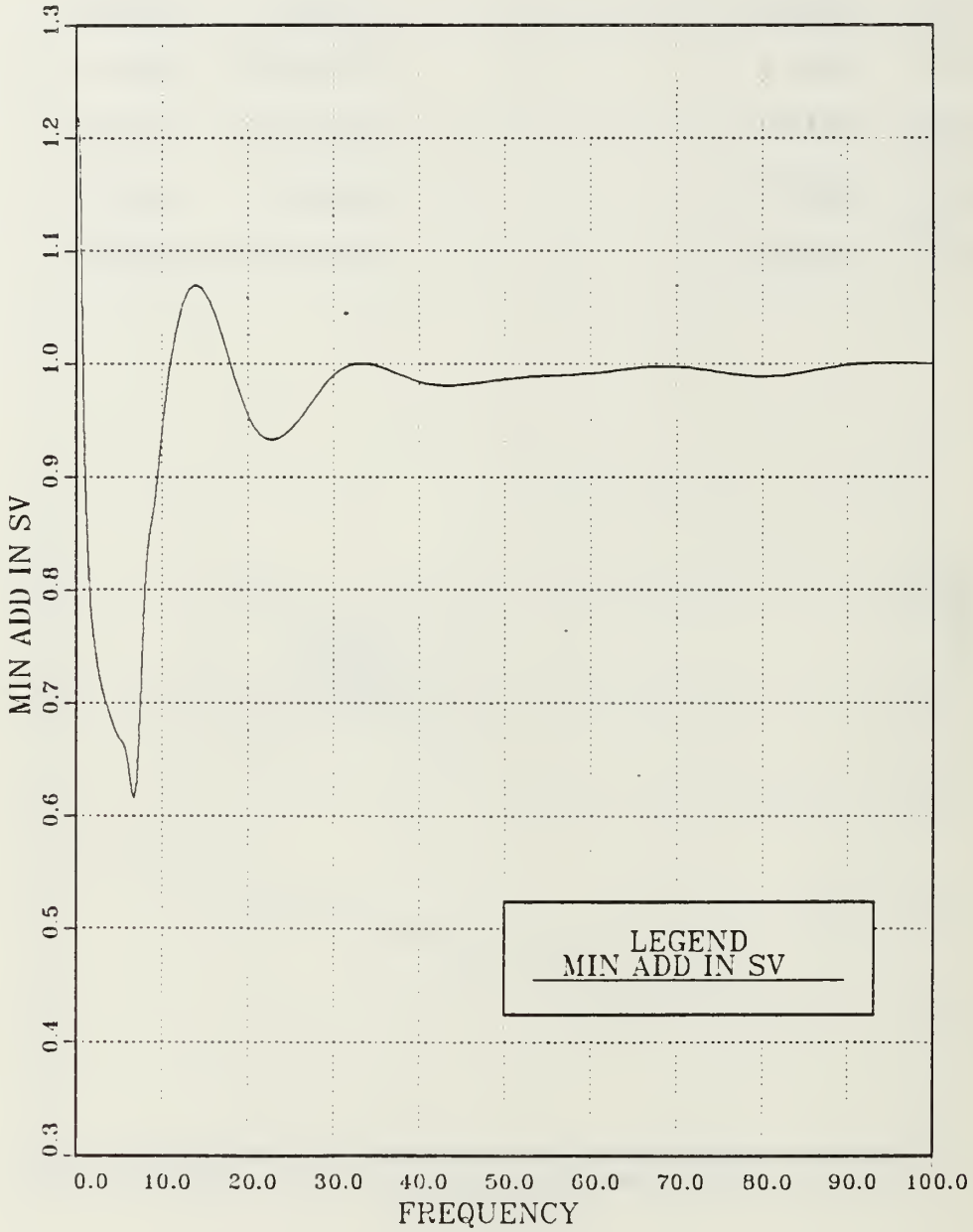

Figure 5.28 MIN ADD IN SV vs. Frequency; Copled Pitch and Roll Channel Autopilot; State-Feedback Design; Continuous Closed Loop Unimpaired System; Circular Airfram.

VI. CONCLUSIONS AND RECOMMENDATIONS

A. CONCLUSIONS

The purpose of this thesis was to examine the control deficiecies in a Bank-to-Turn (B.T.T.) cruise missile, due to specific impairments at its control surfaces during the intermediate phase of its mission. The following are the principal conclusions based on this work.

(1) The original and modified classical designed autopilots which involve separate inputs for each control surface were proved to have identical performance for the longitudinal and lateral channels.

(2) The investigation of specific type of damages at the B.T.T. missile's control surfaces, showed that the hard over case (i.e., one control surface locked at a certain deflection angle) shows greater excursion in the normal acceleration and roll angle with large values being achieved, than the other type of impairments.

(3) It was showed that the impaired missile was able to track the unimpaired missile as long as there was another control surface to provide the appropriate corrective action and the control power of the failed surface.

(4) A discussion was given of a possible method for transitioning from normal control laws to a set of reconfigured control laws for a missile with failed surface. The strategy requires the system to detect and isolate a surface failure and then transfer control to an off-line flight control computer which has been programmed with the new control laws (corrective actions).

(5) The state-feedback autopilot was introduced as additional dynamic design in order to implement control to the unimpaired system. This design, analyzed in terms of its transient response, was found to meet the desired requirements.

(6) The performance of the coupled pitch and roll channel was found to be satisfactory and the unimpaired system proved to be robust.

8. RECOMMENDATIONS

Finally the following recommendations should be taken into consideration:

(1) More complex and other type of impairments could be investigated using the designed autopilot, in order to examine the overall controllability of the missile.

(2) In order to make the system simpler, some of the returning gain loops of the state-feedback design must be eliminated. A further investigation must then be conducted in order to examine if the performance of the resulting design remains robust.

(3) Further analysis should be conducted if robustness were required in both the input and output case simultaneously.

APPENDIX A

PLANT SYSTEM AND INPUT MATRICES OF CONTINUOUS OPEN LOOP PITCH CHANNEL AUTOPILOT (UNIMPAIRED SYSTEM)

OPEN LOOP DYNAMICS MATRIX.....F..

-0.1500D+03	0.0000D+00	0.0000D+00	0.0000D+00	0.0000D+00	0.0000D+00	0.0000D+00	0.0000D+00	0.0000D+00	0.0000D+00
0.0000D+00	0.0000D+00	0.1500D+03							
0.1353D+01	0.0000D+00	0.1000D+01	0.0000D+00	0.0000D+00	0.0000D+00	0.0000D+00	0.0000D+00	0.0000D+00	0.0000D+00
0.0000D+00	0.0000D+00	0.0000D+00							
-0.6572D+01	0.0000D+00	-0.5000D+01	0.0000D+00	0.0000D+00	0.0000D+00	0.0000D+00	0.0000D+00	0.0000D+00	0.0000D+00
0.0000D+00	0.0000D+00	0.0000D+00							
0.0000D+00	0.0000D+00	0.0000D+00	0.0000D+00	0.1000D+01	0.0000D+00	0.0000D+00	-0.5926D+02	0.0000D+00	0.0000D+00
0.0000D+00	0.0000D+00	0.0000D+00							
0.0000D+00	0.0000D+00	0.0000D+00	-0.4436D+02	-0.1492D+00	0.0000D+00	0.0000D+00	0.1789D+01	0.0000D+00	0.0000D+00
0.0000D+00	0.0000D+00	0.0000D+00							
0.0000D+00	0.0000D+00	0.0000D+00	0.0000D+00	0.0000D+00	0.0000D+00	0.1000D+01	-0.7019D+00	0.0000D+00	0.0000D+00
0.0000D+00	0.0000D+00	0.0000D+00							
0.0000D+00	0.0000D+00	0.0000D+00	0.0000D+00	0.0000D+00	-0.4436D+02	-0.1492D+00	-0.1043D+04	0.0000D+00	0.0000D+00
0.0000D+00	0.0000D+00	0.0000D+00							
0.0000D+00	0.0000D+00	0.0000D+00	0.0000D+00	0.0000D+00	0.0000D+00	0.0000D+00	-0.1884D+03	-0.9420D+02	0.9420D+02
-0.9420D+02	0.9420D+02	0.0000D+00							
0.2304D+00	0.1115D+01	0.1703D+00	-0.1115D+01	-0.1703D+00	0.0000D+00	0.0000D+00	0.1009D+02	-0.1430D+00	0.0000D+00
0.0000D+00	0.0000D+00	0.0000D+00							
-0.2304D+00	-0.1115D+01	-0.1703D+00	0.1115D+01	0.1703D+00	0.0000D+00	0.0000D+00	-0.1009D+02	0.0000D+00	-0.1430D+00
0.0000D+00	0.0000D+00	0.0000D+00							
0.2304D+00	0.1115D+01	0.1703D+00	-0.1115D+01	-0.1703D+00	0.0000D+00	0.0000D+00	0.1009D+02	0.0000D+00	0.0000D+00
-0.1430D+00	0.0000D+00	0.0000D+00							
-0.2304D+00	-0.1115D+01	-0.1703D+00	0.1115D+01	0.1703D+00	0.0000D+00	0.0000D+00	-0.1009D+02	0.0000D+00	0.0000D+00
0.0000D+00	-0.1430D+00	0.0000D+00							
0.0000D+00	0.0000D+00	0.0000D+00	0.0000D+00	0.0000D+00	0.0000D+00	-0.1000D+01	0.8871D+03	0.4432D+03	-0.4432D+03
0.4432D+03	-0.4432D+03	0.0000D+00							

OPEN LOOP EIGENVALUES.....DET(SI-F)..

-1.59724E+02, 1.89922E+01:-8.29043E+00, 8.05911E+00:-3.75933E+00, 2.51441E+00:
-1.43935E-01:-5.31417E-06:-7.46000E-02, 6.65991E+00:-1.43000E-01:-1.43000E-01:
-1.43000E-01:

THE CONTROL DISTRIBUTION MATRIX.....G..

0.0000D+00	0.0000D+00	0.0000D+00	0.0000D+00	0.0000D+00
0.0000D+00	0.0000D+00	0.0000D+00	0.0000D+00	-0.1353D+01
0.0000D+00	0.0000D+00	0.0000D+00	0.0000D+00	0.6572D+01
0.0000D+00	0.0000D+00	0.0000D+00	0.0000D+00	0.0000D+00
0.0000D+00	0.0000D+00	0.0000D+00	0.0000D+00	0.0000D+00
0.0000D+00	0.0000D+00	0.0000D+00	0.0000D+00	0.0000D+00
0.0000D+00	0.0000D+00	0.0000D+00	0.0000D+00	0.0000D+00
-0.9420D+02	0.9420D+02	-0.9420D+02	0.9420D+02	0.0000D+00
-0.1430D+00	0.0000D+00	0.0000D+00	0.0000D+00	-0.2304D+00
0.0000D+00	-0.1430D+00	0.0000D+00	0.0000D+00	0.2304D+00
0.0000D+00	0.0000D+00	-0.1430D+00	0.0000D+00	-0.2304D+00
0.0000D+00	0.0000D+00	0.0000D+00	-0.1430D+00	0.2304D+00
0.4432D+03	-0.4432D+03	0.4432D+03	-0.4432D+03	0.0000D+00

THE OPTIMAL FEEDBACK GAIN CONTROL MATRIX...C=BINV*GT*S...

```
 1.4313D-01  -8.1227D-01  -1.5452D-01   1.5704D-02   3.2362D-03  -2.4426D-01
 9.3121D-02  -9.3121D-02  -8.1741D-01
-1.4313D-01   8.1227D-01   1.5452D-01  -1.5704D-02  -3.2362D-03   2.4426D-01
-9.3121D-02   9.3121D-02   8.1741D-01
 1.4313D-01  -8.1227D-01  -1.5452D-01   1.5704D-02   3.2362D-03  -2.4426D-01
 9.3121D-02  -9.3121D-02  -8.1741D-01
-1.4313D-01   8.1227D-01   1.5452D-01  -1.5704D-02  -3.2362D-03   2.4426D-01
-9.3121D-02   9.3121D-02   8.1741D-01
-5.5193D-03  -2.3641D+00  -4.3398D-01  -2.4758D-01   4.0967D-02   1.7860D-01
-3.8930D-01   3.8930D-01   9.2404D-02
```

C-LOOP OPTIMAL REG. E-VALUES...DET(SI-F+G*C)..

```
-9.09132E+02:-2.11193E+02:-1.78501E+01:-9.79306E+00:-5.22654E+00:-6.87901E-01:
-7.46000E-02, 6.65991E+00:-1.46233E-01:-5.42351E-06:-1.43000E-01:-1.43000E-01:
-1.43000E-01:
```

APPENDIX B

PLANT SYSTEM AND INPUT MATRICES OF CONTINUOUS OPEN LOOP ROLL CHANNEL AUTOPILOT (UNIMPAIRED SYSTEM)

THE SYSTEM MATRIX "F"-MATRIX ...

0.00000	0.00000	0.00000	0.00000	0.00000	0.00000
0.00000	0.00000	0.00000	8.03462		
1.00000	0.00000	0.00000	0.00000	0.00000	0.00000
0.00000	0.00000	0.00000	0.00000		
0.00000	-17.60000	-8.00000	0.00000	0.00000	0.00000
0.00000	0.00000	0.00000	0.00000		
-0.75325	-0.88352	0.35165	-5.00000	0.00000	0.00000
0.00000	0.00000	0.00000	-0.40334		
0.00000	0.00000	0.00000	0.00000	-6.00000	0.00000
0.00000	0.00000	0.00000	0.68291		
-0.10271	-0.12048	0.04795	14.31820	-14.18184	-15.00000
0.00000	0.00000	0.00000	-0.14067		
0.10271	0.12048	-0.04795	-14.31820	14.18184	0.00000
-15.00000	0.00000	0.00000	0.14067		
0.10271	0.12048	-0.04795	-14.31820	14.18184	0.00000
0.00000	-15.00000	0.00000	0.14067		
-0.10271	-0.12048	0.04795	14.31820	-14.18184	0.00000
0.00000	0.00000	-15.00000	-0.14067		
0.00000	0.00000	0.00000	0.00000	0.00000	2698.83000
-2698.83000	-2698.83000	2698.83000	-188.40000		

OPEN LOOP EIGENVALUES.....DET(SI-F)..

-1.85057E+02:-9.27462E+00, 2.92679E+01:-2.35821E+00, 2.70296E+00:-8.89209E+00:
-5.18517E+00:-1.50000E+01:-1.50000E+01:-1.50000E+01:

THE CONTROL DISTRIBUTION MATRIX "G"-MATRIX ...

0.00000	0.00000	0.00000	0.00000	0.00000
0.00000	0.00000	0.00000	0.00000	0.00000
0.00000	0.00000	0.00000	0.00000	17.60000
0.00000	0.00000	0.00000	0.00000	0.88352
0.00000	0.00000	0.00000	0.00000	0.00000
-15.00000	0.00000	0.00000	0.00000	0.12048
0.00000	-15.00000	0.00000	0.00000	-0.12048
0.00000	0.00000	-15.00000	0.00000	-0.12048
0.00000	0.00000	0.00000	-15.00000	0.12048
2698.83000	-2698.83000	-2698.83000	2698.83000	0.00000

THE OPTIMAL FEEDBACK GAIN CONTROL MATRIX...C=BINV*GT*S...

5.0881D-01	5.6129D-01	-3.0819D-02	-1.1772D+00	1.0775D+00	-2.7569D-01
-5.0881D-01	-5.6129D-01	3.0819D-02	1.1772D+00	-1.0775D+00	-1.3852D-01
-5.0881D-01	-5.6129D-01	3.0819D-02	1.1772D+00	-1.0775D+00	-1.3852D-01
5.0881D-01	5.6129D-01	-3.0819D-02	-1.1772D+00	1.0775D+00	1.3852D-01
1.7841D-01	-1.3987D-01	1.1148D-01	3.8252D+00	-3.4606D+00	5.6129D-01

C-LOOP OPTIMAL REG. E-VALUES...DET(SI-F+G*C)..

-5.40070E+03:-5.99206E+00, 5.34991E+00:-9.29732E+00:-6.57672E+00, 8.26712E-01:
-1.45396E+00:-2.12132E+01:-2.12132E+01:-2.12132E+01:

APPENDIX C

PLANT SYSTEM AND INPUT MATRICES OF CONTINUOUS OPEN LOOP COUPLED PITCH AND ROLL CHANNELS AUTOPILOTS (UNIMPAIRED SYSTEM)

THE CONTROL DISTRIBUTION MATRIX...........G..

0.0000D+00	0.0000D+00	0.0000D+00	0.0000D+00	0.0000D+00	0.0000D+00	0.0000D+00	0.0000D+00	0.0000D+00	0.0000D+00
0.0000D+00	0.0000D+00	0.0000D+00	0.0000D+00	-0.1353D+01	0.0000D+00	0.0000D+00	0.0000D+00	0.0000D+00	0.0000D+00
0.0000D+00	0.0000D+00	0.0000D+00	0.0000D+00	0.6572D+01	0.0000D+00	0.0000D+00	0.0000D+00	0.0000D+00	0.0000D+00
0.0000D+00	0.0000D+00	0.0000D+00	0.0000D+00	0.0000D+00	0.0000D+00	0.0000D+00	0.0000D+00	0.0000D+00	0.0000D+00
0.0000D+00	0.0000D+00	0.0000D+00	0.0000D+00	0.0000D+00	0.0000D+00	0.0000D+00	0.0000D+00	0.0000D+00	0.0000D+00
0.0000D+00	0.0000D+00	0.0000D+00	0.0000D+00	0.0000D+00	0.0000D+00	0.0000D+00	0.0000D+00	0.0000D+00	0.0000D+00
0.0000D+00	0.0000D+00	0.0000D+00	0.0000D+00	0.0000D+00	0.0000D+00	0.0000D+00	0.0000D+00	0.0000D+00	0.0000D+00
-0.9420D+02	0.9420D+02	-0.9420D+02	0.9420D+02	0.0000D+00	0.0000D+00	0.0000D+00	0.0000D+00	0.0000D+00	0.0000D+00
-0.1430D+00	0.0000D+00	0.0000D+00	0.0000D+00	-0.2304D+00	0.0000D+00	0.0000D+00	0.0000D+00	0.0000D+00	0.0000D+00
0.0000D+00	-0.1430D+00	0.0000D+00	0.0000D+00	0.2304D+00	0.0000D+00	0.0000D+00	0.0000D+00	0.0000D+00	0.0000D+00
0.0000D+00	0.0000D+00	-0.1430D+00	0.0000D+00	-0.2304D+00	0.0000D+00	0.0000D+00	0.0000D+00	0.0000D+00	0.0000D+00
0.0000D+00	0.0000D+00	0.0000D+00	-0.1430D+00	0.2304D+00	0.0000D+00	0.0000D+00	0.0000D+00	0.0000D+00	0.0000D+00
0.4432D+03	-0.4432D+03	0.4432D+03	-0.4432D+03	0.0000D+00	0.0000D+00	0.0000D+00	0.0000D+00	0.0000D+00	0.0000D+00
0.0000D+00	0.0000D+00	0.0000D+00	0.0000D+00	0.0000D+00	0.0000D+00	0.0000D+00	0.0000D+00	0.0000D+00	0.0000D+00
0.0000D+00	0.0000D+00	0.0000D+00	0.0000D+00	0.0000D+00	0.0000D+00	0.0000D+00	0.0000D+00	0.0000D+00	0.0000D+00
0.0000D+00	0.0000D+00	0.0000D+00	0.0000D+00	0.0000D+00	0.0000D+00	0.0000D+00	0.0000D+00	0.0000D+00	0.1760D+02
0.0000D+00	0.0000D+00	0.0000D+00	0.0000D+00	0.0000D+00	0.0000D+00	0.0000D+00	0.0000D+00	0.0000D+00	0.8835D+00
0.0000D+00	0.0000D+00	0.0000D+00	0.0000D+00	0.0000D+00	0.0000D+00	0.0000D+00	0.0000D+00	0.0000D+00	0.0000D+00
0.0000D+00	0.0000D+00	0.0000D+00	0.0000D+00	0.0000D+00	-0.1500D+02	0.0000D+00	0.0000D+00	0.0000D+00	0.1205D+00
0.0000D+00	0.0000D+00	0.0000D+00	0.0000D+00	0.0000D+00	0.0000D+00	-0.1500D+02	0.0000D+00	0.0000D+00	-0.1205D+00
0.0000D+00	0.0000D+00	0.0000D+00	0.0000D+00	0.0000D+00	0.0000D+00	0.0000D+00	-0.1500D+02	0.0000D+00	-0.1205D+00
0.0000D+00	0.0000D+00	0.0000D+00	0.0000D+00	0.0000D+00	0.0000D+00	0.0000D+00	0.0000D+00	-0.1500D+02	0.1205D+00
0.0000D+00	0.0000D+00	0.0000D+00	0.0000D+00	0.0000D+00	0.2699D+04	-0.2699D+04	-0.2699D+04	0.2699D+04	0.0000D+00

OPEN LOOP EIGENVALUES..........DET(SI-F)..

-1.59724E+02, 1.89922E+01:-8.29043E+00, 8.05911E+00:-3.75933E+00, 2.51441E+00:
-1.43935E-01:-5.31417E-06:-7.46000E-02, 6.65991E+00:-1.43000E-01:-1.43000E-01:
-1.43000E-01:-1.85057E+02:-9.27462E+00, 2.92679E+01:-2.35821E+00, 2.70296E+00:
-8.89209E+00:-5.18517E+00:-1.50000E+01:-1.50000E+01:-1.50000E+01:

OPEN LOOP DYNAMICS MATRIX.....F..

```
-0.1500D+03  0.0000D+00  0.0000D+00  0.0000D+00  0.0000D+00  0.0000D+00  0.0000D+00  0.0000D+00  0.0000D+00  0.0000D+00
 0.0000D+00  0.0000D+00  0.1500D+03  0.0000D+00  0.0000D+00  0.0000D+00  0.0000D+00  0.0000D+00  0.0000D+00  0.0000D+00
 0.0000D+00  0.0000D+00  0.0000D+00
 0.1351D+01  0.0000D+00  0.1000D+01  0.0000D+00  0.0000D+00  0.0000D+00  0.0000D+00  0.0000D+00  0.0000D+00  0.0000D+00
 0.0000D+00  0.0000D+00  0.0000D+00  0.0000D+00  0.0000D+00  0.0000D+00  0.0000D+00  0.0000D+00  0.0000D+00  0.0000D+00
 0.0000D+00  0.0000D+00  0.0000D+00
-0.6572D+01  0.0000D+00 -0.5000D+01  0.0000D+00  0.0000D+00  0.0000D+00  0.0000D+00  0.0000D+00  0.0000D+00  0.0000D+00
 0.0000D+00  0.0000D+00  0.0000D+00  0.0000D+00  0.0000D+00  0.0000D+00  0.0000D+00  0.0000D+00  0.0000D+00  0.0000D+00
 0.0000D+00  0.0000D+00  0.0000D+00
 0.0000D+00  0.0000D+00  0.0000D+00  0.0000D+00  0.1000D+01  0.0000D+00  0.0000D+00 -0.5926D+02  0.0000D+00  0.0000D+00
 0.0000D+00  0.0000D+00  0.0000D+00  0.0000D+00  0.0000D+00  0.0000D+00  0.0000D+00  0.0000D+00  0.0000D+00  0.0000D+00
 0.0000D+00  0.0000D+00  0.0000D+00
 0.0000D+00  0.0000D+00  0.0000D+00 -0.4436D+02 -0.1492D+00  0.0000D+00  0.0000D+00  0.1789D+01  0.0000D+00  0.0000D+00
 0.0000D+00  0.0000D+00  0.0000D+00  0.0000D+00  0.0000D+00  0.0000D+00  0.0000D+00  0.0000D+00  0.0000D+00  0.0000D+00
 0.0000D+00  0.0000D+00  0.0000D+00
 0.0000D+00  0.0000D+00  0.0000D+00  0.0000D+00  0.0000D+00  0.0000D+00  0.1000D+01 -0.7019D+00  0.0000D+00  0.0000D+00
 0.0000D+00  0.0000D+00  0.0000D+00  0.0000D+00  0.0000D+00  0.0000D+00  0.0000D+00  0.0000D+00  0.0000D+00  0.0000D+00
 0.0000D+00  0.0000D+00  0.0000D+00
 0.0000D+00  0.0000D+00  0.0000D+00  0.0000D+00  0.0000D+00 -0.4436D+02 -0.1492D+00 -0.1043D+04  0.0000D+00  0.0000D+00
 0.0000D+00  0.0000D+00  0.0000D+00  0.0000D+00  0.0000D+00  0.0000D+00  0.0000D+00  0.0000D+00  0.0000D+00  0.0000D+00
 0.0000D+00  0.0000D+00  0.0000D+00
 0.0000D+00  0.0000D+00  0.0000D+00  0.0000D+00  0.0000D+00  0.0000D+00  0.0000D+00 -0.1884D+03 -0.9420D+02  0.9420D+02
-0.9420D+02  0.9420D+02  0.0000D+00  0.0000D+00  0.0000D+00  0.0000D+00  0.0000D+00  0.0000D+00  0.0000D+00  0.0000D+00
 0.0000D+00  0.0000D+00  0.0000D+00
 0.2304D+00  0.1115D+01  0.1703D+00 -0.1115D+01 -0.1703D+00  0.0000D+00  0.0000D+00  0.1009D+02 -0.1430D+00  0.0000D+00
 0.0000D+00  0.0000D+00  0.0000D+00  0.0000D+00  0.0000D+00  0.0000D+00  0.0000D+00  0.0000D+00  0.0000D+00  0.0000D+00
 0.0000D+00  0.0000D+00  0.0000D+00
-0.2304D+00 -0.1115D+01 -0.1703D+00  0.1115D+01  0.1703D+00  0.0000D+00  0.0000D+00 -0.1009D+02  0.0000D+00 -0.1430D+00
 0.0000D+00  0.0000D+00  0.0000D+00  0.0000D+00  0.0000D+00  0.0000D+00  0.0000D+00  0.0000D+00  0.0000D+00  0.0000D+00
 0.0000D+00  0.0000D+00  0.0000D+00
 0.2304D+00  0.1115D+01  0.1703D+00 -0.1115D+01 -0.1703D+00  0.0000D+00  0.0000D+00  0.1009D+02  0.0000D+00  0.0000D+00
-0.1430D+00  0.0000D+00  0.0000D+00  0.0000D+00  0.0000D+00  0.0000D+00  0.0000D+00  0.0000D+00  0.0000D+00  0.0000D+00
 0.0000D+00  0.0000D+00  0.0000D+00
-0.2304D+00 -0.1115D+01 -0.1703D+00  0.1115D+01  0.1703D+00  0.0000D+00  0.0000D+00 -0.1009D+02  0.0000D+00  0.0000D+00
 0.0000D+00 -0.1430D+00  0.0000D+00  0.0000D+00  0.0000D+00  0.0000D+00  0.0000D+00  0.0000D+00  0.0000D+00  0.0000D+00
 0.0000D+00  0.0000D+00  0.0000D+00
 0.0000D+00  0.0000D+00  0.0000D+00  0.0000D+00  0.0000D+00  0.0000D+00 -0.1000D+01  0.8871D+03  0.4432D+03 -0.4432D+03
 0.4432D+03 -0.4432D+03  0.0000D+00  0.0000D+00  0.0000D+00  0.0000D+00  0.0000D+00  0.0000D+00  0.0000D+00  0.0000D+00
 0.0000D+00  0.0000D+00  0.0000D+00
 0.0000D+00  0.0000D+00  0.0000D+00  0.0000D+00  0.0000D+00  0.0000D+00  0.0000D+00  0.0000D+00  0.0000D+00  0.0000D+00
 0.0000D+00  0.0000D+00  0.0000D+00  0.0000D+00  0.0000D+00  0.0000D+00  0.0000D+00  0.0000D+00  0.0000D+00  0.0000D+00
 0.0000D+00  0.0000D+00  0.8035D+01
 0.0000D+00  0.0000D+00  0.0000D+00  0.0000D+00  0.0000D+00  0.0000D+00  0.0000D+00  0.0000D+00  0.0000D+00  0.0000D+00
 0.0000D+00  0.0000D+00  0.0000D+00  0.1000D+01  0.0000D+00  0.0000D+00  0.0000D+00  0.0000D+00  0.0000D+00  0.0000D+00
 0.0000D+00  0.0000D+00  0.0000D+00
 0.0000D+00  0.0000D+00  0.0000D+00  0.0000D+00  0.0000D+00  0.0000D+00  0.0000D+00  0.0000D+00  0.0000D+00  0.0000D+00
 0.0000D+00  0.0000D+00  0.0000D+00  0.0000D+00 -0.1760D+02 -0.8000D+01  0.0000D+00  0.0000D+00  0.0000D+00  0.0000D+00
 0.0000D+00  0.0000D+00  0.0000D+00
 0.0000D+00  0.0000D+00  0.0000D+00  0.0000D+00  0.0000D+00  0.0000D+00  0.0000D+00  0.0000D+00  0.0000D+00  0.0000D+00
 0.0000D+00  0.0000D+00  0.0000D+00 -0.7533D+00 -0.8835D+00  0.3517D+00 -0.5000D+01  0.0000D+00  0.0000D+00  0.0000D+00
 0.0000D+00  0.0000D+00 -0.4033D+00
 0.0000D+00  0.0000D+00  0.0000D+00  0.0000D+00  0.0000D+00  0.0000D+00  0.0000D+00  0.0000D+00  0.0000D+00  0.0000D+00
 0.0000D+00  0.0000D+00  0.0000D+00  0.0000D+00  0.0000D+00  0.0000D+00  0.0000D+00 -0.6000D+01  0.0000D+00  0.0000D+00
 0.0000D+00  0.0000D+00  0.6829D+00
 0.0000D+00  0.0000D+00  0.0000D+00  0.0000D+00  0.0000D+00  0.0000D+00  0.0000D+00  0.0000D+00  0.0000D+00  0.0000D+00
 0.0000D+00  0.0000D+00  0.0000D+00 -0.1027D+00 -0.1205D+00  0.4795D-01  0.1432D+02 -0.1418D+02 -0.1500D+02  0.0000D+00
 0.0000D+00  0.0000D+00 -0.1407D+00
 0.0000D+00  0.0000D+00  0.0000D+00  0.0000D+00  0.0000D+00  0.0000D+00  0.0000D+00  0.0000D+00  0.0000D+00  0.0000D+00
 0.0000D+00  0.0000D+00  0.0000D+00  0.1027D+00  0.1205D+00 -0.4795D-01 -0.1432D+02  0.1418D+02  0.0000D+00 -0.1500D+02
 0.0000D+00  0.0000D+00  0.1407D+00
 0.0000D+00  0.0000D+00  0.0000D+00  0.0000D+00  0.0000D+00  0.0000D+00  0.0000D+00  0.0000D+00  0.0000D+00  0.0000D+00
 0.0000D+00  0.0000D+00  0.0000D+00  0.1027D+00  0.1205D+00 -0.4795D-01 -0.1432D+02  0.1418D+02  0.0000D+00  0.0000D+00
-0.1500D+02  0.0000D+00  0.1407D+00
 0.0000D+00  0.0000D+00  0.0000D+00  0.0000D+00  0.0000D+00  0.0000D+00  0.0000D+00  0.0000D+00  0.0000D+00  0.0000D+00
 0.0000D+00  0.0000D+00  0.0000D+00 -0.1027D+00 -0.1205D+00  0.4795D-01  0.1432D+02 -0.1418D+02  0.0000D+00  0.0000D+00
 0.0000D+00 -0.1500D+02 -0.1407D+00
 0.0000D+00  0.0000D+00  0.0000D+00  0.0000D+00  0.0000D+00  0.0000D+00  0.0000D+00  0.0000D+00  0.0000D+00  0.0000D+00
 0.0000D+00  0.0000D+00  0.0000D+00  0.0000D+00  0.0000D+00  0.0000D+00  0.0000D+00  0.0000D+00  0.2699D+04 -0.2699D+04
-0.2699D+04  0.2699D+04 -0.1884D+03
```

APPENDIX D

COMPUTER PROGRAMS

In order to plot the state variables of interest and compare them, the following computer programs were developed in WATFIV and used, in order to change the format of the OPTPLOT DATA, into a fixed format data file, 80 characters in length with space between the values, to be used as input file for the EASYPLOT program.

1. Uncoupled Pitch Channel and for q, δ_P and n_Z

```
      $JOB
 1          REAL A,B,C,D
 2          N=1
 3          WHILE (N.LE.100) DO
 4          READ(5,10)A
 5          READ(5,15)B
 6          READ(5,20)C
 7          READ(5,25)D
 8          WRITE(6,30)A,B,C,D
 9       10 FORMAT(E14.7)
10       15 FORMAT(56X,E14.7)
11       20 FORMAT(42X,E14.7)
12       25 FORMAT(42X,E14.7)
13       30 FORMAT(8F15.8)
14          N=N+1
15          END WHILE
16          STOP
17          END

      $ENTRY
```

2. Uncoupled Roll Channel and for P, Ψ and δ_R

```
      $JOB
 1          REAL A,B,C,D,E
 2          N=1
 3          WHILE (N.LE.100) DO
 4          READ(5,10)A
 5          READ(5,15)B,C
 6          READ(5,20)D
 7          READ(5,25)E
 8          WRITE(6,30)A,B,C,E
 9       10 FORMAT(E14.7)
10       15 FORMAT(14X,2E14.7)
11       20 FORMAT(E14.7)
12       25 FORMAT(E14.7)
13       30 FORMAT(4F15.8)
14          N=N+1
15          END WHILE
16          STOP
17          END

      $ENTRY
```

3. Coupled Pitch and Roll Channels and for q, δ_P and n_z

```
      $JOB
 1          REAL A,B,C,D,E,L,G
 2          N=1
 3          WHILE (N.LE.100) DO
 4          READ(5,10)A
 5          READ(5,15)B
 6          READ(5,20)C
 7          READ(5,25)D
 8          READ(5,30)E
 9          READ(5,35)L
10          READ(5,40)G
11          WRITE(6,45)A,C,D,E
12       10 FORMAT(E14.7)
13       15 FORMAT(E14.7)
14       20 FORMAT(56X,E14.7)
15       25 FORMAT(42X,E14.7)
16       30 FORMAT(42X,E14.7)
17       35 FORMAT(E14.7)
18       40 FORMAT(E14.7)
19       45 FORMAT(4F15.8)
20          N=N+1
21          END WHILE
22          STOP
23          END

      $ENTRY
```

4. Coupled Pitch and Roll Channels and for P, Ψ and δ_R

```
      $JOB
 1          REAL A,B,C,D,E,F,G
 2          N=1
 3          WHILE (N.LE.100) DO
 4          READ(5,10)A
 5          READ(5,15)B
 6          READ(5,20)C
 7          READ(5,25)D
 8          READ(5,30)E
 9          READ(5,35)F
10          READ(5,40)G
11          WRITE(6,45)A,E,F,G
12       10 FORMAT(E14.7)
13       15 FORMAT(E14.7)
14       20 FORMAT(E14.7)
15       25 FORMAT(E14.7)
16       30 FORMAT(56X,E14.7)
17       35 FORMAT(E14.7)
18       40 FORMAT(42X,E14.7)
19       45 FORMAT(4F15.8)
20          N=N+1
21          END WHILE
22          STOP
23          END

      $ENTRY
```

APPENDIX E

COUPLED STATE-FEEDBACK DESIGN INPUT DATA FOR POPLAR PROGRAM (UNIMPAIRED SYSTEM)

```
    1    1
  100.0      0.1       0.1
    1.0      0.00        0.0
    0.5       0.6        .1          0
    0   10     0    5    -5     3 1000     0
232323102323102323
-0.15000000000000D+03 0.00000000000000D+00 0.00000000000000D+00 0.00000000000000D+00
 0.00000000000000D+00 0.00000000000000D+00 0.00000000000000D+00 0.00000000000000D+00
 0.00000000000000D+00 0.00000000000000D+00 0.00000000000000D+00 0.00000000000000D+00
 0.15000000000000D+03 0.00000000000000D+00 0.00000000000000D+00 0.00000000000000D+00
 0.00000000000000D+00 0.00000000000000D+00 0.00000000000000D+00 0.00000000000000D+00
 0.00000000000000D+00 0.00000000000000D+00 0.00000000000000D+00 0.13531000000000D+01
 0.00000000000000D+00 0.10000000000000D+01 0.00000000000000D+00 0.00000000000000D+00
 0.00000000000000D+00 0.00000000000000D+00 0.00000000000000D+00 0.00000000000000D+00
 0.00000000000000D+00 0.00000000000000D+00 0.00000000000000D+00 0.00000000000000D+00
 0.00000000000000D+00 0.00000000000000D+00 0.00000000000000D+00 0.00000000000000D+00
 0.00000000000000D+00 0.00000000000000D+00 0.00000000000000D+00 0.00000000000000D+00
 0.00000000000000D+00 0.00000000000000D+00-0.65720000000000D+01 0.00000000000000D+00
-0.50000000000000D+01 0.00000000000000D+00 0.00000000000000D+00 0.00000000000000D+00
 0.00000000000000D+00 0.00000000000000D+00 0.00000000000000D+00 0.00000000000000D+00
 0.00000000000000D+00 0.00000000000000D+00 0.00000000000000D+00 0.00000000000000D+00
 0.00000000000000D+00 0.00000000000000D+00 0.00000000000000D+00 0.00000000000000D+00
 0.00000000000000D+00 0.00000000000000D+00 0.00000000000000D+00 0.00000000000000D+00
 0.00000000000000D+00 0.00000000000000D+00 0.00000000000000D+00 0.00000000000000D+00
 0.00000000000000D+00 0.10000000000000D+01 0.00000000000000D+00 0.00000000000000D+00
-0.59260000000000D+02 0.00000000000000D+00 0.00000000000000D+00 0.00000000000000D+00
 0.00000000000000D+00 0.00000000000000D+00 0.00000000000000D+00 0.00000000000000D+00
 0.00000000000000D+00 0.00000000000000D+00 0.00000000000000D+00 0.00000000000000D+00
 0.00000000000000D+00 0.00000000000000D+00 0.00000000000000D+00 0.00000000000000D+00
 0.00000000000000D+00 0.00000000000000D+00 0.00000000000000D+00-0.44360000000000D+02
-0.14920000000000D+00 0.00000000000000D+00 0.00000000000000D+00 0.17887000000000D+01
 0.00000000000000D+00 0.00000000000000D+00 0.00000000000000D+00 0.00000000000000D+00
 0.00000000000000D+00 0.00000000000000D+00 0.00000000000000D+00 0.00000000000000D+00
 0.00000000000000D+00 0.00000000000000D+00 0.00000000000000D+00 0.00000000000000D+00
 0.00000000000000D+00 0.00000000000000D+00 0.00000000000000D+00 0.00000000000000D+00
 0.00000000000000D+00 0.00000000000000D+00 0.00000000000000D+00 0.00000000000000D+00
 0.00000000000000D+00 0.10000000000000D+01-0.70190000000000D+00 0.00000000000000D+00
 0.00000000000000D+00 0.00000000000000D+00 0.00000000000000D+00 0.00000000000000D+00
 0.00000000000000D+00 0.00000000000000D+00 0.00000000000000D+00 0.00000000000000D+00
 0.00000000000000D+00 0.00000000000000D+00 0.00000000000000D+00 0.00000000000000D+00
 0.00000000000000D+00 0.00000000000000D+00 0.00000000000000D+00 0.00000000000000D+00
 0.00000000000000D+00 0.00000000000000D+00 0.00000000000000D+00-0.44360000000000D+02
-0.14920000000000D+00-0.10433600000000D+04 0.00000000000000D+00 0.00000000000000D+00
 0.00000000000000D+00 0.00000000000000D+00 0.00000000000000D+00 0.00000000000000D+00
 0.00000000000000D+00 0.00000000000000D+00 0.00000000000000D+00 0.00000000000000D+00
 0.00000000000000D+00 0.00000000000000D+00 0.00000000000000D+00 0.00000000000000D+00
 0.00000000000000D+00 0.00000000000000D+00 0.00000000000000D+00 0.00000000000000D+00
 0.00000000000000D+00 0.00000000000000D+00 0.00000000000000D+00 0.00000000000000D+00
-0.18840000000000D+03-0.94200000000000D+02 0.94200000000000D+02-0.94200000000000D+02
 0.94200000000000D+02 0.00000000000000D+00 0.00000000000000D+00 0.00000000000000D+00
 0.00000000000000D+00 0.00000000000000D+00 0.00000000000000D+00 0.00000000000000D+00
 0.00000000000000D+00 0.00000000000000D+00 0.00000000000000D+00 0.00000000000000D+00
 0.23042000000000D+00 0.11154000000000D+01 0.17030000000000D+00-0.11154000000000D+01
-0.17030000000000D+00 0.00000000000000D+00 0.00000000000000D+00 0.10092000000000D+02
-0.14300000000000D+00 0.00000000000000D+00 0.00000000000000D+00 0.00000000000000D+00
```

```
 0.0000000000000D+00 0.0000000000000D+00 0.0000000000000D+00 0.0000000000000D+00
 0.0000000000000D+00 0.0000000000000D+00 0.0000000000000D+00 0.0000000000000D+00
 0.0000000000000D+00 0.0000000000000D+00 0.0000000000000D+00-0.2304200000000D+00
-0.1115400000000D+01-0.1703000000000D+00 0.1115400000000D+01 0.1703000000000D+00
 0.0000000000000D+00 0.0000000000000D+00-0.1009200000000D+02 0.0000000000000D+00
-0.1430000000000D+00 0.0000000000000D+00 0.0000000000000D+00 0.0000000000000D+00
 0.0000000000000D+00 0.0000000000000D+00 0.0000000000000D+00 0.0000000000000D+00
 0.0000000000000D+00 0.0000000000000D+00 0.0000000000000D+00 0.0000000000000D+00
 0.0000000000000D+00 0.0000000000000D+00 0.2304200000000D+00 0.1115400000000D+01
 0.1703000000000D+00-0.1115400000000D+01-0.1703000000000D+00 0.0000000000000D+00
 0.0000000000000D+00 0.1009200000000D+02 0.0000000000000D+00 0.0000000000000D+00
-0.1430000000000D+00 0.0000000000000D+00 0.0000000000000D+00 0.0000000000000D+00
 0.0000000000000D+00 0.0000000000000D+00 0.0000000000000D+00 0.0000000000000D+00
 0.0000000000000D+00 0.0000000000000D+00 0.0000000000000D+00 0.0000000000000D+00
 0.0000000000000D+00-0.2304200000000D+00-0.1115400000000D+01-0.1703000000000D+00
 0.1115400000000D+01 0.1703000000000D+00 0.0000000000000D+00 0.0000000000000D+00
-0.1009200000000D+02 0.0000000000000D+00 0.0000000000000D+00 0.0000000000000D+00
-0.1430000000000D+00 0.0000000000000D+00 0.0000000000000D+00 0.0000000000000D+00
 0.0000000000000D+00 0.0000000000000D+00 0.0000000000000D+00 0.0000000000000D+00
 0.0000000000000D+00 0.0000000000000D+00 0.0000000000000D+00 0.0000000000000D+00
 0.0000000000000D+00 0.0000000000000D+00 0.0000000000000D+00 0.0000000000000D+00
 0.0000000000000D+00 0.0000000000000D+00-0.1000000000000D+01 0.8871240000000D+03
 0.4432110000000D+03-0.4432110000000D+03 0.4432110000000D+03-0.4432110000000D+03
 0.0000000000000D+00 0.0000000000000D+00 0.0000000000000D+00 0.0000000000000D+00
 0.0000000000000D+00 0.0000000000000D+00 0.0000000000000D+00 0.0000000000000D+00
 0.0000000000000D+00 0.0000000000000D+00 0.0000000000000D+00 0.0000000000000D+00
 0.0000000000000D+00 0.0000000000000D+00 0.0000000000000D+00 0.0000000000000D+00
 0.0000000000000D+00 0.0000000000000D+00 0.0000000000000D+00 0.0000000000000D+00
 0.0000000000000D+00 0.0000000000000D+00 0.0000000000000D+00 0.0000000000000D+00
 0.0000000000000D+00 0.0000000000000D+00 0.0000000000000D+00 0.0000000000000D+00
 0.0000000000000D+00 0.0000000000000D+00 0.0000000000000D+00 0.0000000000000D+00
 0.0000000000000D+00 0.8034620000000D+01 0.0000000000000D+00 0.0000000000000D+00
 0.0000000000000D+00 0.0000000000000D+00 0.0000000000000D+00 0.0000000000000D+00
 0.0000000000000D+00 0.0000000000000D+00 0.0000000000000D+00 0.0000000000000D+00
 0.0000000000000D+00 0.0000000000000D+00 0.0000000000000D+00 0.1000000000000D+01
 0.0000000000000D+00 0.0000000000000D+00 0.0000000000000D+00 0.0000000000000D+00
 0.0000000000000D+00 0.0000000000000D+00 0.0000000000000D+00 0.0000000000000D+00
 0.0000000000000D+00 0.0000000000000D+00 0.0000000000000D+00 0.0000000000000D+00
 0.0000000000000D+00 0.0000000000000D+00 0.0000000000000D+00 0.0000000000000D+00
 0.0000000000000D+00 0.0000000000000D+00 0.0000000000000D+00 0.0000000000000D+00
 0.0000000000000D+00 0.0000000000000D+00 0.0000000000000D+00-0.1760000000000D+02
-0.8000000000000D+01 0.0000000000000D+00 0.0000000000000D+00 0.0000000000000D+00
 0.0000000000000D+00 0.0000000000000D+00 0.0000000000000D+00 0.0000000000000D+00
 0.0000000000000D+00 0.0000000000000D+00 0.0000000000000D+00 0.0000000000000D+00
 0.0000000000000D+00 0.0000000000000D+00 0.0000000000000D+00 0.0000000000000D+00
 0.0000000000000D+00 0.0000000000000D+00 0.0000000000000D+00 0.0000000000000D+00
 0.0000000000000D+00-0.7532500000000D+00-0.8835200000000D+00 0.3516500000000D+00
-0.5000000000000D+01 0.0000000000000D+00 0.0000000000000D+00 0.0000000000000D+00
 0.0000000000000D+00 0.0000000000000D+00-0.4033400000000D+00 0.0000000000000D+00
 0.0000000000000D+00 0.0000000000000D+00 0.0000000000000D+00 0.0000000000000D+00
 0.0000000000000D+00 0.0000000000000D+00 0.0000000000000D+00 0.0000000000000D+00
 0.0000000000000D+00 0.0000000000000D+00 0.0000000000000D+00 0.0000000000000D+00
 0.0000000000000D+00 0.0000000000000D+00 0.0000000000000D+00 0.0000000000000D+00
-0.6000000000000D+01 0.0000000000000D+00 0.0000000000000D+00 0.0000000000000D+00
 0.0000000000000D+00 0.6829100000000D+00 0.0000000000000D+00 0.0000000000000D+00
 0.0000000000000D+00 0.0000000000000D+00 0.0000000000000D+00 0.0000000000000D+00
 0.0000000000000D+00 0.0000000000000D+00 0.0000000000000D+00 0.0000000000000D+00
 0.0000000000000D+00 0.0000000000000D+00 0.0000000000000D+00-0.1027100000000D+00
-0.1204800000000D+00 0.4795000000000D-01 0.1431820000000D+02-0.1418184000000D+02
-0.1500000000000D+02 0.0000000000000D+00 0.0000000000000D+00 0.0000000000000D+00
-0.1406700000000D+00 0.0000000000000D+00 0.0000000000000D+00 0.0000000000000D+00
 0.0000000000000D+00 0.0000000000000D+00 0.0000000000000D+00 0.0000000000000D+00
 0.0000000000000D+00 0.0000000000000D+00 0.0000000000000D+00 0.0000000000000D+00
 0.0000000000000D+00 0.0000000000000D+00 0.1027100000000D+00 0.1204800000000D+00
-0.4795000000000D-01-0.1431820000000D+02 0.1418184000000D+02 0.0000000000000D+00
-0.1500000000000D+02 0.0000000000000D+00 0.0000000000000D+00 0.1406700000000D+00
 0.0000000000000D+00 0.0000000000000D+00 0.0000000000000D+00 0.0000000000000D+00
 0.0000000000000D+00 0.0000000000000D+00 0.0000000000000D+00 0.0000000000000D+00
```

```
 0.0000000000000D+00 0.0000000000000D+00 0.0000000000000D+00 0.0000000000000D+00
 0.0000000000000D+00 0.1027100000000D+00 0.1204800000000D+00-0.4795000000000D-01
-0.1431820000000D+02 0.1418184000000D+02 0.0000000000000D+00 0.0000000000000D+00
-0.1500000000000D+02 0.0000000000000D+00 0.1406700000000D+00 0.0000000000000D+00
 0.0000000000000D+00 0.0000000000000D+00 0.0000000000000D+00 0.0000000000000D+00
 0.0000000000000D+00 0.0000000000000D+00 0.0000000000000D+00 0.0000000000000D+00
 0.0000000000000D+00 0.0000000000000D+00 0.0000000000000D+00 0.0000000000000D+00
-0.1027100000000D+00-0.1204800000000D+00 0.4795000000000D-01 0.1431820000000D+02
-0.1418184000000D+02 0.0000000000000D+00 0.0000000000000D+00 0.0000000000000D+00
-0.1500000000000D+02-0.1406700000000D+00 0.0000000000000D+00 0.0000000000000D+00
 0.0000000000000D+00 0.0000000000000D+00 0.0000000000000D+00 0.0000000000000D+00
 0.0000000000000D+00 0.0000000000000D+00 0.0000000000000D+00 0.0000000000000D+00
 0.0000000000000D+00 0.0000000000000D+00 0.0000000000000D+00 0.0000000000000D+00
 0.0000000000000D+00 0.0000000000000D+00 0.0000000000000D+00 0.0000000000000D+00
 0.2698830000000D+04-0.2698830000000D+04-0.2698830000000D+04 0.2698830000000D+04
-0.1884000000000D+03
 0.0000000000000D+00 0.0000000000000D+00 0.0000000000000D+00 0.0000000000000D+00
 0.0000000000000D+00 0.0000000000000D+00 0.0000000000000D+00 0.0000000000000D+00
 0.0000000000000D+00 0.0000000000000D+00 0.0000000000000D+00 0.0000000000000D+00
 0.0000000000000D+00 0.0000000000000D+00-0.1353100000000D+01 0.0000000000000D+00
 0.0000000000000D+00 0.0000000000000D+00 0.0000000000000D+00 0.0000000000000D+00
 0.0000000000000D+00 0.0000000000000D+00 0.0000000000000D+00 0.0000000000000D+00
 0.6572000000000D+01 0.0000000000000D+00 0.0000000000000D+00 0.0000000000000D+00
 0.0000000000000D+00 0.0000000000000D+00 0.0000000000000D+00 0.0000000000000D+00
 0.0000000000000D+00 0.0000000000000D+00 0.0000000000000D+00 0.0000000000000D+00
 0.0000000000000D+00 0.0000000000000D+00 0.0000000000000D+00 0.0000000000000D+00
 0.0000000000000D+00 0.0000000000000D+00 0.0000000000000D+00 0.0000000000000D+00
 0.0000000000000D+00 0.0000000000000D+00 0.0000000000000D+00 0.0000000000000D+00
 0.0000000000000D+00 0.0000000000000D+00 0.0000000000000D+00 0.0000000000000D+00
 0.0000000000000D+00 0.0000000000000D+00 0.0000000000000D+00 0.0000000000000D+00
 0.0000000000000D+00 0.0000000000000D+00 0.0000000000000D+00 0.0000000000000D+00
 0.0000000000000D+00 0.0000000000000D+00 0.0000000000000D+00 0.0000000000000D+00
 0.0000000000000D+00 0.0000000000000D+00 0.0000000000000D+00 0.0000000000000D+00
 0.0000000000000D+00 0.0000000000000D+00-0.9420000000000D+02 0.9420000000000D+02
-0.9420000000000D+02 0.9420000000000D+02 0.0000000000000D+00 0.0000000000000D+00
 0.0000000000000D+00 0.0000000000000D+00 0.0000000000000D+00 0.0000000000000D+00
-0.1430000000000D+00 0.0000000000000D+00 0.0000000000000D+00 0.0000000000000D+00
-0.2304200000000D+00 0.0000000000000D+00 0.0000000000000D+00 0.0000000000000D+00
 0.0000000000000D+00 0.0000000000000D+00 0.0000000000000D+00-0.1430000000000D+00
 0.0000000000000D+00 0.0000000000000D+00 0.2304200000000D+00 0.0000000000000D+00
 0.0000000000000D+00 0.0000000000000D+00 0.0000000000000D+00 0.0000000000000D+00
 0.0000000000000D+00 0.0000000000000D+00-0.1430000000000D+00 0.0000000000000D+00
-0.2304200000000D+00 0.0000000000000D+00 0.0000000000000D+00 0.0000000000000D+00
 0.0000000000000D+00 0.0000000000000D+00 0.0000000000000D+00 0.0000000000000D+00
 0.0000000000000D+00-0.1430000000000D+00 0.2304200000000D+00 0.0000000000000D+00
 0.0000000000000D+00 0.0000000000000D+00 0.0000000000000D+00 0.0000000000000D+00
 0.4432110000000D+03-0.4432110000000D+03 0.4432110000000D+03-0.4432110000000D+03
 0.0000000000000D+00 0.0000000000000D+00 0.0000000000000D+00 0.0000000000000D+00
 0.0000000000000D+00 0.0000000000000D+00 0.0000000000000D+00 0.0000000000000D+00
 0.0000000000000D+00 0.0000000000000D+00 0.0000000000000D+00 0.0000000000000D+00
 0.0000000000000D+00 0.0000000000000D+00 0.0000000000000D+00 0.0000000000000D+00
 0.0000000000000D+00 0.0000000000000D+00 0.0000000000000D+00 0.0000000000000D+00
 0.0000000000000D+00 0.0000000000000D+00 0.0000000000000D+00 0.0000000000000D+00
 0.0000000000000D+00 0.0000000000000D+00 0.0000000000000D+00 0.0000000000000D+00
 0.0000000000000D+00 0.0000000000000D+00 0.0000000000000D+00 0.0000000000000D+00
 0.0000000000000D+00 0.0000000000000D+00 0.0000000000000D+00 0.1760000000000D+02
 0.0000000000000D+00 0.0000000000000D+00 0.0000000000000D+00 0.0000000000000D+00
 0.0000000000000D+00 0.0000000000000D+00 0.0000000000000D+00 0.0000000000000D+00
 0.0000000000000D+00 0.8835200000000D+00 0.0000000000000D+00 0.0000000000000D+00
 0.0000000000000D+00 0.0000000000000D+00 0.0000000000000D+00 0.0000000000000D+00
 0.0000000000000D+00 0.0000000000000D+00 0.0000000000000D+00 0.0000000000000D+00
 0.0000000000000D+00 0.0000000000000D+00 0.0000000000000D+00 0.0000000000000D+00
 0.0000000000000D+00-0.1500000000000D+02 0.0000000000000D+00 0.0000000000000D+00
 0.0000000000000D+00 0.1204800000000D+00 0.0000000000000D+00 0.0000000000000D+00
 0.0000000000000D+00 0.0000000000000D+00 0.0000000000000D+00 0.0000000000000D+00
-0.1500000000000D+02 0.0000000000000D+00 0.0000000000000D+00-0.1204800000000D+00
 0.0000000000000D+00 0.0000000000000D+00 0.0000000000000D+00 0.0000000000000D+00
```

0.0000000000000D+00	0.0000000000000D+00	0.0000000000000D+00	-0.1500000000000D+02
0.0000000000000D+00	-0.1204800000000D+00	0.0000000000000D+00	0.0000000000000D+00
0.0000000000000D+00	0.0000000000000D+00	0.0000000000000D+00	0.0000000000000D+00
0.0000000000000D+00	0.0000000000000D+00	-0.1500000000000D+02	0.1204800000000D+00
0.0000000000000D+00	0.0000000000000D+00	0.0000000000000D+00	0.0000000000000D+00
0.0000000000000D+00	0.2698830000000D+04	-0.2698830000000D+04	-0.2698830000000D+04
0.2698830000000D+04	0.0000000000000D+00		
0.1000000000000D+01	0.0000000000000D+00	0.0000000000000D+00	0.0000000000000D+00
0.0000000000000D+00	0.0000000000000D+00	0.0000000000000D+00	0.0000000000000D+00
0.0000000000000D+00	0.0000000000000D+00	0.0000000000000D+00	0.0000000000000D+00
0.0000000000000D+00	0.0000000000000D+00	0.0000000000000D+00	0.0000000000000D+00
0.0000000000000D+00	0.0000000000000D+00	0.0000000000000D+00	0.0000000000000D+00
0.0000000000000D+00	0.0000000000000D+00	0.0000000000000D+00	0.0000000000000D+00
0.1000000000000D+01	0.0000000000000D+00	0.0000000000000D+00	0.0000000000000D+00
0.0000000000000D+00	0.0000000000000D+00	0.0000000000000D+00	0.0000000000000D+00
0.0000000000000D+00	0.0000000000000D+00	0.0000000000000D+00	0.0000000000000D+00
0.0000000000000D+00	0.0000000000000D+00	0.0000000000000D+00	0.0000000000000D+00
0.0000000000000D+00	0.0000000000000D+00	0.0000000000000D+00	0.0000000000000D+00
0.0000000000000D+00	0.0000000000000D+00	0.0000000000000D+00	0.0000000000000D+00
0.1000000000000D+01	0.0000000000000D+00	0.0000000000000D+00	0.0000000000000D+00
0.0000000000000D+00	0.0000000000000D+00	0.0000000000000D+00	0.0000000000000D+00
0.0000000000000D+00	0.0000000000000D+00	0.0000000000000D+00	0.0000000000000D+00
0.0000000000000D+00	0.0000000000000D+00	0.0000000000000D+00	0.0000000000000D+00
0.0000000000000D+00	0.0000000000000D+00	0.0000000000000D+00	0.0000000000000D+00
0.0000000000000D+00	0.0000000000000D+00	0.0000000000000D+00	0.0000000000000D+00
0.1000000000000D+01	0.0000000000000D+00	0.0000000000000D+00	0.0000000000000D+00
0.0000000000000D+00	0.0000000000000D+00	0.0000000000000D+00	0.0000000000000D+00
0.0000000000000D+00	0.0000000000000D+00	0.0000000000000D+00	0.0000000000000D+00
0.0000000000000D+00	0.0000000000000D+00	0.0000000000000D+00	0.0000000000000D+00
0.0000000000000D+00	0.0000000000000D+00	0.0000000000000D+00	0.0000000000000D+00
0.0000000000000D+00	0.0000000000000D+00	0.0000000000000D+00	0.0000000000000D+00
0.1000000000000D+01	0.0000000000000D+00	0.0000000000000D+00	0.0000000000000D+00
0.0000000000000D+00	0.0000000000000D+00	0.0000000000000D+00	0.0000000000000D+00
0.0000000000000D+00	0.0000000000000D+00	0.0000000000000D+00	0.0000000000000D+00
0.0000000000000D+00	0.0000000000000D+00	0.0000000000000D+00	0.0000000000000D+00
0.0000000000000D+00	0.0000000000000D+00	0.0000000000000D+00	0.0000000000000D+00
0.0000000000000D+00	0.0000000000000D+00	0.0000000000000D+00	0.0000000000000D+00
0.1000000000000D+01	0.0000000000000D+00	0.0000000000000D+00	0.0000000000000D+00
0.0000000000000D+00	0.0000000000000D+00	0.0000000000000D+00	0.0000000000000D+00
0.0000000000000D+00	0.0000000000000D+00	0.0000000000000D+00	0.0000000000000D+00
0.0000000000000D+00	0.0000000000000D+00	0.0000000000000D+00	0.0000000000000D+00
0.0000000000000D+00	0.0000000000000D+00	0.0000000000000D+00	0.0000000000000D+00
0.0000000000000D+00	0.0000000000000D+00	0.0000000000000D+00	0.0000000000000D+00
0.1000000000000D+01	0.0000000000000D+00	0.0000000000000D+00	0.0000000000000D+00
0.0000000000000D+00	0.0000000000000D+00	0.0000000000000D+00	0.0000000000000D+00
0.0000000000000D+00	0.0000000000000D+00	0.0000000000000D+00	0.0000000000000D+00
0.0000000000000D+00	0.0000000000000D+00	0.0000000000000D+00	0.0000000000000D+00
0.0000000000000D+00	0.0000000000000D+00	0.0000000000000D+00	0.0000000000000D+00
0.0000000000000D+00	0.0000000000000D+00	0.0000000000000D+00	0.0000000000000D+00
0.1000000000000D+01	0.0000000000000D+00	0.0000000000000D+00	0.0000000000000D+00
0.0000000000000D+00	0.0000000000000D+00	0.0000000000000D+00	0.0000000000000D+00
0.0000000000000D+00	0.0000000000000D+00	0.0000000000000D+00	0.0000000000000D+00
0.0000000000000D+00	0.0000000000000D+00	0.0000000000000D+00	0.0000000000000D+00
0.0000000000000D+00	0.0000000000000D+00	0.0000000000000D+00	0.0000000000000D+00
0.0000000000000D+00	0.0000000000000D+00	0.0000000000000D+00	0.0000000000000D+00
0.1000000000000D+01	0.0000000000000D+00	0.0000000000000D+00	0.0000000000000D+00
0.0000000000000D+00	0.0000000000000D+00	0.0000000000000D+00	0.0000000000000D+00
0.0000000000000D+00	0.0000000000000D+00	0.0000000000000D+00	0.0000000000000D+00
0.0000000000000D+00	0.0000000000000D+00	0.0000000000000D+00	0.0000000000000D+00
0.0000000000000D+00	0.0000000000000D+00	0.0000000000000D+00	0.0000000000000D+00
0.0000000000000D+00	0.0000000000000D+00	0.0000000000000D+00	0.0000000000000D+00
0.1000000000000D+01	0.0000000000000D+00	0.0000000000000D+00	0.0000000000000D+00
0.0000000000000D+00	0.0000000000000D+00	0.0000000000000D+00	0.0000000000000D+00
0.0000000000000D+00	0.0000000000000D+00	0.0000000000000D+00	0.0000000000000D+00
0.0000000000000D+00	0.0000000000000D+00	0.0000000000000D+00	0.0000000000000D+00
0.0000000000000D+00	0.0000000000000D+00	0.0000000000000D+00	0.0000000000000D+00
0.0000000000000D+00	0.0000000000000D+00	0.0000000000000D+00	0.0000000000000D+00

0.1000000000000D+01	0.0000000000000D+00	0.0000000000000D+00	0.0000000000000D+00
0.0000000000000D+00	0.0000000000000D+00	0.0000000000000D+00	0.0000000000000D+00
0.0000000000000D+00	0.0000000000000D+00	0.0000000000000D+00	0.0000000000000D+00
0.0000000000000D+00	0.0000000000000D+00	0.0000000000000D+00	0.0000000000000D+00
0.0000000000000D+00	0.0000000000000D+00	0.0000000000000D+00	0.0000000000000D+00
0.0000000000000D+00	0.0000000000000D+00	0.0000000000000D+00	0.0000000000000D+00
0.1000000000000D+01	0.0000000000000D+00	0.0000000000000D+00	0.0000000000000D+00
0.0000000000000D+00	0.0000000000000D+00	0.0000000000000D+00	0.0000000000000D+00
0.0000000000000D+00	0.0000000000000D+00	0.0000000000000D+00	0.0000000000000D+00
0.0000000000000D+00	0.0000000000000D+00	0.0000000000000D+00	0.0000000000000D+00
0.0000000000000D+00	0.0000000000000D+00	0.0000000000000D+00	0.0000000000000D+00
0.0000000000000D+00	0.0000000000000D+00	0.0000000000000D+00	0.0000000000000D+00
0.1000000000000D+01	0.0000000000000D+00	0.0000000000000D+00	0.0000000000000D+00
0.0000000000000D+00	0.0000000000000D+00	0.0000000000000D+00	0.0000000000000D+00
0.0000000000000D+00	0.0000000000000D+00	0.0000000000000D+00	0.0000000000000D+00
0.0000000000000D+00	0.0000000000000D+00	0.0000000000000D+00	0.0000000000000D+00
0.0000000000000D+00	0.0000000000000D+00	0.0000000000000D+00	0.0000000000000D+00
0.0000000000000D+00	0.0000000000000D+00	0.0000000000000D+00	0.0000000000000D+00
0.1000000000000D+01	0.0000000000000D+00	0.0000000000000D+00	0.0000000000000D+00
0.0000000000000D+00	0.0000000000000D+00	0.0000000000000D+00	0.0000000000000D+00
0.0000000000000D+00	0.0000000000000D+00	0.0000000000000D+00	0.0000000000000D+00
0.0000000000000D+00	0.0000000000000D+00	0.0000000000000D+00	0.0000000000000D+00
0.0000000000000D+00	0.0000000000000D+00	0.0000000000000D+00	0.0000000000000D+00
0.0000000000000D+00	0.0000000000000D+00	0.0000000000000D+00	0.0000000000000D+00
0.1000000000000D+01	0.0000000000000D+00	0.0000000000000D+00	0.0000000000000D+00
0.0000000000000D+00	0.0000000000000D+00	0.0000000000000D+00	0.0000000000000D+00
0.0000000000000D+00	0.0000000000000D+00	0.0000000000000D+00	0.0000000000000D+00
0.0000000000000D+00	0.0000000000000D+00	0.0000000000000D+00	0.0000000000000D+00
0.0000000000000D+00	0.0000000000000D+00	0.0000000000000D+00	0.0000000000000D+00
0.0000000000000D+00	0.0000000000000D+00	0.0000000000000D+00	0.0000000000000D+00
0.1000000000000D+01	0.0000000000000D+00	0.0000000000000D+00	0.0000000000000D+00
0.0000000000000D+00	0.0000000000000D+00	0.0000000000000D+00	0.0000000000000D+00
0.0000000000000D+00	0.0000000000000D+00	0.0000000000000D+00	0.0000000000000D+00
0.0000000000000D+00	0.0000000000000D+00	0.0000000000000D+00	0.0000000000000D+00
0.0000000000000D+00	0.0000000000000D+00	0.0000000000000D+00	0.0000000000000D+00
0.0000000000000D+00	0.0000000000000D+00	0.0000000000000D+00	0.0000000000000D+00
0.1000000000000D+01	0.0000000000000D+00	0.0000000000000D+00	0.0000000000000D+00
0.0000000000000D+00	0.0000000000000D+00	0.0000000000000D+00	0.0000000000000D+00
0.0000000000000D+00	0.0000000000000D+00	0.0000000000000D+00	0.0000000000000D+00
0.0000000000000D+00	0.0000000000000D+00	0.0000000000000D+00	0.0000000000000D+00
0.0000000000000D+00	0.0000000000000D+00	0.0000000000000D+00	0.0000000000000D+00
0.0000000000000D+00	0.0000000000000D+00	0.0000000000000D+00	0.0000000000000D+00
0.1000000000000D+01	0.0000000000000D+00	0.0000000000000D+00	0.0000000000000D+00
0.0000000000000D+00	0.0000000000000D+00	0.0000000000000D+00	0.0000000000000D+00
0.0000000000000D+00	0.0000000000000D+00	0.0000000000000D+00	0.0000000000000D+00
0.0000000000000D+00	0.0000000000000D+00	0.0000000000000D+00	0.0000000000000D+00
0.0000000000000D+00	0.0000000000000D+00	0.0000000000000D+00	0.0000000000000D+00
0.0000000000000D+00	0.0000000000000D+00	0.0000000000000D+00	0.0000000000000D+00
0.1000000000000D+01	0.0000000000000D+00	0.0000000000000D+00	0.0000000000000D+00
0.0000000000000D+00	0.0000000000000D+00	0.0000000000000D+00	0.0000000000000D+00
0.0000000000000D+00	0.0000000000000D+00	0.0000000000000D+00	0.0000000000000D+00
0.0000000000000D+00	0.0000000000000D+00	0.0000000000000D+00	0.0000000000000D+00
0.0000000000000D+00	0.0000000000000D+00	0.0000000000000D+00	0.0000000000000D+00
0.0000000000000D+00	0.0000000000000D+00	0.0000000000000D+00	0.0000000000000D+00
0.1000000000000D+01	0.0000000000000D+00	0.0000000000000D+00	0.0000000000000D+00
0.0000000000000D+00	0.0000000000000D+00	0.0000000000000D+00	0.0000000000000D+00
0.0000000000000D+00	0.0000000000000D+00	0.0000000000000D+00	0.0000000000000D+00
0.0000000000000D+00	0.0000000000000D+00	0.0000000000000D+00	0.0000000000000D+00
0.0000000000000D+00	0.0000000000000D+00	0.0000000000000D+00	0.0000000000000D+00
0.0000000000000D+00	0.0000000000000D+00	0.0000000000000D+00	0.0000000000000D+00
0.1000000000000D+01	0.0000000000000D+00	0.0000000000000D+00	0.0000000000000D+00
0.0000000000000D+00	0.0000000000000D+00	0.0000000000000D+00	0.0000000000000D+00
0.0000000000000D+00	0.0000000000000D+00	0.0000000000000D+00	0.0000000000000D+00
0.0000000000000D+00	0.0000000000000D+00	0.0000000000000D+00	0.0000000000000D+00
0.0000000000000D+00	0.0000000000000D+00	0.0000000000000D+00	0.0000000000000D+00
0.0000000000000D+00	0.0000000000000D+00	0.0000000000000D+00	0.0000000000000D+00
0.1000000000000D+01	0.0000000000000D+00	0.0000000000000D+00	0.0000000000000D+00
0.0000000000000D+00	0.0000000000000D+00	0.0000000000000D+00	0.0000000000000D+00

```
0.0000000000000D+00 0.0000000000000D+00 0.0000000000000D+00 0.0000000000000D+00
0.0000000000000D+00 0.0000000000000D+00 0.0000000000000D+00 0.0000000000000D+00
0.0000000000000D+00 0.0000000000000D+00 0.0000000000000D+00 0.0000000000000D+00
0.0000000000000D+00 0.0000000000000D+00 0.0000000000000D+00 0.0000000000000D+00
0.1000000000000D+01
0.1000000000000D+01 0.0000000000000D+00 0.0000000000000D+00 0.0000000000000D+00
0.0000000000000D+00 0.0000000000000D+00 0.0000000000000D+00 0.0000000000000D+00
0.0000000000000D+00 0.0000000000000D+00 0.0000000000000D+00 0.0000000000000D+00
0.0000000000000D+00 0.0000000000000D+00 0.0000000000000D+00 0.0000000000000D+00
0.0000000000000D+00 0.0000000000000D+00 0.0000000000000D+00 0.0000000000000D+00
0.0000000000000D+00 0.0000000000000D+00 0.0000000000000D+00 0.0000000000000D+00
0.1000000000000D+01 0.0000000000000D+00 0.0000000000000D+00 0.0000000000000D+00
0.0000000000000D+00 0.0000000000000D+00 0.0000000000000D+00 0.0000000000000D+00
0.0000000000000D+00 0.0000000000000D+00 0.0000000000000D+00 0.0000000000000D+00
0.0000000000000D+00 0.0000000000000D+00 0.0000000000000D+00 0.0000000000000D+00
0.0000000000000D+00 0.0000000000000D+00 0.0000000000000D+00 0.0000000000000D+00
0.0000000000000D+00 0.0000000000000D+00 0.0000000000000D+00 0.0000000000000D+00
0.1000000000000D+01 0.0000000000000D+00 0.0000000000000D+00 0.0000000000000D+00
0.0000000000000D+00 0.0000000000000D+00 0.0000000000000D+00 0.0000000000000D+00
0.0000000000000D+00 0.0000000000000D+00 0.0000000000000D+00 0.0000000000000D+00
0.0000000000000D+00 0.0000000000000D+00 0.0000000000000D+00 0.0000000000000D+00
0.0000000000000D+00 0.0000000000000D+00 0.0000000000000D+00 0.0000000000000D+00
0.0000000000000D+00 0.0000000000000D+00 0.0000000000000D+00 0.0000000000000D+00
0.1000000000000D+01 0.0000000000000D+00 0.0000000000000D+00 0.0000000000000D+00
0.0000000000000D+00 0.0000000000000D+00 0.0000000000000D+00 0.0000000000000D+00
0.0000000000000D+00 0.0000000000000D+00 0.0000000000000D+00 0.0000000000000D+00
0.0000000000000D+00 0.0000000000000D+00 0.0000000000000D+00 0.0000000000000D+00
0.0000000000000D+00 0.0000000000000D+00 0.0000000000000D+00 0.0000000000000D+00
0.0000000000000D+00 0.0000000000000D+00 0.0000000000000D+00 0.0000000000000D+00
0.0000000000000D+00 0.0000000000000D+00 0.0000000000000D+00 0.0000000000000D+00
0.0000000000000D+00 0.0000000000000D+00 0.0000000000000D+00 0.0000000000000D+00
0.1000000000000D+01 0.0000000000000D+00 0.0000000000000D+00 0.0000000000000D+00
0.0000000000000D+00 0.0000000000000D+00 0.0000000000000D+00 0.0000000000000D+00
0.0000000000000D+00 0.0000000000000D+00 0.0000000000000D+00 0.0000000000000D+00
0.0000000000000D+00 0.0000000000000D+00 0.0000000000000D+00 0.0000000000000D+00
0.0000000000000D+00 0.0000000000000D+00 0.0000000000000D+00 0.0000000000000D+00
0.0000000000000D+00 0.0000000000000D+00 0.0000000000000D+00 0.0000000000000D+00
0.1000000000000D+01 0.0000000000000D+00 0.0000000000000D+00 0.0000000000000D+00
0.0000000000000D+00 0.0000000000000D+00 0.0000000000000D+00 0.0000000000000D+00
0.0000000000000D+00 0.0000000000000D+00 0.0000000000000D+00 0.0000000000000D+00
0.0000000000000D+00 0.0000000000000D+00 0.0000000000000D+00 0.0000000000000D+00
0.0000000000000D+00 0.0000000000000D+00 0.0000000000000D+00 0.0000000000000D+00
0.0000000000000D+00 0.0000000000000D+00 0.0000000000000D+00 0.0000000000000D+00
0.1000000000000D+01 0.0000000000000D+00 0.0000000000000D+00 0.0000000000000D+00
0.0000000000000D+00 0.0000000000000D+00 0.0000000000000D+00 0.0000000000000D+00
0.0000000000000D+00 0.0000000000000D+00 0.0000000000000D+00 0.0000000000000D+00
0.0000000000000D+00 0.0000000000000D+00 0.0000000000000D+00 0.0000000000000D+00
0.0000000000000D+00 0.0000000000000D+00 0.0000000000000D+00 0.0000000000000D+00
0.0000000000000D+00 0.0000000000000D+00 0.0000000000000D+00 0.0000000000000D+00
0.1000000000000D+01 0.0000000000000D+00 0.0000000000000D+00 0.0000000000000D+00
0.0000000000000D+00 0.0000000000000D+00 0.0000000000000D+00 0.0000000000000D+00
0.0000000000000D+00 0.0000000000000D+00 0.0000000000000D+00 0.0000000000000D+00
0.0000000000000D+00 0.0000000000000D+00 0.0000000000000D+00 0.0000000000000D+00
0.0000000000000D+00 0.0000000000000D+00 0.0000000000000D+00 0.0000000000000D+00
0.0000000000000D+00 0.0000000000000D+00 0.0000000000000D+00 0.0000000000000D+00
0.1000000000000D+01 0.0000000000000D+00 0.0000000000000D+00 0.0000000000000D+00
0.0000000000000D+00 0.0000000000000D+00 0.0000000000000D+00 0.0000000000000D+00
0.0000000000000D+00 0.0000000000000D+00 0.0000000000000D+00 0.0000000000000D+00
0.0000000000000D+00 0.0000000000000D+00 0.0000000000000D+00 0.0000000000000D+00
0.0000000000000D+00 0.0000000000000D+00 0.0000000000000D+00 0.0000000000000D+00
0.0000000000000D+00 0.0000000000000D+00 0.0000000000000D+00 0.0000000000000D+00
0.1000000000000D+01 0.0000000000000D+00 0.0000000000000D+00 0.0000000000000D+00
0.0000000000000D+00 0.0000000000000D+00
1 0 0 0 0 0 0 0 0 0 0 0 0 0 0 0 0 0 0 0 0 0 0
0 2 0 0 0 0 0 0 0 0 0 0 0 0 0 0 0 0 0 0 0 0 0
0 0 3 0 0 0 0 0 0 0 0 0 0 0 0 0 0 0 0 0 0 0 0
0 0 0 4 0 0 0 0 0 0 0 0 0 0 0 0 0 0 0 0 0 0 0
```

```
0 0 0 0 5 0 0 0 0 0 0 0 0 0 0 0 0 0 0 0 0 0 0
0 0 0 0 0 0 0 0 0 0 0 0 0 6 0 0 0 0 0 0 0 0 0
0 0 0 0 0 0 0 0 0 0 0 0 0 0 7 0 0 0 0 0 0 0 0
0 0 0 0 0 0 0 0 0 0 0 0 0 0 0 8 0 0 0 0 0 0 0
0 0 0 0 0 0 0 0 0 0 0 0 0 0 0 0 9 0 0 0 0 0 0
0 0 0 0 0 0 0 0 0 0 0 0 0 0 0 0 010 0 0 0 0 0
-10000.     10000.
-10000.     10000.
-10000.     10000.
-10000.     10000.
-10000.     10000.
-10000.     10000.
-10000.     10000.
-10000.     10000.
-10000.     10000.
-10000.     10000.
-2858.4       0.0
-279.49       0.0
-117.77       0.00
-21.844       0.00
-2.9          0.0
-0.07        6.6
-0.07       -6.6
-0.4         0.0
-0.1         0.0
-0.00001     0.00
-0.47        0.0
-0.47        0.0
-0.47        0.0
-17069.0      0.0
-56.0        0.000
-0.77         0.0
-7.058        1.59
-7.058       -1.59
-4.88         2.59
-4.88        -2.59
-4.97         0.0
-4.97         0.0
-4.97         0.0
```

LIST OF REFERENCES

1. Arrow, A., An Analysis of Aerodynamic Requirements for Coordinated Bank-to-Turn Autopilots, NASA CR-3644, November 1982.

2. Karaiskos, I., The Effects of Digital Control on Longitudinal Autopilots for Bank-to-Turn and Skid -to-Turn Missiles, Master Thesis, Naval Postgraduate School, Monterey California, December 1985

3. Ogata, K., Modern Control Engineering, Prentice-Hall Inc., 1970.

4. Karadimas, C., Design and Analysis of Discrete Lateral Autopilots for BTT Missiles, M.S. Thesis, Naval Postgraduate School, Monterey, California, December 1985.

5. Gordon, V.C., Utilization of Numerical Optimization Techniques in the Design of Robust Multi-Input Multi-Output Control Systems, Ph.D. Thesis, Naval Postgraduate School, Monterey, California, September 1984.

INITIAL DISTRIBUTION LIST

		No. Copies
1.	Defense Technical Information Center Cameron Station Alexandria, Virginia 22304-6145	2
2.	Library, Code 0142 Naval Postgraduate School Monterey, California 93943-5000	2
3.	Department Chairman, Code 67 Department of Aeronautical Engineering Naval Postgraduate School Monterey, California 93943-5000	1
4.	Professor D.J. Collins, Code 67Co Department of Aeronautical Engineering Naval Postgraduate School Monterey, California 93943-5000	2
5	Professor H.A. Titus, Code 62Ts Department of Electrical Engineering Naval Postgraduate School Monterey, California 93943-5000	2
6.	Hellenic Navy General Staff 2nd Branch, Education Department Stratopedon Papagou Athens, GREECE	4
7.	LCDR Nicolaos, G. Protonotarios H.N Proodou 10, 11147 Galatsi Athens, GREECE	3
8.	LT Ioannis, Karaiskos H.N Pelopos 1, 18121 Koridallos Piraeus, GREECE	1

9.	John, J. Morrow, Code 338 Naval Weapons Center China Lake, Ca., 93555-6001	1
10.	Dale, B. Atkinson, Air-5164 Naval Air Systems Command Washington, D.C. 20361	1
11.	Tor, W. Jensen, Code 6013 Naval Air Development Center Warminister PA., 18974	1

219320

Thesis
P9452
c.1

Protonotarios
An investigation of
B.T.T. missiles.